THE PHOTOLYSIS AND CO-IRRADIATED DECOMPOSITION OF BARIUM AND STRONTIUM AZIDES

The University of Cape Town

A thesis submitted to the
UNIVERSITY OF CAPE TOWN
in fulfilment of the requirements for the degree of
DOCTOR OF PHILOSOPHY

by

ENID GWENDOLYN SHEPHARD B.Sc. (Hons.) (Cape Town)

Department of Chemistry,
University of Cape Town,
Rondebosch, Cape,
South Africa.

March, 1974.

The copyright of this thesis is held by the University of Cape Town.
Reproduction of the whole or any part may be made for study purposes only, and not for publication.

The copyright of this thesis vests in the author. No quotation from it or information derived from it is to be published without full acknowledgement of the source. The thesis is to be used for private study or non-commercial research purposes only.

Published by the University of Cape Town (UCT) in terms of the non-exclusive license granted to UCT by the author.

The University of Cape Town

ACKNOWLEDGEMENTS

The author wishes to express her sincere thanks to Professor E.G. Prout for all his advice, guidance and discussion throughout the research project and the writing of this thesis.

Sincere thanks are also extended to

Mr. D.W. Lensen for his keen help with all the technical aspects of the project,

Mr. C. Ledger, the glassblower, for his competent work, particularly in silica glass,

Mrs. W. Grobbelaar for typing this thesis,

the Council for Scientific and Industrial Research for financial assistance,

and her husband, Gordon, and parents for their help and encouragement throughout the course of this research.

SUMMARY

The effect of ultraviolet radiation on sieved powders and pellets of barium azide in the temperature range 27,0° - 135,0°C and of strontium azide in the temperature range 30,0° - 135,0°C has been studied. Decompositions in the temperature range 27,0° - 100,0°C for barium azide and 30,0° - 90,0°C for strontium azide have been termed photolytic decompositions, while reactions in the temperature range 110,0° - 135,0°C (the thermal decomposition temperature range) for both compounds have been termed co-irradiated decompositions.

The ultraviolet light source used was a very high intensity 100 watt "point source" high pressure mercury arc lamp. The extent of decomposition was almost the same as a simple thermal decomposition.

Kinetic analyses, activation energy determinations, studies of the dependence of reaction rates on light intensity, the effect of water vapour on the sample at various stages of reaction and the observance of the colour of the sample at various stages of reaction have been carried out. Analogous results were obtained for the two compounds.

In the photolytic temperature range two distinct modes of decomposition are postulated to occur, the transition temperature occurring at 60,0°C for barium azide and at 50,0°C for strontium azide.

During co-irradiation it is proposed that decomposition occurs via the expected thermal decomposition process and the photolytic mechanism or a slight variation thereof, above 60,0°C for barium azide and above 50,0°C for strontium azide.

1 INTRODUCTION

Since the work presented in this thesis involves the photolysis of barium and strontium azides and the effect of irradiating these salts with ultraviolet light during the thermal decomposition (co-irradiation) it is necessary to discuss the effects of the interaction of light with solids and the mechanisms of thermal decomposition. Finally the effects of treatment of solids with ultraviolet light prior to thermal decomposition (pre-irradiation) will be reviewed.

1A THE PHOTOLYSIS OF SOLIDS

(i) The effects of the interaction of ultraviolet light with solids

When crystals of certain inorganic solids are irradiated with ultraviolet light of wavelength corresponding to a characteristic absorption band of the solid, photochemical decomposition (photolysis) takes place. The course of the reaction is generally followed by pressure measurements of the evolved gas at fixed time intervals during the photolysis.

Photolytic decompositions of solids have been interpreted from two different viewpoints (1). In the first approach the solid properties are regarded as relatively unimportant except as a matrix for holding the reacting interface. This chemical approach provides an explanation for only some decomposition effects. The second approach involves all the properties associated with solids, in particular the electronic properties. It assumes that all the electronic properties usually associated with that of semi-conductors and non-metals may be involved in the photodecomposition of solids. The approach provides a natural explanation for a large segment of the effects observed during photolytic decomposition of some substances.

When crystals are exposed to light capable of photolysing the sample, it is absorbed within a few microns below the incident surface where photolysis occurs, and after prolonged irradiation decomposition takes place below the surface at well defined individual locations. This has been observed in the photolysis of sodium (2) and potassium (3) azides. Decomposition occurs initially at crystallographically related locations on the crystal surface which resemble etch pits, and at the intersections of slip and twin planes and the crystal surface.

Photolysis involves an energy carrier, produced by the action of light on solids, to transport the energy imparted by an individual photon to the point in the crystal where decomposition occurs. Since the energy of irradiation is of the order of the energy of the chemical bond and that of the energy gap between the valence and conduction bands in ionic crystals, the rate determining step in photolysis occurs by a low energy mechanism involving these energy carriers.

In order to obtain an insight into the interaction of light with solids one must understand the behaviour of electrons in solids i.e. the structure of solids (4).

The modern theory of the electronic structure of solids follows from the Schrödinger equation with a periodic potential arising from the lattice atoms. If the valence electrons are considered to be free to move throughout the volume of the solid with the metal ion embedded in a sea of electrons with no periodic potential of the lattice, then the solution of the Schrödinger equation is of the form:

$$\Psi = e^{ikx}$$

with all values of k allowed, k being the wave number and related to the wavelength of the electron by:

$$k = 2\pi/\lambda \ .$$

The energy of the free electron is given by

$$E = p^2/2m$$

where p is the momentum and m is the mass of the electron.

From the de Broglie relationship momentum is related to wavenumber by

$$p = \hbar k.$$

Thus $$E = (\hbar^2/2m)k^2$$

which gives a quadratic dependence of energy on wavenumber.

If the periodic potential of the lattice atoms is taken into account solutions to the Schrödinger equation are of the form

$$\Psi_k = e^{ikx} u_k(x)$$

where $u_k(x)$ is the periodic function with the same periodicity as the potential i.e. its period is the lattice constant a.

The function $u_k(x)$ depends generally upon k. At values of k equal to $\pm \pi/a$, $\pm 2\pi/a$, $\pm 3\pi/a$ etc., discontinuities occur in the energy thus giving rise to energy bands and forbidden energy gaps. This arises since the condition for Bragg reflection of the electron wave in the crystal is met, i.e.

$$k = n\pi/a$$

becomes equivalent to the Bragg condition

$$2a \sin\theta = n\lambda .$$

Accordingly at values of k near $\pm n\pi/a$ there are an increasing number of components of reflected waves, in the solution of the wave equation, corresponding to an increase in transfer of momentum between the electron and lattice. At values of k far from $\pm n\pi/a$ the energy of the electron is free from any periodic potential of the lattice and the energy can be given by the free-electron quadratic dependence on k.

The zones (or bands) defined by values of k which are integral multiples of π/a are called Brillouin zones. Discontinuities in the energy (energy gaps) occur at the zone boundaries. The first zone includes the segment

$$-\pi/a \text{ and } +\pi/a \ .$$

The second zone includes the two segments

$$-2\pi/a < k < -\pi/a \qquad \text{and} \qquad \pi/a < k < 2\pi/a \qquad \text{etc.},$$

the zones being separated by a few electron volts.

The energy states within these bands are distributed in a quasi-continuous fashion. Electrons progressively fill all the allowed states starting with those lowest in energy and continuing until the supply of electrons is used up. The topmost band that contains electrons (valence electrons) will be completely or partially filled depending on the nature of the constituent atoms in the solid. In the filling of these states the Pauli Exclusion Principle holds i.e. only one electron can occupy a given allowed state at a time, spin being taken into account.

If the highest occupied band contains only a small concentration of occupied or empty states the material is an n-type or p-type semi-conductor respectively. When the highest occupied band contains large fractions of both occupied and empty states the solid is a metal. If the bands which contain electrons are completely filled, the material is an insulator. The completely occupied band is called the "full band" and is separated from the completely empty band (conduction band) by a few electron volts, the magnitude of the energy gap depending on the electronegativity of the constituent atoms. Owing to the Pauli Exclusion Principle electronic conductivity is impossible since accompaning any change for one electron there are changes in the other electrons which add up to an exactly opposite counter balancing change. Thus all ionic

solids are insulators, ignoring the possibility of ionic conduction which can possibly occur.

Chemical activity within solids is closely connected to physical properties such as transport of matter, electrical conductivity, optical behaviour, and magnetic, thermal and mechanical properties. These physical properties in turn depend upon defects in electronic structure and deviation from ideal atomic arrangements in solids (5). Lattice defects which are arbitrarily scattered throughout the crystal give rise to regions of disturbance localized about individual points. Crystal defects such as inhomogeneities, point and line defects, influence the energy levels available for electrons and the properties of growth of new phases. In addition these defects act as traps for energy carriers.

Optical properties of solids are related to bulk properties and imperfections. Several kinds of transitions characteristic of the host atoms or electrons of a solid give rise to optical absorption. An electron on absorbing a quantum of electromagnetic energy may acquire sufficient energy to be raised to a higher-lying (empty) state and absorption by atoms can raise them to higher-lying rotational and vibrational states. Also, the electronic and atomic levels may interact, allowing excitation of both by the absorption of light.

If an insulator is irradiated with light of a suitable wavelength an electron from the full band can be excited to the empty band above it, enabling the excited electron to move freely through the conduction band. The positive hole, remaining behind in the valence band on removal of the excited electron, may remain at the point where it originated or migrate throughout the valence band.

On irradiating an insulator with light of wavelength less than that of the gap between the valence and conduction bands, electrons from

an anion may be excited into the exciton levels which exist between the valence and conduction bands. These levels can be thought of as corresponding to possible "Bohr orbits" with their convergence limit at the lowest level of the conduction band. In this case an electron-hole pair is produced, the electron being bound to the positive hole by coulombic attraction. This excited electron-hole pair can remain at the point of production and is then called a molecular exciton, or migrate throughout the crystal when it is called an exciton. With this movement no charge transport occurs but only energy transfer, therefore it does not contribute to electrical conduction. However they may aid photoconductivity indirectly by thermally dissociating to yield positive holes and electrons in the conduction band. These exciton levels can be observed from the long wavelength edge in the low temperature optical absorption spectra. Exciton transitions have been observed in the optical absorption spectra of sodium, potassium, rubidium and caesium azides (6) as well as thallous and silver azides (7,8) in the wavelength range 1400 - 2200 Å. From these spectra the spacings between the exciton levels and their separation from the valence band have been calculated.

Due to the production of imperfections such as free electrons and their conjugate positive holes or excitons, from the absorption of light of characteristic wavelengths, the total energy of the crystal is increased and can now dispose of its energy in various ways. Thus these imperfections can be considered as energy carriers for the transport of energy imparted by an individual photon.

The existence of an excited ion or exciton in the crystal produces a change in the interaction of this ion with neighbouring ions, and the lattice will not be in its configuration of minimum energy. This excess energy can be transferred thermally to the lattice through vibration about the new equilibrium position. Excitons move through the crystal with velocity corresponding to an energy of the order of a

thermal electron (i.e. ~ kT). This will lead to interaction with the vibrational modes of the lattice resulting in considerable scattering and loss of kinetic energy. The lifetime of an unperturbed exciton is 10^{-8} sec., but can be shortened by collisions with imperfections in radiationless processes (9).

Other methods by which this thermal dissipation occurs is dependent on the relative positions of the ground and excited state potential energy curves. When the two curves intersect, but the excited state has a minimum within the ground state curve, after optical excitation there will be a radiationless transition to the point where the two curves intersect. But if the minimum in the potential energy curve of the excited state lies outside the potential energy of the ground state, an electron could remain in the excited state until a radiationless transition occurs. This would then correspond to a meta-stable state.

Besides thermal dissipation of energy absorbed during optical excitation, an electron can revert to the ground state by luminescence i.e. emission of radiation. This includes fluorescence and phosphorescence. The former involves spontaneous re-emission of quanta of the same transition or of photons resulting from a return to the ground state by a different route. Phosphorescence occurs when the excited electron is transferred to a meta-stable state from which a direct transition to the ground state cannot occur.

Owing to electron traps, hole traps and/or recombination centres on the surfaces of crystals, electronic processes occurring at these surface sites or surface states, can release sufficient energy to produce reactions at the crystal surface. Also defects or impurities in the crystal lattice or Tamm states (10) (a consequence of the quantum mechanical nature of the electronic properties of the crystal) are responsible for trapping free electrons and their conjugate positive

holes and excitons. In particular, decomposition sites are carrier traps. When the decomposition site contains the initially trapped carrier (an electron, hole or exciton) it is in the first excited state. The lifetime of the first excited state must be finite and could range from a few nanoseconds to many hours or even days. In this first excited state the trap is capable of trapping a carrier whose charge is opposite of the initially trapped charge, or of trapping an exciton and facilitating the release of the exciton potential energy. Alternatively it may produce an additional decomposition site without destroying itself. The final step occurs when the energy released facilitates a photolytic reaction.

An electron excited into the conduction band can be trapped immediately or migrate through the band and then be trapped at the trapping centre. The pertinent defect in this case responsible for the trapping, is the absence of an anion from its normal negative lattice site. The result of the trapping is the production of an F-centre, one of the simplest colour centres. An F-centre absorbs in the visible region of the spectrum, and is observed when ionic solids, in particular the alkali halides, are exposed to ultraviolet light, X-radiation and electron bombardment, exhibiting a deep colouration characteristic of the crystal as a whole. The optical absorption of an F-centre arises from an electronic dipole transition to a bound excited state of the F-centre (11). This colouration has been shown by Pohl (12) to be due to a bell shaped absorption band about 4000 to 8000 Å. The electronic structure of an F-centre viz an electron bound to a negative ion vacancy was first suggested by De Boer (13). This description has been found to be correct from e.s.r. data (9). F-centres have been identified by e.s.r. methods in sodium azide when irradiated with ultraviolet light at 77^{o}K (14, 15, 16).

The positive hole, produced on removal of the electron from the valence band can be trapped by a hole trap, the lifetime of the migrating hole generally being shorter than that of the migrating electron. The character of this trap must necessarily be the absence of a cation from the positive site, the colour centre being called a V-centre according to Seitz (9).

Five V-bands (V_1 to V_5) have been distinguished in the ultraviolet absorption of potassium bromide exposed to bromine vapour (17), and are identified with the centres formed by the interaction of positive holes with cation vacancies. V-centres have been observed from the ultraviolet absorption spectrum of sodium azide at $77^{o}K$ (15).

When crystals containing F-centres are irradiated with light within the F-band photoconductivity can result owing to the close proximity of the excited state to the conduction band allowing electrons to be thermally ionized. The free electron can now migrate through the crystal until it is once again trapped. The lifetime of this wandering electron has been found for KCl, at $-100^{o}C$, to be inversely proportional to the F-centre concentration. This has proved that the trapping centres are themselves F-centres. Hence an anion vacancy can trap two electrons. This effect has been observed in optical spectra (4).

During irradiation with light within the F-band at low temperatures there is an appearance of a broad band on the long wavelength region of the F-band, with a corresponding disappearance of the F-band. The new band is called an F'-band which is only stable at low temperatures and decomposes on warming, the F-band being regenerated. The quantum yield in this process is two (18) since each quantum liberates an electron from an F'-centre and on combination with an anion vacancy a second F-centre is formed

$$\text{i.e. } F' \xrightarrow{h\nu} F + e$$

$$e + \boxminus \longrightarrow F$$

where ⊟ represents a vacant anion site.

On irradiating crystals within the F-band at low temperatures, thus causing the formation of F'-centres, an absorption band called the α-band appears simultaneously while the β-band bleaches at the same rate as the F-band. The β-band reappears on warming to a temperature which decomposes the F'-centres and there is a corresponding disappearance of the α-band. The α-band appears superimposed on the normal lattice absorption edge. This absorption band is due to perturbation caused to the first excited anion levels (exciton levels) by a neighbouring anion vacancy, leading to exciton levels somewhat lower than the normal exciton levels. The β-band occurs between the α-band and the main exciton level and is due to promotion of electrons to perturbed exciton levels in the immediate neighbourhood of F-centres. Thus exciton formation occurs in the α-band and not the β-band on irradiation within the F-band, owing to enhancement of perturbations on ions adjacent to those bleached F-centres (i.e. anion vacancies).

Fluorescence occurs on irradiation within the α-band which indicates that the formed exciton is trapped by the anion vacancy but the resulting complex does not dissociate into an F-centre and a free positive hole.

The α- and β- bands have been observed in KI, KBr and RbCl (19).

Irradiation within the F-band at room temperature with light or X-rays produces new bands on the long wavelength side of the F-band. These bands are designated the R_1-, R_2- and M-bands. An M-centre is the combination of an F-centre with a cation-anion vacancy pair (9). Capture of a second electron causes instability and the positive ion vacancy will diffuse away leaving a double F-centre called the R_2-centre. An R_1-centre is formed if the R_2-centre loses one of its electrons through being trapped by an anion vacancy, M-centre or a vacancy pair. These bands have been observed in KCl (20) and sodium azide (16).

Symbolically the process may be represented by

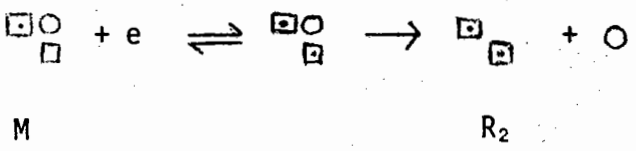

M R_2

□ = anion vacancy

○ = cation vacancy.

Irradiation of KCl at 100°C within the F-band produces a broad band (21) called the R'-band, on the long wavelength side of the F-band. This band is made up of a large number of components since on cooling to 78°K no resolution was found. At 100°C there is an increase in vacancy mobility resulting in electrons combining with groups of vacancies including R_1-, R_2-, and M-centres. R'-centre formation from F-centres increases with temperature up to about 500°C at which temperature there is a dissociation of R'-centres to F-centres.

V-bands are bleached when crystals are irradiated within the F-band. A V_1-centre appears when a crystal is X-irradiated at liquid air temperatures, but warming of the crystal causes this band to be bleached with a marked reduction in the size of the F-band. This results in photoconductance and luminescence supporting the model of a positive hole trapped at a cation vacancy for the V_1-centre. Bleaching of the F- and V_1-bands occurs with low quantum yield owing to low probability of thermal ionization of an electron from the excited state of an F-centre. These free electrons annihilate the trapped holes. V_1- and F-bands are bleached simultaneously by irradiation within the V_1-band through recombination of electrons and holes. The V_2-centres are bleached by irradiation within the F-band at room temperature which is too high a temperature for the V_1-centres to be stable. Temperatures greater than room temperature are needed to bleach the V_3-band. This band is bleached when the crystal is irradiated simultaneously with F-light

and V-light. This supports the theory by Seitz (9) that V_2- and V_3-centres comprise a hole trapped by two cation vacancies, and two holes trapped by two cation vacancies respectively.

Since about 2 e.v. is required to bleach F-centres thermally, no bleaching is expected at room temperature. This arises from the small probability that a trapped electron can escape from an F-centre on acquiring a small thermal energy. Bleaching can occur by tunnelling through the potential barrier. A process of recombination with nearby positive holes and with V_2- and V_3-centres then occurs.

These phenomena, observed when light interacts with solids, have been used by many workers in the field of photolysis to explain the photolytic results obtained. The first theoretical mechanism was postulated by Mott(22) for the photolysis of barium azide and was based on the work of Garner, Maggs and Wischin (23, 24).

Barium azide was treated as an ionic conductor with mobile metal ions in interstial positions. Irradiation produced electrons and positive holes capable of diffusing through the crystal lattice. Neutralization of the mobile metal ions was caused by trapping of electrons at unspecified "sensitivity specks". Thus metal atoms accumulated. A secondary growth mechanism for the product now operated whereby further electrons were trapped by the metal to form metal anions which could then neutralise the mobile metal cations. This mechanism supported the observed formation of nuclei on the surface of crystals accompanied by evolution of gas.

This mechanism has also been the basis for the explanation of photolytic decomposition of other inorganic compounds, although in recent years subsequent workers have criticised and modified Mott's original mechanism or replaced it with new concepts.

At this stage it would be appropriate to review the work done on the photolysis of barium azide and to put forward some of the evidence

for these changes in the original postulated mechanism. The application of the Mott Principle to other ionic inorganic compounds, with developments of new mechanisms for these compounds, will then be discussed.

(ii) The photolysis of barium azide

Following the mechanism proposed by Mott (22), Thomas and Tompkins (55) restudied the photolysis of barium azide using a low pressure mercury arc in the temperature range -106° to 45°C. They found that the rate of photolysis was constant at constant temperature and constant light intensity, when light of wavelength 2537 Å was used. The rate varied as the square of the light intensity at constant temperature but increased in a complex manner with variation of temperature at constant intensity.

A mechanism for the photolysis was proposed, involving the production and trapping of excitons, to satisfactorily fit the found results. Nitrogen was produced from the interaction of excitons at the imperfections, possibly vacant lattice sites.

It was suggested by Baidins (56) that metallic reaction product, produced during the photolysis of barium azide, was not inert. This lead to a re-investigation of the photolysis of barium azide (57, 40). New kinetic measurements were made (57) using high and low pressure mercury lamps over the temperature range -25° to 25°C. The reactions appeared to be more complex than first realized and a theory involving the production of both excitons and positive holes was postulated. The rate of the chemical reaction was proved to be dependent on the nature of the light source, the extent of the decomposition and the intensity of the ultraviolet radiation. It was observed (40) that the rate of photolysis with time first decreased then increased after which it became constant, when light of wavelength 2537 Å or a lamp emitting a

more or less continuous spectrum with spectral lines superimposed was used.

The initial rate was found to be proportional to the square of the light intensity and had an activation energy of 5 Kcal.mol^{-1}. A mechanism which involved a bimolecular recombination of excitons at an unidentified trap T was proposed

$$\text{i.e. } N_3^-T \overset{h\nu}{\rightleftharpoons} N_3^-{}^*T \rightleftharpoons (N_3T)^{-*}$$

$$N_3^-(N_3T)^{-*} \overset{h\nu}{\rightleftharpoons} N_3^-{}^*(N_3T)^{-*} \rightleftharpoons (N_3TN_3)^{2-**}$$

$$(N_3TN_3)^{2-**} \xrightarrow{Ba^{++},\ 5\ \text{Kcal.mol.}^{-1}} 3N_2 + Ba + 2\square$$

where $\square$ represents a vacancy

and * the excited state of the anion or complex.

After prolonged photolysis the square law was not applicable and the rate of nitrogen evolution increased. They assumed that in the initial deceleratory reaction the traps T were completely consumed and thus in the following acceleratory period a new mechanism was taking place. The constant rate of gas evolution had an activation energy of 20 Kcal.mol.$^{-1}$.

The possibility of photo-emission from barium atoms, formed in the first part of the reaction, was considered the reason for the increasing rate period. These generated electrons caused an acceleration of the reaction by facilitating the combination of excitons and radicals. Barium metal was thought to form via aggregation of barium atoms

$$\text{viz} \quad Ba \overset{h\nu}{\rightleftharpoons} Ba^+ + e$$

$$Ba^+ + N_3^- \longrightarrow Ba + N_3$$

$$N_3^- \overset{h\nu}{\rightleftharpoons} N_3^-{}^*$$

$$N_3^{-*} + N_3 \longrightarrow 2N_3 + e$$

$$2N_3 \longrightarrow 3N_2$$

$$Ba + Ba^{2+} + 2e \longrightarrow Ba_2 \quad .$$

The dark rate observed when the light was switched off was explained by postulating the following thermal decomposition:

$$Ba + Ba^{2+} \xrightarrow{kT} (Ba_2)^{2+}$$

$$(Ba_2)^{2+} + 2N_3^- \longrightarrow Ba_2 + 2N_3$$

$$2N_3 \longrightarrow 3N_2 \quad .$$

The effect of filtering the 2537 Å wavelength from the source (with the use of a Chance OY10) was investigated. It was concluded that the 2537 Å wavelength was responsible for the acceleratory reaction.

In another investigation into the importance of wavelength of ultraviolet light on the photochemical decomposition of barium azide Verneker (52) found that light of wavelength 1849 + 2537 Å or light of wavelength 2000 - 3000 Å gave rise to the rate-time plot previously reported (40). However unlike the results found by Jacobs (40), light of wavelength 2537 Å produced no acceleratory reaction and the product after each reaction, regardless of temperature, gave a positive nitride test. Barium nitride showed an acceleratory reaction when photolysed with light of wavelength between 2000 - 3000 Å. This led to the development of a new mechanism.

Verneker maintained that the initial decreasing rate was due to consumption of defects, as previously reported. Consumption of these defects should cause the rate to proceed to zero but since this was not observed a photo-emission process was envisaged viz electrons from metal specks, produced in the process of consumption of defects, keep

the reaction going. After the minimum value, the acceleratory period was proposed to be due to photolysis of the nitride formed.

Tompkins (58) has recently suggested that photolysis of barium azide could involve the trapping of excitons at anion vacancies:

$$N_3^- \quad \underset{\rightleftharpoons}{h\nu} \quad N_3^{-*} \quad \xrightarrow{Vac^-} \quad N_3^{-*}\ Vac^- \ .$$

The trapped exciton can decay via two processes:

$$N_3^{-*}\ Vac^- \begin{cases} \nearrow N_2^-\ Vac^- + N^0 \\ \searrow \overset{N_3^{-*}}{} \ 3N_2 + F' \end{cases}$$

where an F'-centre is two electrons trapped at an anion vacancy. This F'-centre may now react with Ba^{2+} to form the embryo nucleus Ba^0. At the surface bimolecular combination of N atoms produces gaseous nitrogen.

In order to clear up the anomalous results found previously for the photolysis of barium azide, Prout and Sears (61) have recently made a study of the photolysis of pellets of powdered dehydrated barium azide monohydrate. The temperature range of photolysis was 20^o to -197^oC and the effect of both high and low pressure mercury arcs was investigated. High reproducibility was obtained when 8 mg pellets (0,3 mm thick and 5 mm in diameter) were used.

The pressure-time plots obtained when using a high intensity arc comprised two main features viz a short acceleratory region and a decay region which was very protracted and incomplete after 20 hr of irradiation. In the later stages of photolysis the plot appeared to be linear. In the temperature range 0^o to 20^oC an activation energy of 3,0 Kcal.mol.$^{-1}$ and 2,3 Kcal.mol.$^{-1}$ was obtained for the acceleratory and decay reactions respectively. The acceleratory and decay

reactions in the temperature range 0^{o} to $-197^{o}C$ had activation energies of 1,1 and 0,9 Kcal.mol.$^{-1}$ respectively.

The acceleratory reaction appeared to vary as the square of the light intensity and the decay reaction varied linearly with light intensity.

The use of filters with the high pressure lamp indicated that the effective wavelength for phtolysis lies in the narrow region 2000 - 2200 Å.

The low pressure lamp gave similar rate-time plots. The activation energy in the range 21^{o} to $-10^{o}C$ was found to be 2,5 Kcal. mol.$^{-1}$.

Mechanisms were proposed to fit the above experimental results. Since the acceleratory reaction depended on the square of the intensity of radiation, a bimolecular reaction involving two excited ions was proposed. The acceleratory reaction in the temperature range 0^{o} to $22^{o}C$ was thought to be initiated at points of thermodynamic instability such as emergent grain boundaries and dislocations on the surface. The following scheme was proposed:

$$N_3^- \rightleftharpoons N_3^{-*} \quad \text{(excited ion)}$$

$$N_3^{-*} + \boxminus \longrightarrow (N_3 \boxminus)^{-*} \quad \text{(trapping of excited ion at anion vacancies).}$$

These entities are thought to react on neighbouring sites, the reaction being bimolecular with respect to azide ions:

$$2(N_3 \boxminus)^{-*} \longrightarrow (N_3 \boxminus_2 N_3)^{2-*}$$

then $$(N_3 \boxminus_2 N_3)^{2-*} \longrightarrow N_2^- + 2N_2 + 3\boxminus + e \ .$$

Owing to the temperature of irradiation F-centres were not postulated.

Barium atoms are formed by

$$Ba^{2+} + 2e \longrightarrow Ba \ .$$

This mechanism has been supported by e.s.r. measurements which have detected N_2^- ions (59, 60).

In the temperature range 0^o to -197^oC a free radical type reaction was proposed:

$$N_3^- \overset{h\nu}{\rightleftharpoons} N_3^{-*}$$

$$2N_3^{-*} \longrightarrow 2N_3 + 2e$$

$$e + \boxminus \longrightarrow e\boxminus$$

$$N_3 + N_3^- \longrightarrow N_4^- + N_2$$

$$N_3 \longrightarrow N + N_2$$

$$N + N_3^- \longrightarrow N_2^- + N_2 \ .$$

The decrease in the rate of reaction was thought to be due to the consumption of reactive surface material. The initial layer of product could consist of Ba atoms. After a particular time aggregation of these to form discrete nuclei of metal can take place i.e.

$$Ba_n \overset{h\nu}{\rightleftharpoons} Ba_n^+ + e \quad \text{(photo-electric effect)}$$

$$N_2^- \overset{h\nu}{\rightleftharpoons} N_2^{-*}$$

$$Ba_n^+ + N_2^{-*} \longrightarrow N_2 + Ba_n \ .$$

This is a unimolecular reaction with respect to N_2^- ions in accordance with the observed dependence of the decay reaction on light intensity.

No dark rate was observed when the light was switched off, but

an increase in photolytic rate was observed following the dark period. This was accounted for by assuming aggregation of barium atoms continues to take place in the dark period and some crystallization occurs.

(iii) The photolysis of other inorganic azides

Following the original investigations, and proposals of mechanisms, for the photolysis of barium azide an investigation was made into the photolysis of other azides. Mechanisms for the observed photolytic decompositions were postulated with correlations to the already proposed mechanisms for the photolysis of barium azide.

The first comparative study was made at the International Symposium on the Reactivity of Solids in 1964 by Jacobs, Sheppard and Tompkins (39). The kinetics of sodium, potassium and strontium azides were compared with data previously obtained for barium azide (40). Photolysis of potassium and strontium azides showed an initial deceleratory reaction followed by an acceleration after which the rate of photolysis became constant, as was observed for barium azide (40). For sodium azide the rate-time curve showed no acceleration after the initial deceleration and filtering the arc made no difference to the rate-time plot. The acceleratory reaction was removed from the rate-time plot of strontium and potassium azides, by filtering the ultraviolet light. This led to the conclusion that the acceleratory reaction in potassium azide is dependent on light of wavelength 1849 Å and the corresponding region for strontium azide dependent on light of wavelength 2100 Å. The initial deceleratory reaction was found to be dependent on light of wavelength 2537 Å. This indicated that at least two mechanisms were involved in the photolysis of these azides. Thus a mechanism was proposed for sodium and potassium azides based on measurements from absorption spectra (41), photo-electric properties (41, 42), colour centre

absorption bands (43, 15, 44, 45) and electron spin resonance data (46, 14, 47, 16, 48, 49, 50) to date. No mechanism was proposed for strontium azide since no information was as yet available on colour centres or e.s.r. results.

The mechanism for the deceleratory region involved the production of N_3^{-*} (excited azide ions) and their destruction at adjacent imperfections in the following way

$$N_3^- \rightleftharpoons (N_3^-)^* \quad h\nu$$

$$(N_3^-)^* + (N_3^-)^* \longrightarrow N_4^- + \boxminus e + N_2 \quad \ldots\ (1)$$

$$(N_3^-)^* + (N_3^-)^* \longrightarrow N_2^- + \boxminus e + 2N_2 \quad \ldots\ (2)$$

$$(N_3^-)^* + (N_3^-)^* \longrightarrow \boxminus e \boxminus + 3N_2 \quad \ldots\ (3)$$

where $\boxminus$ is an anion vacancy,

$e \boxminus$ is an F-centre

and $\boxminus e \boxminus$ is an F_2^+-centre.

Mechanism (3) is most likely for sodium azide since F-centres and F_2^+-centres have been identified from e.s.r. measurements (14, 16); while paths (1) and (2) are possible for potassium azide since N_2^- and N_4^- ions have been identified from e.s.r. measurements (48, 49, 50).

On warming potassium azide the N_2^- bands have been observed to decrease while the N_4^- resonance band increases, thus the reaction could be

$$N_2^- + N_2^- \longrightarrow N_4^- + \boxminus e$$

followed by aggregation of F-centres with the eventual formation of metal specks.

For sodium azide aggregation of F- and F_2^+-centres leads to the formation of metal specks.

The dark reaction observed in potassium azide was thought to be due to the reaction of N_4^- ions viz

$$N_4^- \longrightarrow N_3^- + N$$

$$N + N \longrightarrow N_2 .$$

The acceleratory phase was thought to be catalysed by the metal product produced in the deceleratory phase. In crystals containing metal specks, photons of the requisite energy were thought to produce electrons through photo-emission from the metal into the conduction band, as was proposed for barium azide (40). Production of nitrogen occurs when azide ions adjacent to metal specks decompose.

Since the absorption spectra of sodium and potassium azides are similar Jacobs and Tariq Kureishy (51) concluded that the lack of the acceleratory process in sodium azide was not due to the band structure of the salt. They tried to determine whether two mechanisms were taking place during the photolysis of the sodium salt as observed in the case of potassium, strontium (39) and barium azides (40). This was investigated by successive interruptions of photolysis in the constant rate period followed by further irradiation.

It was found that, if during the interruption the salt was left in contact with nitrogen, the rate increased and then reached a constant rate on further irradiation. The rate of photolysis after interruption remained constant when the sample was pumped during the interruption. These results indicated that two mechanisms were taking place and the second mechanism (constant rate) is dependent on sodium metal.

The increase in rate after interruption when the sample is kept in contact with nitrogen was thought to be due to chemisorption of nitrogen on the metal during interruption. This chemisorption is sufficient to prevent the catalysis of photolysis by sodium metal until

the metal has been reformed.

They found the primary deceleratory reaction to be proportional to the square of the light intensity and thus proposed the following mechanism:

$$N_3^- \rightleftharpoons (N_3^-)^* \quad \text{..... (1)}$$

$$(N_3^-)^* + S \rightleftharpoons N_3eS \quad \text{..... (2)}$$

$$(N_3^-)^* + N_3eS \longrightarrow 3N_2 + \boxminus e \boxminus + S^- \quad \text{.... (3)}$$

where e is an electron,

* represents an excited state,

S represents a trapping site

and $\boxminus$ represents an anion vacancy.

This process has been supported by e.s.r. measurements which have shown that F_2^+-centres are the major products (16).

At room temperature the F_2^+-centre reacts with a sodium ion to give two anion vacancies

$$\text{i.e.} \quad Na^+ + \boxminus e \boxminus \longrightarrow Na + 2\boxminus \quad \text{..... (4)}$$

The electron attached to the site S can also react with a sodium atom viz

$$S^- + Na^+ \longrightarrow S' + Na \quad \text{..... (5)}$$

where the trapping site S' does not have the same properties as S since it is associated with two sodium atoms and two anion vacancies. Thus S' is now unreactive. The rate of nucleus formation is therefore a deceleratory process since potential nucleus-forming sites S are being consumed during reaction.

The subsequent constant rate reaction is associated with growth of these nuclei. During this constant rate period photo-emission takes place from sodium metal specks

i.e. $$Na_n \overset{h\nu}{\rightleftharpoons} Na_n^+ + e \quad \ldots\ldots\ldots \quad (6)$$

$$(N_3^-)^* + Na_n^+ \longrightarrow Na_n + N_3 \quad \ldots\ldots\ldots \quad (7)$$

$$(N_3^-)^* + N_3 \longrightarrow 3N_2 + 2\square + e \quad \ldots\ldots \quad (8)$$

The electrons produced in (6) and (8) are trapped by anion vacancy pairs to form F_2^+-centres which then react to form Na atoms. The net result being:

$$Na_n + 2e + 2Na^+ \longrightarrow Na_{n+2} \ .$$

The effect of different wavelengths on the photolysis of sodium, potassium, barium, lead and silver azides has been investigated by Verneker (52). The rate of photolysis of sodium, potassium and barium azides became constant after a deceleratory reaction followed by an acceleratory reaction when light of wavelengths 1849 Å + 2537 Å was used. Silver azide showed an acceleratory reaction only when light of wavelengths between 2000 Å - 3000 Å was used. Lead azide showed no acceleratory reaction when light of either 1849 Å + 2537 Å or 2000 Å - 3000 Å was used.

Positive nitride tests were obtained when the products of photolysed sodium, potassium, barium and silver azides were tested.

On filtering light of wavelength 1849 Å, the acceleratory reaction was removed from sodium and barium azides. Filtering the light did not change the photolytic curve of potassium azide.

The decrease in photolytic rate was thought, as before, to be due to consumption of defects. The fact that it did not decrease to zero was explained by photo-emission from metal specks produced through consumption of defects.

To explain the acceleration the value of the work functions were considered for all the metals of the salts studied. It was concluded that photo-emission was possible from these metals if light of wavelength 1849 Å + 2537 Å was used for photolysis. But since no acceleration was observed with light of wavelength 1849 Å + 2537 Å in lead and silver azides the ionization potentials of the metal atoms were thought to be important. This would account for the loss of electron release from lead and silver azides. The nitrides of sodium, potassium and silver all showed acceleratory reactions when irradiated with light of wavelengths ranging from 2000 Å - 3000 Å, thus it was proposed that the acceleration observed is due to photodecomposition of the nitride.

Caesium and rubidium azides have been subjected to ultraviolet photolysis by Jacobs and Tariq Kureishy (53). The rate of photolysis of rubidium azide resembled that of potassium azide viz a constant rate after an initial decay and acceleratory reaction. Caesium azide showed an initial decrease in rate followed by a brief constant rate period after which the rate decreased once more before becoming constant again.

It was suggested that three mechanisms were responsible for the rate-time curves. The first two mechanisms as proposed for barium azide by Jacobs and coworkers (40), was thought to be valid. A third mechanism was proposed in addition which involved the reaction of excitons and excited azide ions at metallic nuclei, with the formation of N_4^- ions. The observed dark rate was thought to be due to thermal decomposition of N_4^- ions. The following mechanism was proposed for the acceleratory reaction (the third mechanism of photolysis) :

$$N_3^- \overset{h\nu}{\rightleftharpoons} N_3^{-*} \quad \text{(exciton)}$$

$$M_n \overset{h\nu}{\rightleftharpoons} M_n^+ + e \quad (M_n = \text{metal nucleus})$$

$$N_3^- \overset{h\nu}{\rightleftharpoons} (N_3^-)^* \quad \text{(excited azide ion)}$$

$$(N_3^-)^* + M_n^+ \longrightarrow N_3M_n$$

$$N_3^{-*} + N_3M_n \longrightarrow M_n + N_4^- + N_2 + \boxminus \text{(anion vacancy)}$$

$$M_n + M^+ + e \longrightarrow M_{n+1} .$$

Recently the photolysis of lithium azide pellets has been investigated by Prout and Sears (54) in the temperature range -60^o to 20^{o}C. A high pressure mercury arc of 100 W was used as the source of ultraviolet light. A plot of pressure of nitrogen gas evolved against time was found to be sigmoid in shape. The acceleratory reaction obeyed the Avrami-Erofeyev equation with the exponent n taking the value 3, while the decay reaction was fitted by the equation log α = kt + c.

Activation energies were calculated and found to be 816 cal.mol.$^{-1}$ and 852 cal.mol.$^{-1}$ over the temperature range -60^{o}C to -30^{o}C. Over the temperature range -20^o to 20^{o}C activation energies of 1000 cal.mol.$^{-1}$ and 1050 cal.mol.$^{-1}$ for the acceleratory and decay reactions respectively were found. Both the rate of the acceleratory and decay reactions were found to be dependent on the square of the light intensity. This led to the proposal of the following mechanism :

$$N_3^- \overset{h\nu}{\rightleftharpoons} N_3^{-*}$$

$$N_3^{-*} + \boxminus \longrightarrow (N_3 \boxminus)^{-*} .$$

These entities react on neighbouring sites as follows:

$$2(N_3\boxminus)^{-*} \longrightarrow (N_3\boxminus_2N_3)^{2-*}$$

$$(N_3\boxminus_2N_3)^{2-*} \longrightarrow 2N_3 + 2e\boxminus$$

$$2N_3 \longrightarrow 3N_2 + 2\boxminus$$

where $e\boxminus$ is an F-centre,

N_3^{-*} is an excited azide ion

and $\boxminus$ is an anion vacancy.

Lithium metal forms via the reaction

$$2Li^{+} + 2e\boxminus \longrightarrow 2Li + 2\boxminus .$$

Pre-irradiation with γ- or X-rays caused a decrease in the acceleratory reaction but did not markedly change the decay reaction. This was thought to be due to F-centre formation by the γ- or X-rays thus decreasing the concentration of vacancies - the propagating entity in the acceleratory reaction.

(iv) The photolysis of other inorganic compounds

In the study of the photolysis of silver halides the mechanism of decomposition has been based on the Mott Principle (4, 25). It was postulated that the absorption of energy occurred principally within the volume elements of the substructure of the silver halide crystal, with the subsequent photochemical change taking place at the surface through secondary effects, resulting in the formation of either excitons or pairs of electrons and positive holes. Due to their mobility they can decay transfering their energy to lattice vibrations or by either interacting with photons to dissociate into free electrons and positive holes or interacting with atoms, ions or molecules on the bounding surfaces of the volume elements of the substructure of the silver halide crystal and so produce a photochemical change.

With the photolysis of silver bromide the excitons are postulated to transfer their energy at room temperature to bromide ions occupying either kink sites on the free surfaces of the crystal or jogs along edge dislocation lines on kink sites associated with internal surfaces, to eject electrons from them. This results in the formation of bromine atoms. Owing to the small range of the electron it can possibly combine with an adjacent silver ion which represents a localized excess

positive charge. From the Frank-Condon Principle it was deduced that the probability of an electron being immediately trapped by silver ions on the surface is small. Thus the silver ion can diffuse from the bromine atom to an adjacent subboundary. It may then combine with the electron to form a silver atom. This separation of bromine atoms and silver ions can only occur when the bromine atoms diffuse to the surface and escape, without combining with previously separated silver atoms.

If free electrons and positive holes are created directly by the absorption of light then the mechanism for photolysis has been postulated to be similar to the above mechanism. The holes would be trapped by bromide ions, prior to electrons being trapped by silver ions, producing bromine atoms at the free surface or on internal surfaces. The silver ions with positive charge can now combine with electrons.

The quantum yield of bromine production at various wavelengths and temperatures during the photolysis of silver bromide, has been investigated by Luckey (26). He found an increase in quantum yield with decrease in wavelength and a decrease with increase in temperature. Irradiations with short wavelengths was thought to produce a higher concentration of positive holes and electrons than irradiation with long wavelengths of light. Since the quantum yield was high it was concluded that recombination cannot occur at short wavelengths. This increase in yield has been attributed to increased absorption of the incident radiation at the surface with decrease in wavelength, since most absorption which is effective in producing gaseous bromine occurs in a layer of 0,3μ. High yields at long wavelengths was only observed with thin crystals with thickness comparable with that of the active layer. With increase in temperature of irradiation there is a decrease in the stability of the trapped electrons thus leading to decreased quantum yields,

the decrease being most marked at short wavelength. At short wavelengths the concentration of holes and electrons, already large, is increased by increase in absorption coefficient with temperature. Thus the number of electrons in shallow traps at short wavelengths would be larger than those at long wavelengths resulting in the rate of recombination of bromine to increase and a decrease in yield.

In the study of photolysis of lead halides (27) the absorption of a photon has been assumed to lead to the production of an electron-hole pair. Due to this assumption three modes of photolysis have been postulated:

i) transport and trapping of photogenerated electrons and holes - colour centre mode,

ii) transport of ionic motion at room temperature irradiation - print out mode, and

iii) the substance is completely evaporated from the surface - photo-enhanced evaporation mode.

Holes generated photolytically in $PbBr_2$ are trapped at surface bromide ions forming bromine atoms which are desorbed either directly or after combination with other halogen atoms to give halogen molecules, the rate of desorption being dependent on ambient conditions. Anion vacancies remaining are transported through the crystal resetting bromide ion sites at the surface for subsequent trapping of a hole and desorption of bromine. Aggregates of lead atoms are formed by Pb^{2+} ions trapping electrons produced by the photons. Monovalent cation impurities have been found to increase the rate of photolysis owing to anion vacancy production (28). This increase in rate is due to the mass transport current of anions to the surface by anion vacancies. The enhanced anion vacancy concentration is accompanied by a reduction of cation vacancy, $V_{Pb^{2+}}$ concentration. Since $V_{Pb^{2+}}$ are shallow traps for

holes, the reduced concentration increases the hole current to the surface. Also annihilation of anion vacancies supplies room for the lead nuclei since lead atoms have a larger radius than lead ions.

A transition from one mode of photolysis to another has been observed during the photolysis of $PbCl_2$ (29), the mechanism operating during photolysis being dependent on ~~temperature~~ intensity of irradiation. At low light intensities holes are trapped at surface halogen ions which can be desorbed. The excess metal condenses inside the crystal (print-out mode). At higher intensities there is an increase in photolysis. Complete $PbCl_2$ molecules are desorbed from the surface (photo-enhanced evaporation mode). This change in photolytic mechanism at high intensity has been explained by Levine (30). A potential barrier, set up at the surface by trapped holes, causes the acceleration of photogenerated electrons towards the surface. The electrons will not reach the surface when their lifetime is shorter than the transit time to cross the barrier. This transit time is reduced with increase in intensity of radiation. When electrons produced during the photolysis of $PbCl_2$ cross the potential barrier and become trapped at surface states connected with Pb^{2+} ions (Pb^{+} states (31)) recombination centres for holes and electrons may form. Pb^{+} states have been identified from e.s.r. measurements during irradiation with ultraviolet light at liquid nitrogen temperatures (32).

When molecular-like structure between a Pb^{+} state and a Cl atom (formed by a hole trapped at a neighbouring Cl^{-} state) is formed, surface breakdown by evaporation occurs.

The intensity dependence of photolysis for $PbBr_2$ and $PbCl_2$ was found to be a function of irradiation time. For $PbBr_2$ the rate was proportional to intensity for irradiation times shorter than one second. At low intensity values the rate of photolysis of $PbCl_2$ was proportional

to $I^{0,17}$ and $I^{3,2}$ (29) at high intensities.

From the ionic conductivity of $PbBr_2$ (27) and $PbCl_2$ (29) and from samples doped with cation impurities (27) it was concluded that the anion vacancies are the dominant mobile lattice vacancy.

Using ultraviolet light centred around 5000 Å for the photolysis of PbI_2 mobile excitons are thought to be created near the surface. The rate of photodecomposition was found to vary as the square of the light intensity indicating that photolysis is a bimolecular process in which two excitons are trapped at anion vacancies situated at surface imperfections (such as surface kink sites at the edges of crystals and at the edges of cracks in crystals) to give an iodine molecule, two electrons and two anion vacancies. This interaction with imperfections leads to the production of both charge separated carriers forming a positive hole and an electron which can be trapped at an anion vacancy to form an F-centre. When two such positive holes react a molecule of iodine gas is formed. If the F-centres are stable at the temperature of decomposition aggregation of such centres will lead to the formation of metallic nuclei, but when the F-centres are unstable two electrons are trapped by lead ions to form lead atoms. Lead nuclei have been postulated to grow by two mechanisms depending on temperature. At high temperatures excitons decompose into electrons and positive holes causing the growth of lead nuclei to proceed via alternate trapping of interstitial lead ions and pairs of electrons. At low temperatures there is a transport of neutral excitons rather than charged lattice ions. Pairs of excitons decompose at a surface adjacent to a nucleus of lead.

An activation energy of 4 Kcal.mol.$^{-1}$ was obtained for photolysis of PbI_2 and thought to be related either to the reaction of two excitons or for the diffusion of iodine molecules through a surface layer.

The importance of anion vacancies in photolysis of PbI_2 has been verified by the increase in rate of samples doped with Ag^+ ions.

Photodecompositions have been carried out on several perchlorates. Photolysis of nitronium perchlorate (34), using a high pressure lamp, yielded O_2 and NO identified by mass spectrometry methods. The rate of evolution of gas reached a finite constant value with time after an initial acceleration and decay. The rate of gas evolution at all stages was found to be proportional to the square of the light intensity. The acceleratory and decay reactions were thought to be dependent on the existence of impurity trapping centres. After total consumption of these centres the reaction dies out and a second process continues independent of trapping centres. During acceleration excitation of a ClO_4^- ion in the vicinity of an electron acceptor trap (T) causes a transfer of the electron to the trap

viz $$ClO_4^- \overset{h\nu}{\rightleftharpoons} (ClO_4^-)^* \overset{T}{\rightleftharpoons} (T\,ClO_4^-)^* .$$

The bimolecular rate determining step proposed is :

$$(ClO_4^-)^* + (TClO_4^-)^* \longrightarrow T + Cl_2 + 4O_2 + 2e .$$

The free electrons are absorbed by NO_2^+ ions :

$$2NO_2^+ + 2e \longrightarrow 2NO_2 + 2 \text{ vacancies.}$$

Thus the trap is associated with two anion vacancies and cannot participate as before, causing a decrease in photolytic rate. The NO_2 produced may be photolysed directly by incident radiation, may evolve as a gas or remain as an impurity in the crystal lattice. The activation energy for this mechanism was found to be 9 Kcal.$mol.^{-1}$.

The second process taking place simultaneously with the above process has no self consuming features and can be represented by

$$NO_2^+ \overset{h\nu}{\rightleftharpoons} (NO_2^+)^*$$

$$ClO_4^- \rightleftharpoons^{h\nu} (ClO_4^-)^*$$

$$(NO_2^+)^* + (ClO_4^-)^* \longrightarrow NO + ClO + 2O_2 \quad \text{-bimolecular decomposition.}$$

The kinetics of gas evolution from anhydrous silver perchlorate (35) using a low pressure lamp has been studied by Verneker and Maycock. As found with nitronium perchlorate the rate became constant after an initial acceleration and decay. The rate of evolution of oxygen at all stages of the reaction was found to be proportional to the first power of intensity of radiation.

A mechanism for the acceleratory reaction was postulated to involve the production of a defect centre:

$$ClO_4^- + \boxed{\ } \xrightarrow{h\nu} ClO_4^{\,o} + \boxed{e}$$

$$ClO_4^{\,o} \longrightarrow \text{products} + \boxed{\ }$$

$$Ag^+ + \boxed{e} \longrightarrow Ag^o + \boxed{\ } \ .$$

For the deceleratory reaction a mechanism involving consumable trapping centres was postulated. These centres were concluded to be anion vacancies since samples doped with SO_4^{2-} ions showed an increase in the maximum rate. Thus the defects created during acceleration must be anion vacancies. Since the deceleratory reaction did not decrease to zero but became a finite constant value a new mechanism, not involving consumable trapping centres, was thought to become active. The activation energy for this process was found to be 4,5 Kcal.mol.$^{-1}$ and has been associated with photo-emission of electrons from silver metal formed during the initial acceleration.

Thus the process

$$Ag_m^o \xrightarrow{h\nu} Ag_m^+ + e$$

$$Ag_m^+ + ClO_4^- \longrightarrow Ag_m^o + ClO_4^o$$

$$ClO_4^o \longrightarrow \text{products}$$

$Ag^o_m + Ag^+ + e \longrightarrow Ag^o_{m+1}$ can take place.

Ag^o_{m+1} represents the growth of colloidal metal.

The photolysis of sodium bromate has been investigated by Herley and Levy (36) using a high pressure mercury lamp. The rate of evolution of oxygen at 300^oK was found to decrease during the first 100 minutes of the reaction and then reach a constant rate. This constant rate period deviated slightly from a second order dependence on light intensity. (The rate depended on $I^{1,8}$). A phenomenological theory was proposed to account for the photochemical decomposition. A steady state rate equation was derived with the assumptions that:

i) photolysis is essentially a solid state electronic process including charge trapping; sites generated (by precursors such as impurities) or destroyed; sites rendered inactive by precursors, etc. and

ii) photolytic decomposition occurs when an unspecified crystal defect acquires a second excitation after having first acquired an initial excitation.

The rate equation represented, in algebraic form, the most general rate equation that could be obtained from these assumptions. A tentative mechanism was proposed involving excitons since photoconductivity was not detected. These excitons have been thought to be mobile electron-hole pairs or stable excitons. The mechanism involves the

generation of new decomposition sites from existing sites, with the centres generating the new sites maintaining their initial characteristics. A sequence of decompositions taking into account an overall bimolecular character was proposed.

The photolysis of potassium permanganate, in the form of small crystals (approximately 250 μm), powdered crystals (particle size: 40 μm in diameter) and pellets (5 mm in diameter and made under a pressure of 2000 lb/sq.in.) has been investigated by Prout and Lownds (37). A high intensity ultraviolet source which transmitted light of mainly 2537 Å was used. Photolysis was confined to the temperature range 20^{o} - 180^{o}C.

The pressure-time plots for the photolysis of whole crystals and powder exhibited an initial puff followed by a short acceleration and a decay lasting longer than 400 min. The decay period of photolysed pellets passed into an extended region where the gas was evolved at a constant rate. The volume of gas liberated was found to be proportional to the area of salt being irradiated.

Photolysis was thought to be confined to a surface layer and penetration of reaction was estimated to be equivalent to approximately 1000 unit cell layers for the pellet after 400 min. of photolysis.

It has been thought that the acceleration is associated with excitation of MnO_4^- ions at defect surfaces with excitation proceeding until the ion dissociates thermally. Reaction then proceeds in a linear branching manner across the surface, reaction being favoured at the leading reactant-product interface by the strain induced by the product in the original lattice. The decay reaction takes place at less reactive sites on the surface which are being steadily consumed during photolysis.

The intensity dependence of the photolytic rate was found to be proportional to $I^{2,83}$ at 80,0^{o}C and $I^{2,03}$ at 140,0^{o}C. A mechanism was postulated in which either three photons (at 80,0^{o}C) or two photons

(at 140,0^{o}C) are required to raise the energy of the permanganate ion to a level at which the excited ion dissociates thermally.

Activation energies of 4,5 Kcal.mol.$^{-1}$ and 13,6 Kcal.mol.$^{-1}$ were found over the temperature ranges 20,0^{o} - 110,0^{o}C and 120,0^{o} - 180,0^{o}C respectively. These activation energies were concluded to be associated with the thermal dissociation of the excited ions.

1B THE THERMAL DECOMPOSITION OF SOLIDS

The majority of thermal decompositions which have been studied are of the type

$$A_{(solid)} \longrightarrow B_{(solid)} + C_{(gas)} .$$

As with the study of the photolysis of solids, a convenient way of following a thermal decomposition is to measure the pressure of the gas evolved at specified time intervals. The general features of the curve are illustrated in Fig. 1, although any of these features may be absent in specific cases. Features of the decomposition curve include (i) an initial rapid evolution of gas, represented by A followed by (ii) an induction period (represented by B) in which gas may or may not be evolved,

(iii) an acceleratory period following the induction period (shown in C) and

(iv) a decay reaction represented by D.

Boldyrev (62) divided thermal decompositions into two groups viz (i) thermal decomposition taking place via bond cleavage in an anionic or cationic lattice component and accompanied by no transfer of charge. This mechanism depends mainly on defects on the surface and along lines (edge or screw dislocations).

(ii) Decomposition proceeds via the transfer of electrons from an anion to a cation and is mainly dependent on point defects (vacancies, interstitials, impurity atoms, excitons, free electrons and holes).

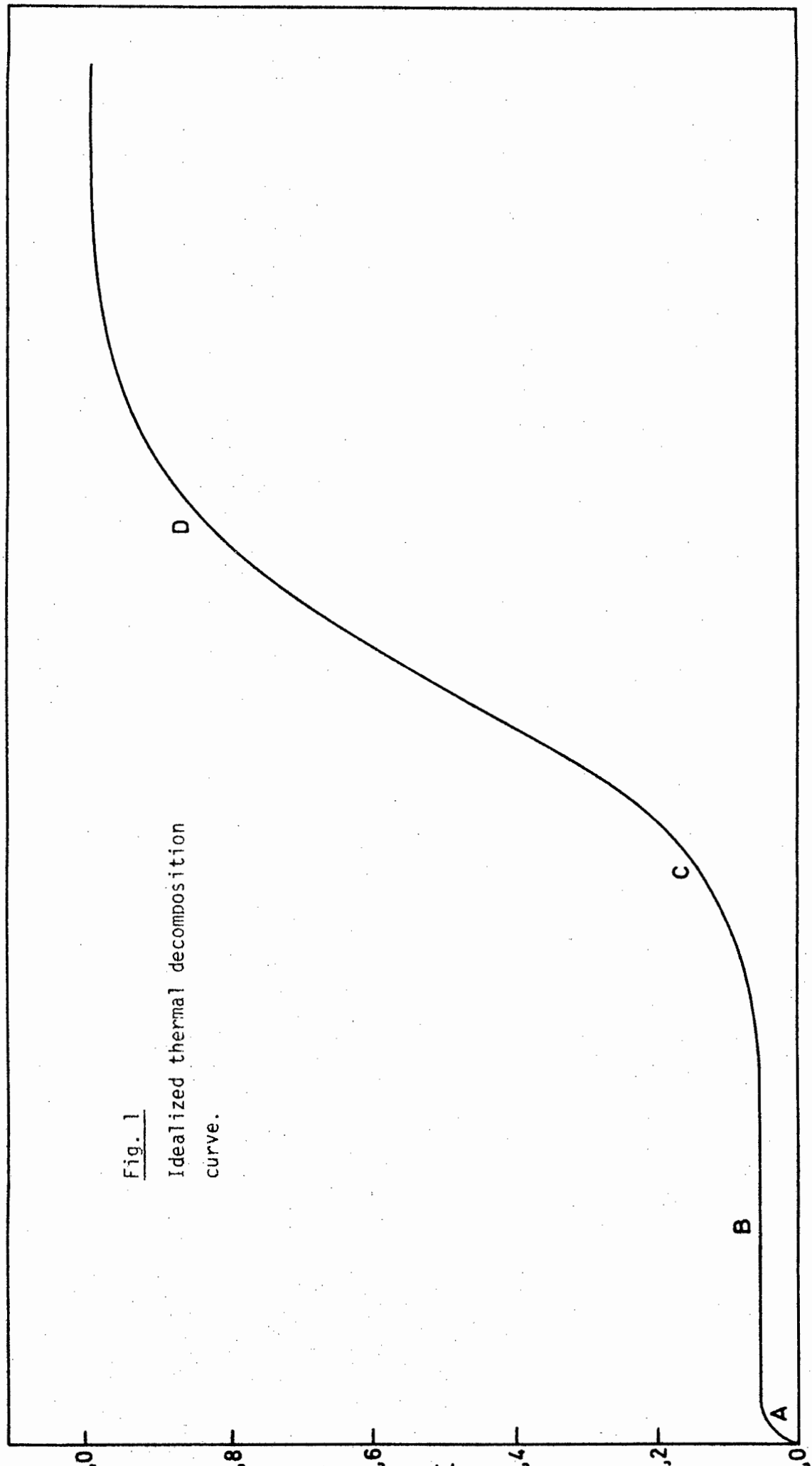

Fig. 1

Idealized thermal decomposition curve.

In either case but in the first to a lesser extent, the electronic environment at the site of decomposition of an individual molecule will influence the activation energy of its decomposition.

Line defects play an important part in the thermal decomposition of solids since reaction commences at the point of emersion of dislocations at the crystal surface and at the boundaries of the groupings (43, 63, 64, 65). The emergence of edge dislocations, bent crystals, twisted crystals, incipient cleavage cracks, and similar families of edge dislocations at the surface of crystals of platinum phthalocyanine has been observed by Menter (134). The concentration of these line defects is dependent on the age of the crystal, thus the rate of thermal decomposition being dependent on age. With age formation of groupings of dislocations is annihilated. The thermal decomposition of carbonates (66) and the azides (67, 68) have been shown to be favoured at dislocations.

The scheme of charge transfer in the thermal decomposition of ionic solids was originally postulated by Mott (22) to be the capture of an electron from the conduction band of the crystal by an impurity centre with the subsequent occurrence of contraction process toward the capture site of interstitial ions and electrons, and the decomposition of a positive hole, formed as a result of the breaking away of an electron from an anion of the radical, after its escape to the surface of the crystal. This scheme has been used to explain topochemical processes accompanied by charge transfer, and has value in many cases at the present time, although, as in the case of mechanisms proposed for photolysis, changes and additions have been made.

Charge transport within an ionic lattice is dependent on the defect structure of the solid and is achieved by ionic conductivity i.e. migration of ions. Ionic conductivity through the crystal results

through migration of either interstitials or by the counter migration of vacancies. Migration rates, for both the interstitial and vacancy mechanisms, depend directly on the concentrations of these point defects. The result of ionic mobility is the migration of product atoms or molecules through the lattice.

Semiconductivity can also influence charge transport in crystals. Intrinsic semiconductivity results when electrons in the valence band are thermally excited to the conduction band leaving behind positive holes in the valence band. Extrinsic semiconductivity is due to impurities which act either as acceptors or donors of electrons. The energy levels of these donors and acceptors lie in the forbidden energy gap near the conduction and valence bands respectively. Promotion of an electron from a level within the forbidden zone into the conduction band is n-type semiconductivity; p-type semiconductivity arises from the demotion of a positive hole from the forbidden band into the valence band. Of particular relevance to solid decompositions is the type of semiconductivity described by Boldyrev, London and Zhuravlev (70), where the product phase, if it has a work function different from that of the reactant will act as an electron donor or acceptor, depending on the relative values of the work functions.

Exciton formation during thermal decomposition results through thermal excitation of an electron to a non-conducting excited state or alternatively from the partial combination of an electron and a positive hole, without reversion to the electronic ground state. As discussed under photolysis, where they play a more significant role, excitons are mobile and can dissociated into free electrons and positive holes, thus aiding charge transport.

A characteristic feature of the thermal decomposition of solids is the initiation and propagation of the reaction from a number of

preferred sites termed nuclei formed at the above mentioned imperfections in the lattice (either at the surface or in the bulk of the reactant matrix) since the activation energy of decomposition is lowest at these sites.

Many workers have obtained photographs showing discrete, non-random nucleation on crystal surfaces. It has been observed from these photographs that the nuclei form in the regions of emergence of dislocations and grain boundaries on the crystal surface. For example this has been shown by Herley and Levy (83, 84, 85, 86) to occur during the thermal decomposition of ammonium perchlorate.

The nature of these nuclei is not always clear but they are thought to be composed of solid reaction products. Movement of reaction through the lattice is due to strain produced by differences in physical properties between product and parent phases. Chemical transformation is facilitated at defects on the internal and external surfaces of the crystal because both the chemical potential and stereochemical environment of ionic species in the immediate vicinity of these points differ from those of similar species at "ideal" lattice sites.

Nuclei are classified either as compact or diffuse. The latter are spread throughout the solid and are not directly observable since they do not grow to a visible size. An example of this occurs in the thermal decomposition of mercury fulminate (71).

Compact nuclei are directly observable and are generally favoured since the activation energy for nucleus growth is less than that for nucleus formation. They have characteristic shapes dependent on the physical properties of the solid. In sodium azide pellets (72) they were observed to be two-dimensional and approximately circular, and

were formed on preferred crystallographic faces. Spherical nuclei have been observed in the thermal decomposition of barium azide (24) and horn-shaped nuclei in the dehydration of copper sulphate pentahydrate (69).

The number of nuclei formed during thermal decomposition can be increased by the pre-reaction treatment of the sample, thereby increasing greatly the number of potential nucleus forming sites, for example grinding (73, 74) or scratching of the crystal surface (75). Pre-irradiation of the solid prior to decomposition with ionizing radiations (γ- and X-rays (76 - 79)), ultraviolet light (23), electrons (80) or reactor radiation (81, 82) has generally been found to enhance the subsequent thermal decomposition of the solid as a result of the formation of crystal defects and deposition of radiolysis products in the crystal lattice.

The induction period (B Fig. 1) is considered to be the time during which nucleus formation takes place. At the end of the induction period the production of nuclei is at a critical stage, and the reaction becomes autocatalytic during the acceleration. At the end of the induction period the crystal is a function of the number of nuclei and their spatial distribution, the size and shape of the nuclei and a variety of properties of the nuclei themselves e.g. their chemical, crystallographic and electronic structure. Growth of these nuclei takes place during the acceleration, although some nucleus formation may also occur during this stage of the reaction.

Beyond the inflection point the decay stage begins. Nucleus growth ceases and the rate of reaction decreases when the nuclei have expanded far enough to begin to overlap and thereby decrease the interfacial area between the reactant and product.

The mechanism of a particular decomposition and the kinetic equation which will describe the acceleration of the reaction will be dependent upon two features viz : the rate of nucleus formation and the rate and mode of growth of the nuclei.

Nucleation can involve either a single step and can then be described as a linear or exponential function of time, or involve multiple steps and then be described as a power of the time. A linear increase in nuclei with time has been observed with the dehydration of copper sulphate dihydrate (69). Photographs of nucleation in ammonium perchlorate crystals have been obtained by Herley, Levy and Jacobs (83, 84, 85, 86). They observed discrete nuclei on the surface of the crystal in preferred crystallographic directions, the nuclei being different on different crystal faces. It appeared that once the nuclei had reached a critical size growth stopped during which time the smaller nuclei continued to grow until they too had reached the critical size. Once decomposition over the external faces was complete nucleation on the subsurfaces was observed.

The kinetics of simultaneous nucleus formation and nucleus growth, or the growth of a constant number of nuclei i.e. the acceleratory region can be described by the following mathematical relationships: (i) power law,

(ii) exponential law,

(iii) the Prout-Tompkins equation and

(iv) the Avrami-Erofeyev equation.

If nucleation proceeds according to a power law, and if it is assumed that nucleus growth is constant, it can be shown that (4)

$$p = kt^n \quad \ldots\ldots\ldots\ldots \quad (1)$$

where p is the gas pressure at time t during an isothermal decomposition,

k is the rate constant

and $n = \beta + \lambda$ where β is an integer representing the number of successive molecular decompositions at a single site required to form a stable growth nucleus; λ has values 1, 2 or 3 depending on whether the nuclei grow 1-, 2- or 3-dimensionally i.e. linear, plate-like or spherical.

In the derivation of the equation overlap of the growing nuclei has been neglected.

The power law can be applied to the acceleratory reaction in the form $p^{1/n} = kt$, thus enabling the determination of the rate constant for the reaction. The equation has been found most useful since it dispenses with the knowledge of the final pressure. The acceleratory reaction of the thermal decomposition of lithium (87), calcium (88) and strontium (89) azides have been analysed using the power law with n = 3. It has also been applied to zinc oxalate (90) with n varying between 1 and 2. Wischin (24) deduced a value of n = 6 corresponding to spherical nuclei increasing in number as the cube of the time in the thermal decomposition of single crystals of barium azide.

The exponential law takes into account constant rate of nucleation, growth of nuclei and branching chains and was derived by Garner and Hailes (71). It has been applied in the form

$$p = c \exp(kt) \quad \ldots\ldots\ldots \quad (2)$$

where c = constant and is a function of temperature and contains the constants for nucleation, growth and branching.

Although it has been applied to the decomposition of mercury fulminate and large crystals of lead styphnate (91), the concept of propagation of linear chains through the crystal and hence a division

of the crystal into mosaic blocks resulting in slow decomposition, was not thought to be a favourable mechanism. Thus a modification postulating the propagation of branching plate-like nuclei through the crystal (92), was made to the theory. This idea was applied to silver oxalate (93) and it was suggested that decomposition proceeded along grain boundaries and dislocation lines, with branching occurring at intersections of these defects in the crystal lattice.

Interference between these branching nuclei has been considered by Prout and Tompkins (94) which is a modification to the theory of the exponential law. Thus a term for the probability of chain termination was introduced into the equation formulated by Garner and Hailes (71) for linear branching chains. The Prout-Tompkins equation was obtained on integrating the equation derived to represent the rate of decomposition $d\alpha/dt$ and has the form

$$\log(p/p_f - p) = kt + c \quad \ldots\ldots\ldots (3)$$

where p is the pressure at time t,

p_f is the final pressure

and k is the branching coefficient.

It has been applied to the thermal decomposition of unirradiated and pre-irradiated permanganates (95) as well as the co-irradiated decomposition of potassium permanganate (96). In addition the equation has been used for the analysis of the entire thermal decomposition of nitronium perchlorate (97) and lead oxalate (78); and the acceleratory reactions of potassium metaperiodate (99), lithium perchlorate (100) and pre-irradiated ammonium perchlorate (98).

The equation was modified for the thermal decomposition of silver permanganate (101). In this case the branching coefficient was not assumed to be constant but to vary inversely with time. Thus the

equation became

$$\log(p/p_f - p) = k't + c' \quad \ldots\ldots\ldots\ldots\ldots\ldots \quad (4)$$

The Avrami equation takes into account the effects of ingestion of potential nucleus forming sites by growing nuclei or the overlapping of such nuclei. Avrami (102) in a mathematical study of the kinetics of phase changes analysed reaction-time curves using the concept of a random nucleation process at potential nucleus forming sites, followed by nuclear growth. The potential nucleus forming sites were termed "germ nuclei" and those which became active and started growing were termed "grains" or "growth nuclei". "Phantom nuclei" were the sites ingested by growing nuclei thus never becoming active.

He developed an equation which represented a general solution to the problem of random nucleation followed by three-dimensional growth. It had the form:

$$-\log(1-\alpha) = \frac{6SN_o\, k_2'^3}{V_o\, k_1'^3}\left[e^{-k_1't} - 1 + k_1't - \frac{(k_1't)^2}{2!} + \frac{(k_1't)^3}{3!}\right] \ldots.(5)$$

where S = shape factor,

V_o = final volume of product obtained from complete decomposition of reactant,

N_o = total number of germ nuclei at time $t = o$,

k_i' = constant

and α = fractional decomposition = p/p_f.

Several limiting cases were obtained from this equation. When α is small the contribution of overlapping and phantom nuclei were considered to be negligible and the general equation reduces to the power law i.e.

$$\alpha = ct^n \quad \ldots\ldots\ldots\ldots\ldots\ldots\ldots\ldots\ldots\ldots \quad (6)$$

where n has the same meaning as before.

In particular n = 4 corresponds to random nucleation of three-dimensional nuclei, n = 3 corresponds to instantaneous nucleation followed by three-dimensional growth and n = 2 corresponds to linear growth.

When t is large i.e. in the decay period, the general equation reduces to

$$-\log(1-\alpha) = \left[SN_o\, k_2'^3/V_o\right]t^3 \quad \ldots\ldots\ldots\ldots (7)$$

$$= kt^3 \quad \ldots\ldots\ldots\ldots\ldots\ldots (8)$$

Using a different approach Erofeyev (103) first derived a general kinetic equation

$$\alpha = 1-\exp\left(-\int_0^t p\,dt\right) \quad \ldots\ldots\ldots (9)$$

$$\text{or} \quad -\log(1-\alpha) = \int_0^t p\,dt \quad \ldots\ldots\ldots\ldots\ldots (10)$$

α = fractional decomposition

and p = probability of the reaction of an individual molecule in an interval dt.

The equation was then applied to the formation and growth of nuclei in the solid state. He obtained the equation

$$\alpha = 1 - \exp(-kt^4) \quad \ldots\ldots\ldots\ldots (11)$$

corresponding to three-dimensional nuclei increasing in number at a constant rate. For cylindrical nuclei

$$\alpha = 1 - \exp(-kt^3) \quad \ldots\ldots\ldots\ldots (12)$$

and for flat nuclei

$$\alpha = 1 - \exp(-kt^2) \quad \ldots\ldots\ldots\ldots (13)$$

Thus in general according to the shape of the nuclei and their rate of increase

$$\alpha = 1 - \exp(-kt^n) \quad \ldots\ldots\ldots (14)$$

or $$-\log(1-\alpha) = kt^n \quad \ldots\ldots\ldots\ldots\ldots (15)$$

which is of the same general form as derived by Avrami. Equations 7, 8 and 15 are the general equations for the kinetics of reactions which proceed by way of formation and growth of reaction nuclei in a solid. These equations are known as the Avrami-Erofeyev equation.

The Avrami-Erofeyev equation has been found to be versatile because of the variable n. Using the equation with n = 3 it has been applied to the acceleration of sodium nitrate (104). The acceleratory reaction of barium azide (68), ammonium perchlorate (105) and silver oxalate (106) have been described using this equation with n = 4.

During the decay reaction contraction of the area of the interface between the reactant and product phases takes place. In certain cases the product phase may catalyse the reaction as a result of intimate contact between the two solid phases. Topokinetic equations applicable to the decay therefore describe a contracting envelope of product enclosing a volume of reactant which is free of defects such as dislocations, since these represent sites of preferential decomposition, and are usually consumed by the product during the acceleration.

Analysis of the decay may be achieved using the Avrami-Erofeyev equation in the form

$$\alpha = 1 - \exp(-kt^3) \quad \ldots\ldots\ldots (16)$$

This equation is only applicable when the interface remains intact. Thus the value of n is necessarily 3 since in the decay stage ingestion of potential nucleus forming sites will be virtually complete. However this situation is not always the case since strain produced by differences in the molecular volumes of parent and product phases produces a collapse of the interface thus leaving isolated blocks of reactant containing no nuclei in which the rate of reaction is proportional to the amount of substance undecomposed.

Hence $$d\alpha/dt = k(1-\alpha) \quad \ldots\ldots\ldots\ldots \quad (17)$$

$$\therefore \quad -\log(1-\alpha) = kt \text{ (unimolecular law)} \ldots \quad (18)$$

or $$\log(p_f/p_f-p) = kt \quad \ldots\ldots\ldots\ldots\ldots \quad (19)$$

The decay reaction was considered by Prout and Tompkins (94) to be proportional to the number of unreacted molecules i.e. proportional to (p_f-p). Also only those molecules adjacent to product molecules will be able to decompose. Thus the rate of reaction is

$$dp/dt = k(p_f-p)P \quad \ldots\ldots\ldots\ldots \quad (20)$$

where P is the probability of the favoured situation and is determined by $\alpha = p/p_f$. Thus

$$dp/dt = k(p_f-p)p/p_f \quad \ldots\ldots\ldots \quad (21)$$

Integration between limits led to the equation

$$\log(p/p_f-p) = kt + c \quad \ldots\ldots\ldots\ldots \quad (22)$$

which is the Prout-Tompkins equation as found for acceleratory reactions except that the two rate constants, k, are different.

An examination of the topological change of a contracting envelope with time leads to several possible kinetic equations for the description of the decay stage. An example of this is the contracting sphere equation. This equation describes the rate of penetration of the product interface into particles which have become coated with a layer of product in the early stages of the reaction. It has the algebraic form

$$1 - (1-\alpha)^{1/3} = kt \quad \ldots\ldots\ldots\ldots (23)$$

Other shapes of contracting interfaces are for example a contracting parallelopiped, or rectangle, or circle depending on the geometry of both the particles and the interface.

These equations, developed for the decay reaction have, as in the case of the equations for the acceleratory region, been extensively used. The decay reaction of sodium nitrate (104) and ammonium perchlorate (105) have been described using the Avrami-Erofeyev equation with n = 3. The decay stage of lithium perchlorate (100) and pre-irradiated ammonium perchlorate (98) have been described by the unimolecular decay law.

Prout and coworkers have applied the contracting sphere equation to the decay stage of the decomposition of lithium azide (87), calcium azide (88), nickel oxalate (107) and barium azide (68).

When none of the standard equations described above fit the experimental data, empirical equations (82, 105), or a general method for the calculation of rate constants described by Jacobs and coworkers (108) have been used. It must be noted that where an empirical equation is used to describe the kinetics of a particular stage of decomposition, the rate constant has no physical meaning.

It must be noted that the applicability of a particular equation to an actual decomposition should not be regarded as proof of the relevance of the model from which the equation was derived, but rather as a postulate upon which experimentation designed to support this postulate can be based. Also the observed behaviour of a particular solid need not be describable by only one kinetic equation. An example of this is the use of the Prout-Tompkins equation, by Prout and coworkers (94) and the Avrami-Erofeyev equation (n = 4) by Boldyrev (109) to the kinetics of the thermal decomposition of potassium permanganate.

However the theoretical approach to the decomposition kinetics of solids has led to greater understanding of the macro-processes occurring during the reactions, and has also provided equations which yield rate constants. Regardless of their significance these rate constants can be used to investigate the dependence of reaction rate on a variety of experimental variables e.g. temperature of decomposition, size of particles and age or history of the material.

1C THE EFFECTS OF PRE-IRRADIATION WITH ULTRAVIOLET LIGHT ON THE THERMAL DECOMPOSITION OF SOLIDS

Much work has been done in the field of treatment of ionic solids with radiation at room temperature prior to thermal decomposition. This has led to a better understanding of the mechanism of thermal decomposition of unirradiated salts since photo- and thermal processes can frequently be equated. This is especially the case for the processes of nuclear formation and growth in solid state decomposition.

Of particular importance to this work is the pre-treatment of the solid with ultraviolet light. Thus a detailed review of the effect of pre-irradiation of solids with ultraviolet light at room temperature on the subsequent thermal decomposition will be undertaken.

The general effects of pre-irradiation on the subsequent thermal decomposition are:

(i) a shortening of the induction period,

(ii) acceleration of the reaction,

(iii) changes in the activation energies associated with the decomposition process and

(iv) changes in mathematical analyses governing the pressure-time plots, and their extent of fit.

Since thermal decomposition of many inorganic solids has been thought to proceed via an electron transfer it can be concluded, when the effects of the interaction of ultraviolet light on ionic solids is taken into account, that pre-irradiation with ultraviolet light will have a positive effect on the subsequent thermal decomposition. In order to observe the effect of pre-irradiation, irradiation nuclei must create sufficient strain to crack or fracture the solid

and thus create new reactive surfaces.

The inorganic azides were the first class of ionic solids to be subjected to pre-treatment with ultraviolet light, the barium and strontium salts being the initial salts, studied by Garner and Maggs (23). They found that the induction periods of these two azides were shortened in the subsequent thermal decomposition and in the case of barium azide an increase in rate constant in the equation $\alpha = kt^6$ was observed. These workers concluded that the nature of the reaction mechanisms was not markedly affected by pre-illumination with ultraviolet light. They proposed that ultraviolet light produced "holes" and diffusion of metal atoms to these holes resulted in the formation of nuclei, from which the reaction was initiated.

Following this study Thomas and Tompkins (55) studied the effect of high and low doses of ultraviolet light at room temperature on the subsequent thermal decomposition of barium azide. As found by the previous workers, a decrease in induction period and an increase in the rate of the acceleratory reaction was observed. At high irradiation doses the exponent changed from 6 to 3. These results were explained by assuming that with low doses of irradiation there is an increase in the number of potential nucleus forming sites, assumed to be anion vacancies. As the dose increases these sites could become activated by trapping electrons and so relaxing the requirement for thermal activation. In the limit this means that all the potential nucleus forming sites become both activated and equivalent, and accordingly a cubic acceleratory period is obtained.

Prout and Moore (114) found that the Avrami-Erofeyev equation with $n = 4$ fitted the acceleratory reaction of the thermal decomposition of barium azide. With pre-irradiation at room temperature (111) the

exponent changed from 4 to 6. During pre-irradiation it was assumed that a large number of F-centres were formed which, during heating, aggregate and collapse to give barium atoms. These atoms migrate and accumulate at favourable sites (dislocations) to give metal nuclei. The increase in exponent was accounted for by assuming that after irradiation the number of nuclei no longer increase linearly with time but with the cube of the time.

Pre-irradiaiton of potassium azide (74) had no subsequent effect on the thermal decomposition. Following irradiation, evolution of nitrogen was detected. A blue colouration was observed after irradiation which disappeared on heating. The colouration was thought to be due to the formation of F-centres and positive holes. During irradiation mobile excitons are formed and the electron from the exciton can tunnel to a vacant site to form a single entity. A second exciton can then form a complex adjacent to the first resulting in a reaction to give three molecules of nitrogen. Heating presumably reversed this process through the bimolecular combination of electrons from F-centres by the tunnel effect.

Colloidal sodium has been identified from electron spin resonance studies during the thermal decomposition of sodium azide following pre-irradiation with ultraviolet light at room temperature (46). Colloidal sodium was thought to form due to photochemical reduction by irradiation clusters during thermal diffusion. Aggregation took place via vacancy or electron diffusion.

A shortening of the induction period and an increase in the acceleratory rate constant with no effect on the decay constant was observed when lithium azide, pre-irradiated with ultraviolet light, was decomposed thermally (110).

The acceleratory reaction of unirradiated lithium azide was described by the Avrami-Erofeyev equation with n = 3, and thus nuclear growth was considered to be two-dimensional with the number of nuclei increasing linearly with time. The decay reaction was described by the contracting sphere equation. With pre-irradiation the value of n decreased to 2, while the contracting sphere still fitted the decay.

It was supposed that pre-treatment with ultraviolet light produced F-centres as for potassium (74) and barium azides (111). This was concluded since the salt turned a buff colour after irradiation. Collapse of F-centres takes place during heating resulting in lithium atoms and finally lithium metal centres. The change in n from 3 to 2 with pre-irradiation was ascribed to a saturation number of nuclei at the end of the induction period. Thus during the acceleratory period further formation of nuclei would be swamped by the already growing nuclei. The thermal decomposition of pre-irradiated lithium azide thus proceeded via two-dimensional growth of nuclei, growth occurring from a fixed number of nuclei. Since the decay showed little dependence on irradiation it was concluded that the topochemistry of this stage of the reaction was similar to that of the unirradiated material, and after surface nucleation and coverage the product reactant interface moves inwards on the particles of the powder.

By pre-irradiating pellets of equal diameter but varying in weight, the ultraviolet light was found to affect the surface only since thermal decomposition produced the same initial burst of gas irrespective of weight.

Calcium (73, 88, 111) and strontium (23, 111, 112) azides have shown similar results when pre-irradiated with ultraviolet light. Garner and Reeves (112) found that both the unirradiated and pre-irradiated decomposition of calcium and strontium azides could be described

by the power law with n = 3. The fit of the power law was better for the pre-irradiated than the unirradiated decomposition and an increase in rate constant was observed when the sample was pre-irradiated. The nuclei at the end of the induction period of the unirradiated decomposition were assumed to be almost all the same size. Pre-irradiation was thought to cause all the nuclei at the end of the induction period to be the same size hence the better fit of the power law. The increase in rate was concluded to be due to the development of nuclei at dislocation sites which would not have developed during thermal treatment.

Fresh samples of calcium azide (73) showed an increase in rate constant with increase in irradiation dose. The rate constant for aged samples was found to be constant for all doses up to 10^{14} photons/cm^2. The difference was attributed to the activation of excess bulk vacancies in the fresh calcium azide. For the aged material it was supposed that an excess in electrons due to irradiation were captured by surface clusters and these transformed into growth nuclei. In the unirradiated material, the rate was controlled by the slow rate of production of electrons which were always in short supply. In fresh material containing excess grown-in vacancies, pre-irradiation was reported to activate germ nuclei throughout the system. However, Prout and Brown (88) did not find any evidence of this ageing effect for unirradiated calcium azide when kept for a period of four months. They have suggested internal nucleation on pre-irradiating the salt.

Using high ultraviolet doses, Prout and Moore (111) found the pressure-time curves obtained for the thermal decomposition of calcium and strontium azides could be analysed successfully using the power law with n = 2. The point of inflection was found to decrease with increase in ultraviolet dose. It was suggested that surface damage

occurred with two-dimensional nuclei growing linearly with time for high doses of irradiation. The change in n from 3 to 2 when high doses of ultraviolet light were used, was assumed to be due to the high concentration of surface nuclei, due to heavy irradiation doses, and any increase in the number of surface nuclei with subsequent thermal decomposition is virtually "swamped" by the pre-irradiation effect.

The oxalates have been another class of inorganic solids which have been extensively subjected to pre-thermal treatment with ultraviolet light. Prout and Tompkins (113) were the first to study the effect of pre-irradiation on mercuric oxalate. They stated that the pre-irradiated salt decomposed at a higher rate than the unirradiated salt. The acceleratory reaction in the thermal decomposition was replaced by an initial burst of gas followed by a short constant rate period when the pre-irradiated salt was decomposed. A later investigation by Prout and Moore (135) indicated that both the unirradiated and pre-irradiated thermal decomposition could be mathematically represented by the power law with n = 2. They proposed that ultraviolet irradiation produced an unidentified irradiation product, possibly mercurous oxalate, by an electron transfer process which formed and then grew under the action of light on the surface of the mercuric oxalate.

The acceleratory period of the thermal decomposition of unirradiated silver oxalate (115, 116) was described by the power law in the form $\alpha = k(t-t_o)^n$ where $3,5 < n < 4$. It was found that pre-irradiation with ultraviolet light caused an increase in the rate constant with a decrease in the value of n to 3,0. The effects were attributed to the first order formation of certain sites of compact nuclei which grow in three-dimensions, the number of unfertilised sites decreasing as the

ultraviolet dose is increased. The decomposition for silver oxalate has also been postulated (92, 93, 117) to react via a branching chain mechanism. No change in kinetics was found by these workers, other than a change in the pre-exponential factor when the salt was pre-irradiated with small doses of ultraviolet light. Decompositions of single crystals of the unirradiated salt (118) were later observed to follow a cubic law. In later years Haynes and Young (119) have indicated that the exponential law provides the most suitable analysis and explanation of the decomposition behaviour. For the thermal decomposition of pre-irradiated silver oxalate they propose that pre-treatment with ultraviolet light results in an increase in the number of starting points on the surface and these can then develop into growth nuclei with simultaneous decomposition along a line joining two of these nuclei. This explained the use of the exponential equation. Russian workers (120, 121) have concluded that the effect of pre-irradiation on silver oxalate with ultraviolet light is a purely surface one and affects only the initial decomposition.

2 OBJECTS OF RESEARCH

Previous investigations into the photolysis of barium and strontium azides (39, 40, 55, 61) have been confined to temperatures below 25,0°C. The ultraviolet light sources employed have been of low intensity which has resulted in surface reactions only. Consequently it was considered necessary to examine the photodecomposition of barium and strontium azides at temperatures above 25,0°C using light sources of high light intensities in order to attempt to propagate full decomposition of the salt.

Previously only the effect of irradiation with X-rays (122) and radium (123, 124) during the thermal decomposition of barium and strontium azides has been investigated. Thus it was decided that a study of irradiation of barium and strontium azides with ultraviolet light during thermal decomposition would be of interest. This study would also be beneficial in the linking of the mechanisms of photolysis and thermal decomposition since both the low temperature photolysis (61) and the thermal decomposition (114) of barium azide have been found to be characterised by sigmoid curves.

3 APPARATUS AND EXPERIMENTAL METHODS

3A CONSTRUCTION OF HIGH VACUUM SYSTEMS

(i) High vacuum line for photolysis and co-irradiation of powdered material

The course of all photolytic decompositions of powdered material were followed using a high vacuum constant volume line. This vacuum line consisted essentially of a pumping system, a pressure measuring device and a decomposition cell. The line is illustrated in Fig. 3.

The line was pumped by a Pfeiffer TVS 250 turbomolecular pump capable of producing a vacuum of $1,0 \times 10^{-6}$ torr. The pressure was measured by an Edwards "Speedivac" Pirani gauge. This gauge was coupled to a Philips flat bed recorder, PM 8100. Each range of the recorder (1mV, 2mV, 5mV, 10mV) was calibrated against the McLeod gauge using dry nitrogen in the line. The calibration was performed on three different occasions. All three curves were reproducible in the pressure range 0,00 to 0,02 torr. At pressures above 0,02 torr the gauge was highly inaccurate for the work to be undertaken. These curves are illustrated in Fig. 2. Thus decompositions were done in the pressure range 0,00 to 0,02 torr i.e. where the gauge millivolt output is linear.

Two ten litre bulbs were included in the construction of the line. This ensured the use of the linear range of the pirani gauge when samples not larger than 2mg were decomposed. These bulbs were placed such that, when the rate of decomposition was at its maximum, the time required for pressure equilibration throughout the large

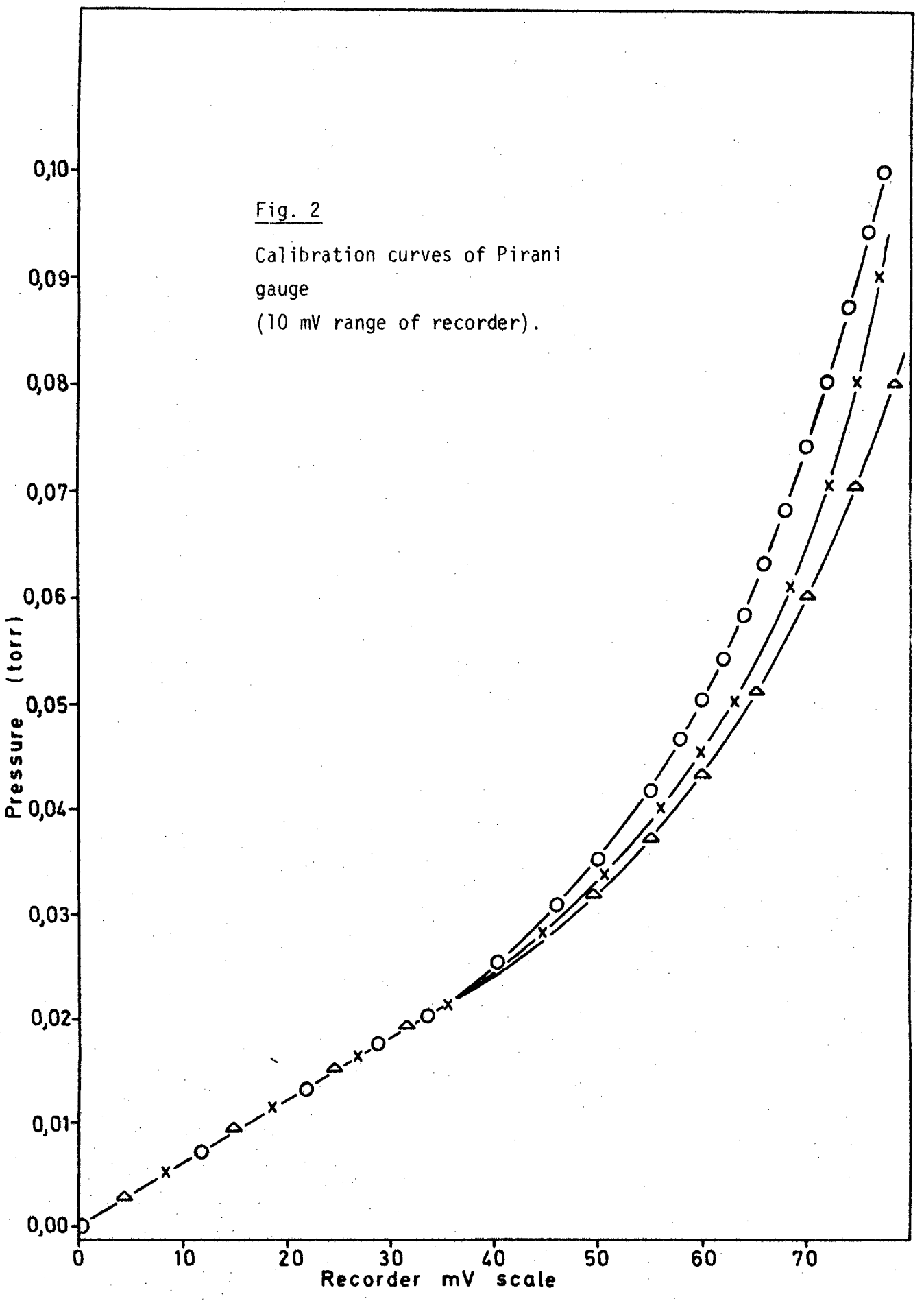

Fig. 2

Calibration curves of Pirani gauge
(10 mV range of recorder).

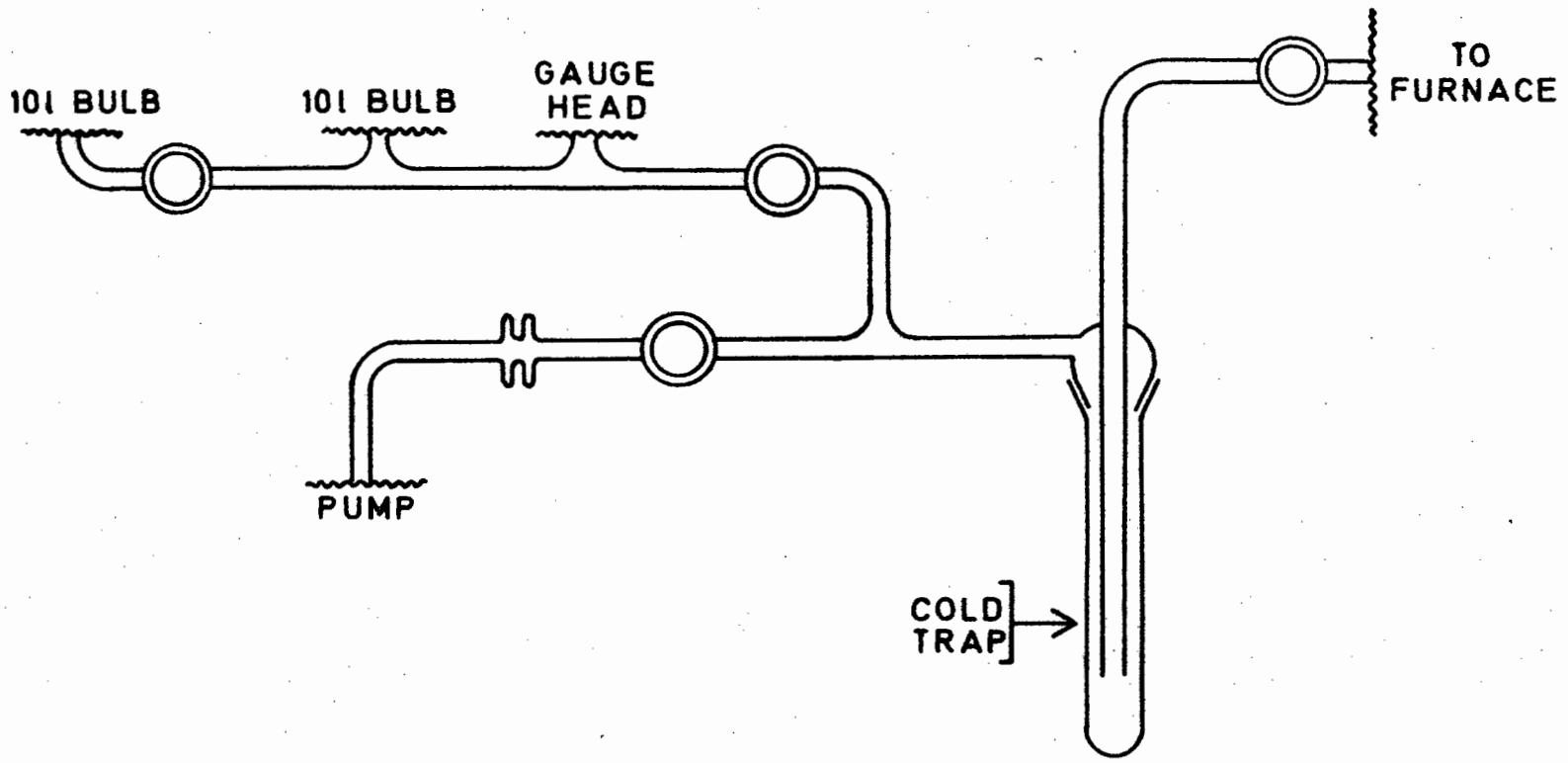

Fig. 3

Vacuum line used for the decomposition of powdered material.

volume was negligible.

A decomposition cell, glass blown from silica glass, was used for all decompositions. The cell used to determine activation energies for the photolysis of barium azide powder in the temperature range $27,0^{o}$ - $100,0^{o}C$, and the dependence of photolytic rate on intensity of ultraviolet source is shown in Fig. 4. This cell was tapered to 5mm in diameter at the bottom and had a plane window glass blown on to the top. A water filter (to remove infrared components from the light), made from silica glass with plane faces 1cm apart, was supported 5mm above this plane window. This cell had many limitations, which will be elucidated later, which called for a modification of it and the water filter. The design was altered and is illustrated in Fig. 5. Essentially it was the same as the old cell but had the water filter glass blown on top of the plane window. Both cells were attached to the line via a greaseless ball and socket joint with a neoprene ring.

The furnace consisted of a brass cylinder (diameter 6cm, height 9cm) with a bore (1,8cm diameter) through the centre to take the decomposition cell. This furnace was mounted on a silver steel rod so that it could be moved freely in a vertical direction and swing freely in a horizontal plane. The cell fitted midway into the furnace and rested on a brass plug which was machined to the shape of the bottom of the cell. The furnace was held in position around the cell by means of a taper pin (see Fig. 4 and 5). Electrical power was supplied to the furnace windings by a CNS Sirect Mk II proportional temperature controller, which had a platinum resistance thermometer as temperature sensor. The temperature of the furnace was measured by a copper/constantan thermocouple placed in an evacuated pyrex cell

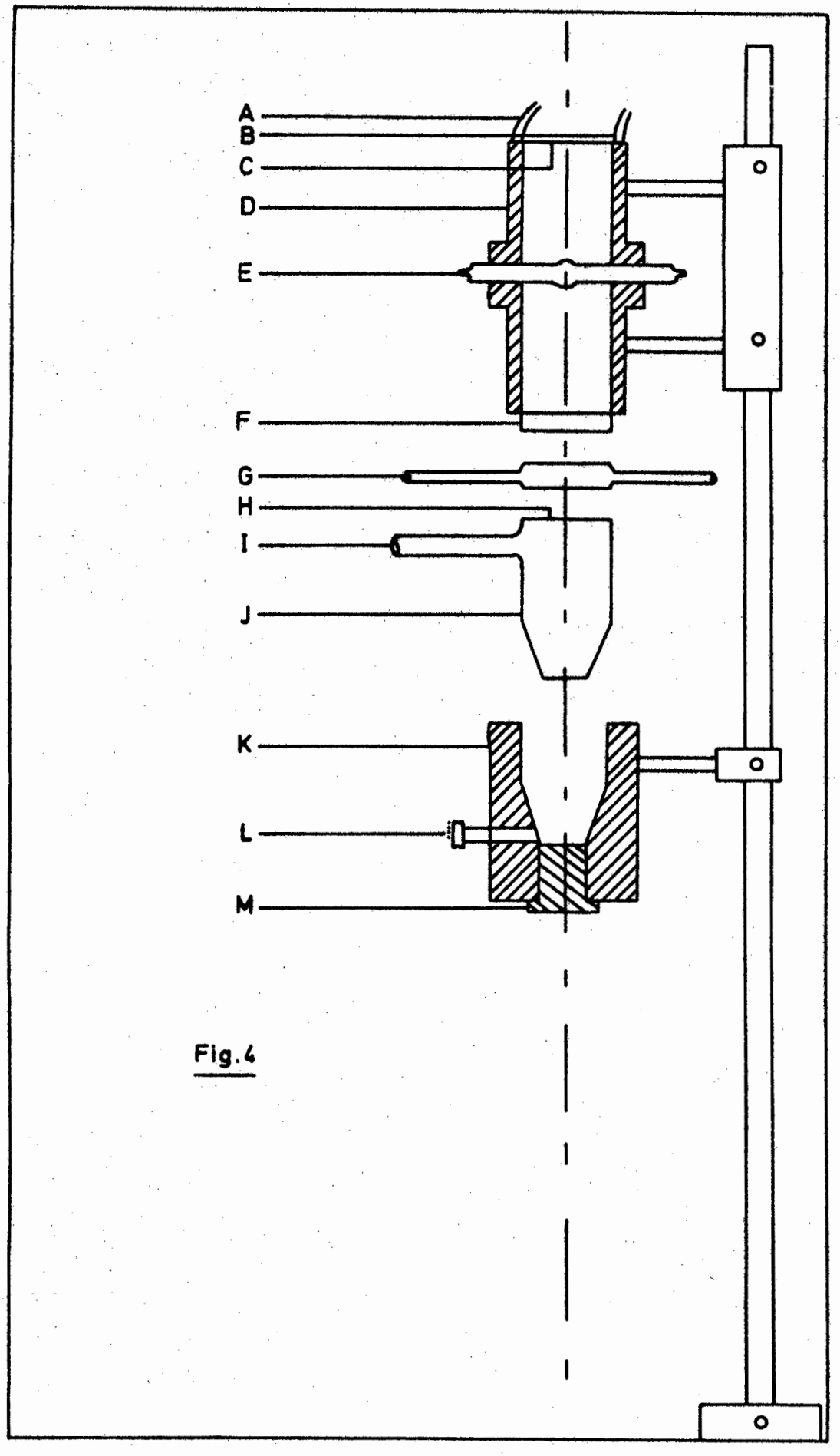

Fig.4

Key to Fig. 4

Cross-sectional view of manufactured lamp housing, water filter, decomposition cell and furnace.

A Water inlet

B Water outlet

C Aluminised mirror

D Lamp housing and water jacket

E Ultraviolet lamp

F Lens holder

G Water filter

H Plane window

I Ball and socket joint with neoprene ring

J Decomposition cell

K Furnace

L Platinum resistance thermometer

M Brass plug

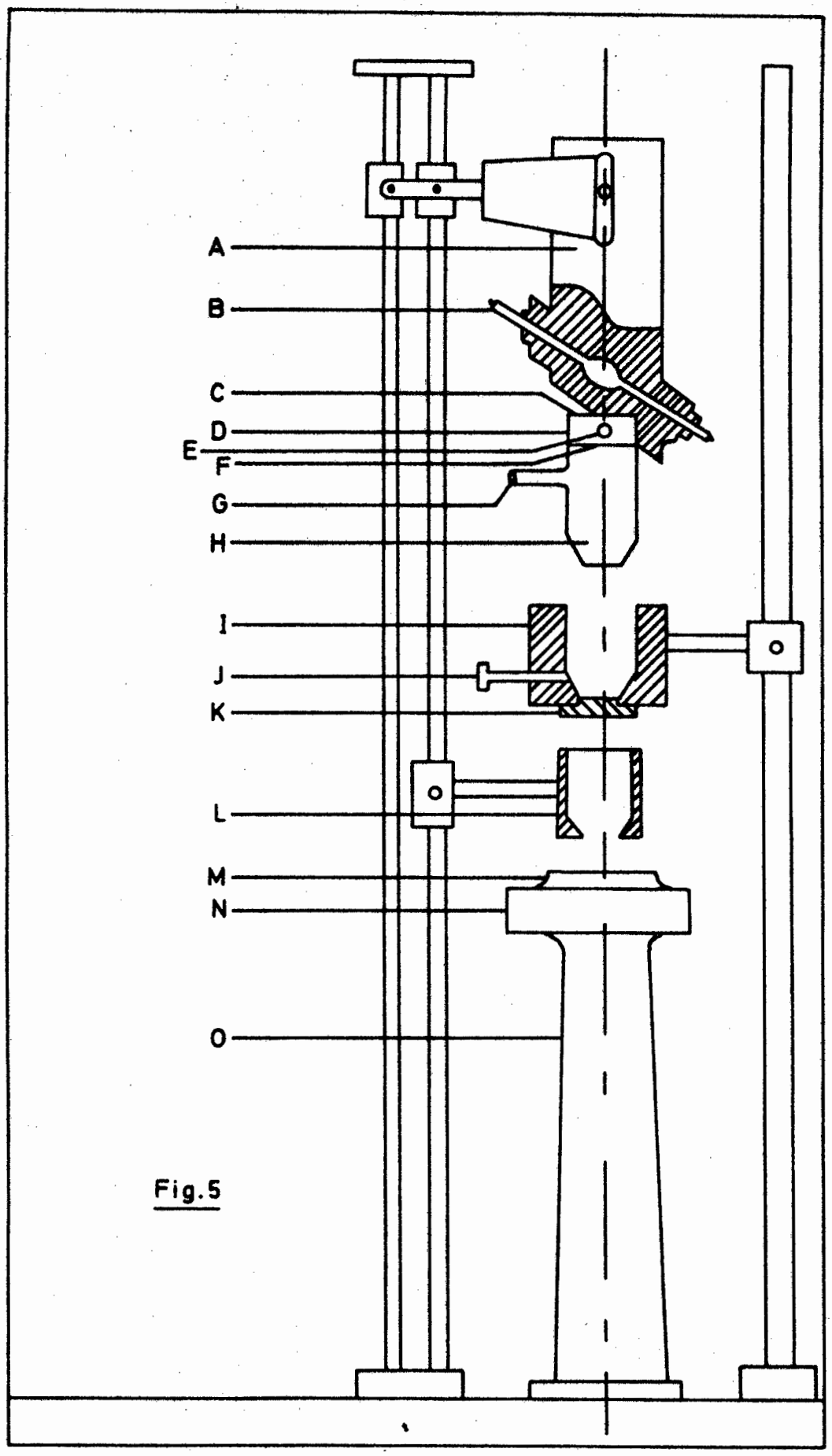

Fig.5

Key to Fig. 5

Cross-sectional view of constructed lamp housing, water filter glass blown to decomposition cell, furnace, cell holder for intensity determinations and perspex support for photometer detector.

A Lamp housing (workshop manufacture)

B Ultraviolet lamp

C Plane window

D Water filter

E Inlet for flow of water through filter

F Plane window

G Ball and socket joint with neoprene ring

H Decomposition cell

I Furnace

J Platinum resistance thermometer

K Brass plug

L Holder for cell during intensity measurements

M Collar over window

N Photometer detector

O Perspex support for photometer detector

with base resembling the shape of the decomposition cell. The thermocouple was connected to a precalibrated scalamp thermocouple galvanometer. It was found that the temperature was controlled to within $\pm$ 0,3^{o}C in the temperature range 25,0^{o} - 135,0^{o}C.

The ultraviolet source used for photolysis and irradiation during thermal decomposition was an Hanovia U.V.-100 source. The intensities of the principal radiations of wavelengths 2970 Å and 3650 Å were 11,96 and 11,86 MWcm^{-2} respectively. The 100 watt high pressure mercury arc lamp gave a "point" source of light which could be focused to a 1cm disc at 12cm from the lens or at 30cm, using an alternative lens. An aluminised mirror brought the light propagated away from the sample back to focus at the centre of the source. The lamp housing provided by the manufacturers was essentially a water jacket which allowed the heat dissipated by the source to be removed from the system (see Fig. 4). The housing allowed an inlet and an outlet for a flow of N_2 gas to prevent ozone formation due to ultraviolet light passing through the atmosphere. The lamp in the manufactured housing, and with the lens that gave a 1cm disc of light 12cm from the lens, was mounted on a rack in a vertical position such that the beam passed through the bore in the furnace and the lens was 12cm from the sample. This system was used for the determination of activation energies for the photolysis of barium azide powder in the temperature range 27,0^{o} - 100,0^{o}C .

The intensity of light at the sample could be increased by moving the lamp housing gradually away from the sample, but on so doing the size of the focused spot decreased until it was an intense point of light with a large area of diffuse light surrounding it. As the distance of the lens from the sample decreased, the size of the

focused spot increased and became less intense. With the water filter supported above the window of the decomposition cell, the lens was prevented from moving to less than 7cm from the sample, (the focused spot at this position was larger than 1cm in diameter). The variation of light intensity with the lens at a distance of 7cm from the sample and at a distance which gave a focused disc 5mm in diameter (the smallest focused spot that could be used since this just covered the area of the bottom of the decomposition cell), was extremely small (28,0 - 22,0 units). Since a larger variation was required in the determination of the variation of the rate of reaction with variation of light intensity, the lens which gave a 1cm (in diameter) focused disc at 30cm from the lens was used. A 1cm diameter disc of focused light on the sample gave an intensity of 26,0 units at the sample. With the lens at its minimum distance from the sample a minimum intensity of 9,0 units was obtained. This variation of intensity was used to determine the variation of rate of reaction with variation of light intensity for barium azide only at a constant photolytic decomposition temperature of 80,0^{o}C. This system was not satisfactory for the above determination at a constant photolytic decomposition temperature of 50,0^{o}C, since at intensities much below 15,0 units the reaction at 50,0^{o}C was extremely slow. This necessitated the use of the lamp without the lens and mirror and the construction of a new decomposition cell so that the distance between the lamp and sample would be minimal, thus increasing the intensity to greater than 26,0 units. The redesigned cell has been described earlier. A new lamp housing was constructed from a copper pipe 4,0cm in diameter. The lamp was mounted inside the housing at an angle of 45^{o} from the horizontal. This was done to ensure that droplets of unvapourised mercury did not sit in the bowl of the lamp

while in operation. The pipe was open to the air at the top and air holes were drilled in the pipe to facilitate cooling. No mirrors or lenses were used to focus the light. Nitrogen was not used to remove ozone since the amount formed while the lamp was in operation was found to be negligible. The construction is illustrated in Fig. 5.

This system allowed the lamp to be moved as close as 5mm from the water filter that was glass blown to the decomposition cell. The maximum intensity that could be obtained was 65,0 units. The intensity was varied by varying the distance of the lamp from the sample. This system was used for all tests on barium azide, (other than the determination of the activation energy of photolysis of barium azide in the temperature range 27,0^{o} - 100,0^{o}C and the variation of the photolytic rate of barium azide with light intensity at 80,0^{o}C) as well as all tests on strontium azide powder.

The intensity was measured by using a "Photovolt" photometer (model 220A) incorporating a photomultiplier probe head. The following construction was made to facilitate accurate readings, (see Fig. 5). A brass cylinder of one half the length of that of the furnace was constructed. This was mounted on a rack such that it could be moved freely in the same manner as the furnace. It was pinned in position by means of a taper pin, when in use, such that the bottom of the cylinder was at the same position as the sample during decomposition. The inside of the cylinder was machined to the shape of the decomposition cell, the aperture at the bottom of the cylinder being 5mm in diameter, the diameter of the bottom of the cell over which the sample lay. The window of the detector was covered with a brass collar machined to fit the brass cylinder. An aperture, 5mm

in diameter, was cut in the collar such that the opening at the bottom of the brass cylinder and thus the bottom of the decomposition cell, fitted over the aperture in the collar, when the detector was positioned. Intensity readings were taken with the cell (under vacuum) surrounded by the brass cylinder. The probe head was supported under the cell by means of a perspex stand.

Due to their short life, new lamps were used for each new series of runs which constituted a particular test. Intensity measurements were made after each run and adjustments were made if necessary by adjusting the distance of the light from the sample.

(ii) High vacuum line for photolysis and co-irradiation of pelleted material

A high vacuum line, similar to that used to study decompositions of powder, was constructed to study the photodecomposition and co-irradiation of barium azide pellets (see Fig. 6). The pumping system and decomposition cell designs were the same as that used for powder - the second cell constructed was used for all decompositions and the lamp was used in the housing constructed in the workshop. The essential difference between the lines was the pressure measuring device. The minimum weight of powder that could be used to make pellets was 8mg. The pressure of the gas produced during decomposition far exceeded 0,02 torr. As shown before the Pirani gauge was inaccurate for measurement of pressures in excess of 0,02 torr. Thus all decompositions of pellets were followed using a calibrated McLeod gauge (vol. 123,1cm^3) to measure the pressure of nitrogen evolved. This line contained one expansion bulb of volume one litre.

Fig. 6

Vacuum line used for the decomposition of pelleted material.

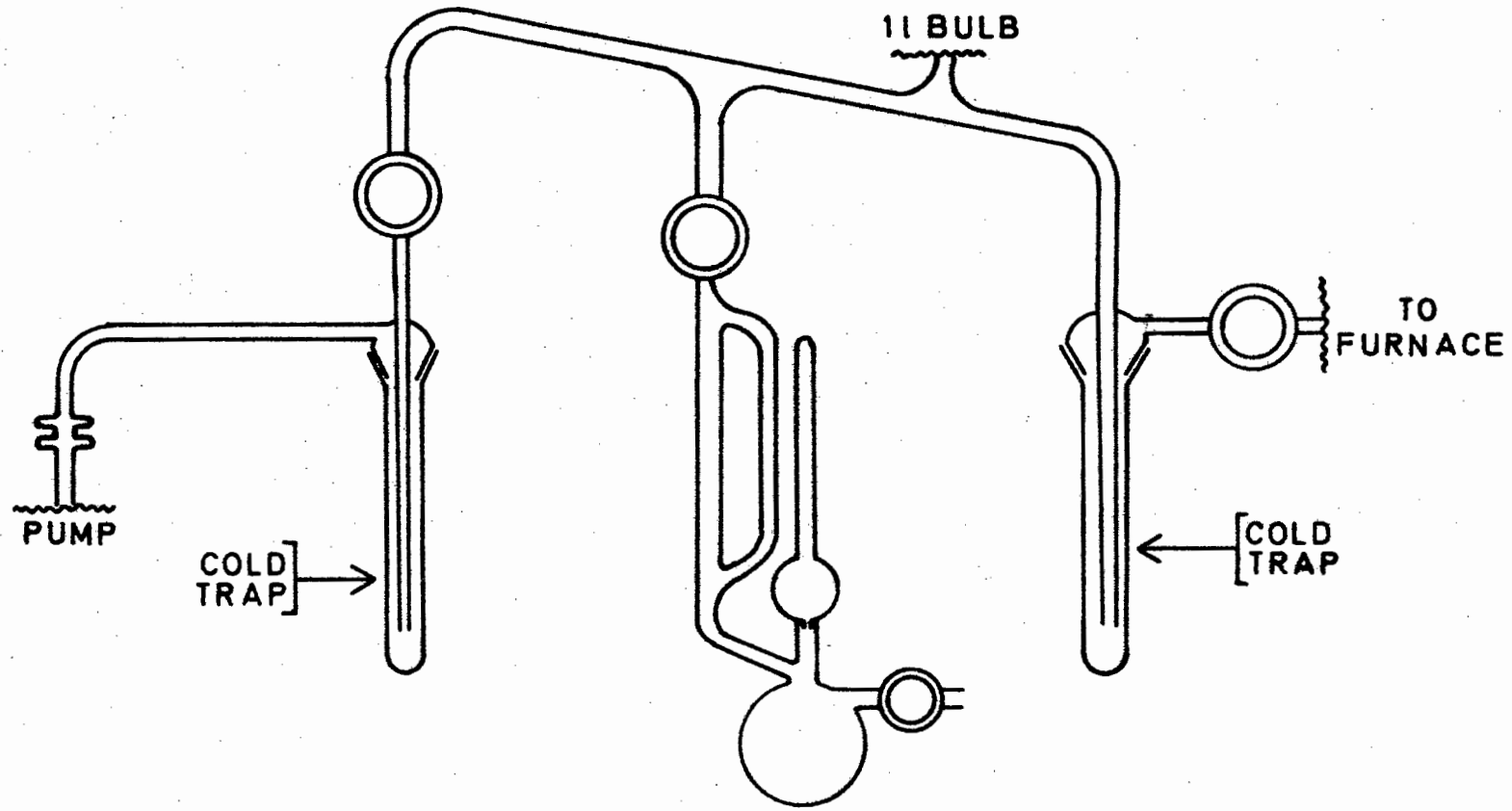

3B EXPERIMENTAL PROCEDURES

(i) Preparation of hydrazoic acid

The hydrazoic acid was prepared by an ion exchange method using "Analar" cationic resin in the H^+ form. A 10% solution of B.D.H. "Analar" grade sodium azide was passed through the bed of resin. This resulted in a 3% solution of hydrazoic acid. It was found to contain no iron or sodium ions using Ferron reagent and flame photometry.

(ii) Preparation of barium azide

Commercial grade barium azide was recrystallized in conductivity water (specific conductance 2,0 x 10^{-6} $ohms^{-1}cm^{-1}$ at 20,0^{o}C) at a temperature of 70,0^{o}C. 3% Hydrazoic acid solution was added to make the solution acid. More acid was added, to prevent the formation of barium hydroxide, during evaporation.

Pure barium azide monohydrate was recrystallised from this acid solution and dried over P_2O_5 in a vacuum dessicator, with constant pumping for 48 hours, to dehydrate it. The dehydrated sample was stored over P_2O_5 in a black vacuum dessicator at all times.

(iii) Preparation of strontium azide

Six grams of strontium hydroxide were dissolved in hydrazoic acid, 3%, until the solution was acid to phenolphthalein (external indicator). The solution was evaporated to dryness, the pH being kept just acid by the addition of hydrazoic acid. The resulting precipitate of strontium azide was then dried for 48 hours over P_2O_5 in

a black vacuum dessicator with constant pumping. It was stored in a black vacuum dessicator at all times to prevent hydrolysis of the salt and its interaction with light.

(iv) Grinding of barium and strontium azide crystals

In order to obtain powders of barium and strontium azide, 500mg of the required crystals were ground for 4 min. in a grindex, using an agate capsule and one nylon ball. The resulting powder was passed through a selection of Endecott test sieves. The powder between mesh size 63μ to 125μ was collected and stored over P_2O_5 in a black vacuum dessicator. For each series of decompositions, which constituted a particular test, a new sample from the original batch of crystals was ground and sieved. A small spoon shaped spatula was constructed to deliver a constant 2mg of powder of either salt into the decomposition cell.

(v) Pelleting the powders of barium and strontium azides

The sieved powder was used to make pellets. A glass scoop, constructed to hold a constant mass of 8mg of the required powder was used to deliver the sample into an evacuable KB-R die. The die was evacuated for 10 min. before a pressure of 2000 lb/sq.in. or 600 lb/sq.in. was applied for 15 min. by a ten-ton Apex Type 341/4 hydraulic press. The resulting pellets were 5mm in diameter and 0,25mm thick.

(vi) Decomposition procedures

The sample in the silica decomposition cell was attached to the line and pumped for 1 hour before decomposition. This was found to be the minimum time required to obtain a good vacuum. During the pumping stage the sample was shielded from daylight by aluminium foil wrapped around the cell. After a one hour pump the pump was isolated and the furnace, preset at the desired temperature for decomposition, was brought into position around the cell. With the shutter closed the light was arced and the whole system was allowed to come to equilibrium over a period of six minutes. The shutter was then opened and decomposition began. For powders the reaction was followed by monitoring the pressure of gas evolved with the Pirani gauge coupled to the recorder. The McLeod gauge was used to follow the reaction of the pellets. During the pumpdown and decomposition the cold trap was filled every 10 minutes. At the end of each decomposition the light intensity was measured. The decomposition cell was cleaned with a dilute solution of hydrafluoric acid then washed thoroughly with distilled water and pumped dry.

(vii) Interrupting a decomposition and admitting water vapour onto the salt

A decomposition was allowed to proceed to a certain stage and then interrupted in order that the sample could be exposed to water vapour for a fixed time, after which the run continued. Before connecting the decomposition cell to the line 1ml distilled water was introduced into the cold trap, the water was then solidified by

liquid nitrogen. After connection of the decomposition cell to the line the system was pumped for 1 hour after which decomposition procedures took place as usual. At the selected point of interruption the shutter was closed and the furnace removed from the sample. The expansion bulbs and decomposition section were now isolated and the liquid nitrogen removed. On vapourization of the water it was allowed to come into contact with the sample for a specific length of time (1 min.), after which the water vapour was pumped from the line for 1 hour. After isolation of the pump, the liquid nitrogen trap was replaced and the furnace repositioned around the sample. After allowing 6 min. for the sample to reach decomposition temperature, the expansion bulbs and shutter were opened and decomposition continued.

4 RESULTS

The results obtained for the photolysis and co-irradiation of barium and strontium azides (powder and pellets) will be reported together since a marked similarity in the behaviour of the two compounds was noticed.

Decompositions of barium azide in the temperature range $27,0^{o}$ - $100,0^{o}C$ and strontium azide in the temperature range $30,0^{o}$ - $90,0^{o}C$ are referred to as photolytic decompositions. Irradiated decompositions, for both barium and strontium azides, in the temperature range $110,0^{o}$ - $135,0^{o}C$ are referred to as co-irradiated decompositions (122).

The variables plotted in the diagrams for barium and strontium azides are α vs t where t = time and $\alpha = p/p_f$ (p = pressure at t and p_f is the observed final pressure), except where indicated.

Throughout this thesis powder of either azide refers to material of particle size ranging from 63μ to 125μ. Pelleted material is powder pressed at either 600 lb/sq.in. or 2000 lb/sq.in. in a 5mm die for 15 min., after evacuation of the die for 10 min. For all decompositions using either barium or strontium azide powder, 2mg was used. For the making of pellets 8mg of the required powder was used which resulted in pellets 0,25mm thick. For each set of decompositions which constituted a particular test, freshly ground and sieved powder was used. Pellets were made when required.

Percentage decompositions were calculated assuming the equations for decomposition to be

$$Ba(N_3)_2 \rightarrow Ba + 3N_2 \quad \text{for barium azide}$$

and

$$Sr(N_3)_2 \rightarrow Sr + 3N_2 \quad \text{for strontium azide.}$$

Intensity units are arbitrary. Due to the short life of the

lamps, new ones were used for each series of decompositions which constituted a particular test.

4A PHOTOLYSIS OF BARIUM AND STRONTIUM AZIDES

(i) Powder

A temperature range of 27,0° - 100,0°C was chosen for the photolysis of barium azide since no dark rate could be detected in this temperature range when the sample was screened from the light. Similarly a temperature range of 30,0° - 90,0°C was chosen for the photolysis of strontium azide. For both these azides the percentage decomposition was found to be the same as that of a corresponding thermal decomposition at 130,0°C, viz 95,0% (114) for barium azide and 71,2% (89) for strontium azide.

(ia) Reproducibility

For both barium and strontium azides, whole crystals and crystals ground for 4 min. in a grindex did not give reproducible results. The crystals of both compounds ground for 4 min., were then sieved and the powder between sieves of mesh size 63μ and 125μ selected. To test the reproducibility of barium azide, three decompositions of the sieved samples were done at 50,0°C (intensity 37,0 units) and three at 83,0°C (intensity 25,0 units). When the sets of curves were superimposed, satisfactory reproducibility was obtained. The two sets of curves are shown in Fig. 7 and 8. Similarly the reproducibility of sieved powder of strontium azide was checked by superimposing three photolytic decomposition curves (decomposition temperature of 80,0°C,

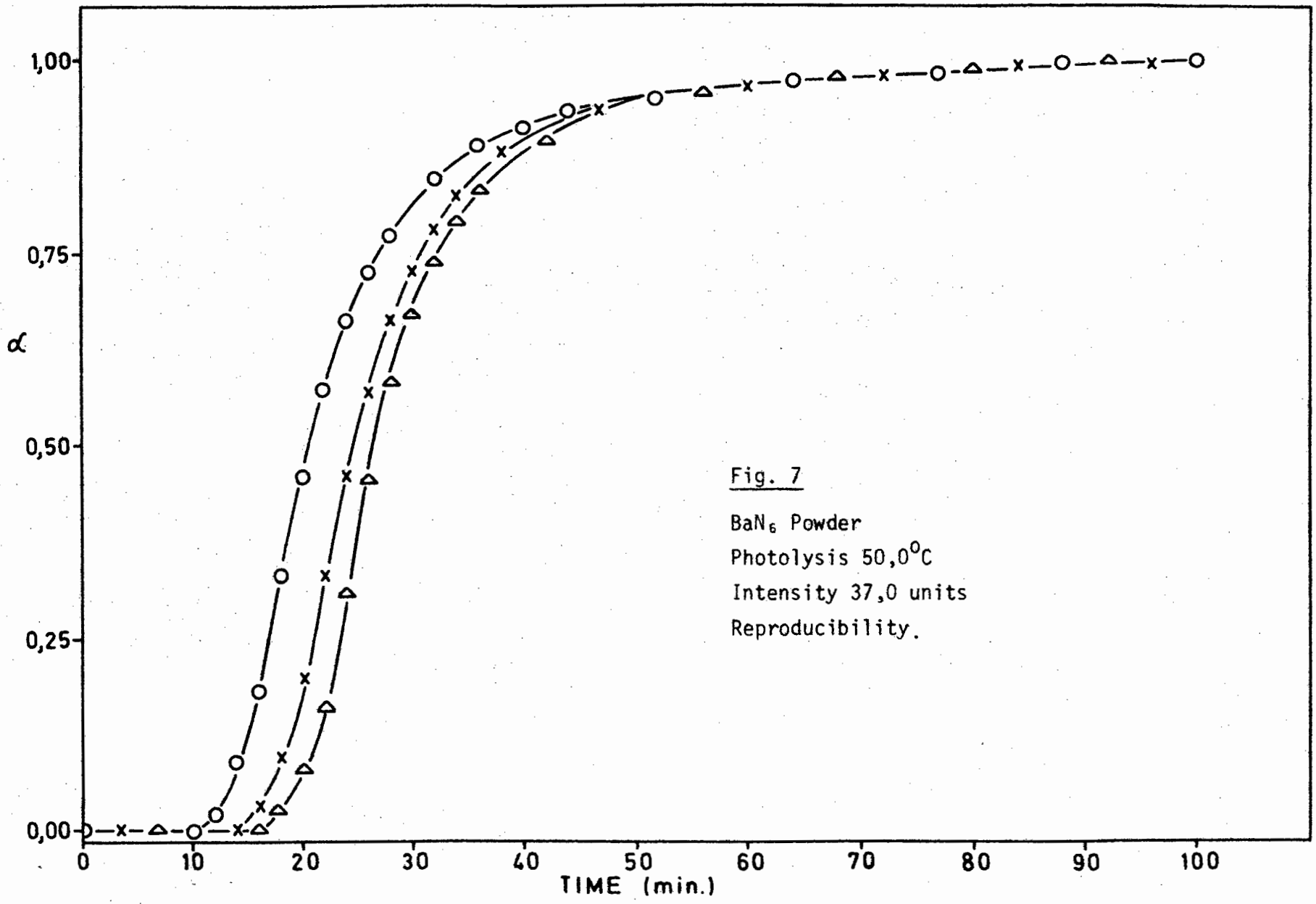

Fig. 7

BaN_6 Powder
Photolysis 50,0°C
Intensity 37,0 units
Reproducibility.

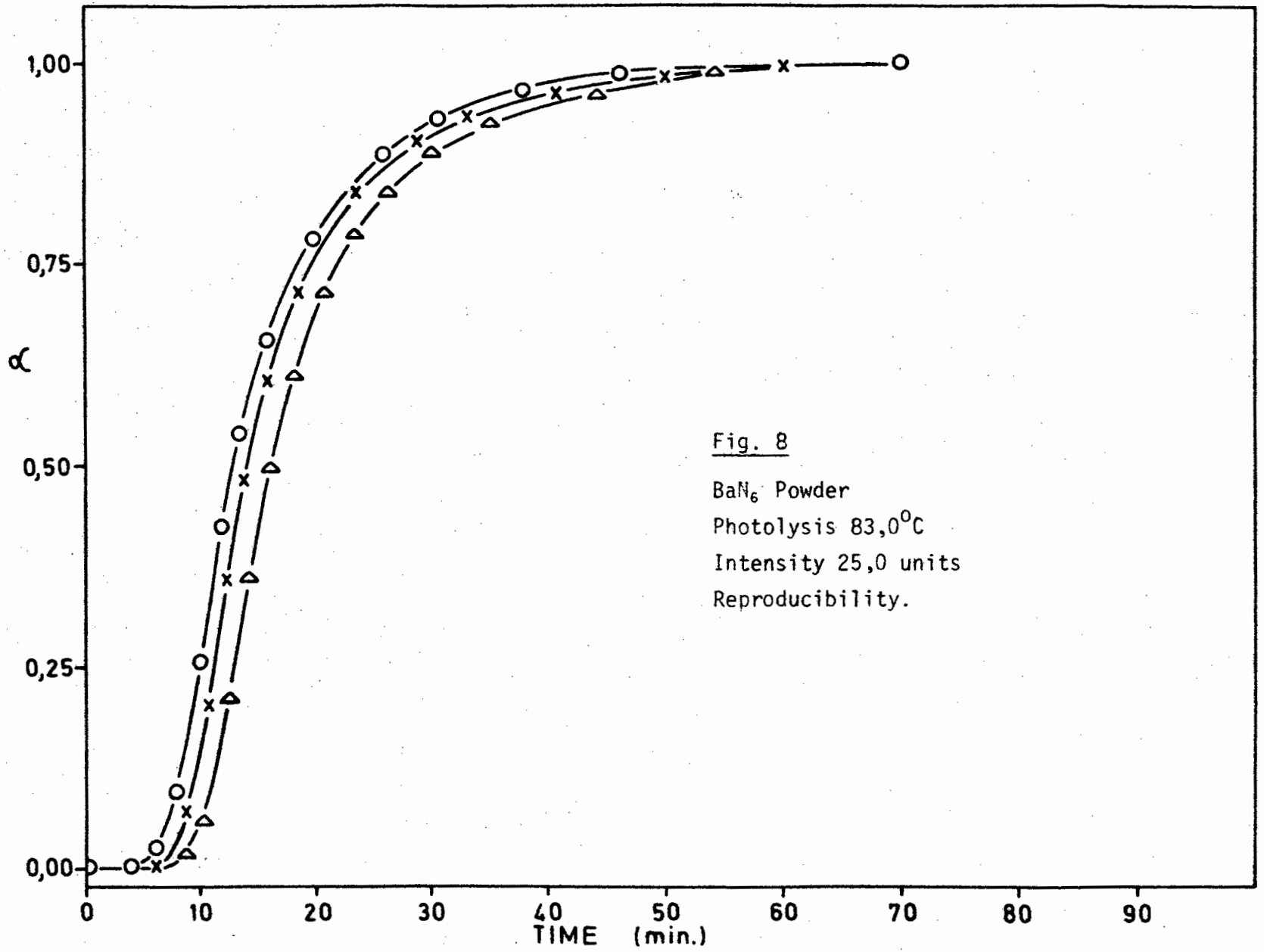

Fig. 8

BaN_6 Powder
Photolysis 83,0°C
Intensity 25,0 units
Reproducibility.

and intensity of 33,0 units). Satisfactory results were found. This is illustrated in Fig. 9. The rate constants for barium azide are tabulated below in Table 1; Table 2 shows the rate constants for strontium azide. The Avrami-Erofeyev equation (n = 2) and the unimolecular law were used to obtain the rate constants of the accelerat-ory and decay reactions respectively, for both barium and strontium azides. The applicability of these equations will be shown later.

For all the following tests, on either azide, only powders of particle sizes 63μ to 125μ were used since these gave reproducible results.

Table 1

Reproducibility constants for the photolysis of barium azide powder.

Temperature ^{o}C	Intensity units	Induction period min.	$k_{acc} \times 10^2$ $min.^{-1}$	$k_{decay} \times 10^2$ $min.^{-1}$
50,0	37,0	10,0	5,21	4,32
		16,0	5,50	4,40
		14,0	5,20	4,29
83,0	25,0	7,0	6,05	4,25
		6,0	6,57	4,54
		4,0	6,34	4,23

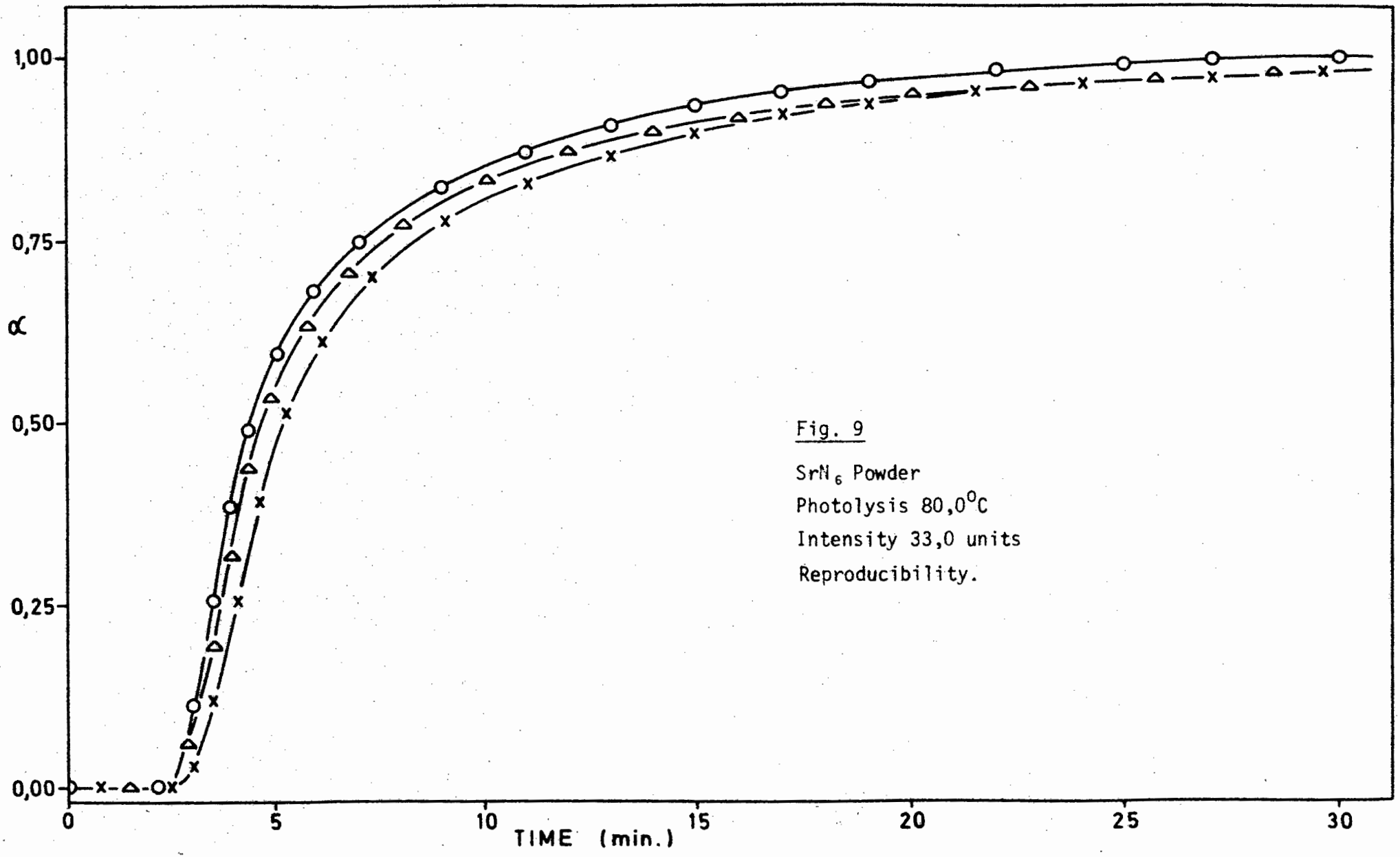

Fig. 9

SrN_6 Powder
Photolysis 80,0°C
Intensity 33,0 units
Reproducibility.

Table 2

Reproducibility constants for the photolysis of strontium azide powder.

Temperature ^{o}C	Intensity units	Induction period min.	k_{acc} x 10 min^{-1}	k_{decay} x 10 min^{-1}
80,0	33,0	2,3	2,46	1,11
		2,2	2,65	1,06
		2,5	2,40	1,01

(ib) Mathematical analyses

Photodecomposition curves of barium azide in the temperature range $27,0^{o}$ - $100,0^{o}C$ showed a well defined induction period during which there was no evolution of gas, followed by an acceleratory and decay reaction. The inflection point occurred at $\alpha = 0,43$.

The acceleratory reaction was described by the Avrami-Erofeyev equation with n = 2

$$\text{i.e.} \quad (-\log(1-\alpha))^{\frac{1}{2}} = k_{acc}t + c \; ; \quad \alpha = p/p_f \; .$$

This equation fitted the curve from $0,01 < \alpha < 0,43$.

The unimolecular law

$$\text{i.e.} \quad -\log(1-\alpha) = k_{decay}t + c \; ; \; \alpha = p/p_f$$

fitted the decay reaction from $0,43 < \alpha < 0,92$.

Since no gas was evolved during the induction period no mathematical analysis for this part of the decomposition was possible.

For comparative purposes the duration of the induction period i.e. the time taken for the reaction to reach $\alpha = 0,01$, was used as the rate constant.

Typical α vs t curves of the photolysis of barium azide powder, with mathematical analyses are indicated at $50,0^{o}C$ (intensity 20,0 units) and at $80,0^{o}C$ (intensity 10,9 units) in Fig. 10 and 11.

Photolytic curves of strontium azide, in the temperature range $30,0^{o}$ - $90,0^{o}C$ showed the same features as those of barium azide i.e. an induction period, acceleratory period and decay period. However the decay reaction was more protracted than that of the barium salt.

The kinetic equations which were tested, where relevant, were the Avrami-Erofeyev, the Prout-Tompkins, the contracting sphere, the exponential laws of acceleration and the unimolecular decay equations, including the power laws of acceleration and decay. The Avrami-Erofeyev equation with $n = 2$ was found to fit the acceleratory reaction. No mathematical analysis could be obtained for the decay reaction of the photolytic decomposition when the observed final pressure (p_f) was used in the appropriate equations. Thus in order to find an analysis for the decay reaction a final pressure p_f' was estimated for this reaction and substituted in the above mentioned kinetic equations. Using this estimated final pressure the Avrami-Erofeyev equation with $n = 2$, (i.e. $\left(-\log(1-\alpha')\right)^{\frac{1}{2}} = k_{acc}t + c$; $\alpha' = p/p_f'$, p_f' = estimated final pressure) was found to fit the acceleratory period from $0,01 < \alpha < 0,36$, as was found using the observed final pressure; and the unimolecular decay law (i.e. $-\log(1-\alpha') = k_{decay}t + c$; $\alpha' = p/p_f'$, p_f' = estimated final pressure) was found to fit the decay reaction from $0,36 < \alpha < 0,95$. The inflection point occurred at $\alpha = 0,36$. (Note: the α values quoted

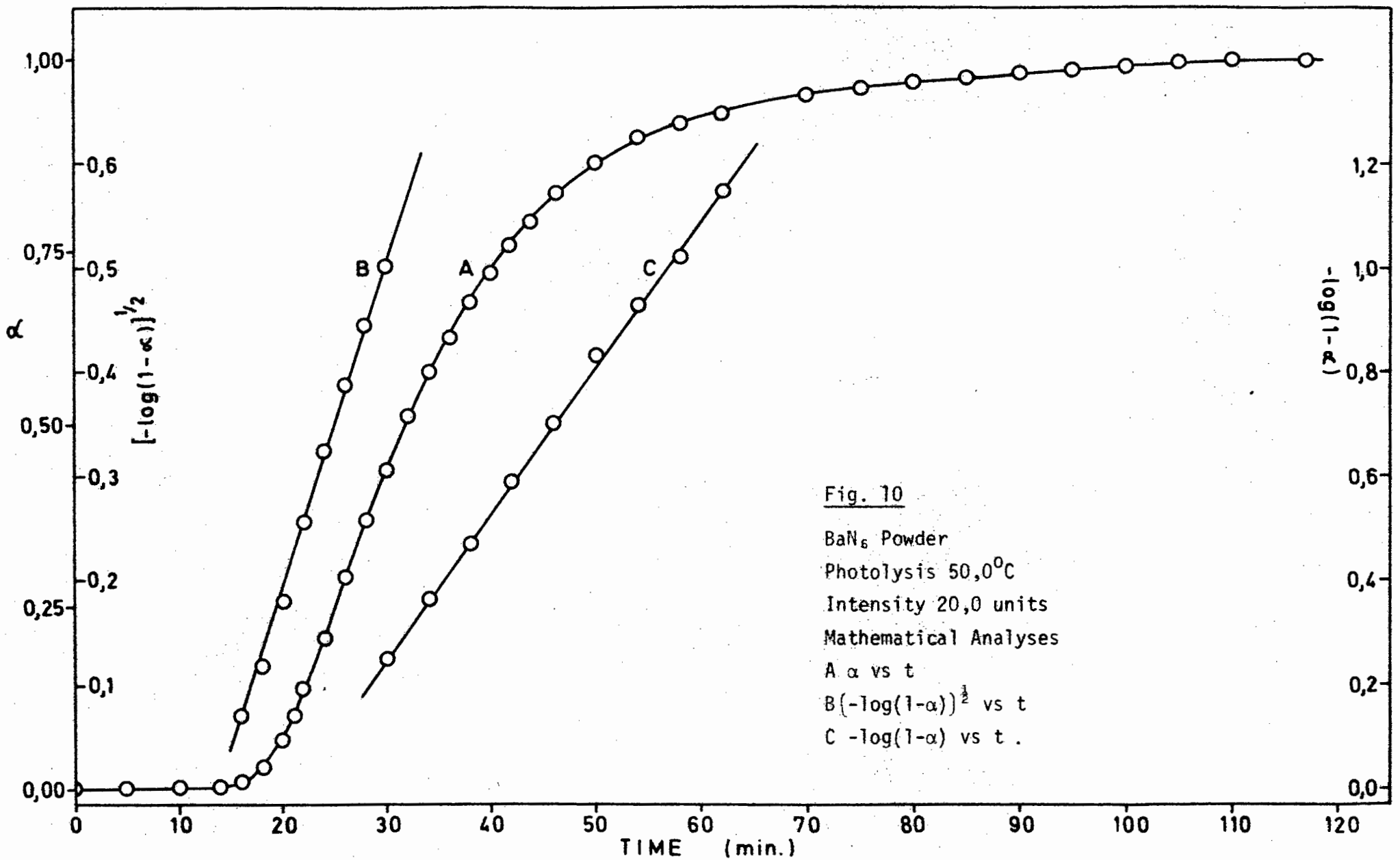

Fig. 10

BaN_6 Powder
Photolysis 50,0°C
Intensity 20,0 units
Mathematical Analyses
A α vs t
B $\{-\log(1-\alpha)\}^{\frac{1}{2}}$ vs t
C $-\log(1-\alpha)$ vs t .

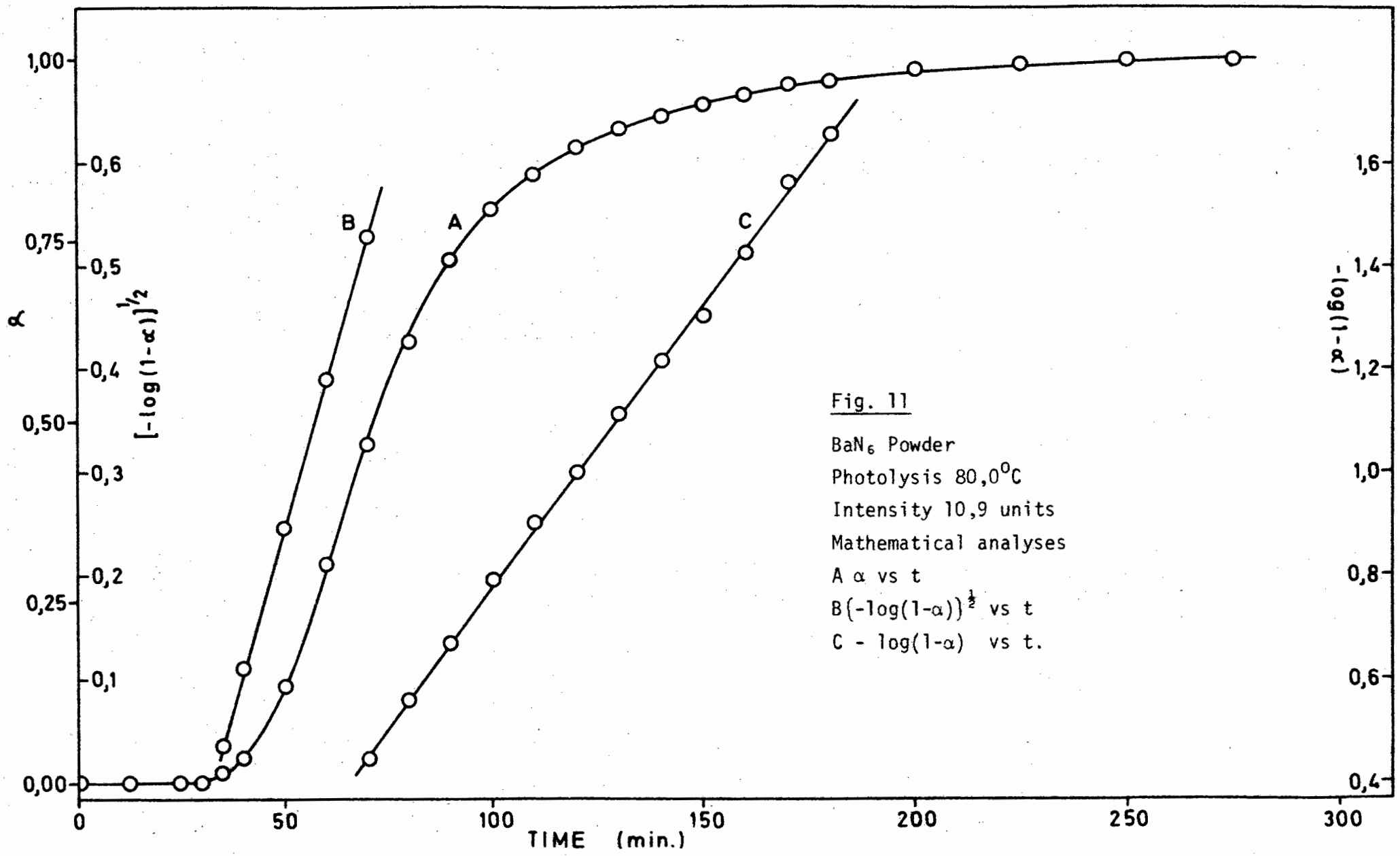

Fig. 11

BaN_6 Powder
Photolysis 80,0°C
Intensity 10,9 units
Mathematical analyses
A α vs t
B $(-\log(1-\alpha))^{\frac{1}{2}}$ vs t
C $-\log(1-\alpha)$ vs t.

were calculated from p/p_f where p = pressure at time = t and p_f is the observed final pressure and not the estimated final pressure). A typical α vs t curve showing the photolysis of strontium azide powder at 80,0^{o}C (intensity 33,0 units) with analyses, is shown in Fig. 12. Curve A shows a plot of α vs t ($\alpha = p/p_f$). The position in the decay reaction where the final pressure was estimated is indicated on this curve (p_f'). Curve B is a plot of the Avrami-Erofeyev equation (n = 2) against time, when p_f the observed final pressure was substituted in the equation, while B' shows a plot of the same equation with p_f', the estimated final pressure substituted for the final pressure. Curves C and C' are plots of the unimolecular law against time. C was obtained by substituting the observed final pressure p_f into the equation; while the latter curve C' was obtained by substituting the estimated final pressure p_f' into the equation. Thus for the determination of all rate constants for the photolytic decompositions of strontium azide powder a final pressure p_f' was estimated.

(ic) Evaluation of activation energies

Activation energies for barium and strontium azides were obtained by decomposing samples at various temperatures in the photolytic temperature range. The light intensity was kept at a constant value throughout the determination. In order to obtain the critical increment of the process(es) occurring during photolysis, the Arrhenius equation was applied. For the induction period the -log(induction period (min.)) was plotted against $10^3/T$, and for the acceleratory and decay reactions log k_{acc} and log k_{decay} respectively were plotted against $10^3/T$ where T is the temperature of decomposition

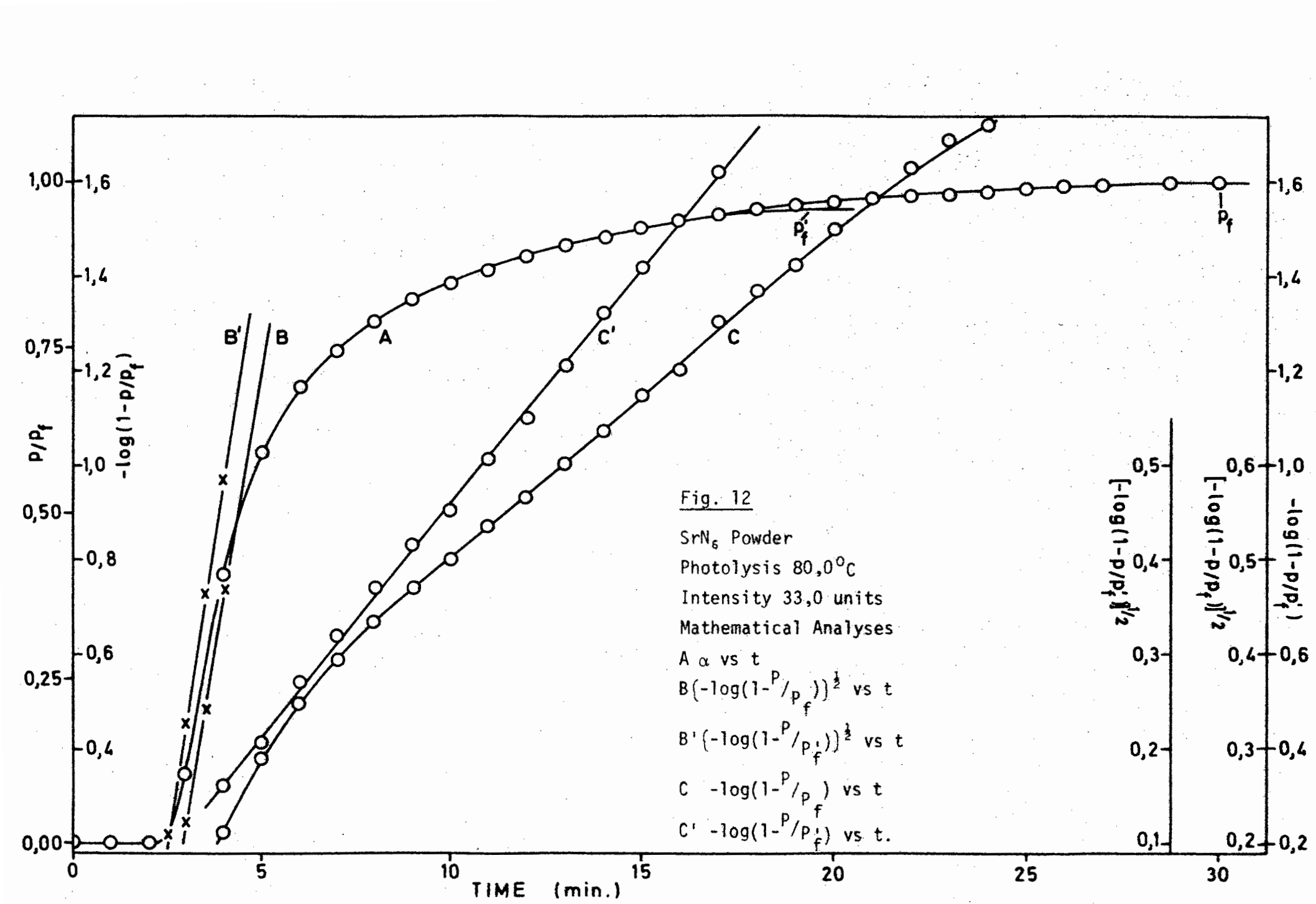

Fig. 12

SrN_6 Powder

Photolysis 80,0°C

Intensity 33,0 units

Mathematical Analyses

A α vs t

B $\left(-\log\left(1-{}^{P}/_{P_f}\right)\right)^{\frac{1}{2}}$ vs t

B' $\left(-\log\left(1-{}^{P}/_{P'_f}\right)\right)^{\frac{1}{2}}$ vs t

C $-\log\left(1-{}^{P}/_{P_f}\right)$ vs t

C' $-\log\left(1-{}^{P}/_{P'_f}\right)$ vs t.

in ^{o}K.

A constant light intensity of 25,0 units was chosen for barium azide while a value of 40,5 units was chosen for strontium azide for the determination of rate constants throughout the respective temperature ranges.

For barium azide a change in activation energy occurred at $60,0^{o}C$, thus activation energies were calculated in the temperature ranges $27,0^{o}$ - $60,0^{o}C$ and $60,0^{o}$ - $100,0^{o}C$. For strontium azide a change in activation energy occurred at $50,0^{o}C$. Thus similarly, activation energies were calculated in the temperature ranges $30,0^{o}$ - $50,0^{o}C$ and $50,0^{o}$ - $90,0^{o}C$.

Table 3 and Table 4 indicate the rate constants for barium and strontium azides respectively while Tables 5 and 6 show the activation energies for barium and strontium azides respectively. Fig. 13 and 14 illustrate the plots of -log I.P., log k_{acc} and log k_{decay} against $10^{3}/T$ in the temperature ranges $27,0^{o}$ - $60,0^{o}C$ and $60,0^{o}$ - $100,0^{o}C$ respectively for barium azide. The plots of -log I.P., log k_{acc} and log k_{decay} against $10^{3}/T$, for strontium azide in the temperature range $30,0^{o}$ - $90,0^{o}C$, are illustrated in Fig. 15 16 and 17.

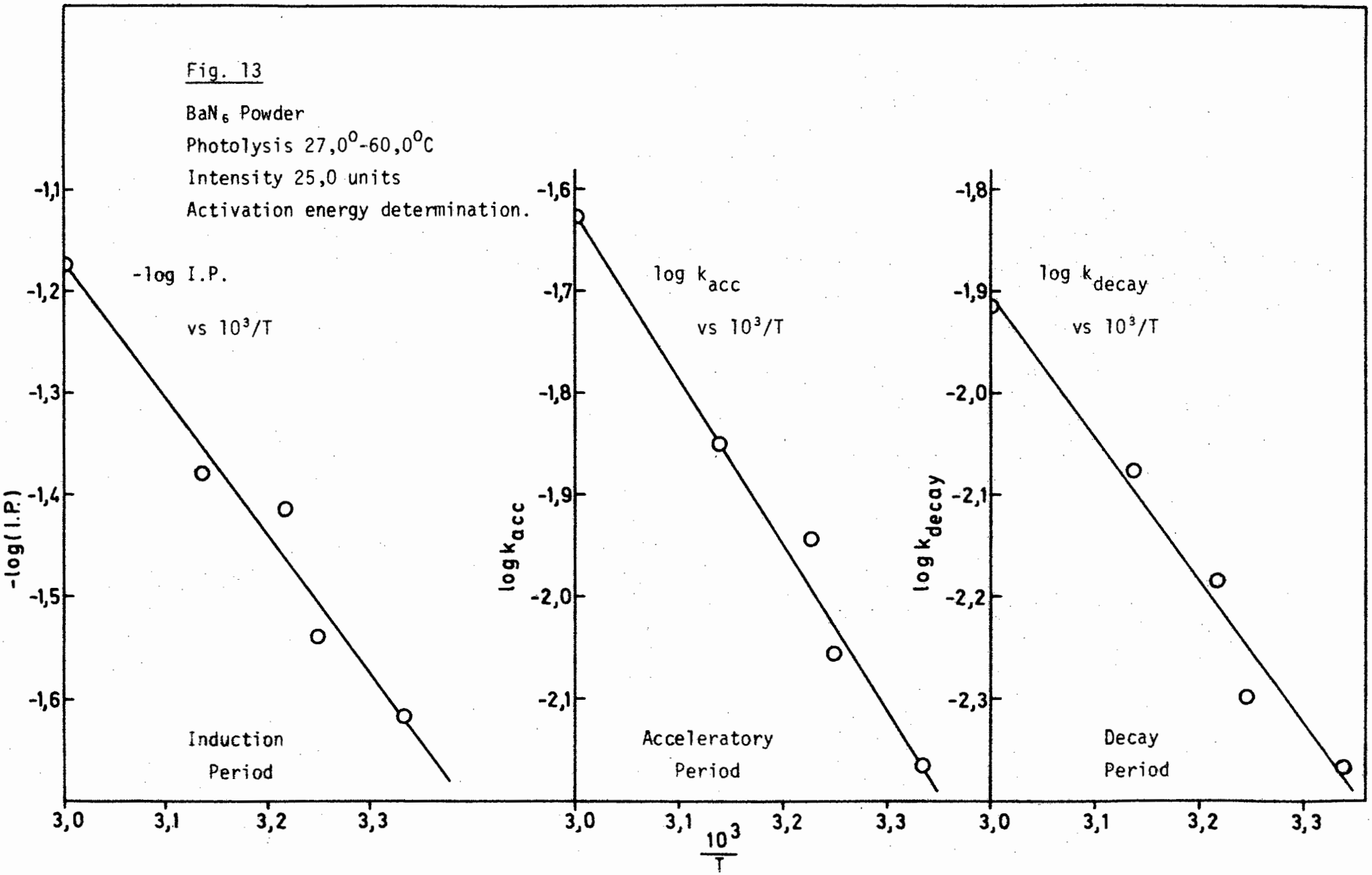
Fig. 13
BaN_6 Powder
Photolysis 27,0°-60,0°C
Intensity 25,0 units
Activation energy determination.
-log I.P.
vs $10^3/T$
Induction Period
$\log k_{acc}$
vs $10^3/T$
Acceleratory Period
$\log k_{decay}$
vs $10^3/T$
Decay Period
$-\log(I.P.)$
$\log k_{acc}$
$\log k_{decay}$
$\frac{10^3}{T}$
-1,1
-1,2
-1,3
-1,4
-1,5
-1,6
-1,6
-1,7
-1,8
-1,9
-2,0
-2,1
-1,8
-1,9
-2,0
-2,1
-2,2
-2,3
3,0
3,1
3,2
3,3

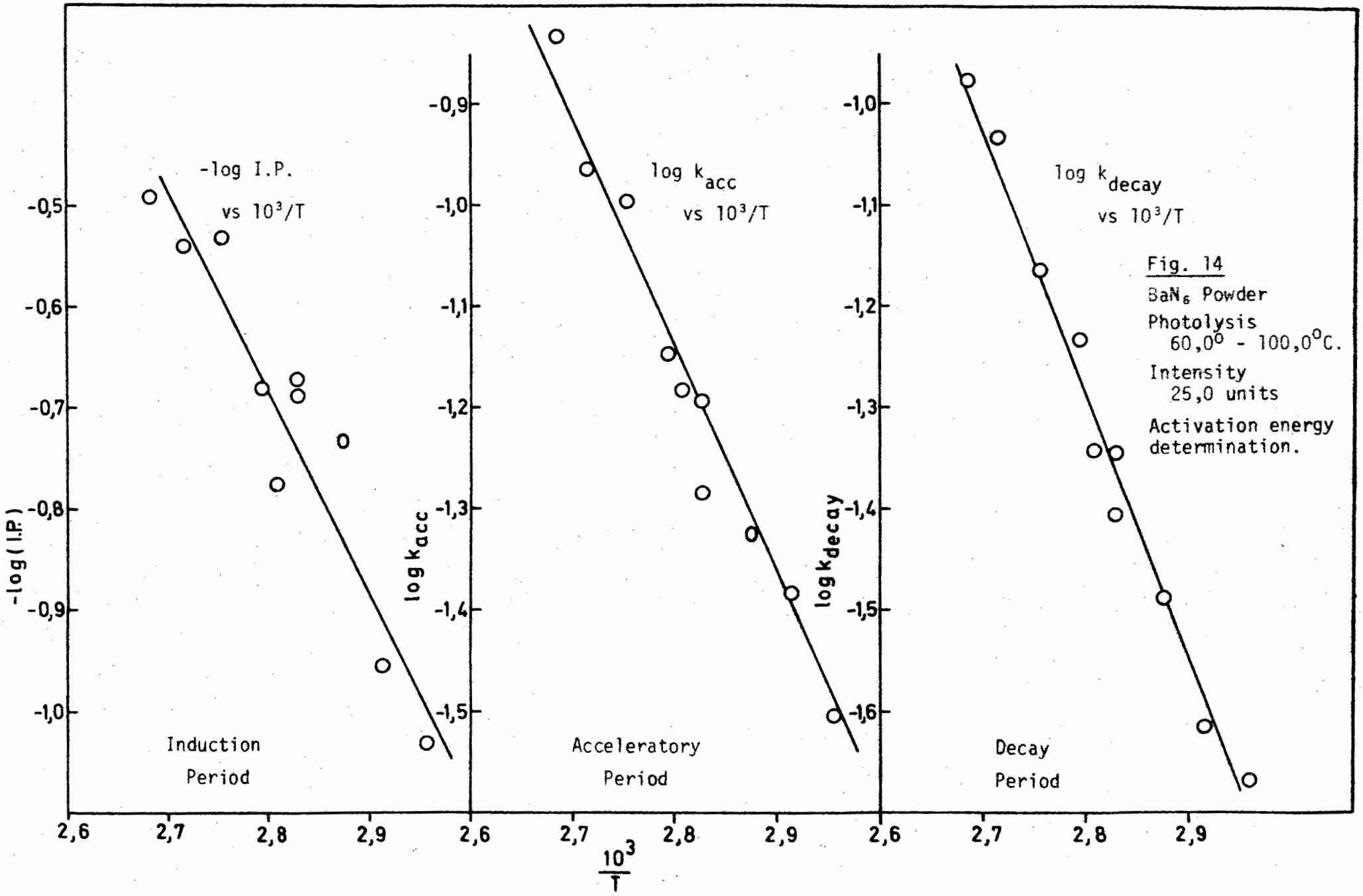

Fig. 14

BaN_6 Powder

Photolysis
60,0° - 100,0°C.

Intensity
25,0 units

Activation energy determination.

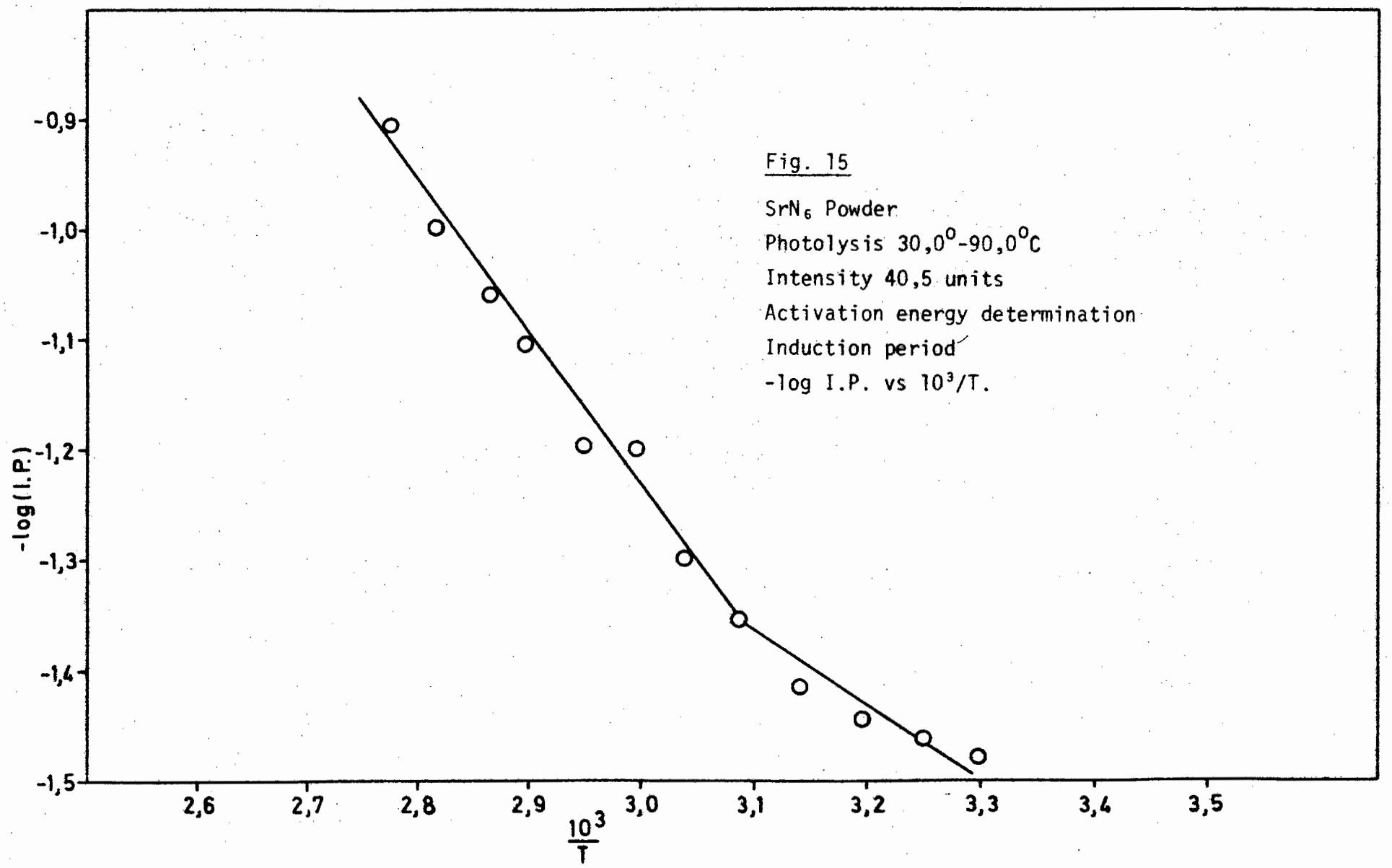

Fig. 15

SrN_6 Powder
Photolysis 30,0°-90,0°C
Intensity 40,5 units
Activation energy determination
Induction period
-log I.P. vs $10^3/T$.

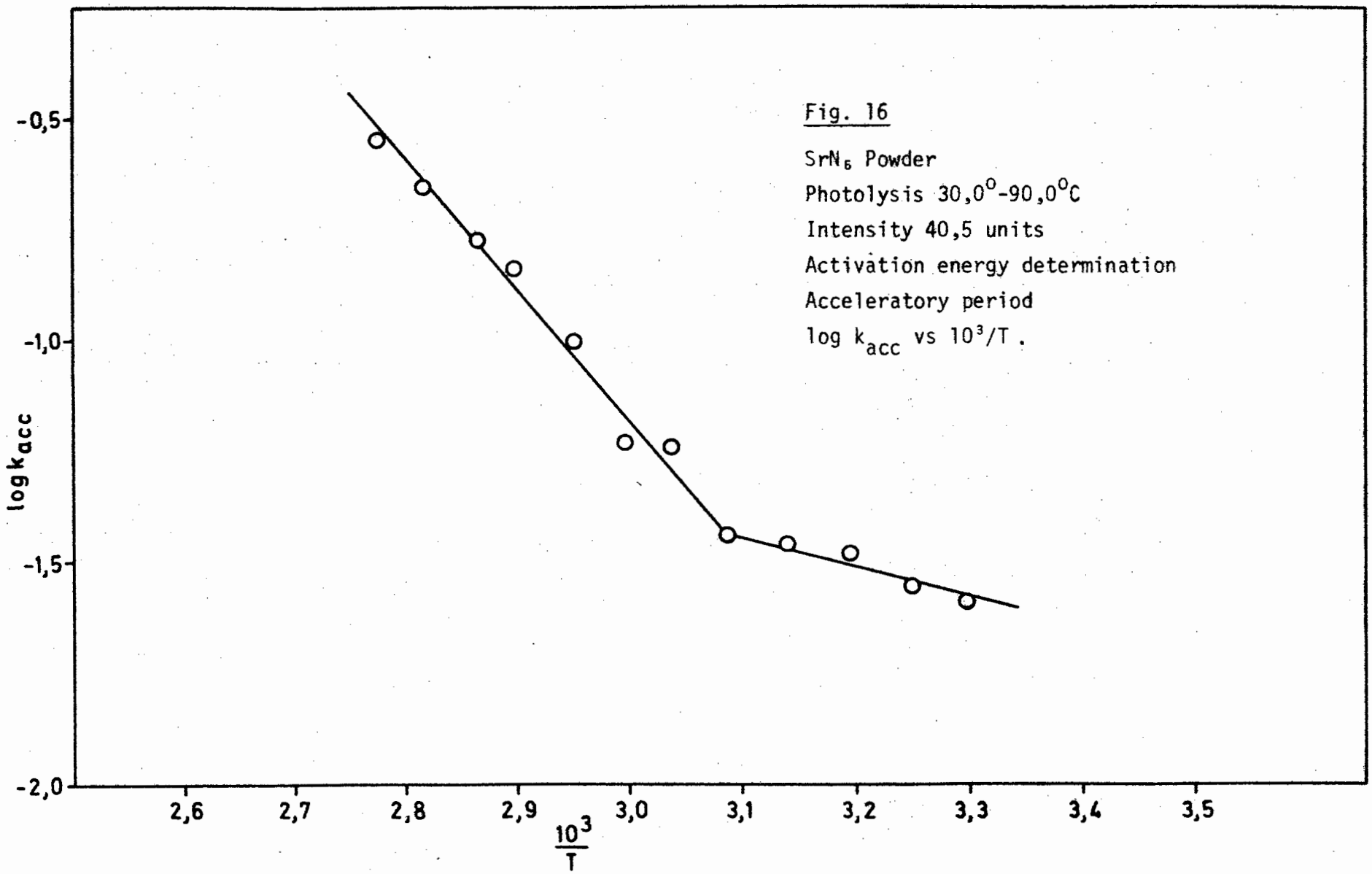

Fig. 16

SrN_6 Powder
Photolysis 30,0°-90,0°C
Intensity 40,5 units
Activation energy determination
Acceleratory period
log k_{acc} vs $10^3/T$.

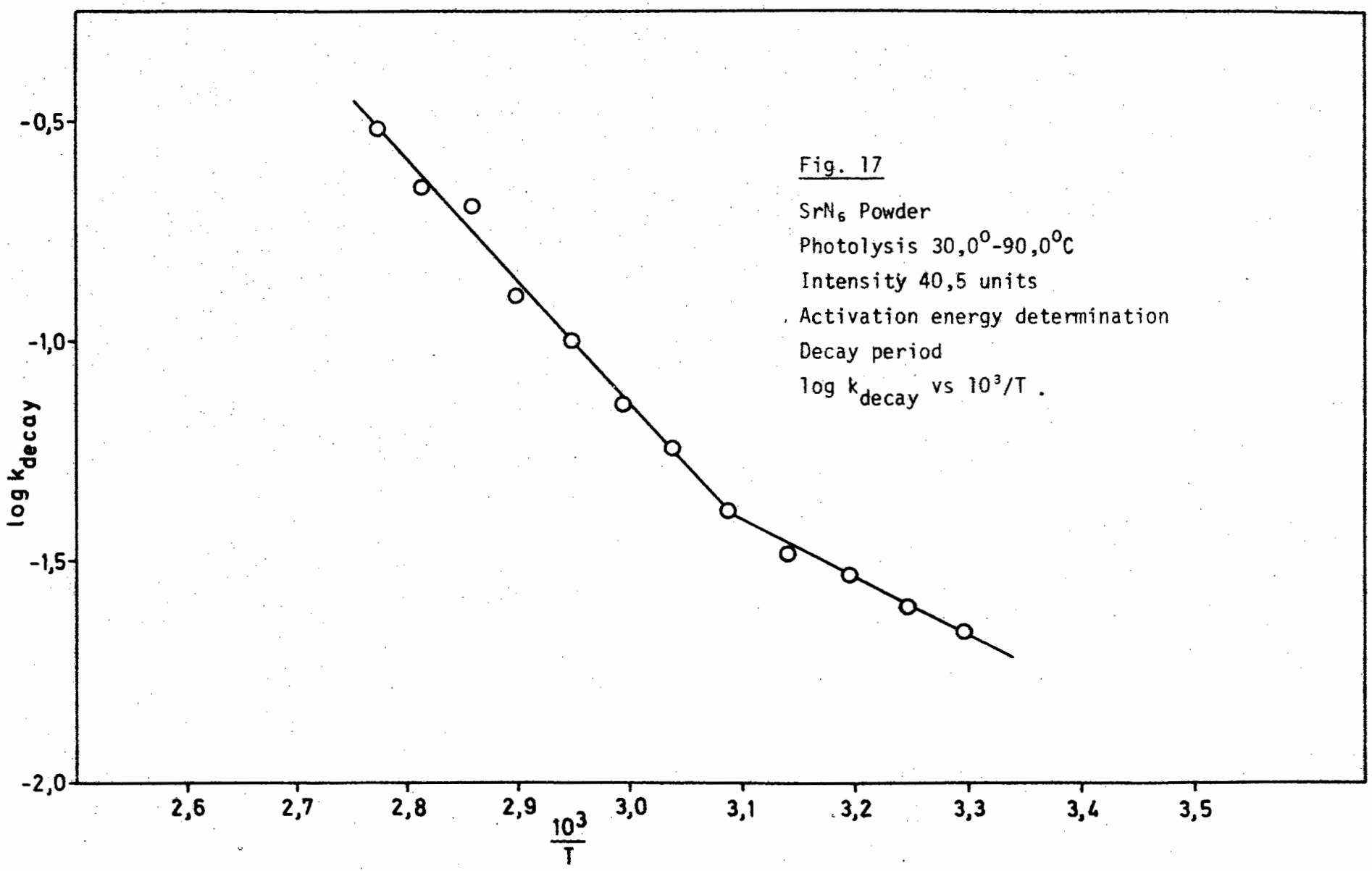

Fig. 17

SrN_6 Powder
Photolysis 30,0°-90,0°C
Intensity 40,5 units
Activation energy determination
Decay period
log k_{decay} vs $10^3/T$.

Table 3

Rate constants for the photolysis of barium azide powder.
Temperature range 27,0° - 100,0°C. Light intensity 25,0 units.

Temperature °C	Induction period min.	$k_{acc} \times 10^2$ min^{-1}	$k_{decay} \times 10^2$ min^{-1}
27,1	41,6	0,67	0,42
35,2	35,0	0,87	0,49
38,0	26,0	1,14	0,65
45,8	24,0	1,46	0,83
60,1	15,0	2,33	1,22
65,5	10,8	3,12	2,13
70,5	9,0	4,15	2,43
75,0	5,4	4,70	7,07
80,5	4,9	6,35	4,48
80,5	4,7	5,13	3,89
83,0	6,0	6,57	4,54
85,0	4,8	7,07	5,79
90,0	3,4	10,20	6,83
95,1	3,5	10,77	9,25
100,0	3,1	14,75	10,50

Table 4

Rate constants for the photolysis of strontium azide powder.
Temperature range 30,0° - 90,0°C. Light intensity 40,5 units.

Temperature °C	Induction period min.	$k_{acc} \times 10^2$ $min.^{-1}$	$k_{decay} \times 10^2$ $min.^{-1}$
30,2	30,0	2,60	2,18
35,0	29,0	2,75	2,42
40,1	28,0	3,25	2,93
45,5	26,0	3,39	3,26
51,0	22,5	3,55	4,70
56,0	20,0	5,70	5,61
61,2	16,0	5,85	7,00
66,2	15,8	9,60	9,92
72,0	12,8	14,30	12,42
76,3	11,5	16,82	20,08
82,0	10,0	21,50	21,90
87,5	8,0	28,10	30,00

Table 5

Activation energies for the photolysis of barium azide powder. Intensity 25,0 units.

Temperature range ^{o}C	Induction period Kcal.mol.$^{-1}$	Acceleratory period Kcal.mol.$^{-1}$	Decay period Kcal.mol.$^{-1}$
27,0 - 60,0	6,2	7,6	6,6
60,0 - 100,0	11,4	11,3	12,9

Table 6

Activation energies for the photolysis of strontium azide powder. Intensity 40,5 units.

Temperature range ^{o}C	Induction period Kcal.mol.$^{-1}$	Acceleratory period Kcal.mol.$^{-1}$	Decay period Kcal.mol.$^{-1}$
30,0 - 50,0	2,6	3,2	5,7
50,0 - 90,0	6,5	12,9	12,9

(id) The effect of variation of intensity of ultraviolet light source

In order to determine the molecularity of the photolytic process(es) taking place, for both barium and strontium azides in the two photolytic temperature ranges, the rate of photolysis was measured at different light intensities, keeping the decomposition temperature constant. The method of variation of light intensity has been described under section 3 on apparatus. For barium azide decomposition temperatures of 80,0°C and 50,0°C were chosen while for strontium azide decomposition temperatures of 40,0°C and 70,0°C were chosen. Thus the dependence of the duration of the induction period and rate constants for the acceleratory and decay reactions, on the intensity of the ultraviolet light source was determined for both azides.

In the equation

$$k = I^m + c \quad (c = \text{constant})$$

the molecularity m was determined by rewriting the equation in the form

$$\log k = m \log I + \log c.$$

The value of m was obtained by a method of least squares. Table 7 gives the rate constants at 50,0°C and 80,0°C at various light intensities for barium azide, and Table 8 gives the corresponding rate constants for strontium azide at decomposition temperatures of 40,0°C and 70,0°C. Table 9 gives the values of m for both compounds.

Table 7

Rate constants for the photolysis of barium azide powder at various light intensities.

Temperature ^{o}C	Intensity units	Induction period min.	$k_{acc} \times 10^2$ $min.^{-1}$	$k_{decay} \times 10^2$ $min.^{-1}$
50,0	41,0	9,5	13,33	10,60
	35,5	7,0	12,80	9,34
	33,5	7,8	8,60	8,30
	30,0	8,4	8,70	7,19
	27,2	9,5	3,62	4,11
	25,0	9,0	7,30	5,73
	22,0	11,0	4,70	3,43
	20,0	14,0	2,75	2,83
	15,1	19,0	1,98	1,27
80,0	25,9	28,0	3,54	3,42
	21,5	32,0	2,83	2,35
	20,8	25,0	2,81	2,19
	19,2	35,0	2,68	2,65
	14,6	35,0	2,19	1,69
	10,9	34,0	1,39	1,07
	9,1	58,0	1,18	1,00

Table 8

Rate constants for the photolysis of strontium azide powder at various light intensities.

Temperature ^{o}C	Intensity units	Induction period min.	$k_{acc} \times 10^2$ $min.^{-1}$	$k_{decay} \times 10^2$ $min.^{-1}$
40,0	64,0	1,5	35,70	14,21
	58,0	2,1	28,75	11,78
	52,0	2,8	22,40	10,61
	46,0	3,8	16,00	7,60
	42,0	4,0	15,25	6,43
	38,0	5,0	10,52	5,30
	35,2	6,0	8,98	4,50
	30,0	8,8	5,75	3,75
70,0	38,0	3,0	19,05	13,37
	34,0	3,6	15,00	9,51
	29,5	5,2	13,00	8,25
	26,1	5,4	10,92	7,00
	21,5	8,0	7,37	4,62
	18,6	10,0	5,08	3,57
	10,4	24,0	2,00	1,06

Table 9				
The value of m in the equation $k = I^m + c$.				
Salt	Temperature ^oC	Induction period	Acceleratory period	Decay period
BaN_6	50,0	0,7	2,0	2,1
	80,0	0,6	1,0	1,2
SrN_6	40,0	2,0	2,3	1,9
	70,0	1,6	1,8	1,9

Plots of k vs I^m (m corrected to the nearest whole number) have been plotted in Fig. 18, 19 and 20 for barium azide and Fig. 21, 22 and 23 for strontium azide.

(ie) Visual observations

The colour of the powder was observed at various stages of the photolytic decomposition. For barium azide photodecompositions were performed at 50,0^{o}C and 80,0^{o}C at an intensity of 33,0 units. The results were found to be identical at both temperatures. The salt had turned light brown on the surface facing the light by the end of the induction period; the lower surfaces were unchanged in colour at this point. At α = 0,08 the surface of the salt facing the light had turned dark brown while the surface away from the light had then turned light brown. The two surfaces changed slowly from these brown shades through to a charcoal black by the time the reaction had

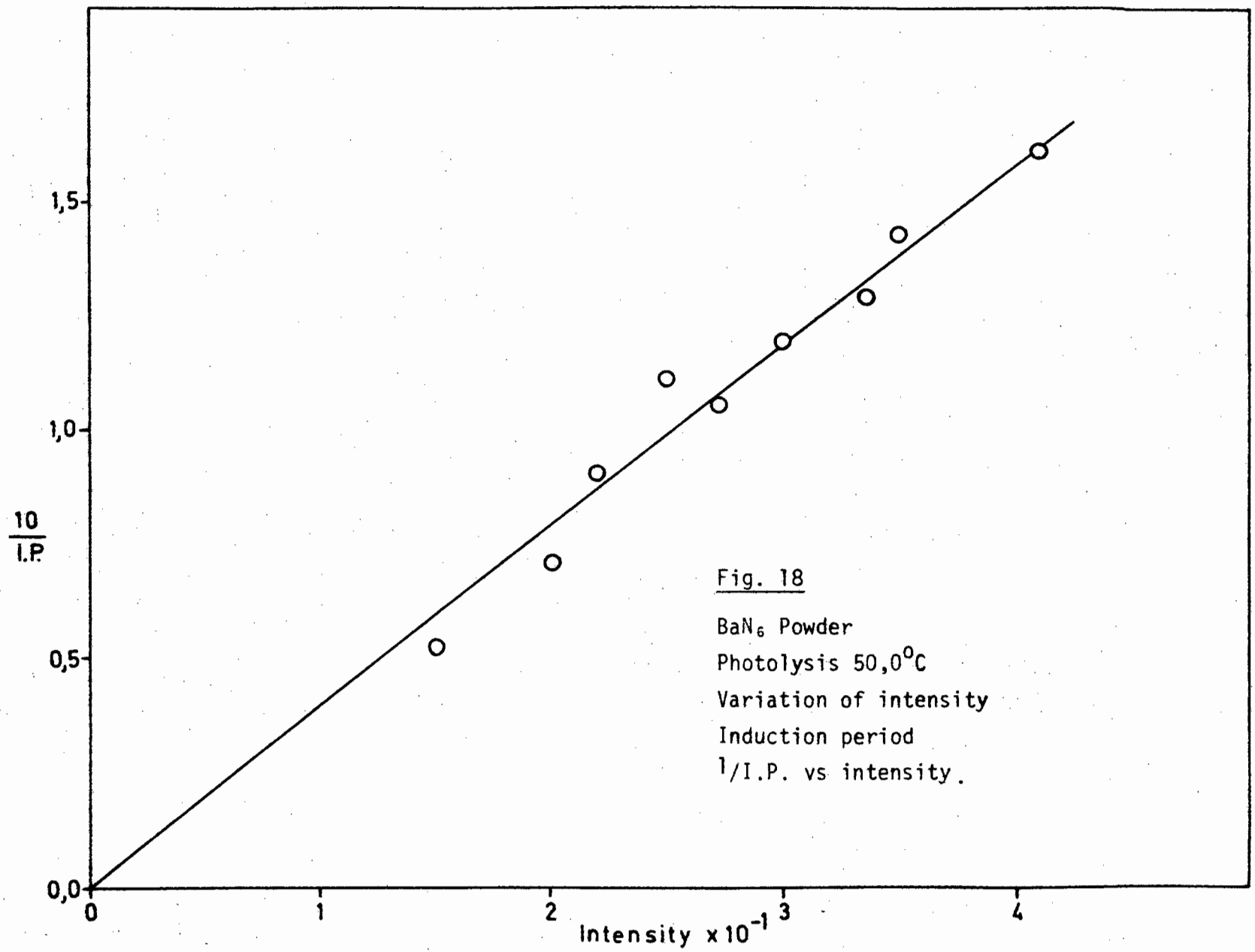

Fig. 18

BaN_6 Powder
Photolysis 50,0°C
Variation of intensity
Induction period
1/I.P. vs intensity.

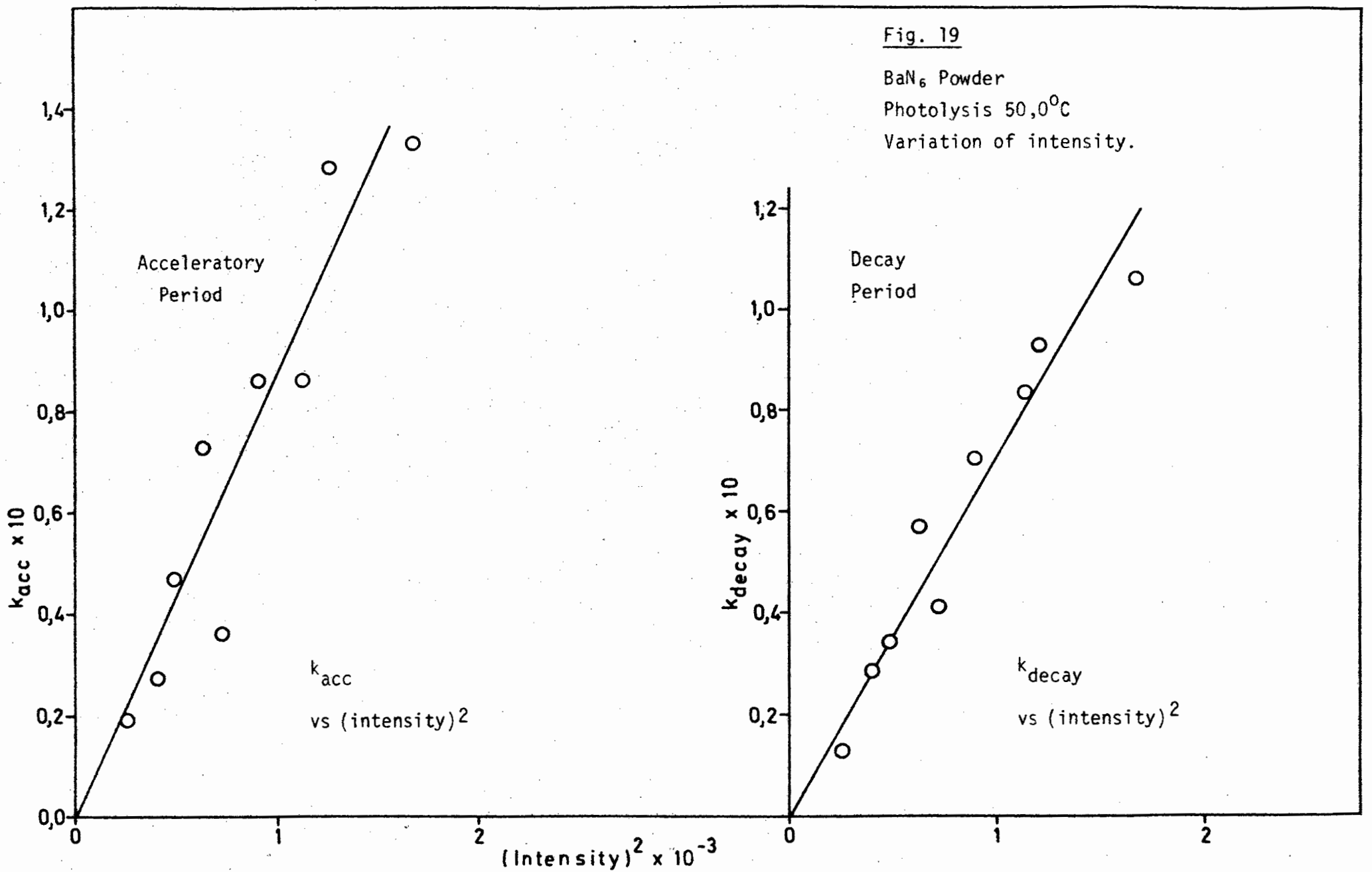

Fig. 19

BaN_6 Powder
Photolysis 50,0°C
Variation of intensity.

Fig. 20

BaN_6 Powder
Photolysis 80,0°C
Variation of intensity.

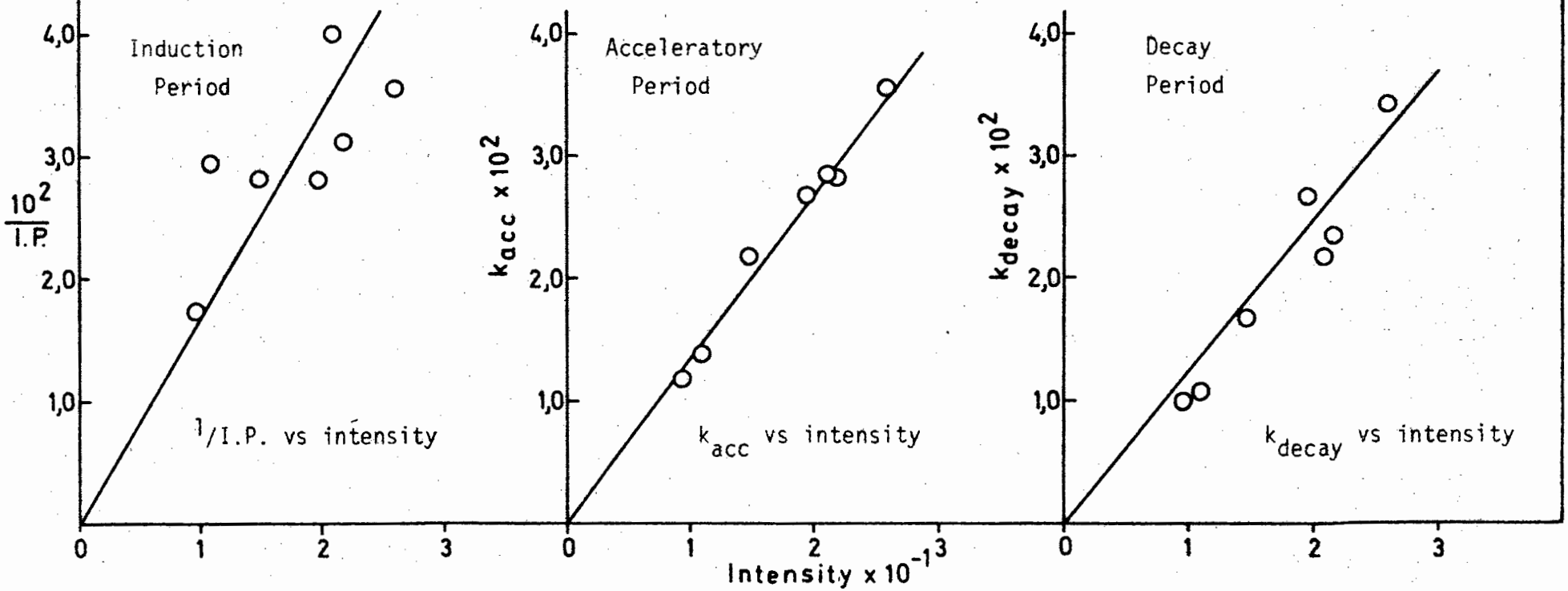

Fig. 21

SrN_6 Powder

Photolysis 40,0°C

Variation of intensity .

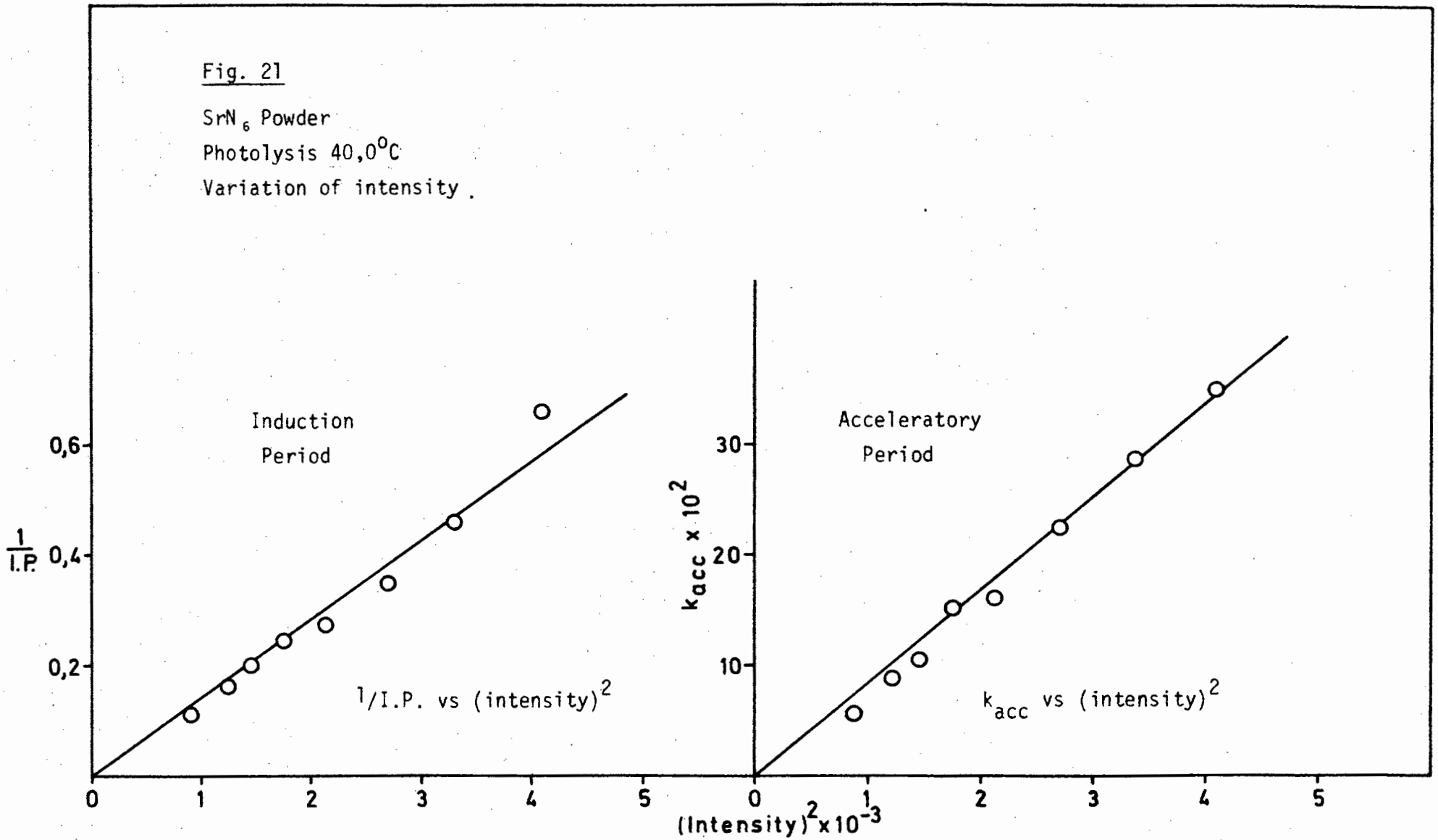

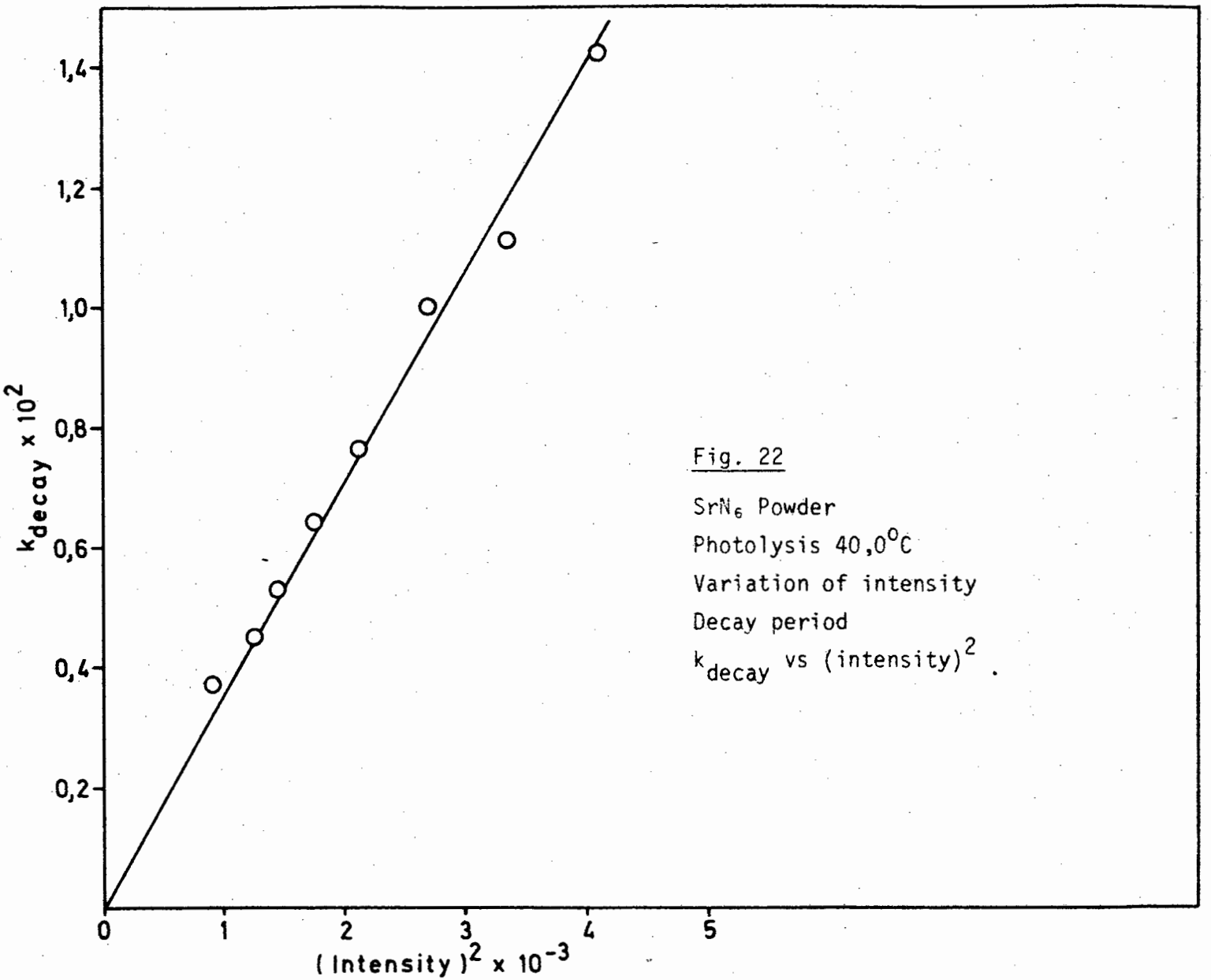

Fig. 22

SrN_6 Powder
Photolysis 40,0°C
Variation of intensity
Decay period
k_{decay} vs $(intensity)^2$.

Fig. 23

SrN_6 Powder

Photolysis 70,0°C

Variation of intensity.

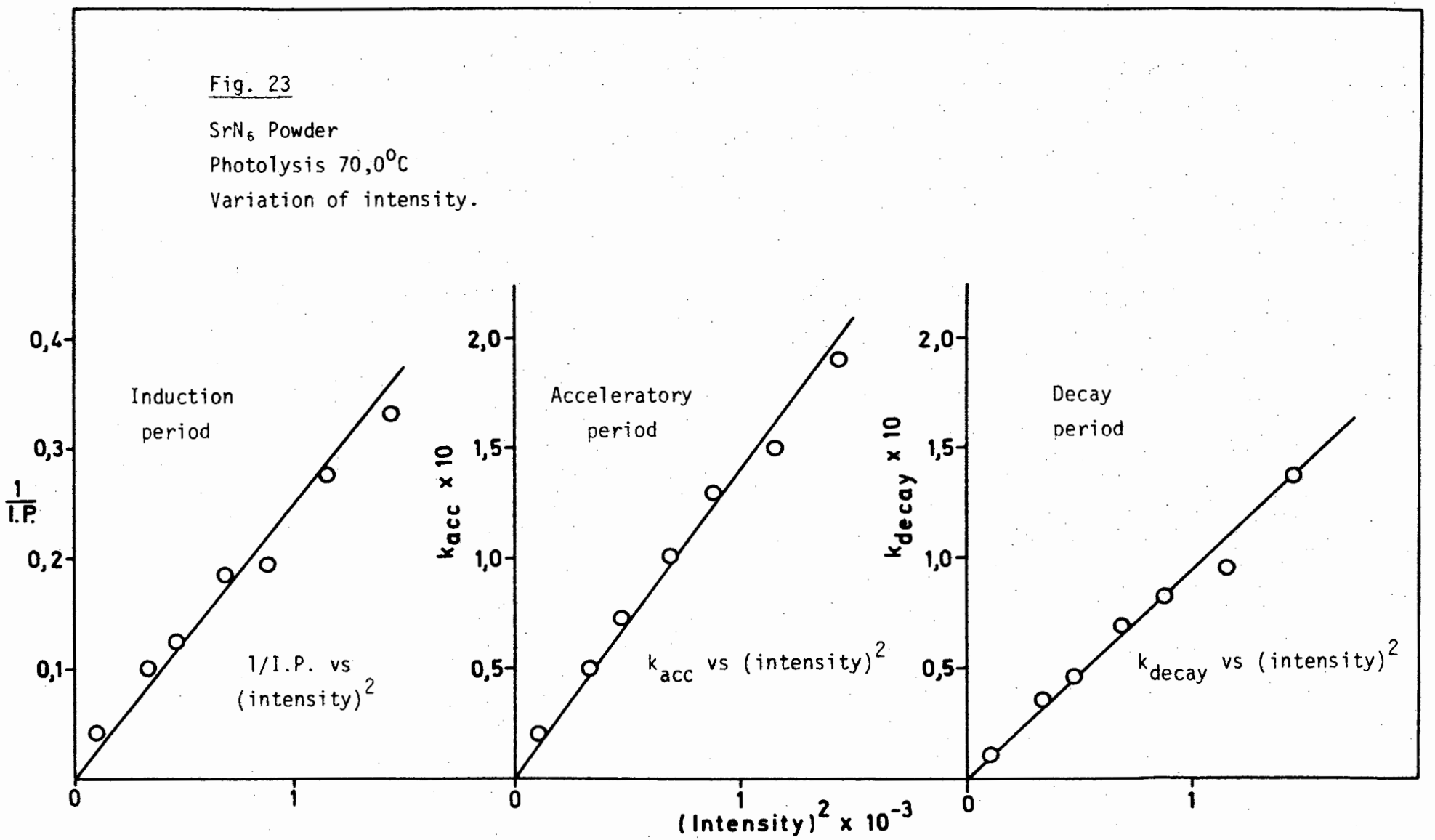

reached α = 0,30 and at α = 0,50 all the external surfaces of the particles were dark black. No further change in the colour of the particles was observed in the decay stage of the reaction.

The change in colour of strontium azide during a photolytic decomposition was observed at decomposition temperatures of 40,0°C and 70,0°C, using a light intensity of 33,0 units. As for barium azide the results at both temperatures were identical. However the changes in colour were different for strontium azide. At α = 0,01 the upper surface had turned light grey. The lower surface changed to this colour at α = 0,09 by which time the upper surface had changed to a darker grey. As the reaction continued these grey surfaces became darker and by the time the reaction had reached α = 0,40 all the external surfaces of the particles were dark black. No further change in the colour of the particles could be observed in the decay stage of the reaction.

(if) Interruption of a photodecomposition : dark rate determination

All photolytic decompositions of barium azide below 100,0°C and strontium azide below 90,0°C ceased the moment the light was switched off. Thus there was no measurable dark rate. On recommencing photolytic decompositions the runs continued as though no interruption had occurred.

(ig) Admittance of water vapour following an interruption

To investigate the presence of metallic nuclei at various stages of the photolytic decomposition of barium and strontium azides, water vapour (17 torr pressure) was introduced after the reaction had

reached a certain point. These decompositions are called "water interruptions".

The general procedure has been described under the experimental section. Prior to performing these tests an investigation was made of the effect of removing the sample from the furnace and allowing it to cool to room temperature after which photodecomposition was recommenced at the same temperature as before. The method was as follows. A photodecomposition was allowed to proceed to a desired point and then the shutter was closed and the furnace removed from the sample. Once the sample had cooled to room temperature, the furnace was repositioned around the sample which was given 6 min. to reach the decomposition temperature before the shutter was opened and photodecomposition resumed. It was found that the reaction continued as if no interruption had taken place. This test was done on barium azide at 50,0^{o}C and 80,0^{o}C using a light intensity of 27,5 units, as these were the decomposition temperatures and light intensities used when investigating the effect of water vapour. The same results were found when this test was carried out on strontium azide at decomposition temperatures of 40,0^{o}C and 80,0^{o}C using a light intensity of 33,0 units. Thus removal of the furnace from the sample and then replacing the furnace after the sample had cooled to room temperature, did not affect the kinetics of the subsequent reaction of either azide.

For barium azide water vapour was introduced for 1 min. at t = 0; midway along the induction period, and at α values of 0,01; 0,08; 0,21; 0,39; 0,43; 0,55 at the decomposition temperature of 50,0^{o}C. Using a decomposition temperature of 80,0^{o}C "water interruptions" for 1 min. were made at t = 0; midway along the induction period and at α values of 0,01; 0,08; 0,17; 0,30; 0,43; 0,58 on different samples of barium azide. Similarly "water interruptions" for 1 min. on strontium azide were made at t = 0; midway along the induction period and at α

values of 0,01; 0,12; 0,31; 0,42 at the decomposition temperature of 40,0°C. At the decomposition temperature of 80,0°C "water interruptions" were made for 1 min. at t = 0; midway along the induction period and at α values of 0,01; 0,14; 0,31; 0,40.

The results of these "water interruptions" were identical for both barium and strontium azides. At t = 0 and midway along the induction period water vapour appeared to have no effect on the subsequent reaction. A new induction period was detected (shorter than that of the uninterrupted run) when water vapour was introduced at α = 0,01. The subsequent reaction showed a decrease in k_{acc} and k_{decay}. Water vapour introduced at positions further along the decomposition curve caused subsequent reactions to proceed after longer induction periods followed by acceleratory and decay reactions. The durations of the new induction periods increased in time and the rates of k_{acc} and k_{decay} decreased as the point of interruption along the curve increased. Water vapour introduced at the inflection point and at positions in the decay reaction destroyed any further reaction. The final pressure of reactions following "water interruptions" at α = 0,01 and at positions further along the decomposition curve was reduced from that of an uninterrupted decomposition.

These results for barium azide are illustrated in Fig. 24 (decomposition temperature 80,0°C, intensity 27,5 units) and 25 (decomposition temperature 50,0°C, intensity 27,5 units); and for strontium azide in Fig. 26 (decomposition temperature 40,0°C, intensity 33,0 units) and Fig. 27 (decomposition temperature 80,0°C, intensity 33,0 units). The curves have not been normalized so as to show the effect of water vapour on the final pressure.

(ih) <u>The effect of filtering the high intensity arc with blue and ultraviolet transmission filters</u>

In order to determine which wavelengths of ultraviolet radiation were most effective for the photolysis of barium and strontium azides,

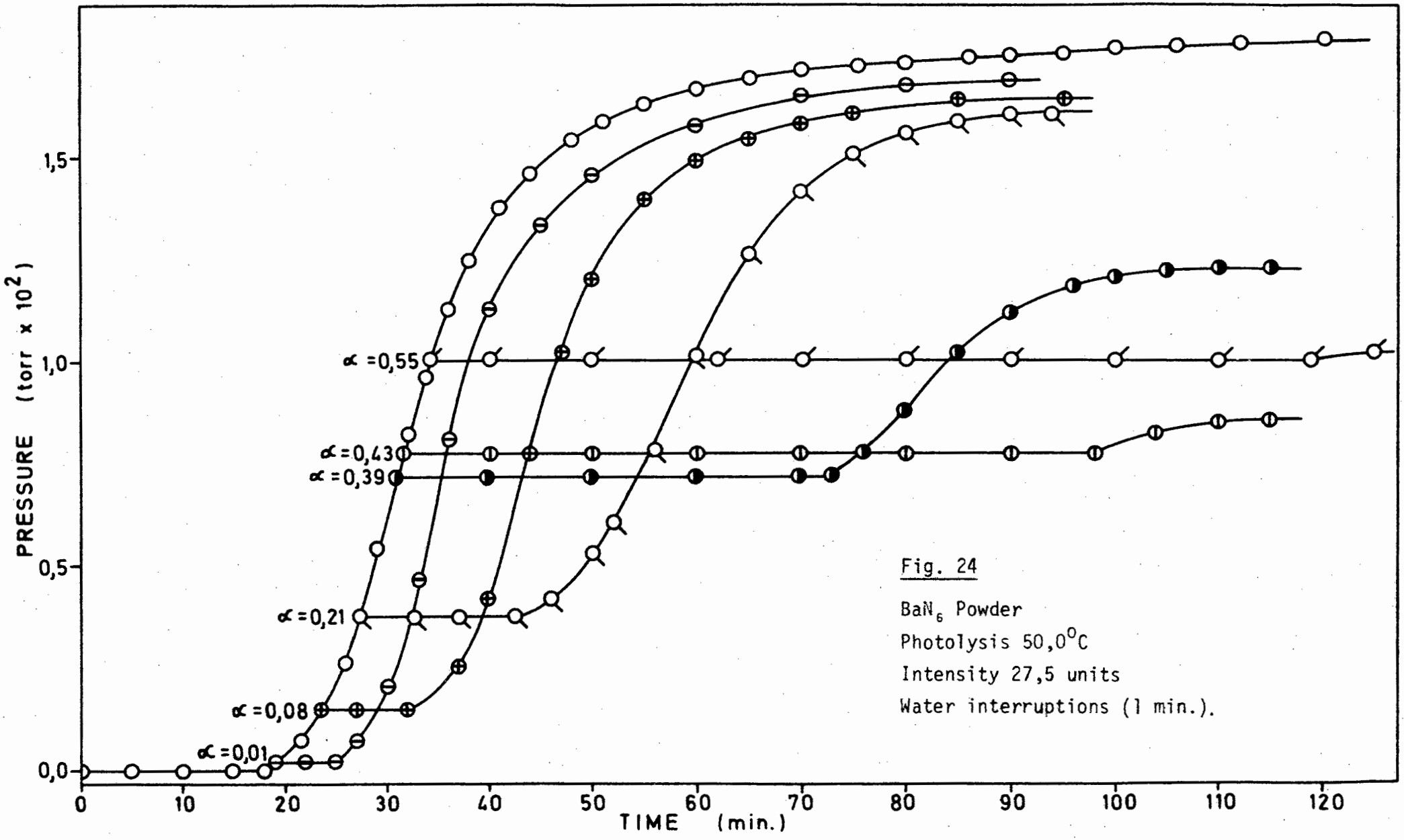

Fig. 24

BaN_6 Powder
Photolysis 50,0°C
Intensity 27,5 units
Water interruptions (1 min.).

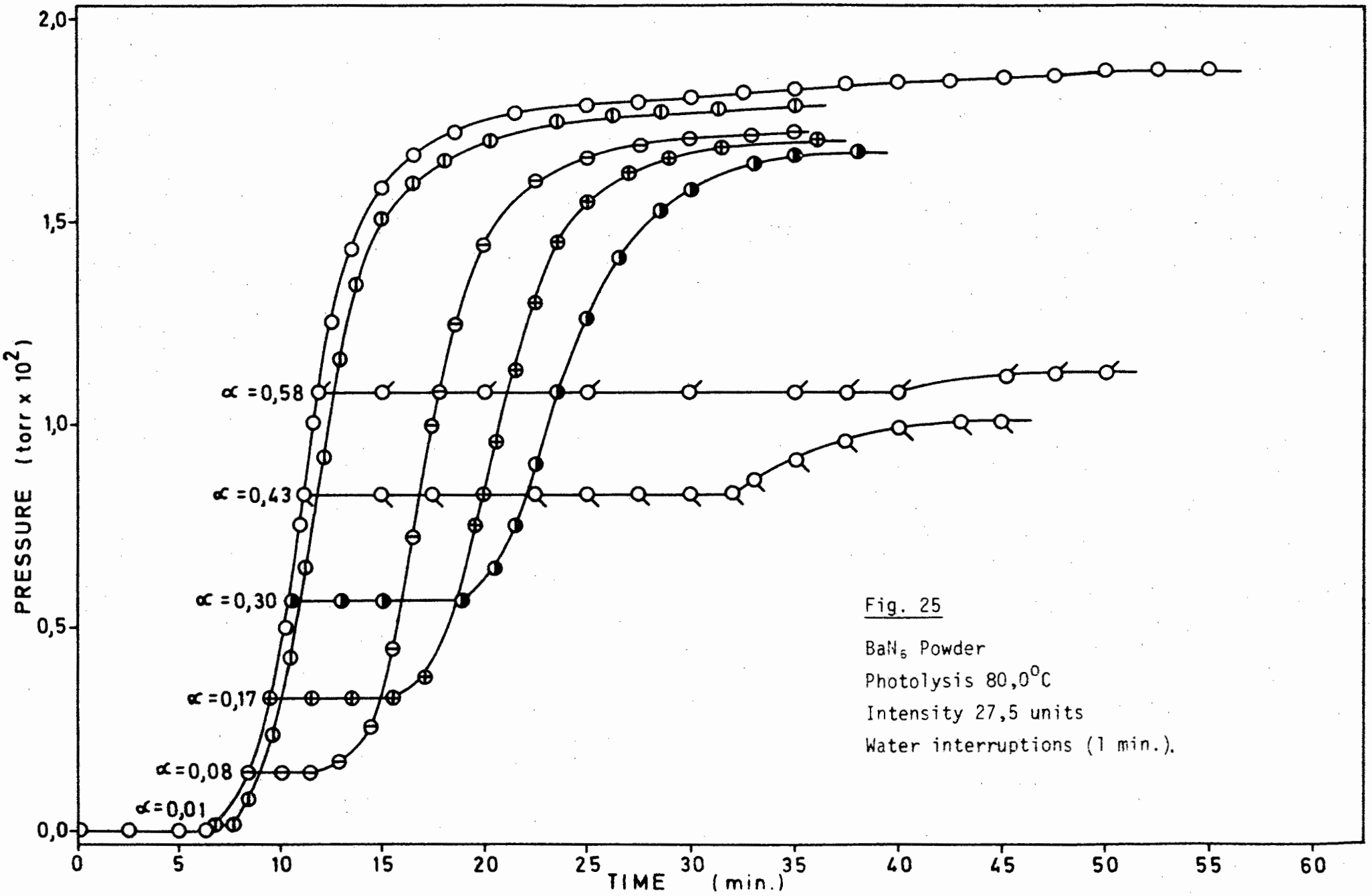

Fig. 25

BaN_6 Powder
Photolysis 80,0°C
Intensity 27,5 units
Water interruptions (1 min.).

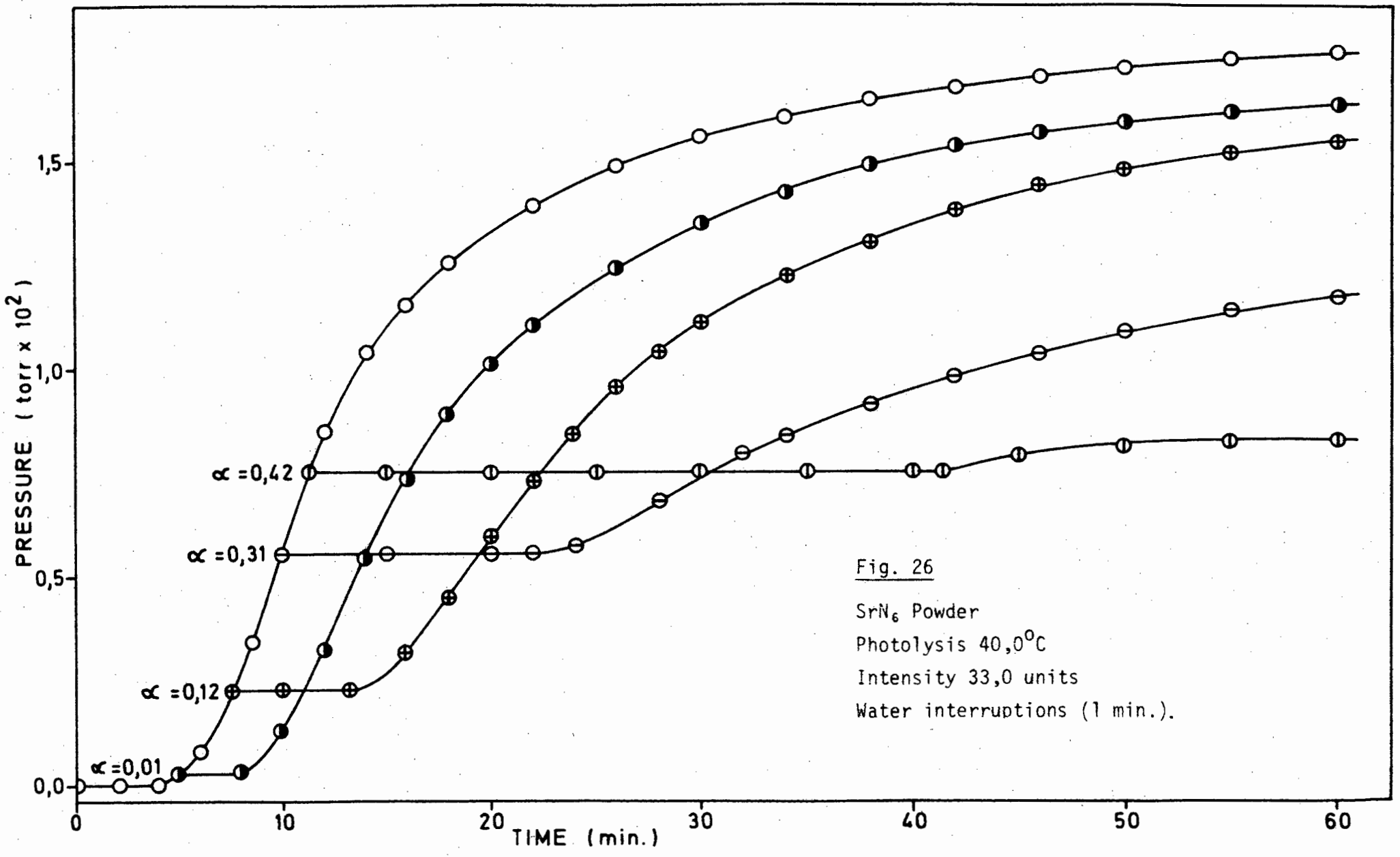

Fig. 26

SrN_6 Powder
Photolysis 40,0°C
Intensity 33,0 units
Water interruptions (1 min.).

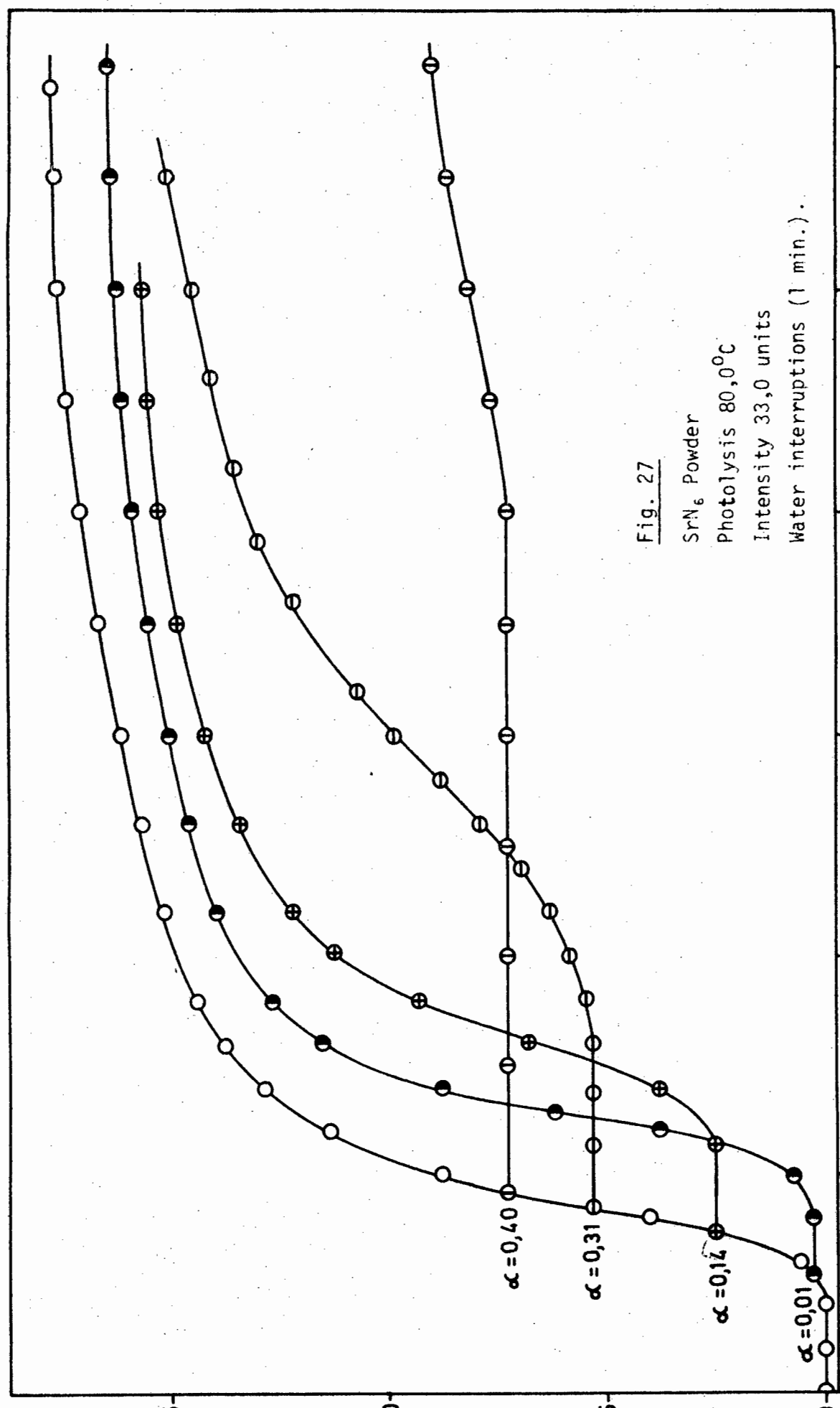

Fig. 27

SrN_6 Powder
Photolysis 80,0°C
Intensity 33,0 units
Water interruptions (1 min.).

various Schott filters were employed.

Photodecompositions were done at 50,0°C and 80,0°C for barium azide and at 70,0°C for strontium azide. An incident light intensity of 27,0 units was used for both salts.

Table 10 lists the Schott filters and their Chance equivalents. The light intensities transmitted by the filters are also listed.

Table 10

Filters used during the photolysis of barium and strontium azide powders.

Schott filter	Chance filter	Transmitted λ Å	Transmitted intensity
3mm UG5	OX7	2200 - 4200	0,16
1mm UG1	-	2800 - 4200	0,20
5mm BG12	OY10	3300 - 4900	0,26

The effects of the filters were identical for both barium and strontium azides. No reaction was observed when the 5mm BG12 filter was used. The 3mm UG5 and the 1mm UG1 filter caused a reduction in reaction rate, the latter filter causing a greater reduction than the former. These results are illustrated in Fig. 28 and 29 for barium azide and Fig. 30 for strontium azide.

(ii) The determination of the nature of photolytic nuclei

At the end of the induction period the crystal is a function of the number of nuclei, their spatial distribution , the size and shape

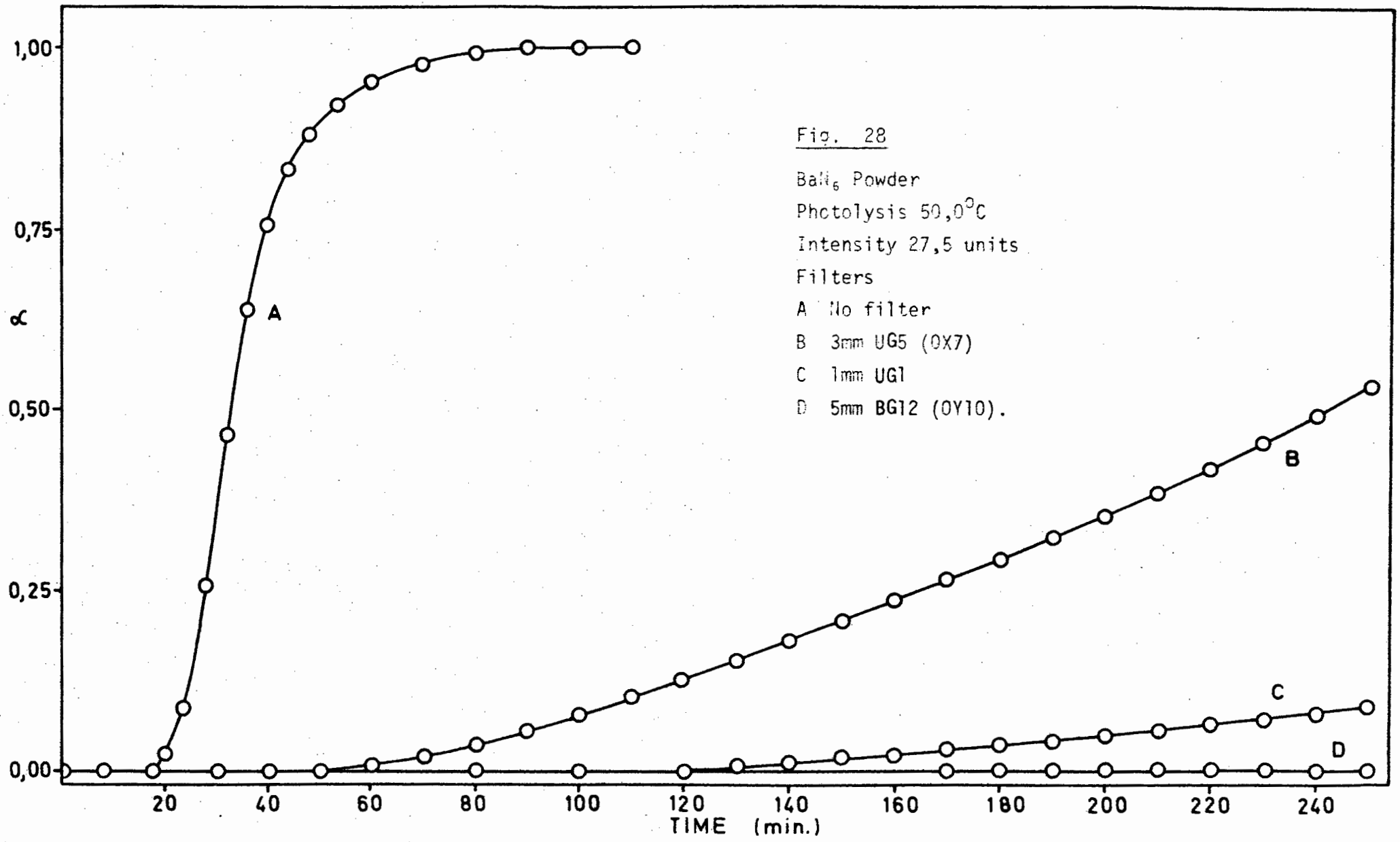

Fig. 28

BaN_6 Powder
Photolysis 50,0°C
Intensity 27,5 units
Filters
A No filter
B 3mm UG5 (OX7)
C 1mm UG1
D 5mm BG12 (OY10).

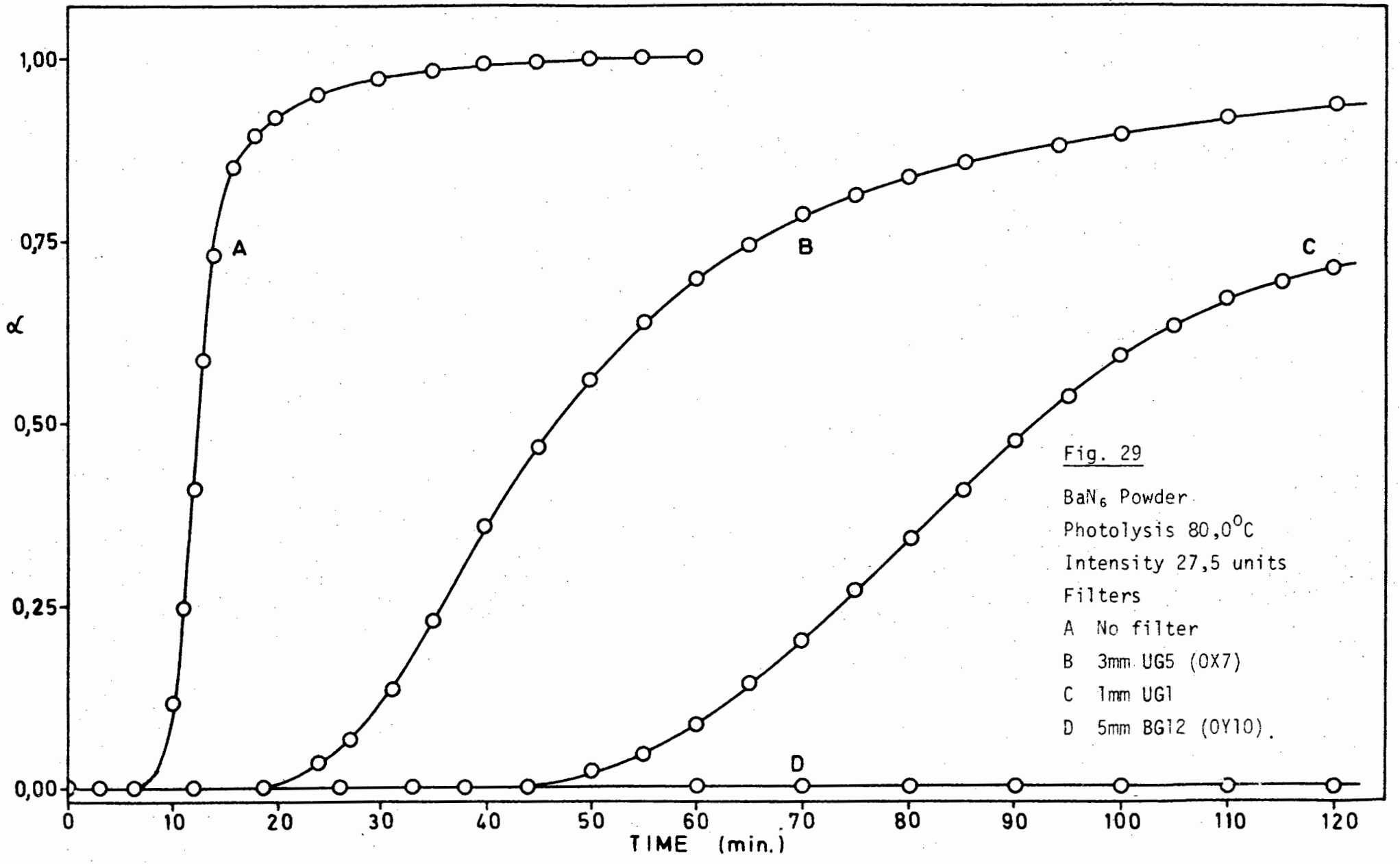

Fig. 29

BaN_6 Powder
Photolysis 80,0°C
Intensity 27,5 units
Filters
A No filter
B 3mm UG5 (0X7)
C 1mm UG1
D 5mm BG12 (0Y10).

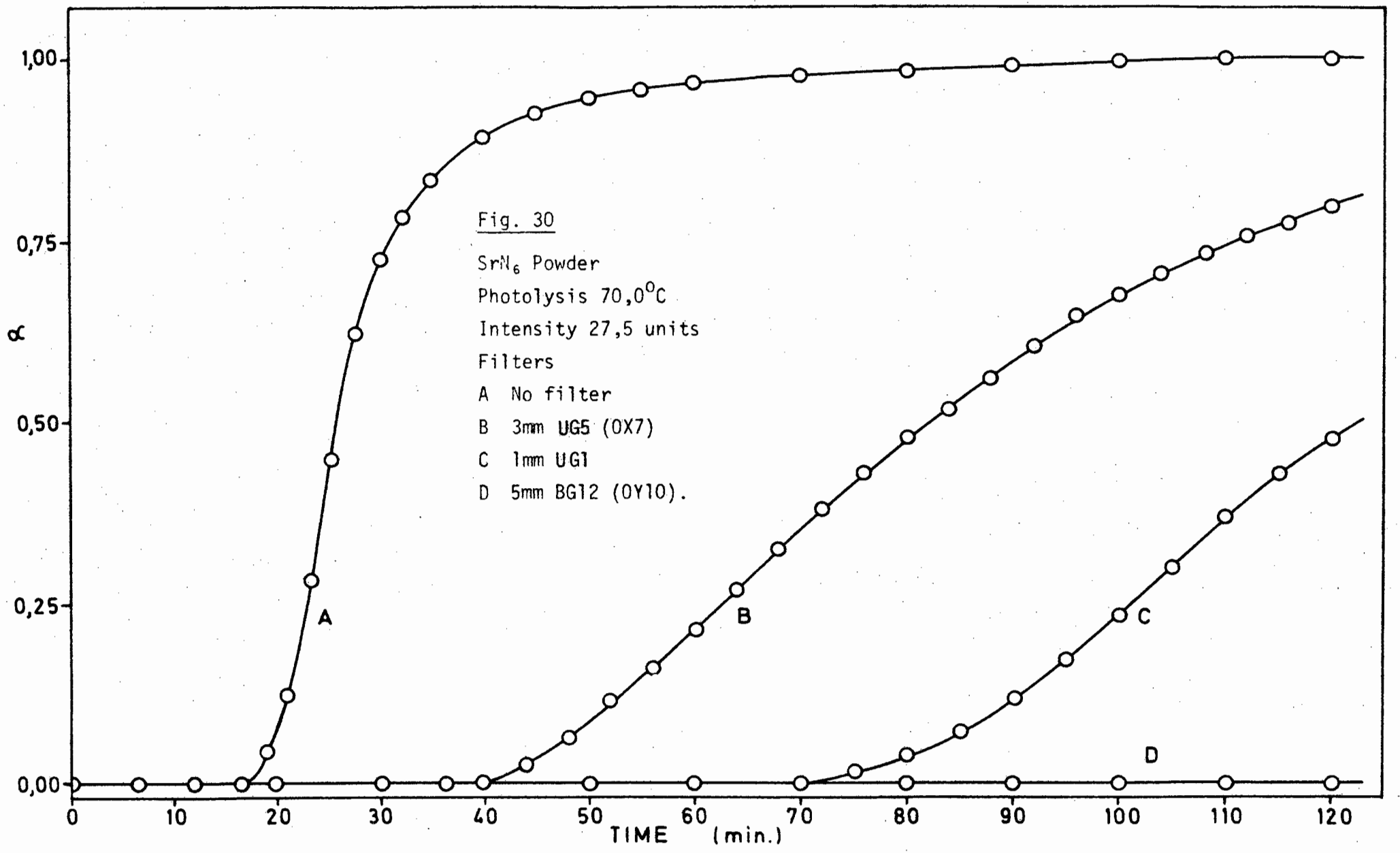

Fig. 30

SrN_6 Powder
Photolysis 70,0°C
Intensity 27,5 units
Filters
A No filter
B 3mm UG5 (0X7)
C 1mm UG1
D 5mm BG12 (0Y10).

of the nuclei and a variety of properties of the nuclei themselves (e.g. chemical, crystallographic and electronic structure). It was desired to ascertain whether the photodecomposition of barium and strontium azides would involve similar reaction centres i.e. nuclei, to those involved in thermal decomposition. This information was obtained in the following manner.

Barium azide was decomposed thermally at 116,0°C until the reaction had reached the end of the induction period. The furnace was then removed from the sample. Once the furnace had cooled to 85,0°C it was replaced in position around the cell. After a warm-up time of 6 min. photolysis commenced using a light intensity of 27,5 units. It was found that photolysis commenced without an induction period and the rate of reaction was the same as that expected if the decomposition had been entirely photolytic. On reversal of the procedure i.e. photolysis of barium azide at 85,0°C (intensity 27,5 units) till the end of the induction period and then thermal decomposition at 116,0°C, the thermal reaction of pre-irradiated barium azide began without an induction period.

Similar treatments were carried out on strontium azide. A thermal decomposition temperature of 126,0°C was used and photolysis was carried out at 73,0°C (light intensity 33,0 units). The results for strontium azide were identical to those found with barium azide.

(ii) Pellets

Photodecompositions in the temperature range 30,0° - 100,0°C for barium azide pellets and strontium azide pellets in the temperature range 30,0° - 90,0°C were found to have the same percentage decomposition as a thermal decomposition of powder at 130,0° i.e. 95,0% for barium azide (114) and 71,2% for strontium azide (89). These pellets

weighed 8mg, were 5mm in diameter and 0,25mm thick. However pellets of either barium or strontium azide, weighing 800mg and having a thickness and diameter of 1,0mm and 5mm respectively had percentage decompositions of 90,0% for barium azide and 65,0% for strontium azide. The reaction of these pellets of both azides, was extremely slow for the last 10 - 13% of decomposition. (This could be due to the increased opacity of the layer of barium or strontium metal to the ultraviolet light.) Pellets weighing 8mg were used for all tests described below.

(iia) Shape of decomposition curve, mathematical analyses and reproducibility

The shape of the decomposition curves obtained from photolysed pellets of barium or strontium azide (pressed at either 600 lb/sq.in. or 2000 lb/sq.in.) differed from those obtained from photolysed powder. The shapes obtained from pellets of the two azides were almost identical, irrespective of pelleting pressure. After an induction period a constant evolution of gas occurred until $\alpha = 0,22$ for barium azide and $\alpha = 0,20$ for strontium azide. This in turn was followed by a decay reaction which obeyed the unimolecular decay law. The fit of this analysis was from $0,22 < \alpha < 0,96$ for barium azide and $0,20 < \alpha < 0,93$ for strontium azide. Fig. 31 and 32 show typical α vs t curves, with analysis for barium azide pellets decomposed at 80,0°C (pelleting pressure of 2000 lb/sq.in.) and 50,0°C (pelleting pressure 600 lb/sq.in.). A light intensity of 25,0 units was used for both decompositions. Similar curves for pellets of strontium azide are shown in Fig. 33 and 34. Fig. 33 shows a pellet (pelleting pressure 2000 lb/sq.in.) photolysed at 73,0°C; Fig. 34 shows a pellet (pelleting pressure 600 lb/sq. in.) photolysed at 47,0°C. A light intensity of 30,0 units was used for the decomposition of both pellets.

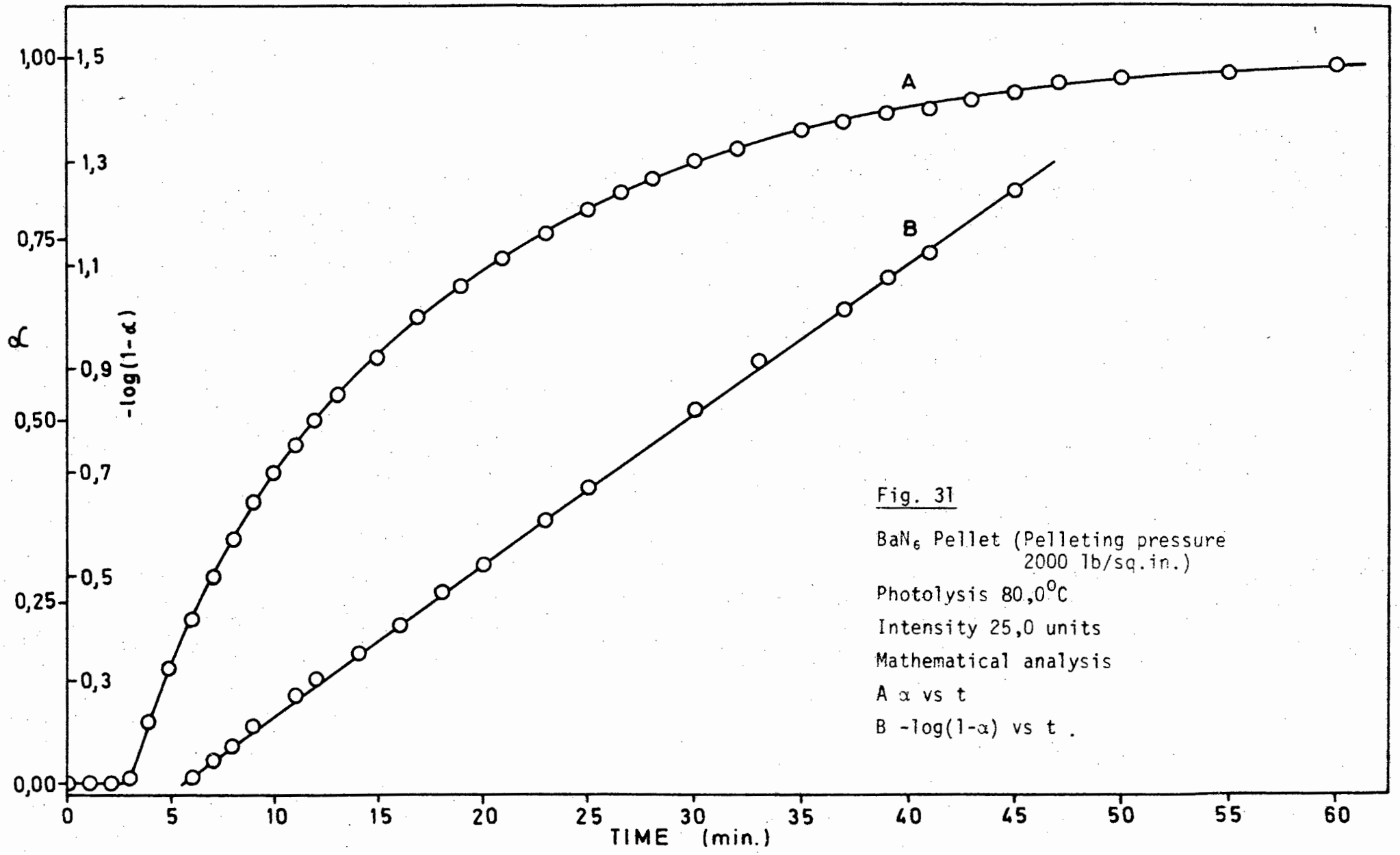

Fig. 31

BaN_6 Pellet (Pelleting pressure 2000 lb/sq.in.)

Photolysis 80,0°C

Intensity 25,0 units

Mathematical analysis

A α vs t

B $-\log(1-\alpha)$ vs t .

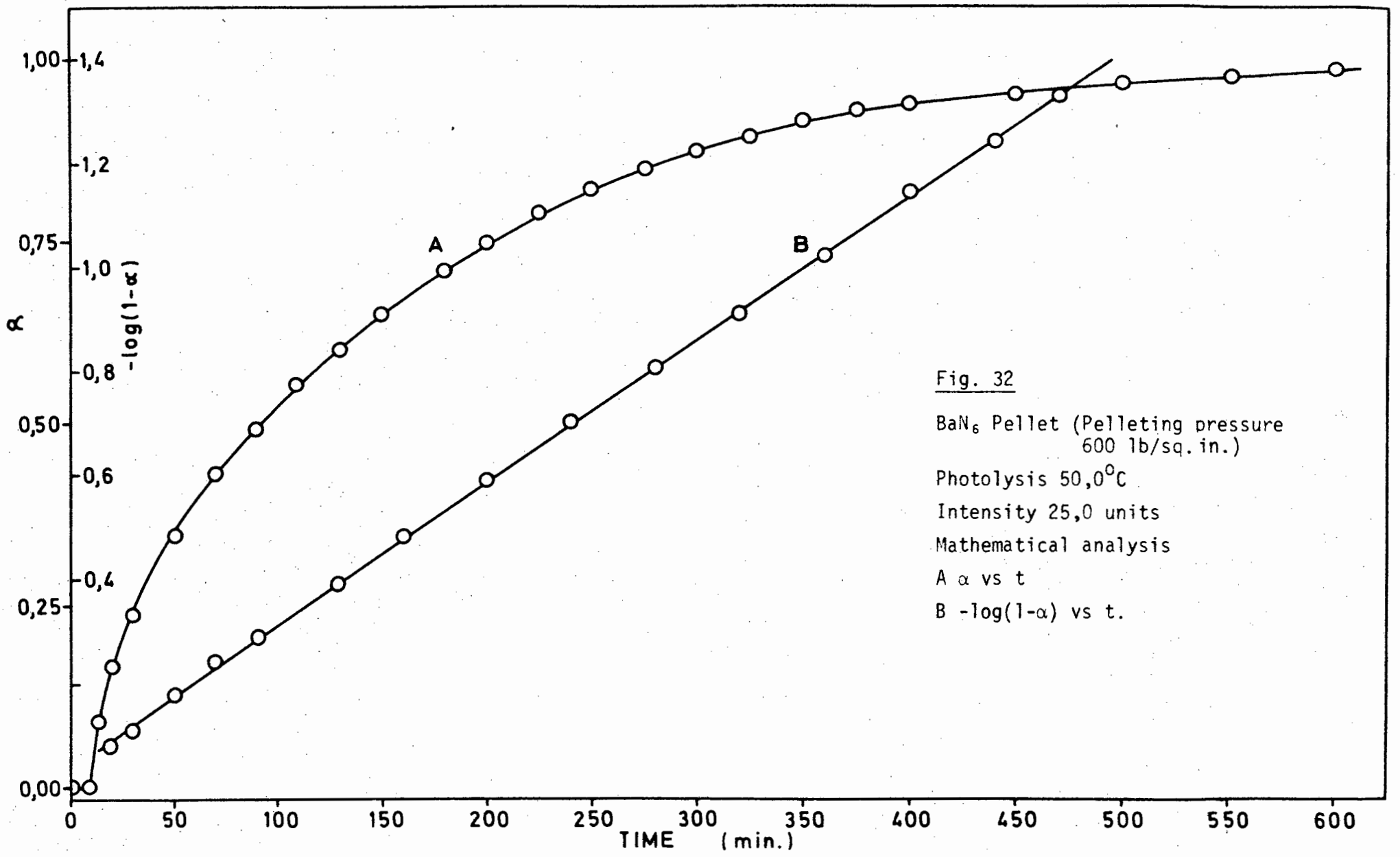

Fig. 32

BaN_6 Pellet (Pelleting pressure 600 lb/sq. in.)

Photolysis 50,0°C

Intensity 25,0 units

Mathematical analysis

A α vs t

B $-\log(1-\alpha)$ vs t.

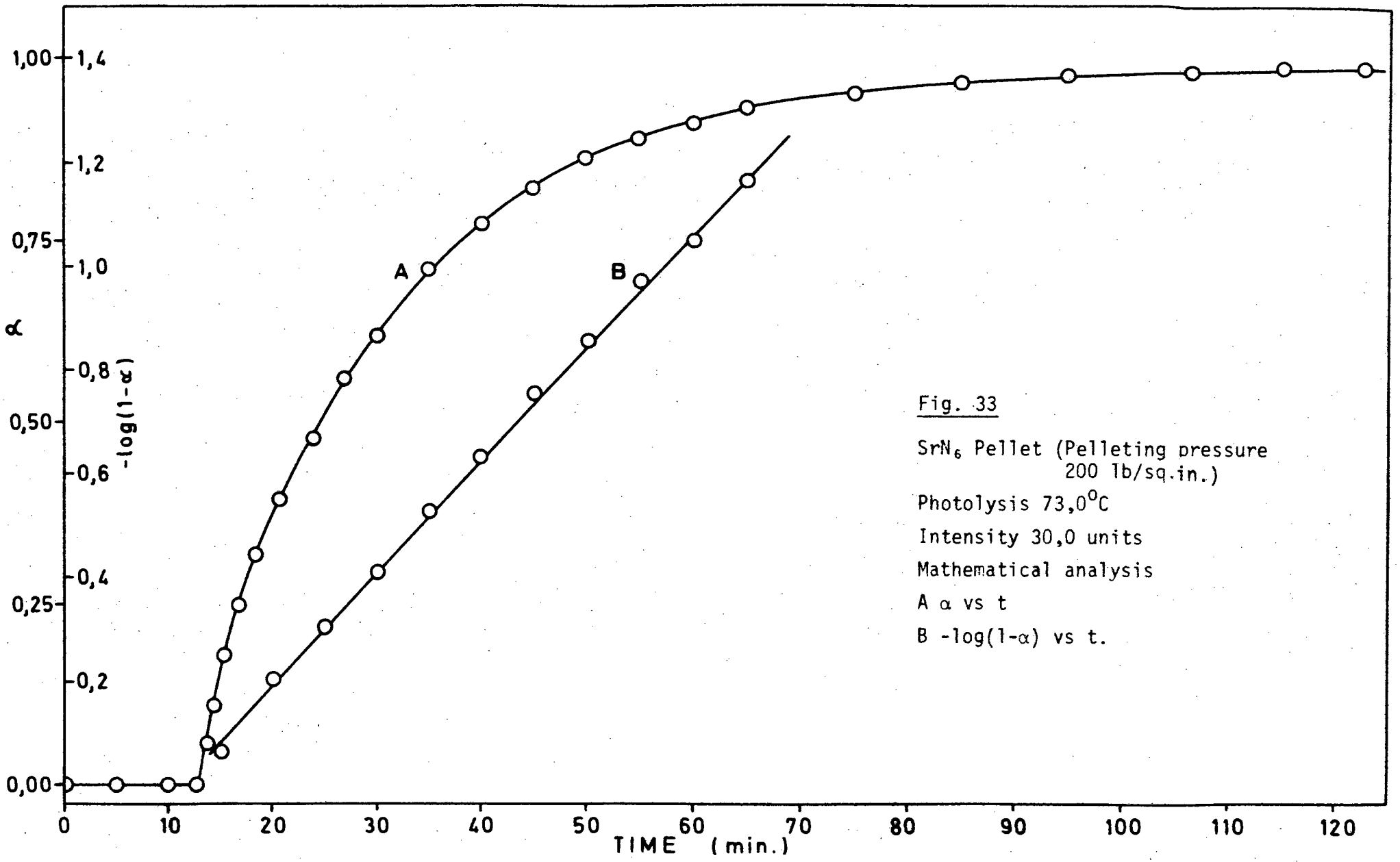

Fig. 33

SrN_6 Pellet (Pelleting pressure 200 lb/sq.in.)

Photolysis 73,0°C

Intensity 30,0 units

Mathematical analysis

A α vs t

B $-\log(1-\alpha)$ vs t.

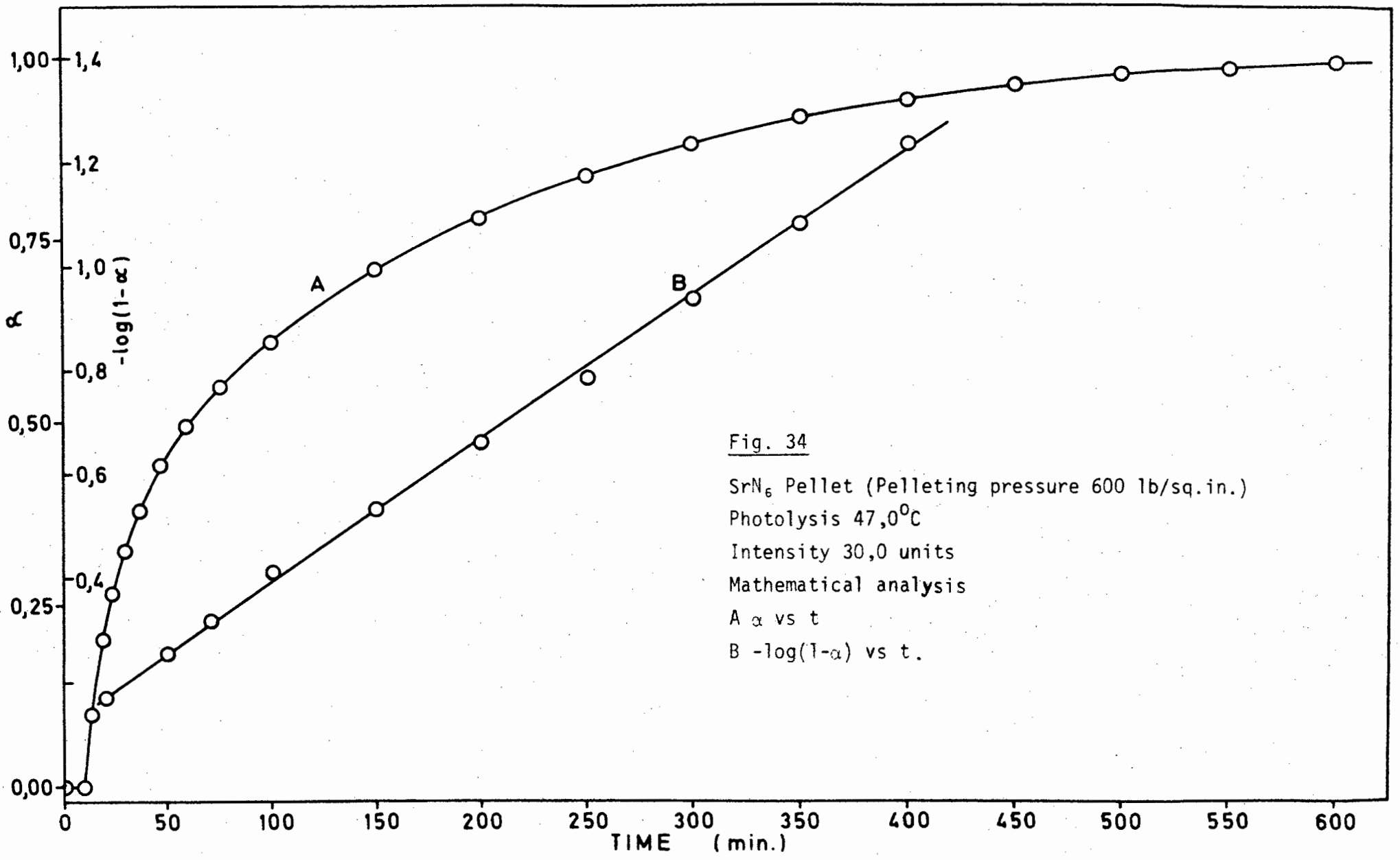

Fig. 34

SrN_6 Pellet (Pelleting pressure 600 lb/sq.in.)
Photolysis 47,0°C
Intensity 30,0 units
Mathematical analysis
A α vs t
B $-\log(1-\alpha)$ vs t.

Photolysis of barium azide pellets irrespective of pelleting pressure, showed no reproducibility. The nature of the irreproducibility of the photolysis of three pellets each pressed at 2000 lb/sq.in. and decomposed at 80,0^{o}C with a light intensity of 25,0 units is shown in Fig. 35. Two of these curves show a burst of gas after the induction period followed by a smooth decomposition curve. This burst of gas coincides with the fracture of the pellet. Analyses for these curves were unobtainable. When a completely smooth decomposition curve was obtained, the pellet was found to be unfractured at the end of the decomposition. Reproducibility for the photolysis of strontium azide pellets was also not obtainable. The nature of the irreproducibility is indicated in Fig. 36 for a pellet pressed at 2000 lb/sq.in. and decomposed at 70,0^{o}C with a light intensity of 30,0 units.

(iib) Evaluation of activation energies

Since no reproducible results could be obtained for either barium or strontium azide pellets, activation energies were determined using the split run technique. Due to the nature of the curve the split run technique was used on the decay reaction, and only on pellets which did not fracture at the end of the induction period. With this method the decomposition was allowed to proceed at the lowest temperature at which the first rate constant was to be calculated. After an appropriate time the run was interrupted by closing the shutter and removing the furnace from the sample. The temperature of the furnace was then adjusted to the next higher temperature, while the sample was allowed to cool to room temperature. When the furnace had reached the new temperature it was replaced in position around the

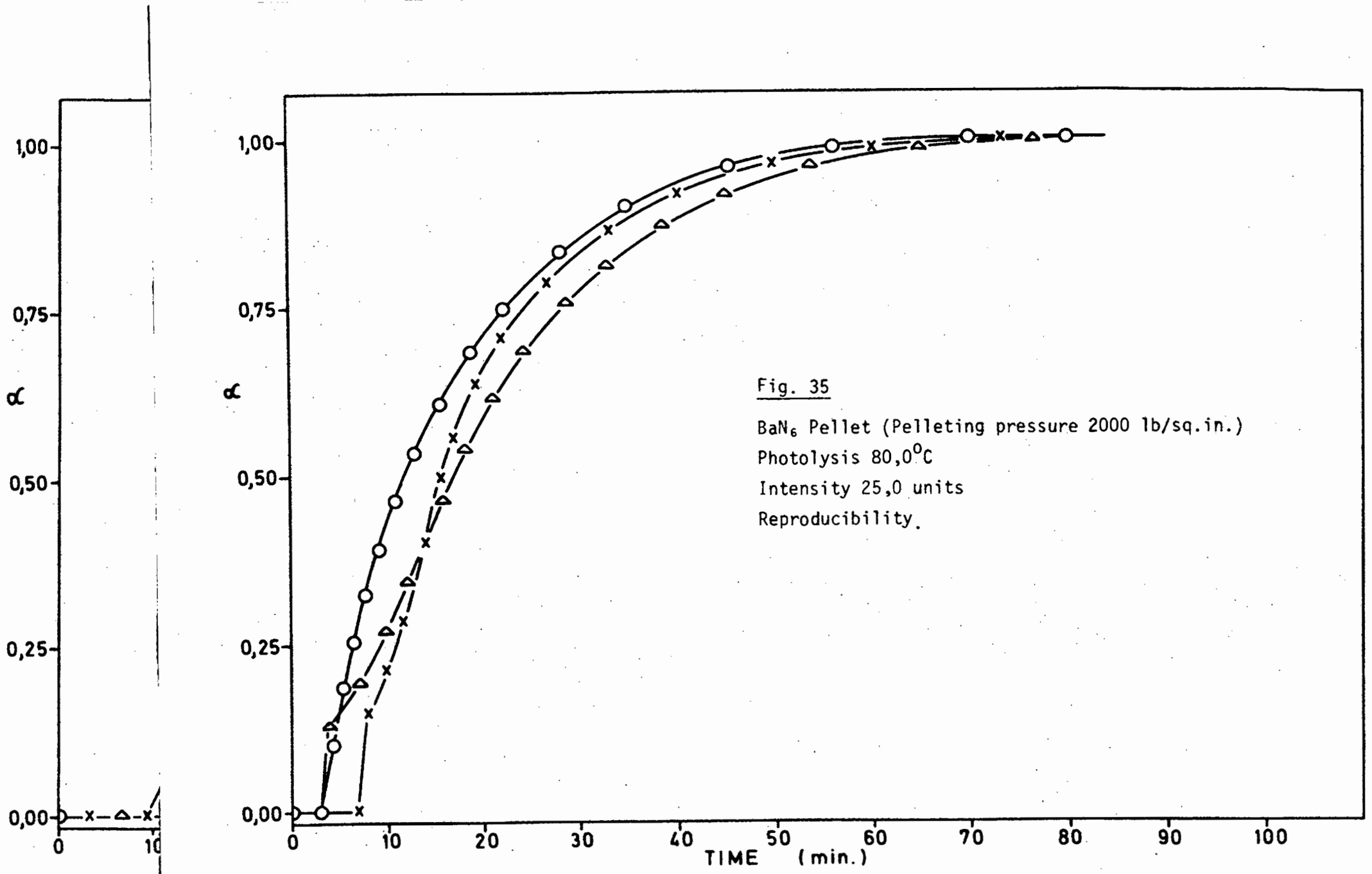

Fig. 35

BaN_6 Pellet (Pelleting pressure 2000 lb/sq.in.)
Photolysis 80,0°C
Intensity 25,0 units
Reproducibility.

decomposition cell and photodecomposition was commenced after the sample had been given 6 min. in which to reach the temperature of the furnace. Five or six rate constants could be found for the decay reaction using one pellet.

Before the split run technique was applied for determination of activation energies a check was made that interrupting a run had no effect on the subsequent photolytic decomposition of both barium and strontium azide pellets. This was done by allowing a decomposition to proceed till a certain point and then interrupting it by removing the furnace from the sample after the shutter had been closed. When the sample had cooled to room temperature the furnace was replaced around the sample. After 6 min. the shutter was opened and photo-decomposition was allowed to continue. It was found that the reaction for both barium and strontium azide pellets continued as though no interruption had taken place.

Activation energies for the decay reactions of both barium and strontium azide pellets pressed at 600 lb/sq.in. and 2000 lb/sq.in. were determined. It was assumed, from the results obtained from powdered barium azide, that a change in activation energy would be expected at 60,0^{o}C. Thus activation energies were determined in the temperature ranges 30,0^{o} - 60,0^{o}C and 60,0^{o} - 100,0^{o}C for pellets of barium azide. Similarly it was expected that a change in activation energy at 50,0^{o}C would be observed for strontium azide pellets, thus demanding the determination of activation energies in the temperature ranges 30,0^{o} - 50,0^{o}C and 50,0^{o} - 90,0^{o}C. A light intensity of 25,0 units was used for the split runs on barium azide pellets while a light intensity of 30,0 units was used for the split runs on strontium azide pellets.

The respective logarithms of the rate constants were plotted against the inverse of the absolute temperatures of decomposition.

Fig. 37

BaN_6 Pellet
Photolysis 30,0° - 60,0°C
Intensity 25,0 units
Activation energy determination (decay reaction).

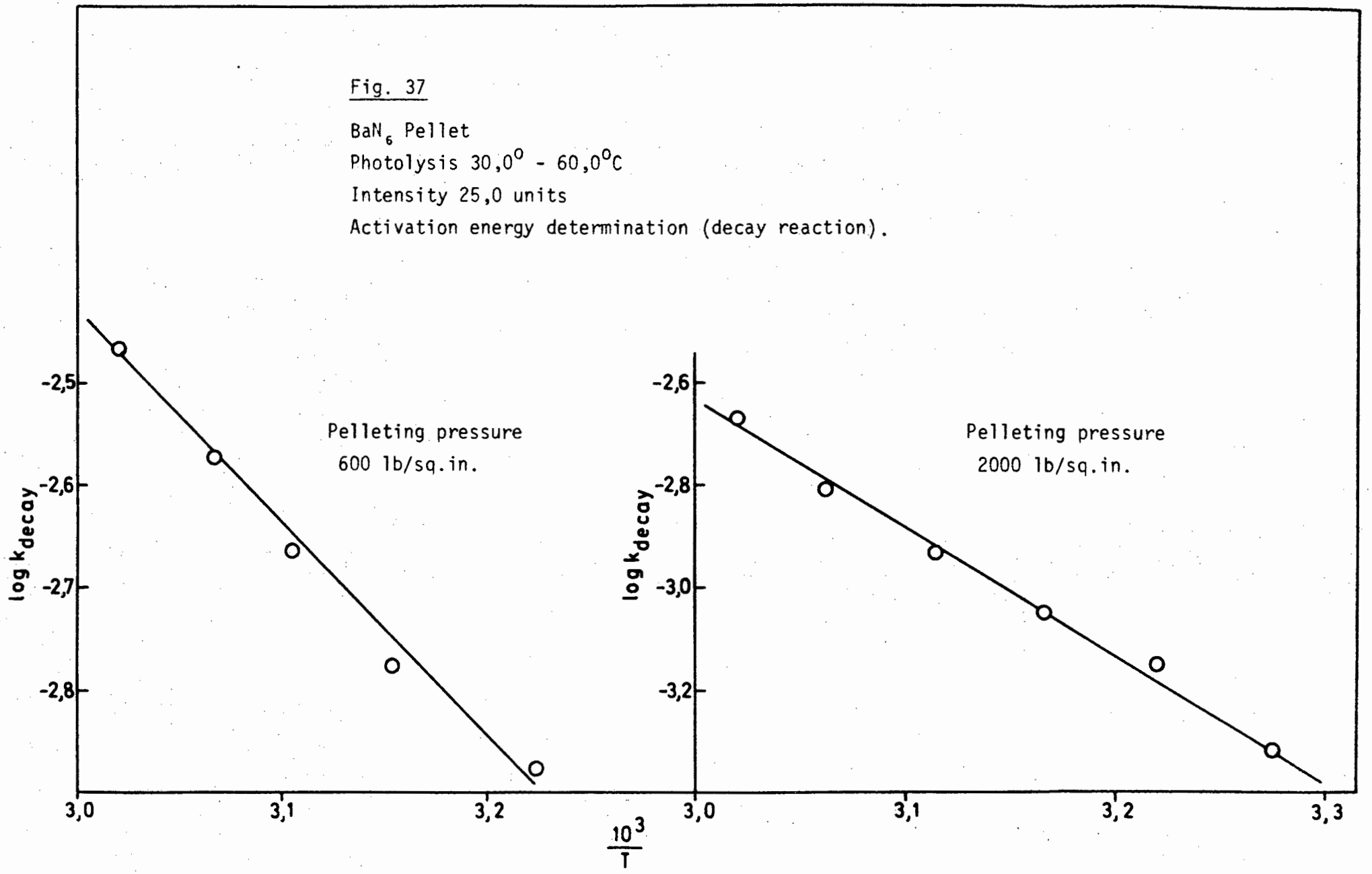

This is illustrated in Fig. 37 (temperature range 30,0° - 60,0°C, intensity 25,0 units, pelleting pressures 600 lb/sq.in. and 2000 lb/sq.in.) and 38 (temperature range 60,0° - 100,0°C, intensity 25,0 units, pelleting pressures 600 lb/sq.in. and 2000 lb/sq.in.) for barium azide and for strontium azide in Fig. 39 (temperature range 30,0° - 50,0°C, intensity 30,0 units, pelleting pressures 600 lb/sq.in. and 2000 lb/sq.in.), 40 (temperature range 50,0° - 90,0°C, intensity 30,0 units, pelleting pressure 600 lb/sq.in.) and 41 (temperature range 50,0° - 90,0°C, intensity 30,0 units, pelleting pressure 2000 lb/sq. in.). Tables 11 and 12 give the rate constants for barium azide and Tables 13 and 14 give the rate constants for strontium azide pellets pressed at 600 lb/sq.in. and 2000 lb/sq.in. respectively. Tables 15 and 16 list the activation energies for the decay reactions of barium and strontium azide pellets respectively.

Table 11

Rate constants for the decay reaction of photolysed barium azide pellets. Pelleting pressure 600 lb/sq.in. Intensity 25,0 units.

Temperature range of split run °C	Temperature °C	$k_{decay} \times 10^2$ min.$^{-1}$
30,0 - 60,0	37,1	0,13
	44,0	0,16
	49,0	0,21
	53,1	0,26
	58,1	0,34
60,0 - 100,0	67,0	0,83
	78,0	1,49
	82,0	1,66
	88,5	2,75
	92,3	4,00

Fig. 38

BaN_6 Pellet

Photolysis 60,0° - 100,0°C

Intensity 25,0 units

Activation energy determination (decay reaction).

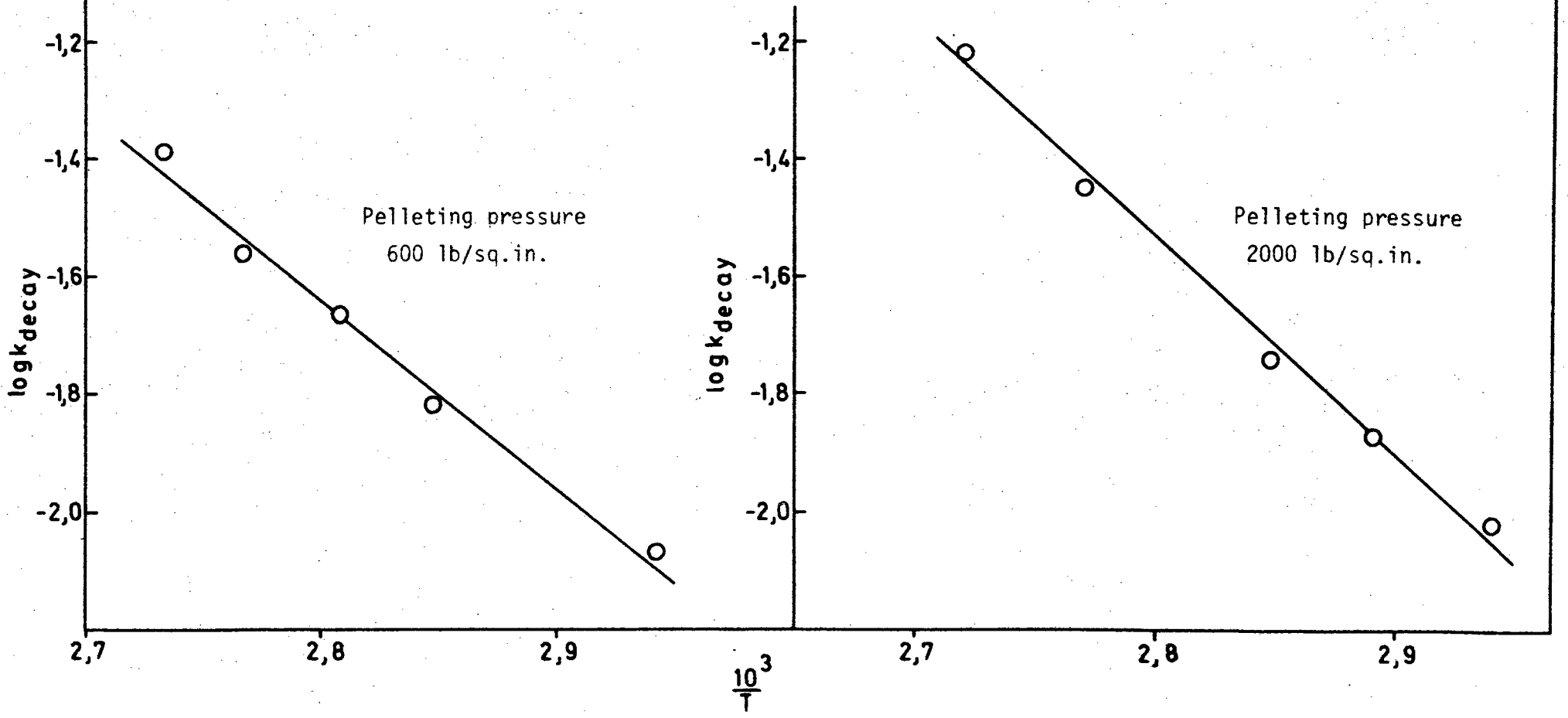

Fig. 39

SrN_6 Pellet

Photolysis 30,0° - 50,0°C

Intensity 30,0 units

Activation energy determination (decay reaction)

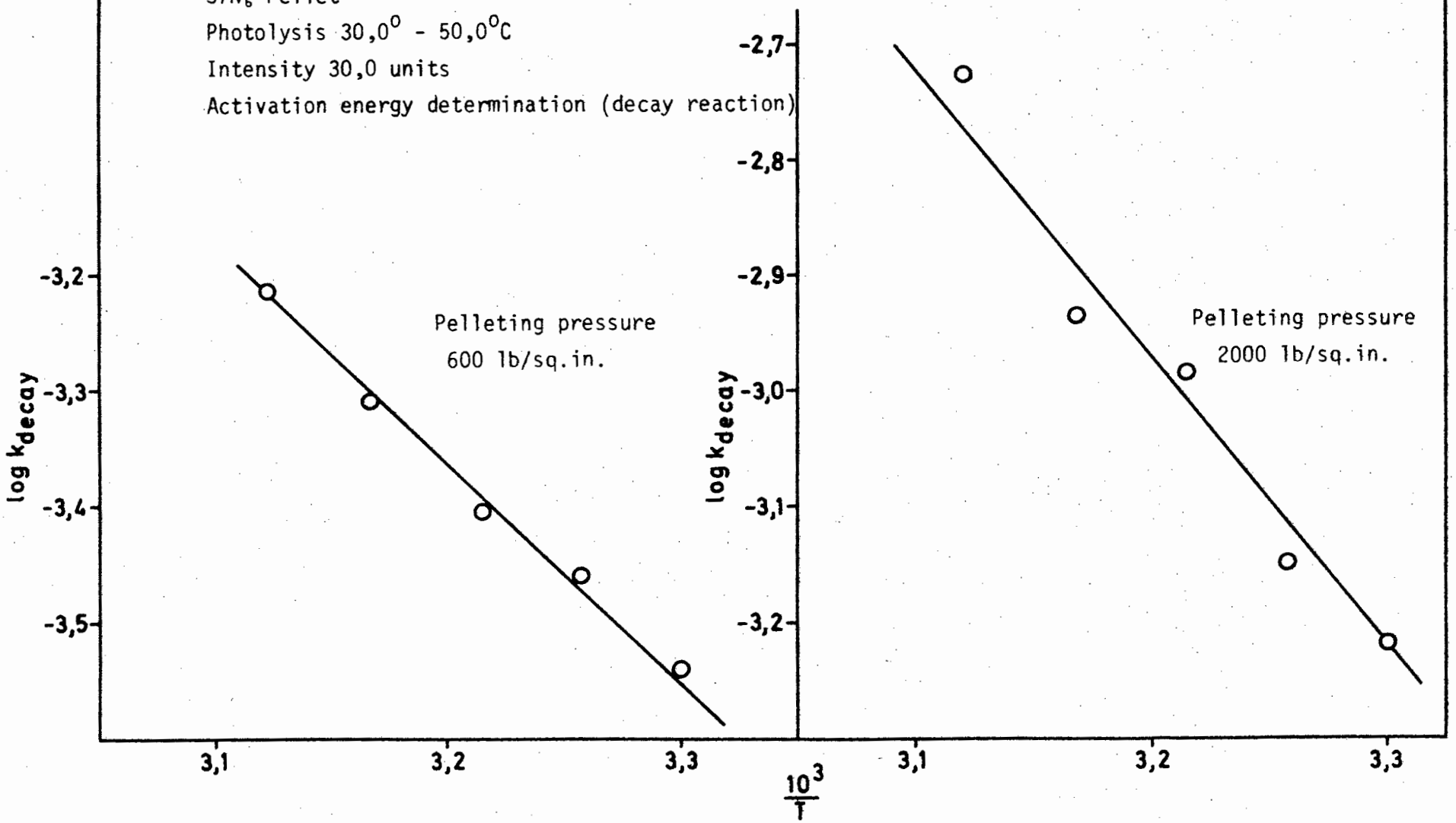

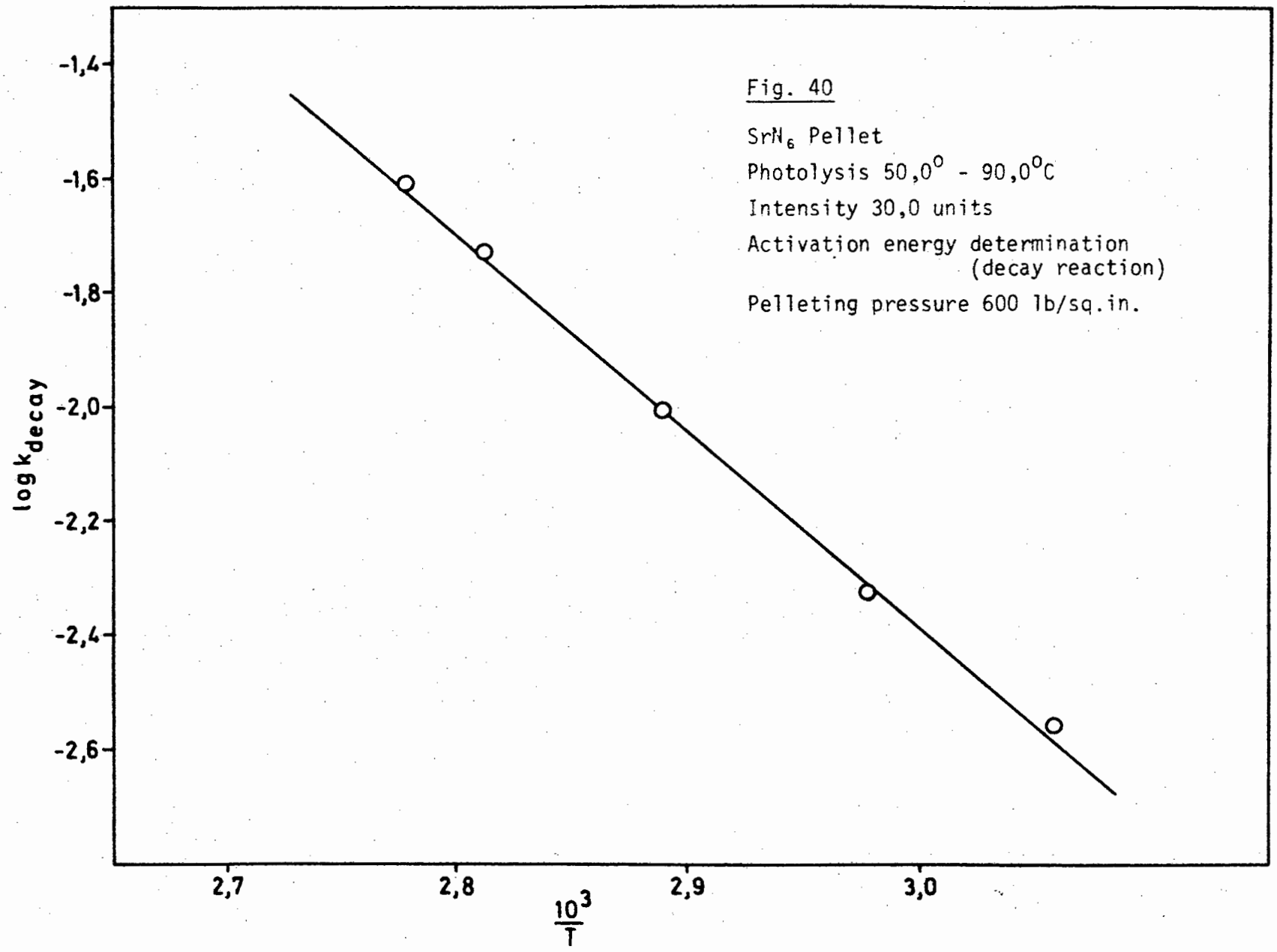

Fig. 40

SrN_6 Pellet

Photolysis 50,0° - 90,0°C

Intensity 30,0 units

Activation energy determination (decay reaction)

Pelleting pressure 600 lb/sq.in.

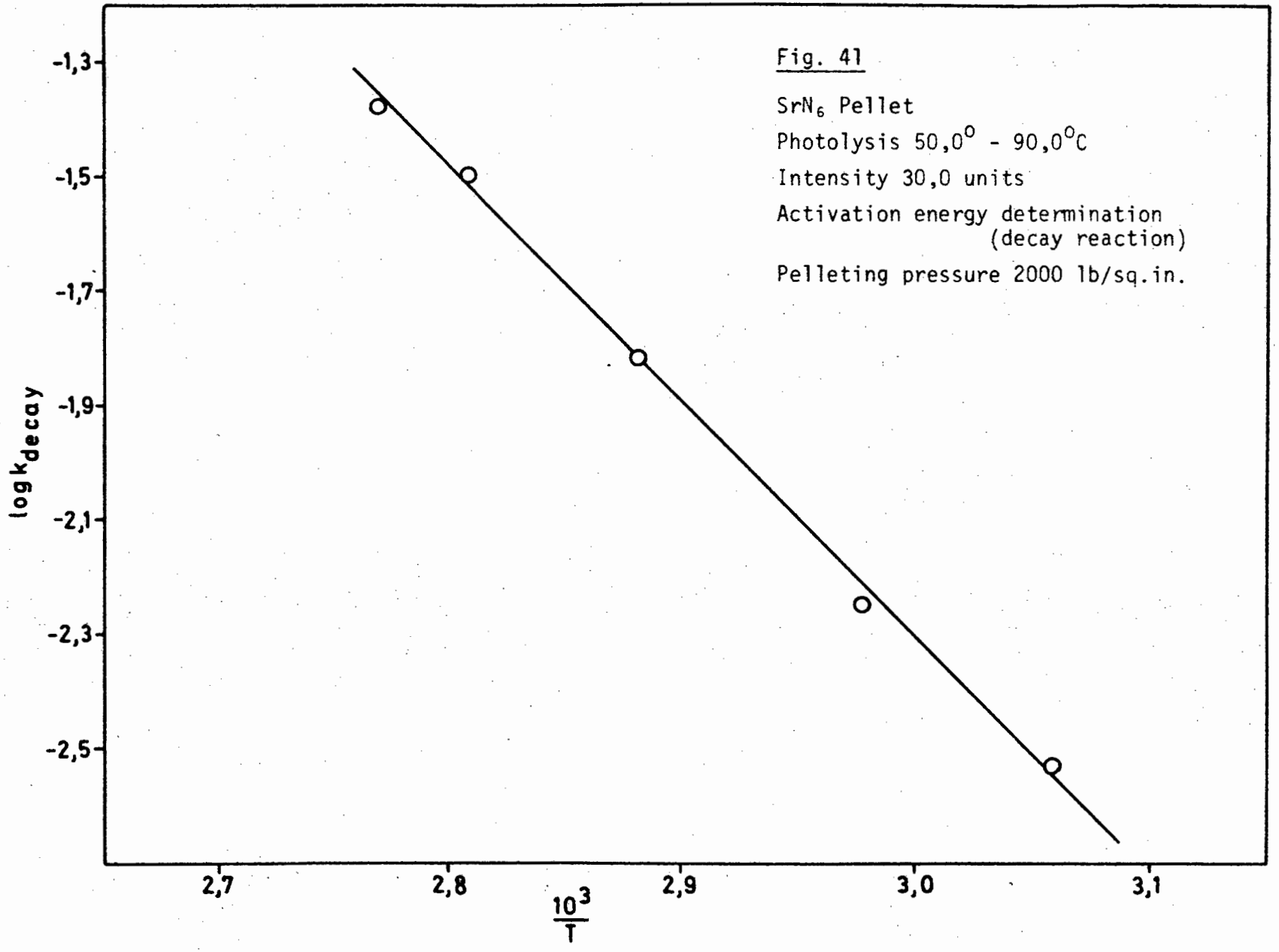

Fig. 41

SrN_6 Pellet

Photolysis 50,0° - 90,0°C

Intensity 30,0 units

Activation energy determination (decay reaction)

Pelleting pressure 2000 lb/sq.in.

Table 12

Rate constants for the decay reaction of photolysed barium azide pellets. Pelleting pressure 2000 lb/sq.in. Intensity 25,0 units.

Temperature range of split run ^{o}C	Temperature ^{o}C	$k_{decay} \times 10^{2}$ $min.^{-1}$
30,0 - 60,0	32,0	0,047
	37,9	0,070
	43,1	0,090
	48.1	0,11
	53,4	0,15
	58,1	0,21
60,0 - 100,0	67,1	1,00
	73,0	1,32
	78,0	1,78
	88,0	3,47
	93,8	6,05

Table 13

Rate constants for the decay reaction of photolysed strontium azide pellets. Pelleting pressure 600 lb/sq.in. Intensity 30,0 units.

Temperature range of split run ^{o}C	Temperature ^{o}C	$k_{decay} \times 10^{2}$ $min.^{-1}$
30,0 - 50,0	30,0	0,028
	34,0	0,034
	38,0	0,039
	42,5	0,048
	47,1	0,061
50,0 - 90,0	54,0	0,27
	63,0	0,46
	73,2	0,96
	82,5	1,83
	87,5	2,46

Table 14

Rate constants for the decay reaction of photolysed strontium azide pellets. Pelleting pressure 2000 lb/sq.in. Intensity 30,0 units.

Temperature range of split run ^{o}C	Temperature ^{o}C	$k_{decay} \times 10^{2}$ $min.^{-1}$
30,0 - 50,0	30,0	0,060
	34,0	0,069
	38,0	0,10
	42,8	0,11
	47,5	0,19
50,0 - 90,0	54,0	0,29
	63,0	0,55
	74,0	1,54
	83,0	3,15
	88,0	4,15

Table 15

Activation energies for the decay reaction of photolysed barium azide pellets.

Pelleting pressure lb/sq.in.	**Temperature** range ^{o}C	Activation **energy** $Kcal.mol.^{-1}$
600	30,0 - 60,0	9,4
2000	30,0 - 60,0	12,4
600	60,0 - 100,0	14,8
2000	60,0 - 100,0	17,0

Table 16		
Activation energies for the decay reaction of photolysed strontium azide pellets.		
Pelleting pressure lb/sq.in.	Temperature range ^{o}C	Activation energy Kcal.mol.$^{-1}$
600	30,0 - 50,0	8,8
2000	30,0 - 50,0	11,7
600	50,0 - 90,0	16,1
2000	50,0 - 90,0	18,9

(iic) Visual observations

This involved the observation of the colour of the pellet at various stages of photolytic decomposition. A temperature of 72,0^{o}C and light intensity of 25,0 units was chosen for a barium azide pellet, pressed at 2000 lb/sq.in. The colour changes were similar to those found for barium azide powder.

By the end of the induction period the surface opposite the light had turned uniformly brown; the lower face was unchanged at this point. By the time the reaction had reached α = 0,18 the lower surface had turned to this light brown colour and the upper surface had changed to a darker brown colour. These surfaces changed slowly from these brown shades to dark black on all external surfaces by the time the reaction had reached α = 0,22. By examination of the pellet in a dry box, flushed with dry nitrogen, it was found that the interior of the pellet was white at α = 0,22. Each external black layer was estimated to be 50 000 unit cell layers thick. At the end of the reaction the interior of the pellet was dark black.

A similar result was found for a barium azide pellet pressed at 600 lb/sq.in.

The change in colour of a strontium azide pellet during photolysis was also found to be similar to that of strontium azide powder. At a decomposition temperature of 70,0°C and light intensity of 30,0 units, a pellet pressed at 2000 lb/sq.in. was found to turn uniformly light grey on the surface facing the light by the end of the induction period. The lower face had changed to this colour by the time the reaction had reached α = 0,15 while the upper face had changed to a darker grey at this point. These grey shades changed progressively to darker shades until at α = 0,20 both faces were dark black. Examination of the pellet at this stage in a dry box, flushed with dry nitrogen, showed that the interior of the pellet had not changed colour. Each black surface was estimated to be approximately 30 000 unit cell layers thick. At the end of the reaction the interior of the pellet was dark black. A similar result was found for a strontium azide pellet pressed at 600 lb/sq.in.

(iid) Interruption of a photodecomposition: dark rate determination

For both barium and strontium azide pellets no measurable dark rate could be observed at any stage of the photolytic reaction. The reaction ceased the moment the light was switched off but commenced as though no interruption had taken place once the light was switched on again.

(iie) Admittance of water vapour following an interruption

In order to obtain an insight into the effect of metallic nuclei on the photolytic decomposition of barium and strontium azide pellets, water vapour (17 torr pressure) was admitted at various stages of the decomposition. The method used was identical to that for "water

interruptions" with powder. Using a temperature of 72,0°C and lamp intensity of 25,0 units a pellet of barium azide (pelleting pressure 2000 lb/sq.in.) was decomposed till α = 0,22 (i.e. at the point where the pellet had turned black on all external faces), and then the water vapour was reacted for 1 min. with the pellet. The subsequent reaction was found to be completely destroyed. The same result was found with strontium azide pellets (pelleting pressure 2000 lb/sq.in.) when water vapour was allowed to react for 1 min. with a pellet which had decomposed to α = 0,20 (i.e. at the point where the pellet had turned completely black on all external faces). Introduction of water vapour before α = 0,22 for a barium azide pellet and before α = 0,20 for a strontium azide pellet, caused the subsequent reaction to proceed after an induction period of the same duration as the uninterrupted pellet. The subsequent photolytic reaction proceeded as though no interruption had been made when the water vapour was introduced at zero time and midway along the induction period of either barium or strontium azide pellets.

It was found that removal of the furnace from the cell and the replacement of it once the cell had cooled to room temperature had no effect on the subsequent reaction, thus validating the above results.

(iif) The decomposition of two pellets simultaneously

It was desired to ascertain whether the ultraviolet light source could activate two pellets (of either barium azide or strontium azide) resting loosely on top of each other and cause them to decompose simultaneously, or separately.

Two pellets of barium azide (pelleting pressure 2000 lb/sq.in.)

resting on top of each other, were decomposed at 72,0°C using a light intensity of 25,0 units. The reaction was found to proceed in two stages. This is illustrated in Fig. 42.

When both surfaces of the top pellet had turned black (pressure = 0,26 torr), the pellet beneath had not changed colour. When the pressure had reached 1,25 torr the underface of the lower pellet had just turned light brown, by which time the upper surface had turned dark brown. These brown shades had changed to a dark black when the pressure of gas evolved had reached a value of 1,65 torr. The percentage decomposition of the total reaction was found to be 93,0%. No dark rate was detected at any stage of the reaction.

A similar result was obtained when two pellets of strontium azide (pelleting pressure 2000 lb/sq.in.) resting on each other were decomposed at 73,0°C and with a light intensity of 30,0 units. The two stages of reaction are illustrated in Fig. 43. The bottom pellet had not changed colour when the top pellet was totally black on all external surfaces (pressure = 0,25 torr). The upper surface of the bottom pellet changed to a dark brown and the lower surface to a light brown when the pressure of gas evolved had reached a value of 1,15 torr. These brown shades had changed to dark black by the time the pressure had risen to 1,30 torr. The percentage decomposition of the two pellets was found to be 69,0%. As with the reaction of two barium azide pellets resting on each other, no dark rate was detected at any stage of the reaction of two pellets of strontium azide.

The effect on photolysis of 8mg of barium azide powder pelleted between two barium metal pellets was now investigated. The pressing of the powder between the two metal pellets was to ensure good contact between product and unreacted material. The metal pellets were

Fig. 42

BaN_6 Pellets (Pelleting pressure 2000 lb/sq.in.)

Photolysis 72,0°C

Intensity 25,0 units

A Photolysis of BaN_6 powder pressed between two barium metal pellets

B Photolysis of a single pellet

C Photolysis of two pellets resting on each other.

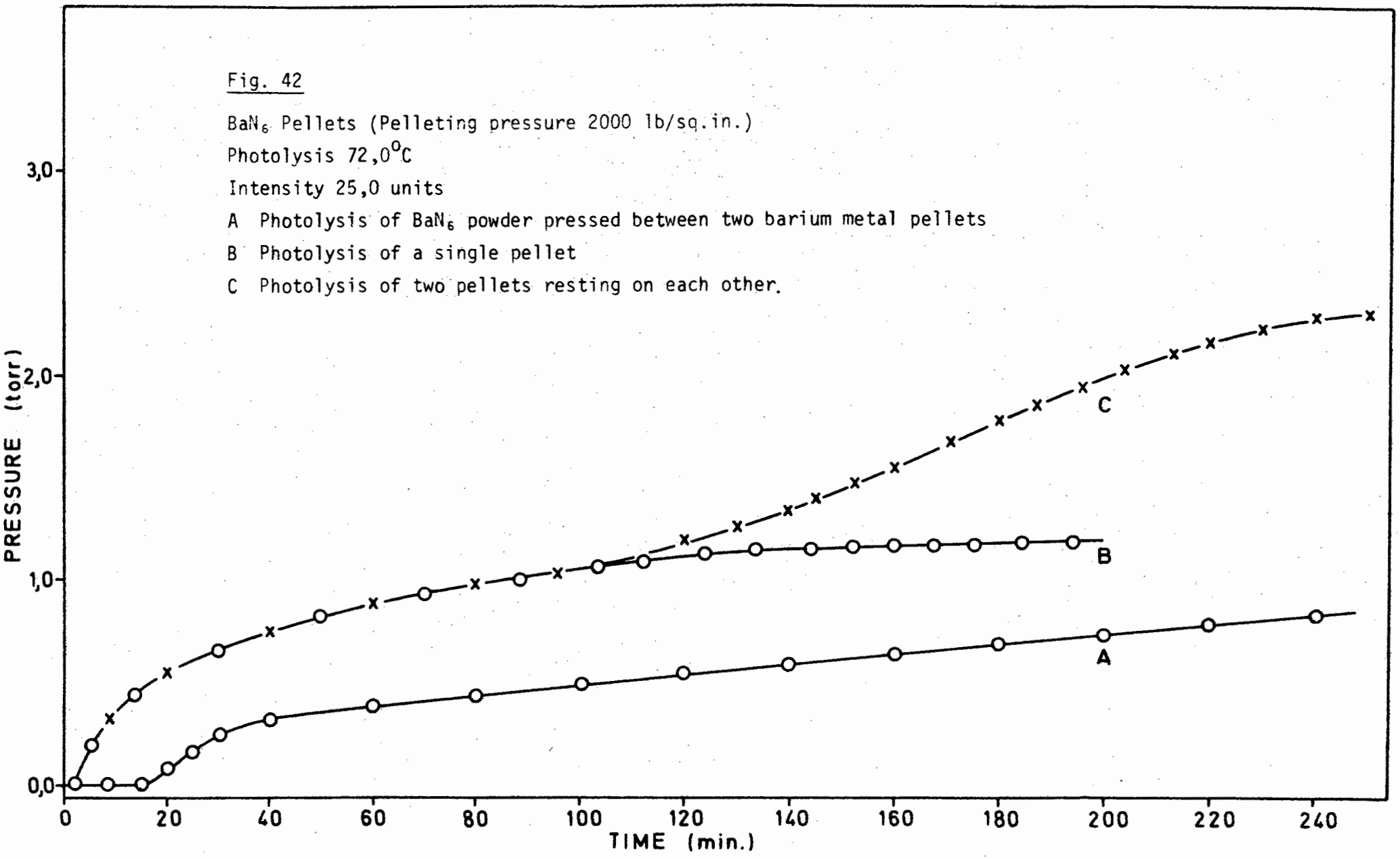

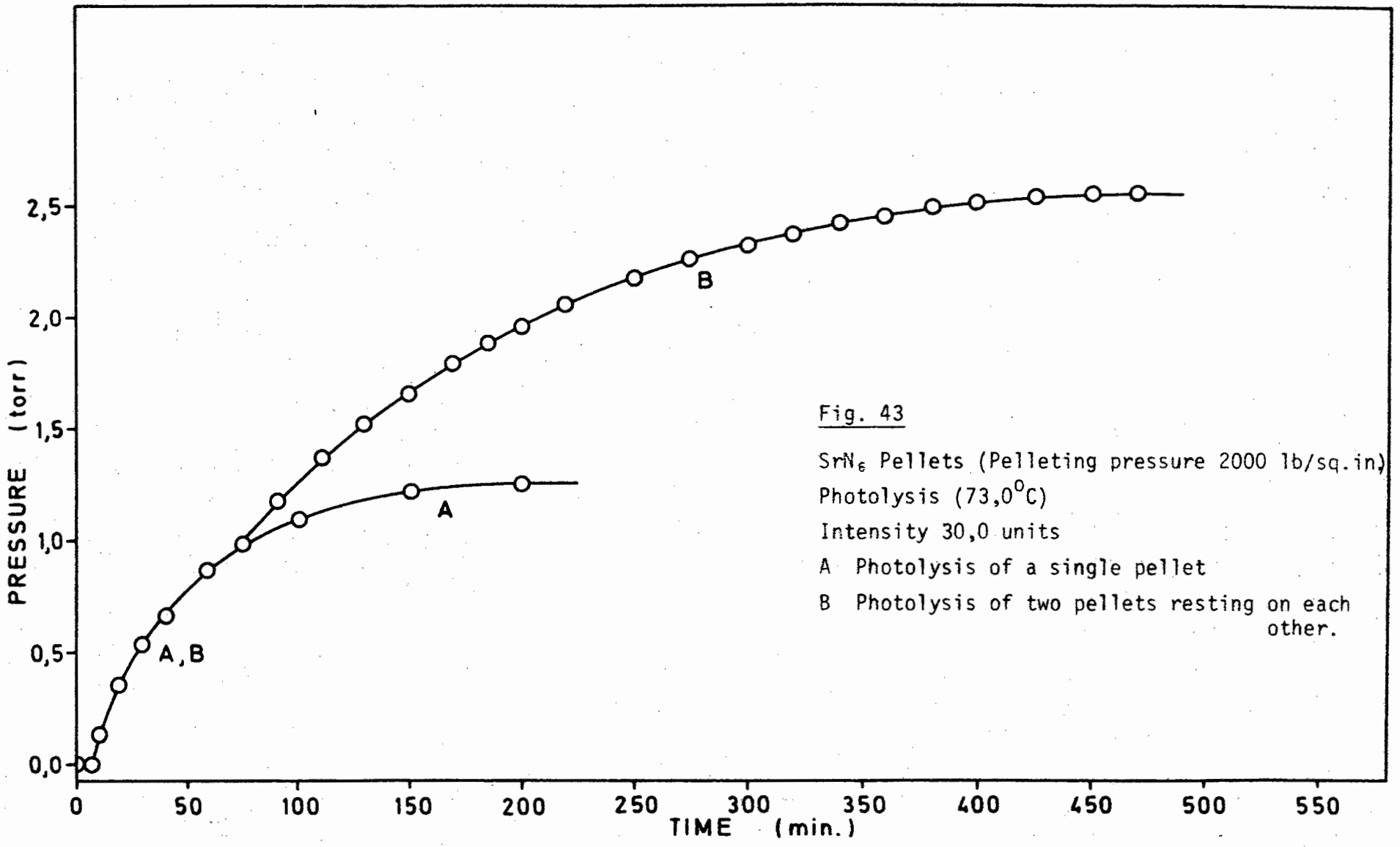

Fig. 43

SrN_6 Pellets (Pelleting pressure 2000 lb/sq.in)
Photolysis (73,0°C)
Intensity 30,0 units
A Photolysis of a single pellet
B Photolysis of two pellets resting on each other.

obtained by decomposing two barium azide pellets (pelleting pressure 2000 lb/sq.in.) each weighing 8mg, thermally at 130,0^{o}C. In an atmosphere of dry nitrogen the pellets were transferred from the line to a dry box flushed with dry nitrogen. The barium metal pellets were placed in the die with 8mg of barium azide powder between them. The die was removed from the dry box and pressed at 2000 lb/sq.in. for 15 min. after the die had been evacuated for 10 min. The die was then replaced in the dry box and the "sandwich" placed in the decomposition cell. The cell was attached to the line and, after pumping the system, photodecomposition took place at 72,0^{o}C (intensity 25,0 units) after the usual procedures. The rate of photolysis appeared to be much reduced. This was thought to be due to the prevention of diffusion of nitrogen from between the two barium metal pellets. At all stages of the reaction no dark rate could be detected.

4B IRRADIATION OF BARIUM AND STRONTIUM AZIDES WITH ULTRAVIOLET LIGHT DURING THERMAL DECOMPOSITION (CO-IRRADIATION)

(i) Powder

Thermal decompositions of barium or strontium azide powders in the temperature range of 110,0° - 135,0°C during which the sample is irradiated with ultraviolet light, are called "co-irradiated" decompositions, after Skorik, Boldyrev and Kamarov (122). The principal feature of this type of decomposition is the existence of a dark rate due to the thermal decomposition of the azide under study.

It was found that irradiation with ultraviolet light of either azide during thermal decomposition had a marked effect on the rate of decomposition viz a decrease in the induction period and an increase in the rate of the acceleratory and decay reactions. A comparison between a thermal decomposition and a co-irradiated decomposition for barium azide powder (decomposition temperature 120,0°C and intensity 15,5 units) is illustrated in Fig. 44 and for strontium azide (decomposition temperature 122,0°C and intensity 15,25 units) in Fig. 45. The percentage decomposition of either azide was found to be unaltered by irradiation with ultraviolet light during thermal decomposition i.e. percentage decomposition was found to be 95,0% for barium azide and 71,2% for strontium azide, the same as for a pure thermal decomposition.

(ia) Reproducibility

To investigate the reproducibility of co-irradiated decompositions three decompositions of barium azide were done at 110,0°C using a light intensity of 15,5 units. The resulting decomposition curves

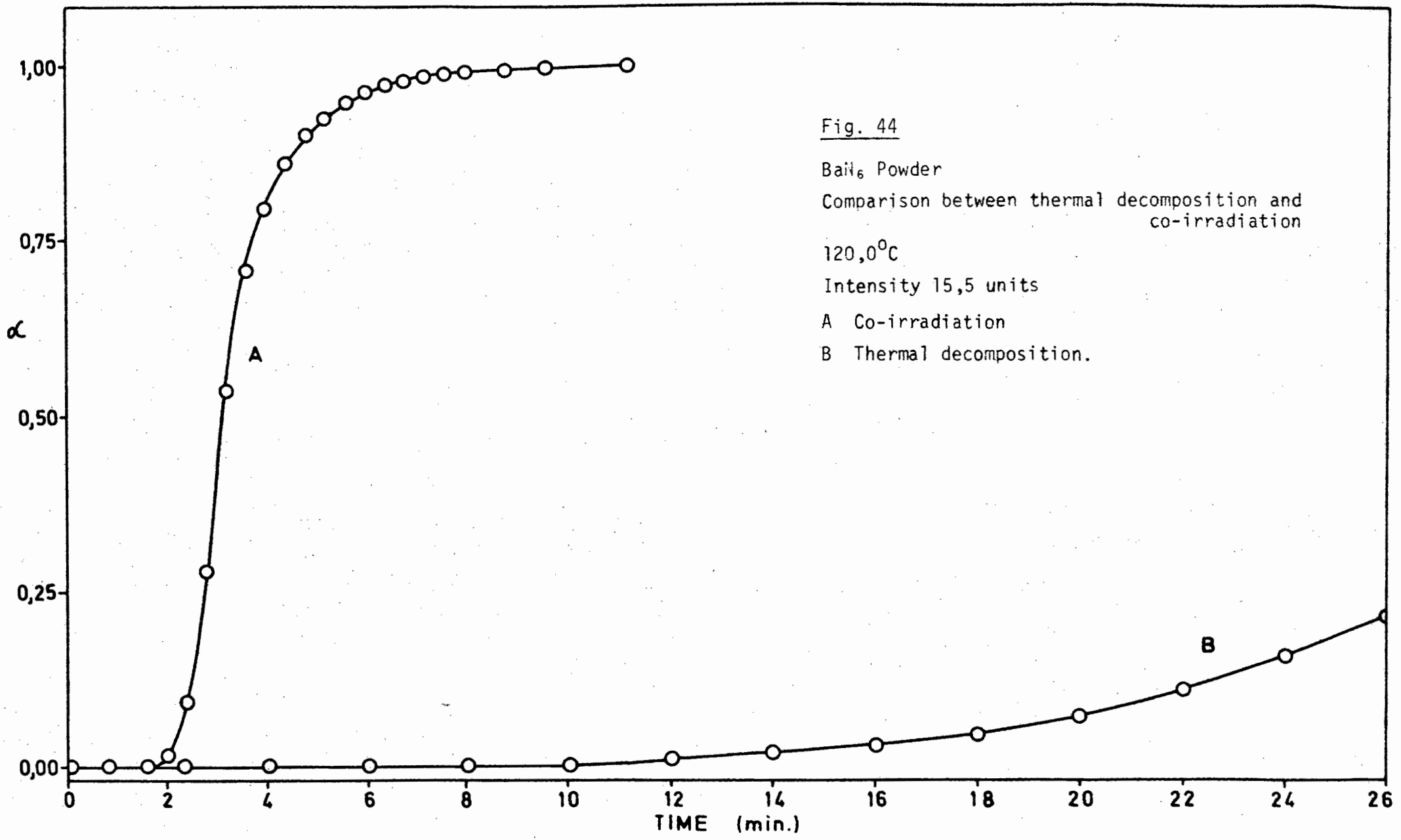

Fig. 44

BaN_6 Powder

Comparison between thermal decomposition and co-irradiation

120,0°C

Intensity 15,5 units

A Co-irradiation

B Thermal decomposition.

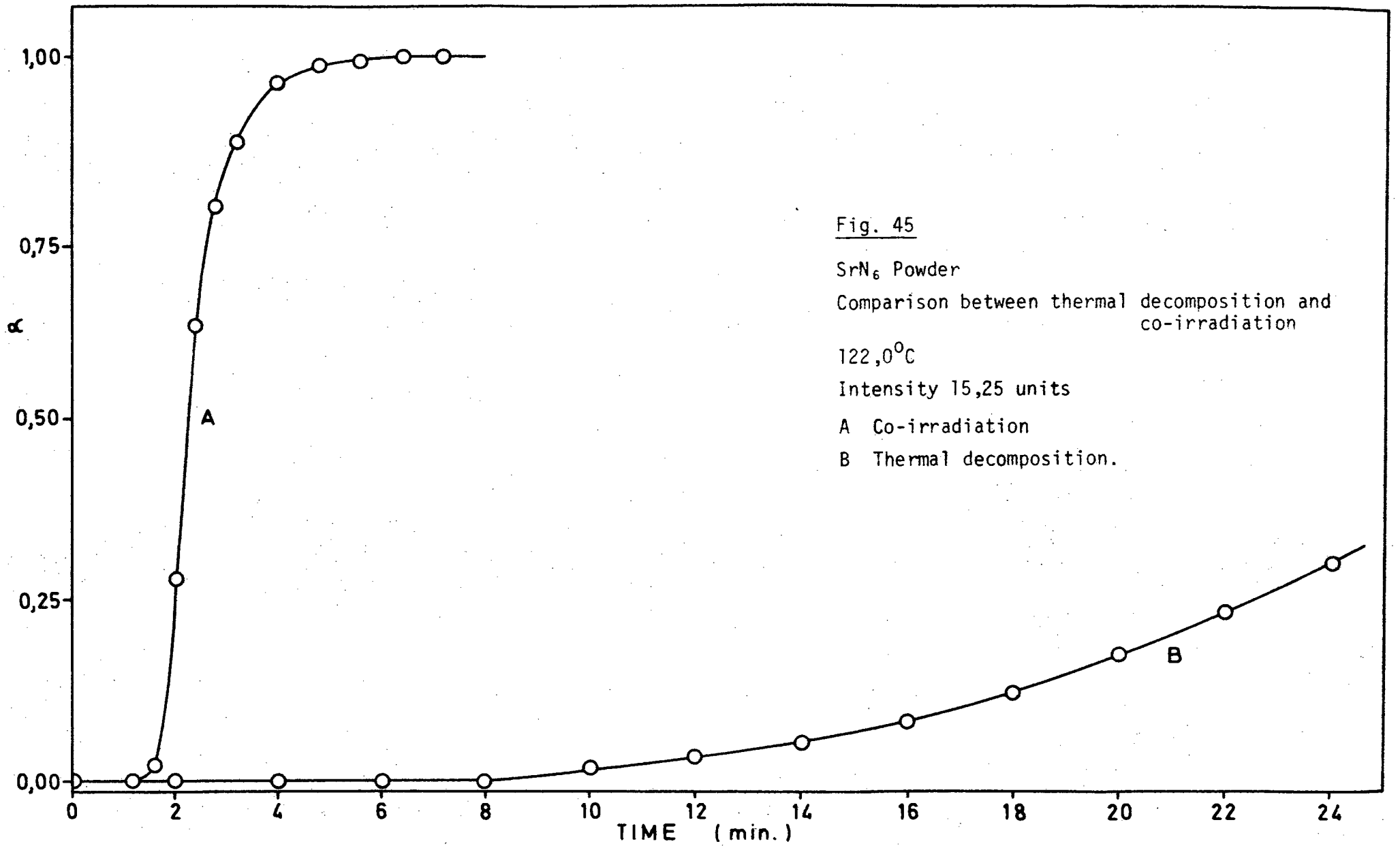

Fig. 45

SrN_6 Powder

Comparison between thermal decomposition and co-irradiation

122,0°C

Intensity 15,25 units

A Co-irradiation

B Thermal decomposition.

obtained were superimposed and satisfactory reproducibility was found. Similarly the reproducibility of co-irradiated strontium azide was investigated at a temperature of 116,0°C using a light intensity of 16,0 units. Satisfactory results were found but the reproducibility was not as good as was found for the barium salt. The curves of barium and strontium azides are illustrated in Fig. 46 and Fig. 47 respectively. Both sets of curves were analysed using the Avrami-Erofeyev equation with n = 2 for the acceleratory period and the unimolecular law for the decay period. The applicability of these equations to the co-irradiated decomposition will be illustrated later. The rate constants for barium azide are tabulated in Table 17 and those found for strontium azide are tabulated in Table 18.

Table 17

Reproducibility constants for co-irradiated barium azide powder.

Temperature °C	Intensity units	Induction period sec.	$k_{acc} \times 10^3$ $sec.^{-1}$	$k_{decay} \times 10^3$ $sec.^{-1}$
110,0	15,5	204,0	3,80	3,51
		216,0	3,88	3,67
		211,2	3,86	3,66

Table 18

Reproducibility constants for co-irradiated strontium azide powder.

Temperature °C	Intensity units	Induction period sec.	$k_{acc} \times 10^3$ $sec.^{-1}$	$k_{decay} \times 10^3$ $sec.^{-1}$
116,0	16,0	108,0	7,23	9,30
		120,0	6,53	8,33
		108,0	8,65	8,00

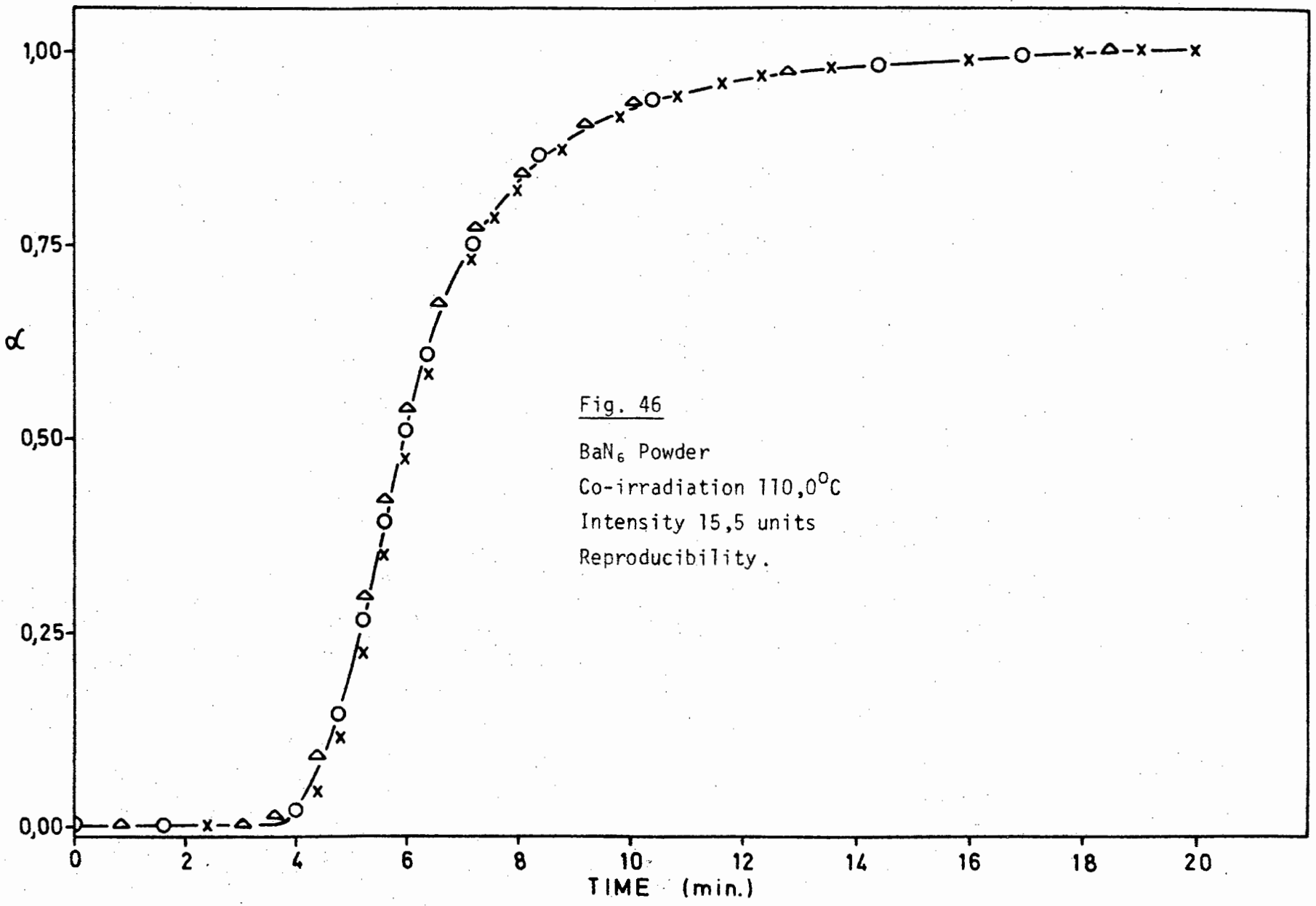

Fig. 46

BaN_6 Powder
Co-irradiation 110,0°C
Intensity 15,5 units
Reproducibility.

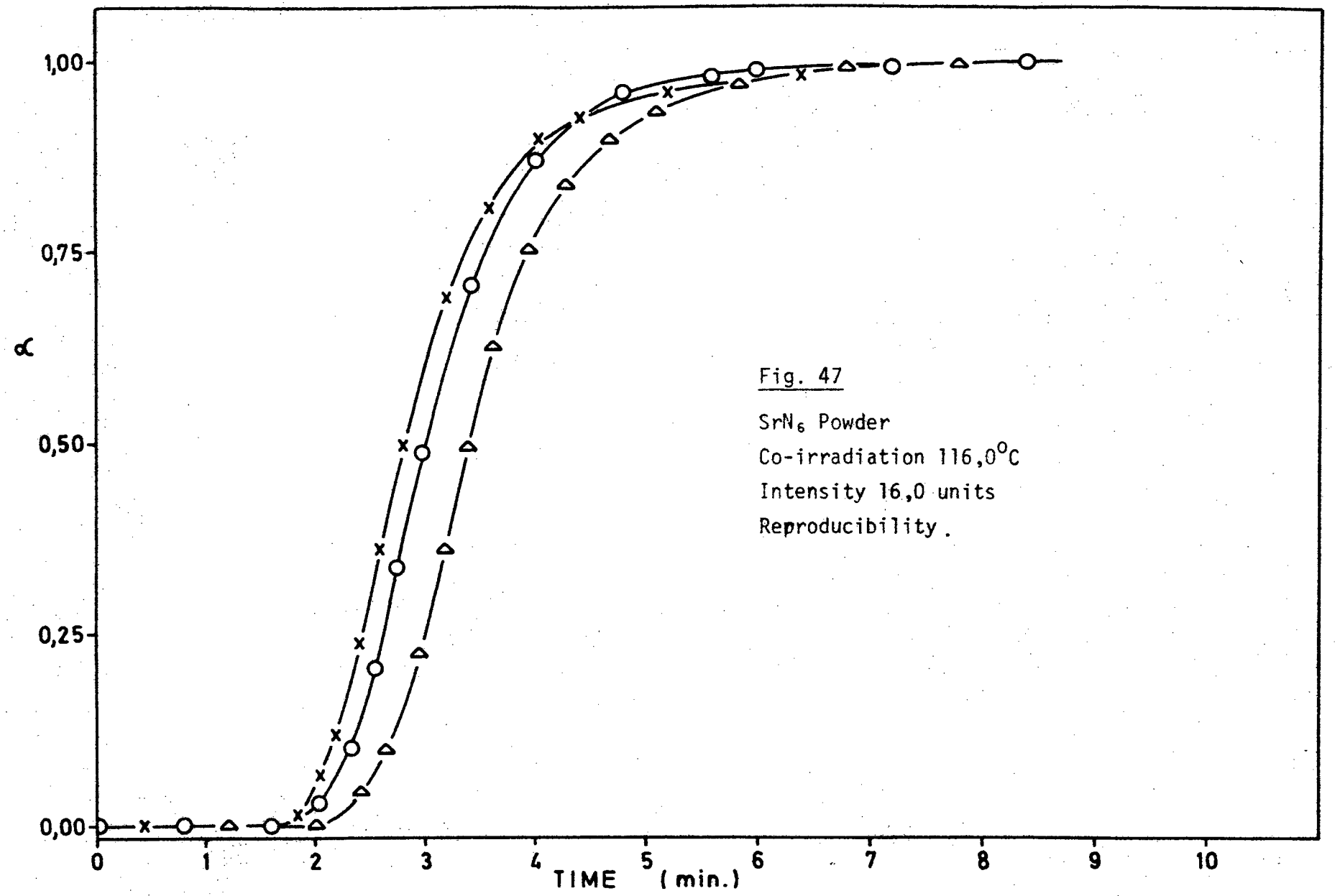

Fig. 47

SrN_6 Powder
Co-irradiation 116,0°C
Intensity 16,0 units
Reproducibility .

(ib) Mathematical Analyses

The shape of the co-irradiated decomposition curves of barium azide, was similar to that obtained from the photolysis of the powder. As for photolysis, the Avrami-Erofeyev equation with n = 2 (i.e. $(-\log(1-\alpha))^{\frac{1}{2}} = k_{acc}t + c$) fitted the acceleratory reaction and the decay reaction was fitted by the unimolecular law (i.e. $-\log(1-\alpha) = k_{decay}t + c$). The former equation fitted the curve from $0,01 < \alpha < 0,47$ and the latter equation fitted the curve from $0,47 < \alpha < 0,97$. The inflection point in the curve occurred at $\alpha = 0,47$. Since no gas was evolved during the induction period no mathematical equation could be applied to it. The inverse of the duration of the induction period was taken as the constant for that part of the curve. A typical α vs t plot for co-irradiated barium azide, at $120,0^{o}C$ (intensity 15,5 units), is illustrated with analyses in Fig. 48.

The co-irradiated decomposition curves of strontium azide were similar in shape to those obtained for the photolysis of the powder. However, the decay reaction for co-irradiated decompositions of strontium azide was less protracted than that found for the photolysis of the powder. Mathematical analyses for the co-irradiated decomposition curves were found using the Avrami-Erofeyev equation with n = 2 for the acceleratory period and the unimolecular law for the decay reaction. These analyses were obtained by using the observed final pressure p_f. A final pressure was not estimated for the decay reaction as was done for the photolysis of the powder.

The inflection point in the curve occurred at $\alpha = 0,48$. The fit of the Avrami-Erofeyev equation (n = 2) was from $0,03 < \alpha < 0,48$

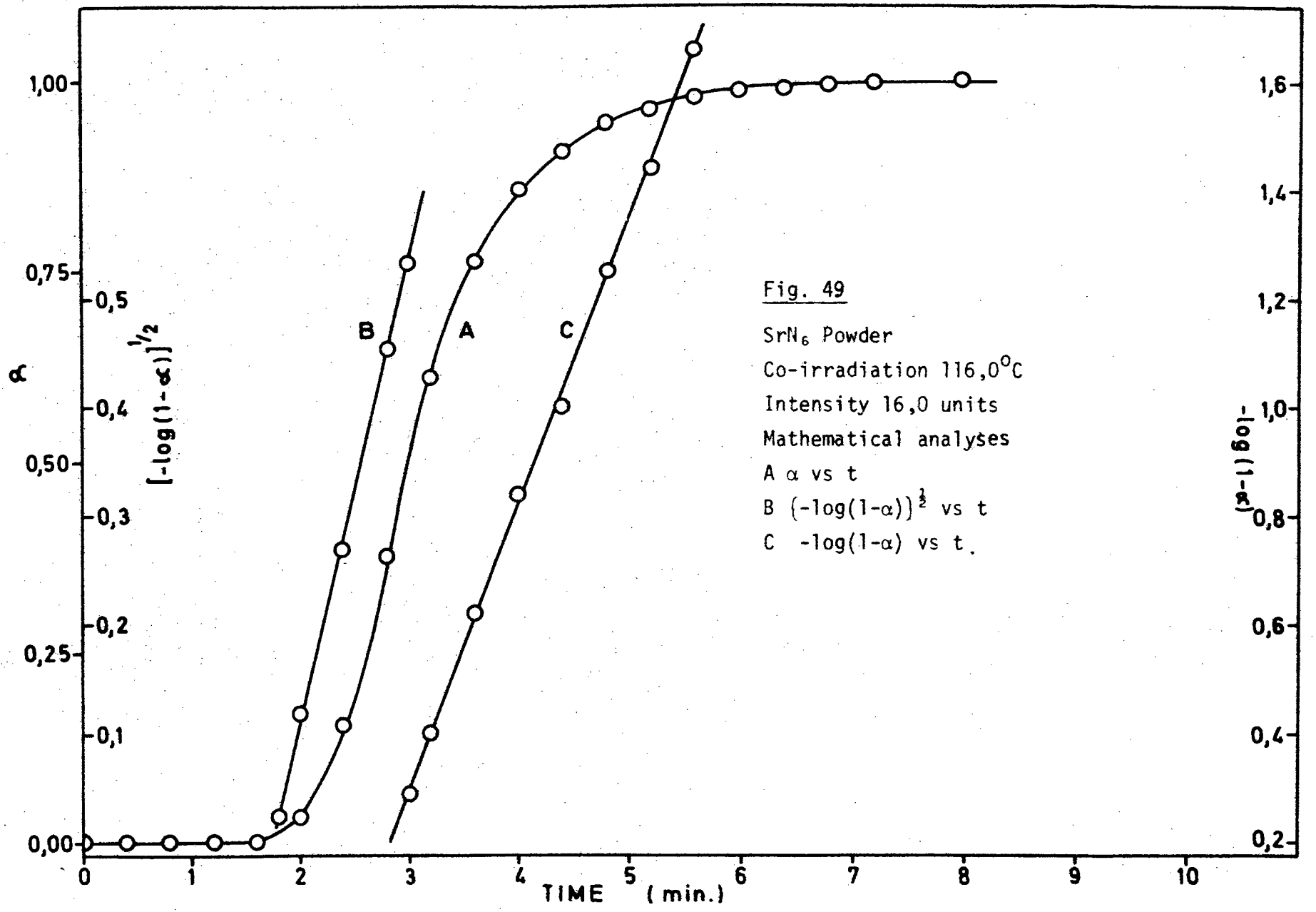

Fig. 49

SrN_6 Powder
Co-irradiation 116,0°C
Intensity 16,0 units
Mathematical analyses
A α vs t
B $(-\log(1-\alpha))^{\frac{1}{2}}$ vs t
C $-\log(1-\alpha)$ vs t.

and the unimolecular decay law fitted the equation from $0,48 < \alpha < 0,98$. A typical α vs t curve with analyses is illustrated in Fig. 49 for a co-irradiated decomposition at $116,0^{o}C$ using a light intensity of 16,0 units.

(ic) Evaluation of activation energies.

A series of runs was done for both barium and strontium azides in which the intensity was kept constant but the decomposition temperature was varied over a temperature range of $110,0^{o}$ - $135,0^{o}C$. Thus Arrhenius activation energies were determined for both compounds by plotting the logarithms of the rate constants against the inverse of the absolute temperatures of decomposition.

In order to find the effect of different light intensities on the value of the activation energies of co-irradiated decompositions, critical increments for the chemical process(es) taking place during co-irradiation of barium and strontium azides were determined using different constant light intensities. Activation energies for barium azide were determined using light intensities of 6,4 and 15,5 units, while the activation energies for strontium azide were determined using light intensities of 7,0 and 15,25 units. An attempt was made to determine activation energies for barium azide at a constant light intensity of 26,5 units. A value for the activation energy of the induction period only could be obtained. Activation energies for the acceleratory and decay reactions could not be determined at this high intensity since the rates of reaction were extremely fast and the time required for pressure equilibration throughout the large volume of the line was considerable. No attempt was made to determine activation energies for strontium azide at this high light intensity. Fig. 50, 51 and 52 show plots of the logarithms of the rate constants against

Fig. 50

BaN_6 Powder

Co-irradiation 110,0° - 135,0°C

Intensity 6,4 units

Activation energy determination.

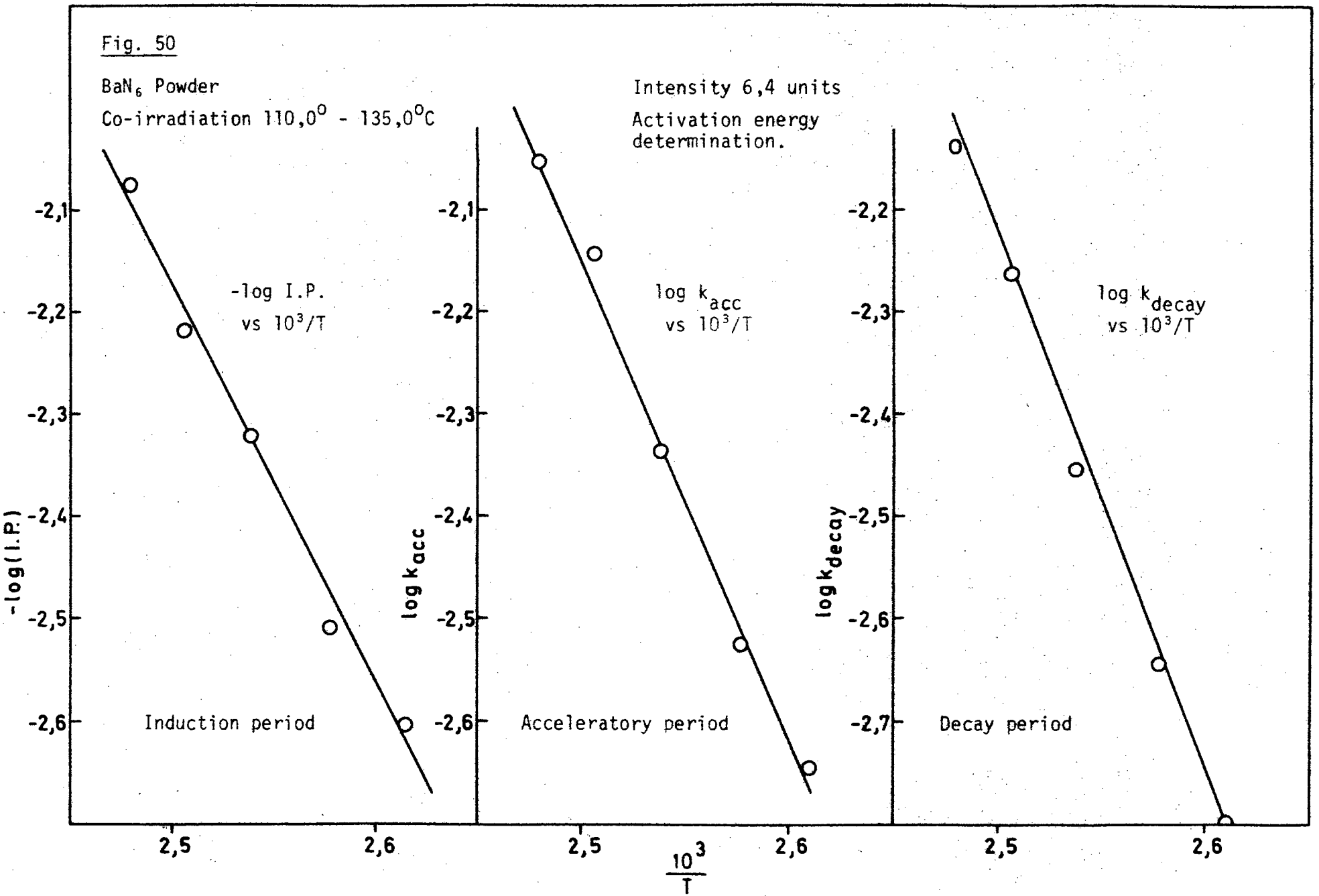

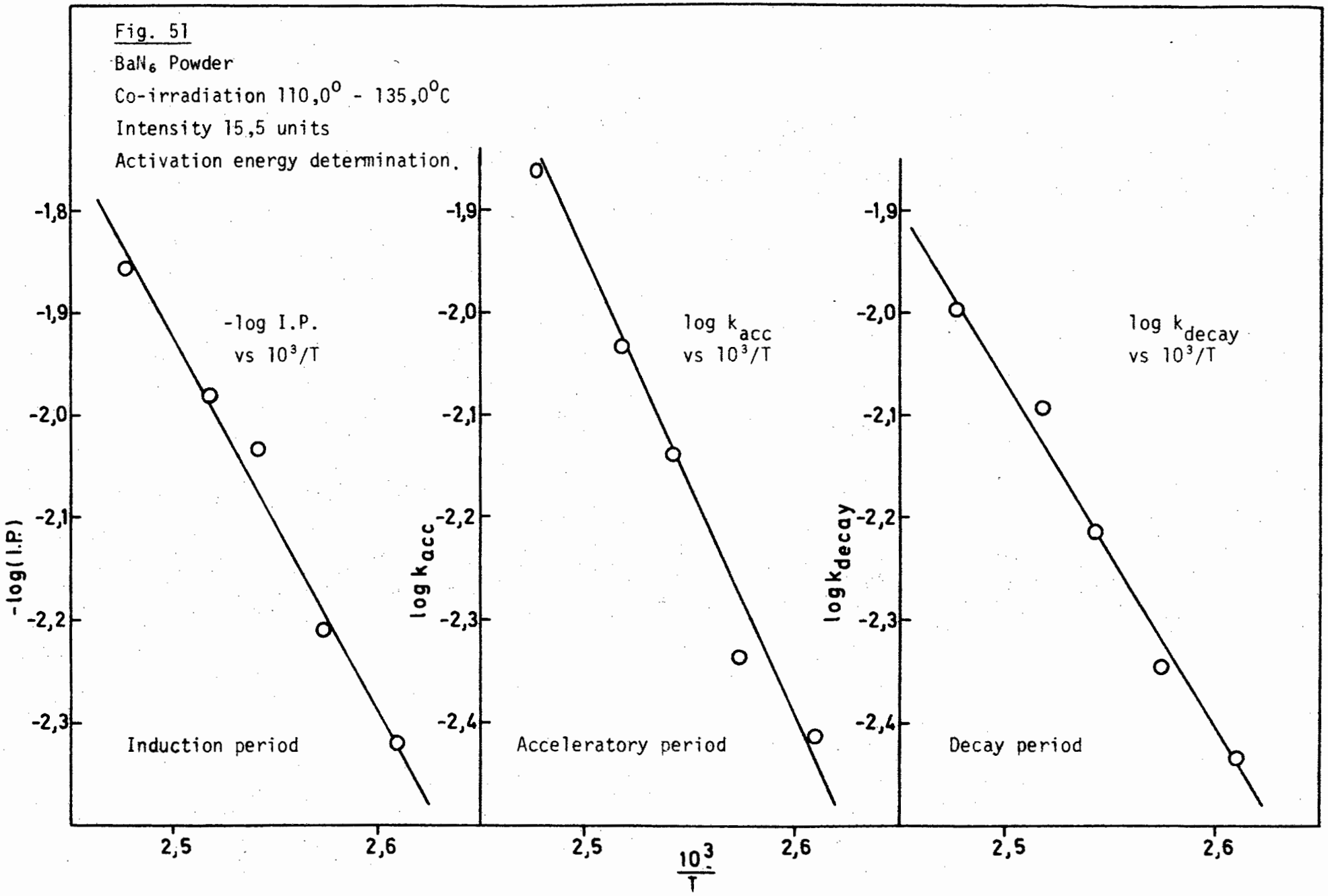
Fig. 51
BaN_6 Powder
Co-irradiation 110,0° - 135,0°C
Intensity 15,5 units
Activation energy determination.
-log I.P. vs $10^3/T$
$\log k_{acc}$ vs $10^3/T$
$\log k_{decay}$ vs $10^3/T$
Induction period
Acceleratory period
Decay period
-log(I.P)
$\log k_{acc}$
$\log k_{decay}$
$\frac{10^3}{T}$
-1,8
-1,9
-2,0
-2,1
-2,2
-2,3
-2,4
2,5
2,6

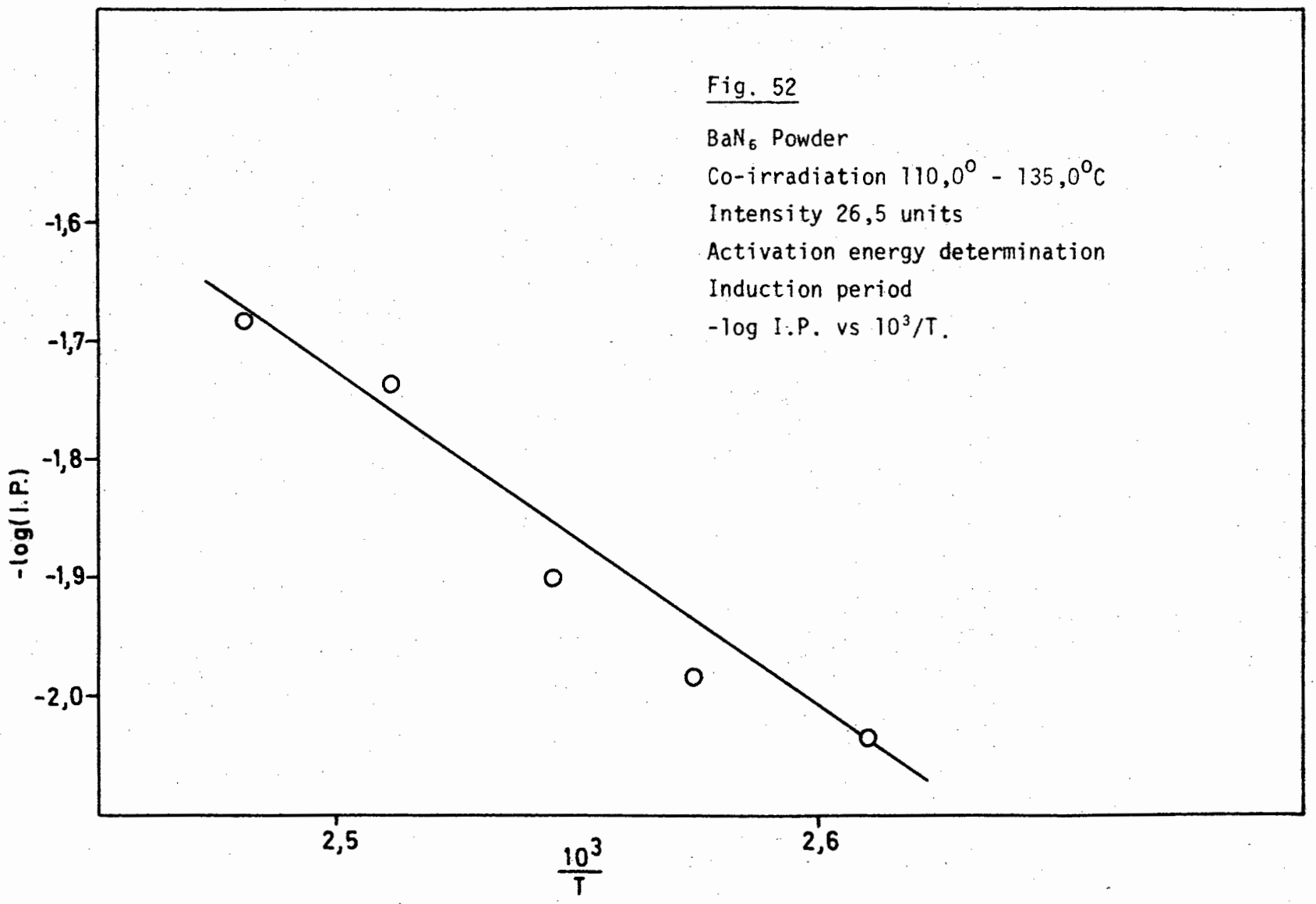

Fig. 52

BaN_6 Powder

Co-irradiation 110,0° - 135,0°C

Intensity 26,5 units

Activation energy determination

Induction period

-log I.P. vs $10^3/T$.

the absolute temperatures of decomposition using constant light intensities of 6,4; 15,5 and 26,5 units respectively for barium azide. Fig. 53 and 54 show similar plots for strontium azide using constant light intensities of 7,0 and 15,25 units respectively.

Both barium and strontium azides showed a decrease in activation energy with increase in light intensity.

Table 19 and Table 20 indicate the rate constants for barium and strontium azides respectively and Table 21 and Table 22 show the activation energies for barium and strontium azides respectively. For comparison Tables 21 and 22 show the activation energies for the thermal decomposition of barium (114) and strontium (89) azides respectively.

Table 19

Rate constants for the co-irradiation of barium azide powder. Temperature range 110,0° - 135,0°C.

Intensity units	Temperature °C	Induction period sec.	$k_{acc} \times 10^3$ $sec.^{-1}$	$k_{decay} \times 10^3$ $sec.^{-1}$
6,4	110,0	402,0	2,26	1,55
	114,9	324,0	2,97	2,26
	120,9	210,0	4,58	3,50
	126,1	168,0	7,16	5,48
	130,2	120,0	8,75	7,33
15,5	110,0	211,2	3,86	3,66
	115,5	163,2	4,58	4,47
	120,5	108,0	7,23	6,13
	125,9	96,0	9,26	8,00
	130,8	72,0	13,88	9,81
26,5	110,0	108,0	-	-
	115,5	96,0	-	-
	120,0	81,0	-	-
	125,1	54,0	-	-
	130,0	48,0	-	-

Fig. 53

SrN_6 Powder

Co-irradiation 110,0° - 135,0°C

Intensity 7,0 units

Activation energy determination .

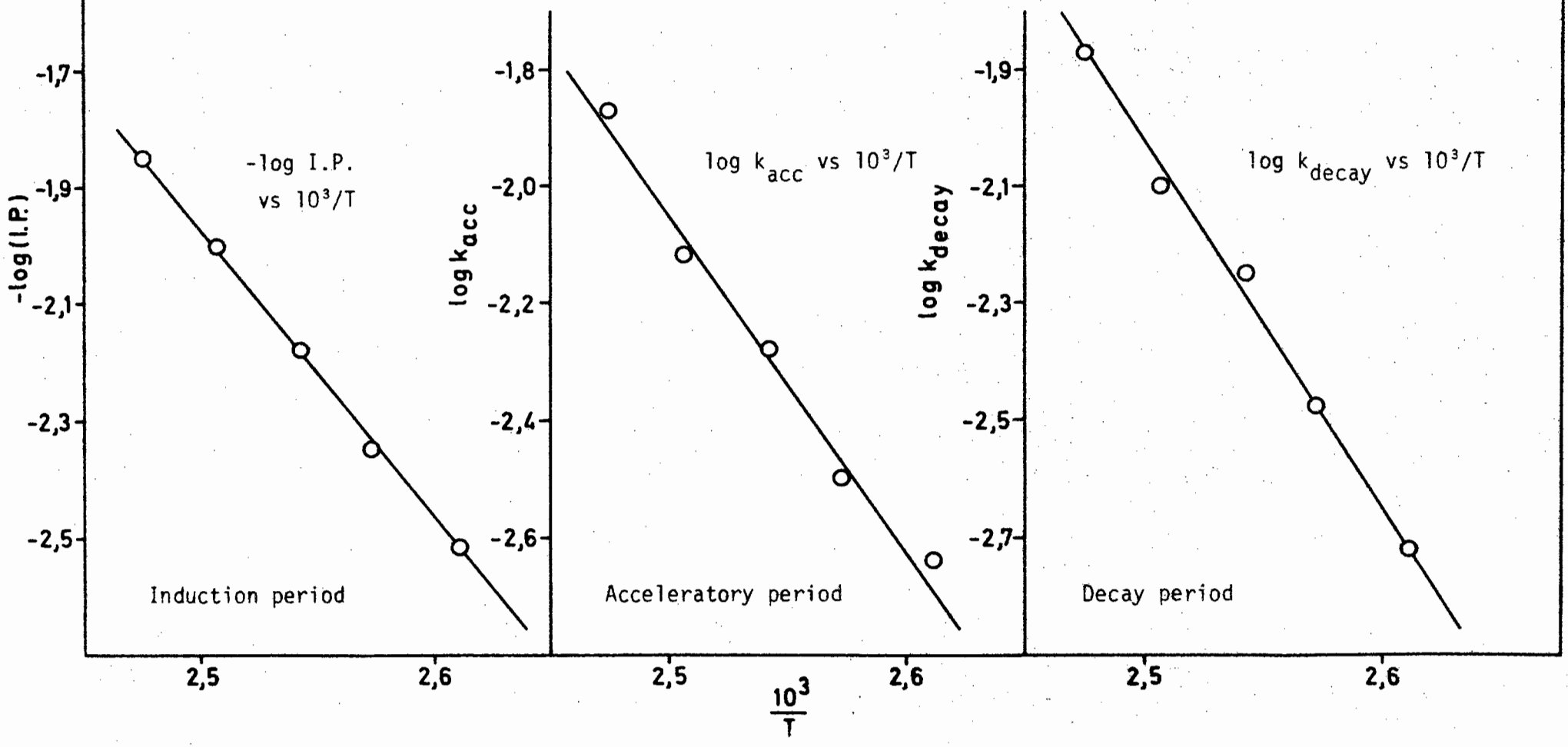

Fig. 54

SrN_6 Powder

Co-irradiation 110,0° - 135,0°C

Intensity 15,25 units

Activation energy determination.

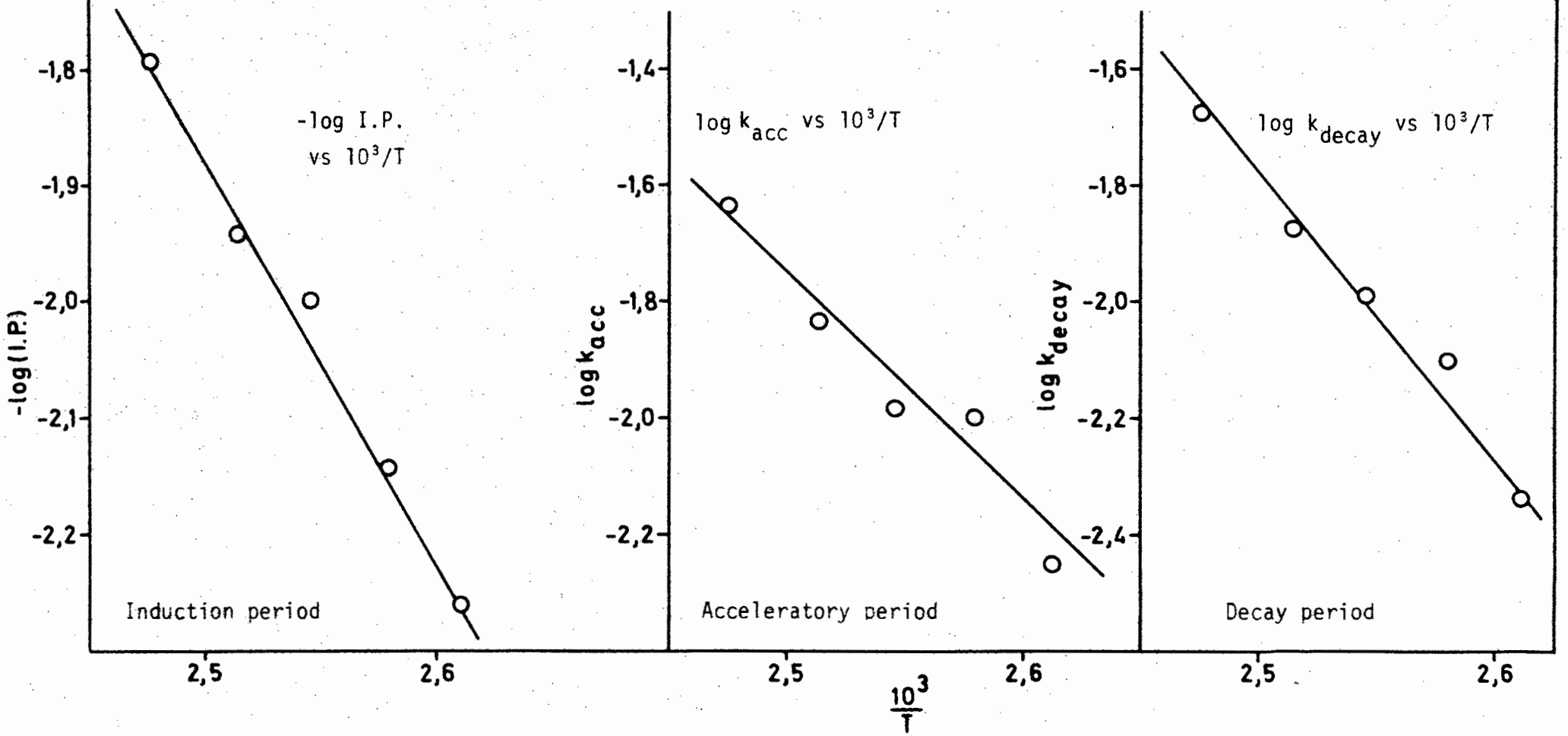

Table 20

Rate constants for the co-irradiation of strontium azide powder. Temperature range 110,0° - 135,0°C.

Intensity units	Temperature °C	Induction period sec.	$k_{acc} \times 10^3$ sec.$^{-1}$	$k_{decay} \times 10^3$ sec.$^{-1}$
7,0	110,0	336,0	2,25	1,77
	115,8	228,0	3,12	3,29
	120,3	153,6	5,16	5,61
	126,0	108,0	7,45	7,83
	131,0	72,0	13,23	13,40
15,25	110,0	182,4	5,59	4,49
	114,8	139,2	9,57	7,83
	120,8	103,2	10,08	10,17
	125,0	87,6	14,13	12,17
	131,0	62,4	22,50	20,71

Table 21

Activation energies for the co-irradiation of barium azide powder. Temperature range 110,0° - 135,0°C.

Intensity units	Induction period Kcal.mol.$^{-1}$	Acceleratory period Kcal.mol.$^{-1}$	Decay period Kcal.mol.$^{-1}$
0,0 (114)	26,5	26,8	26,1
6,4	18,5	21,7	24,1
15,5	16,5	19,2	15,6
26,5	12,1	-	-

Table 22			
Activation energies for the co-irradiation of strontium azide powder. Temperature range 110,0° - 135,0°C.			
Intensity units	Induction period Kcal.mol.$^{-1}$	Acceleratory period Kcal.mol.$^{-1}$	Decay period Kcal.mol.$^{-1}$
0,0 (89)	23,0	25,0	21,7
7,0	22,6	25,9	28,3
15,25	15,4	18,8	20,9

(id) The effect of variation of intensity of ultraviolet light source

The molecularity of the co-irradiation process in barium and strontium azide powders was determined by doing a series of decompositions at a constant temperature of 115,0°C for barium azide and 116,5°C for strontium azide, at various light intensities. Thus the dependence of induction period and subsequent acceleratory and decay reactions of the two azides, on the intensity of light source could be determined. The method of variation of light intensity has been described under section 3 on apparatus.

The molecularity (m) of the co-irradiation process was calculated from the equation

$$k = I^m + c$$

rewritten in the form

$$\log k = m\log I + \log c.$$

The value of m could now be calculated by a method of least squares.

Table 23 and Table 24 list the rate constants for barium and strontium azides respectively at various light intensities. Table 25 gives the value of m for both compounds.

Table 23

Rate constants for co-irradiated barium azide powder at various light intensities. Temperature 115,0°C.

Intensity units	Induction period sec.	$k_{acc} \times 10^3$ $sec.^{-1}$	$k_{decay} \times 10^3$ $sec.^{-1}$
25,8	114,0	7,95	6,45
21,9	130,0	6,95	5,85
16,6	150,0	5,33	4,24
10,8	216,0	3,86	3,58
6,8	288,0	2,97	2,45

Table 24

Rate constants for co-irradiated strontium azide powder at various light intensities. Temperature 116,5°C.

Intensity units	Induction period sec.	$k_{acc} \times 10^3$ $sec.^{-1}$	$k_{decay} \times 10^3$ $sec.^{-1}$
27,2	67,2	9,61	11,80
23,5	80,4	8,75	10,53
20,0	90,0	8,23	9,43
18,0	100,0	7,06	7,66
15,0	124,2	6,53	7,66
13,5	130,2	6,66	6,48
10,25	156,0	4,76	4,55
7,5	204,0	4,90	4,83

Table 25				
The value of m in the equation $k = I^m + c$.				
Salt	Temperature ^oC	Induction period	Acceleratory period	Decay period
BaN_6	115,0	0,7	0,7	0,7
SrN_6	116,5	0,8	0,6	0,8

Plots of k vs I^m are shown in Fig. 55 for barium azide and Fig. 56 and 57 for strontium azide.

(ie) Visual observations

Samples of barium and strontium azides, each decomposed at 115,0^oC and at a light intensity of 14,0 units, were observed at various stages of the co-irradiated decomposition. Both salts showed the same colour changes during decomposition. At α = 0,01 i.e. at the end of the induction period, the surfaces facing the light had changed to a light grey colour which then turned to a darker grey by the time the reaction had reached α = 0,20. No colour change of the lower surface was noticeable until α = 0,20 - a change to light grey was noticeable at this point. These grey shades changed slowly to black and at α = 0,50 all external surfaces, of either salt, were dark black. No further change in the colour of the particles could be observed in the decay stage of the decomposition of either salt.

Fig. 55

BaN_6 Powder

Co-irradiation 115,0°C

Variation of intensity .

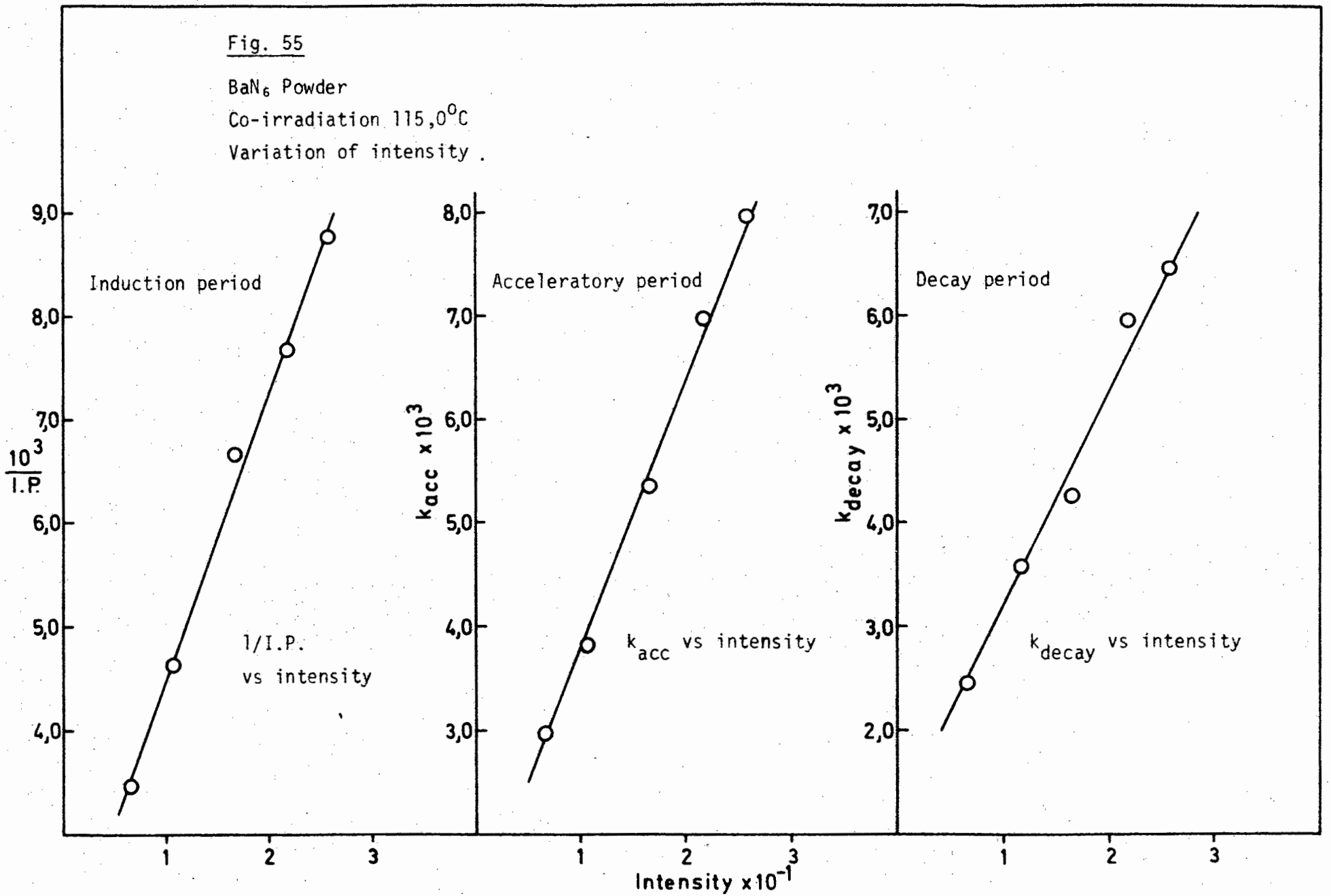

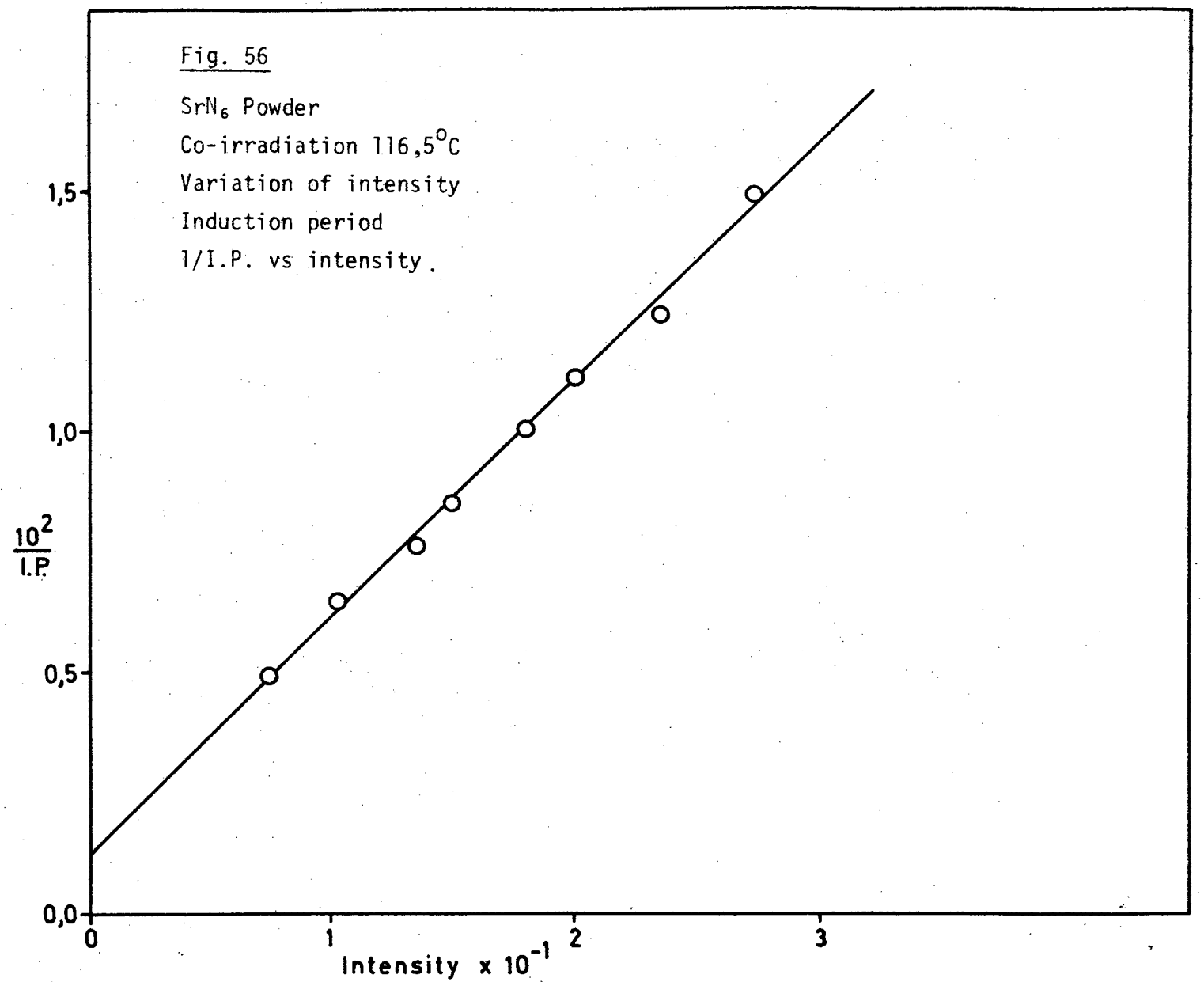
Fig. 56
SrN_6 Powder
Co-irradiation 116,5°C
Variation of intensity
Induction period
1/I.P. vs intensity.
1,5
1,0
0,5
0,0
$\frac{10^2}{I.P.}$
0
1
2
3
Intensity x 10^{-1}

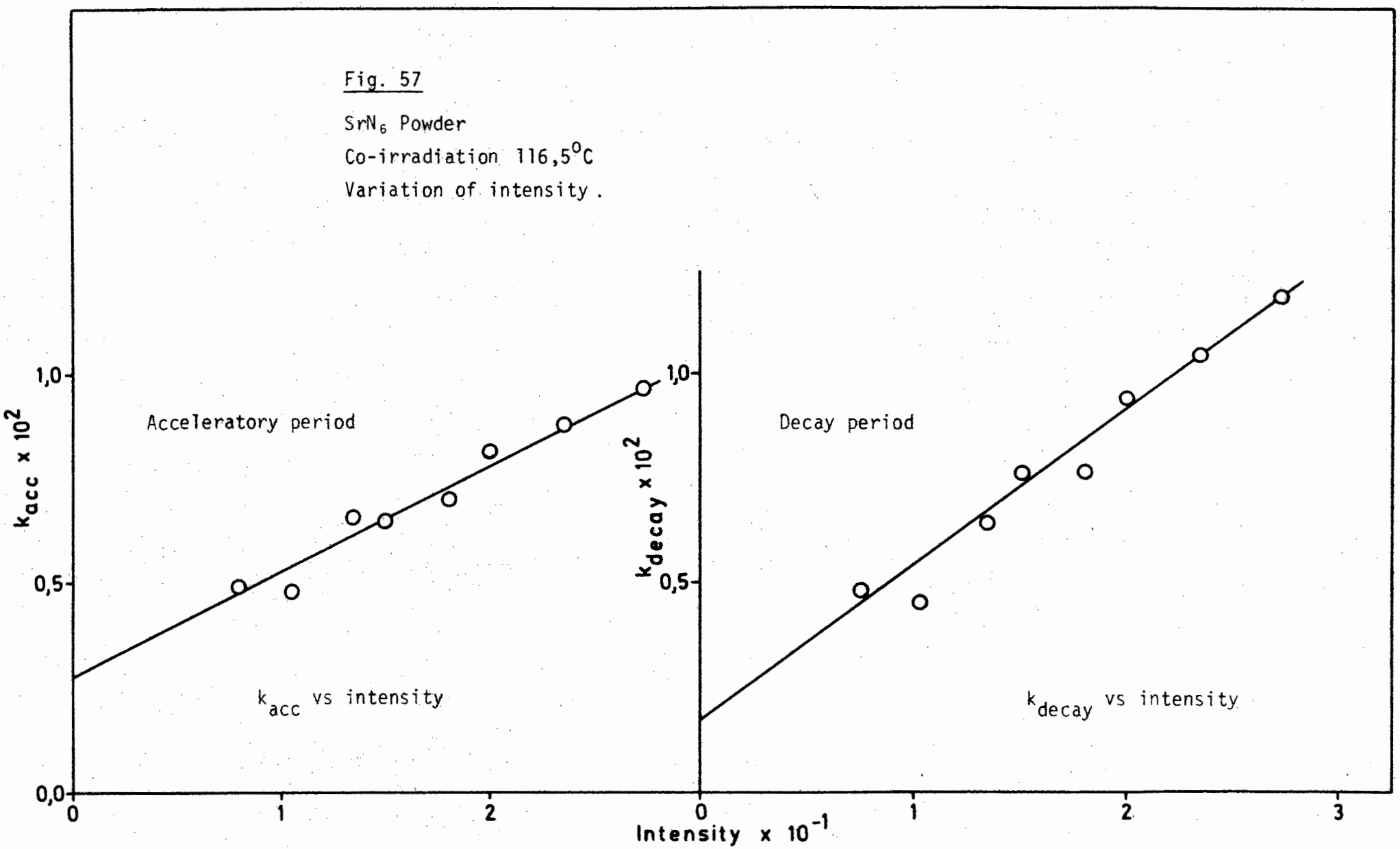

Fig. 57

SrN_6 Powder

Co-irradiation 116,5°C

Variation of intensity .

(if) Interruption of a co-irradiated decomposition : dark rate determination

For decompositions of either barium or strontium azide above 100,0°C the reaction did not cease when the light was switched off - the dark rate was considerable. After co-irradiation had ceased i.e. when the shutter was closed during co-irradiation, the samples did not decompose as they would have done had the initial decomposition been entirely thermal. This is due to the high sensitivity of either azide to pre-irradiation by ultraviolet light.

Dark rates are illustrated in Fig. 58 (decomposition temperature 122,0°C and light intensity 14,25 units) and Fig. 59 (decomposition temperature 130,0°C and light intensity 6,4 units) for barium azide. Fig. 60 and 61 show dark rates for strontium azide when temperatures of 120,0°C (intensity 15,25 units) and 130,0°C (intensity 7,0 units) are used for decomposition.

(ig) Admittance of water vapour following an interruption

Water vapour (17 torr pressure) was introduced at various stages of co-irradiated decompositions of barium and strontium azides in order to investigate the presence of metallic nuclei. The procedure has been described under the experimental section.

A decomposition temperature of 115,0°C and light intensity of 13,0 units were chosen for the "water interruptions" of barium azide and a decomposition temperature of 116,0°C and light intensity of 16,0 units for strontium azide.

Water vapour was allowed to react with both azides for 1 min. at the desired point of interruption. For barium azide water vapour

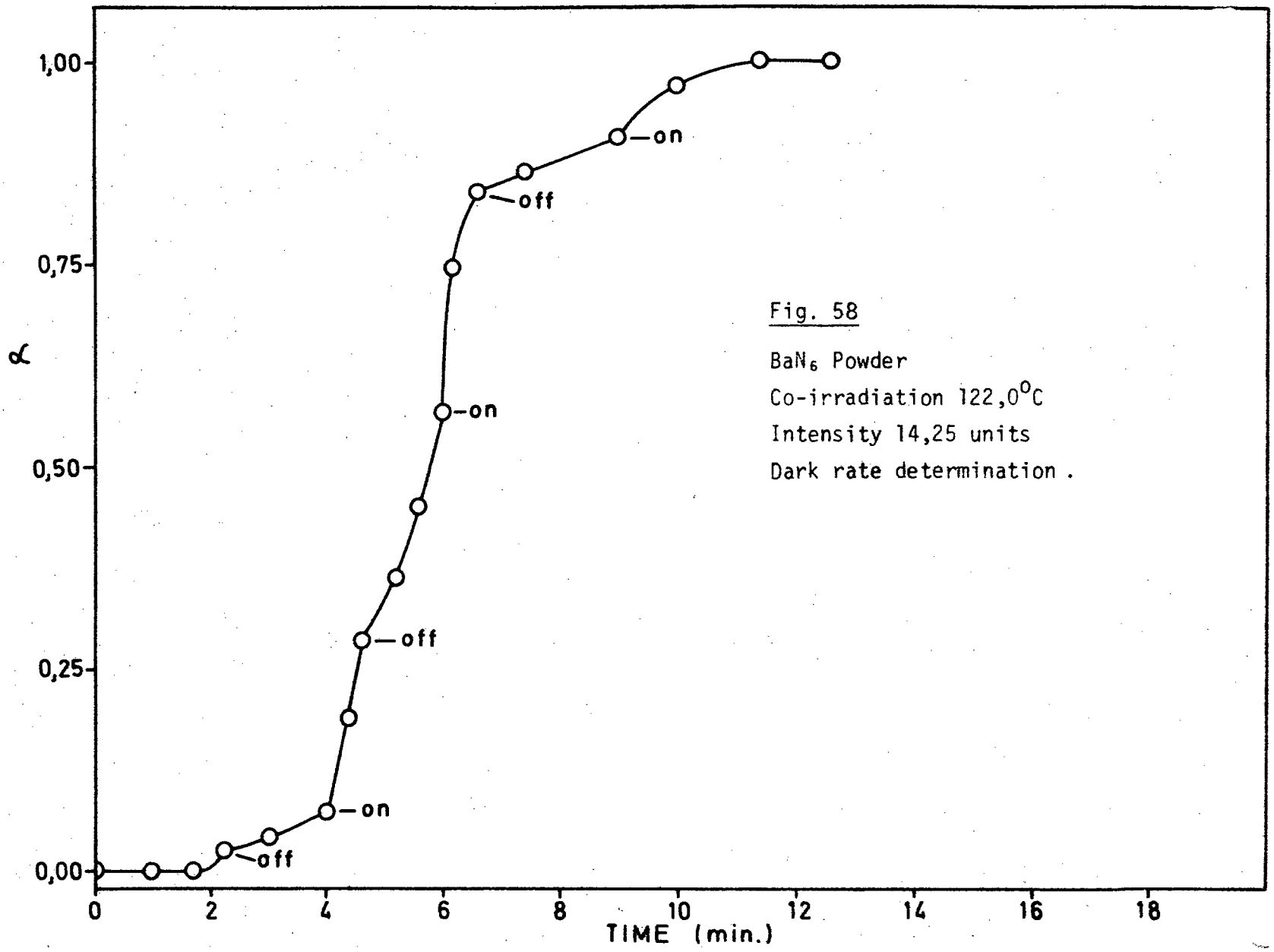

Fig. 58

BaN_6 Powder
Co-irradiation 122,0°C
Intensity 14,25 units
Dark rate determination .

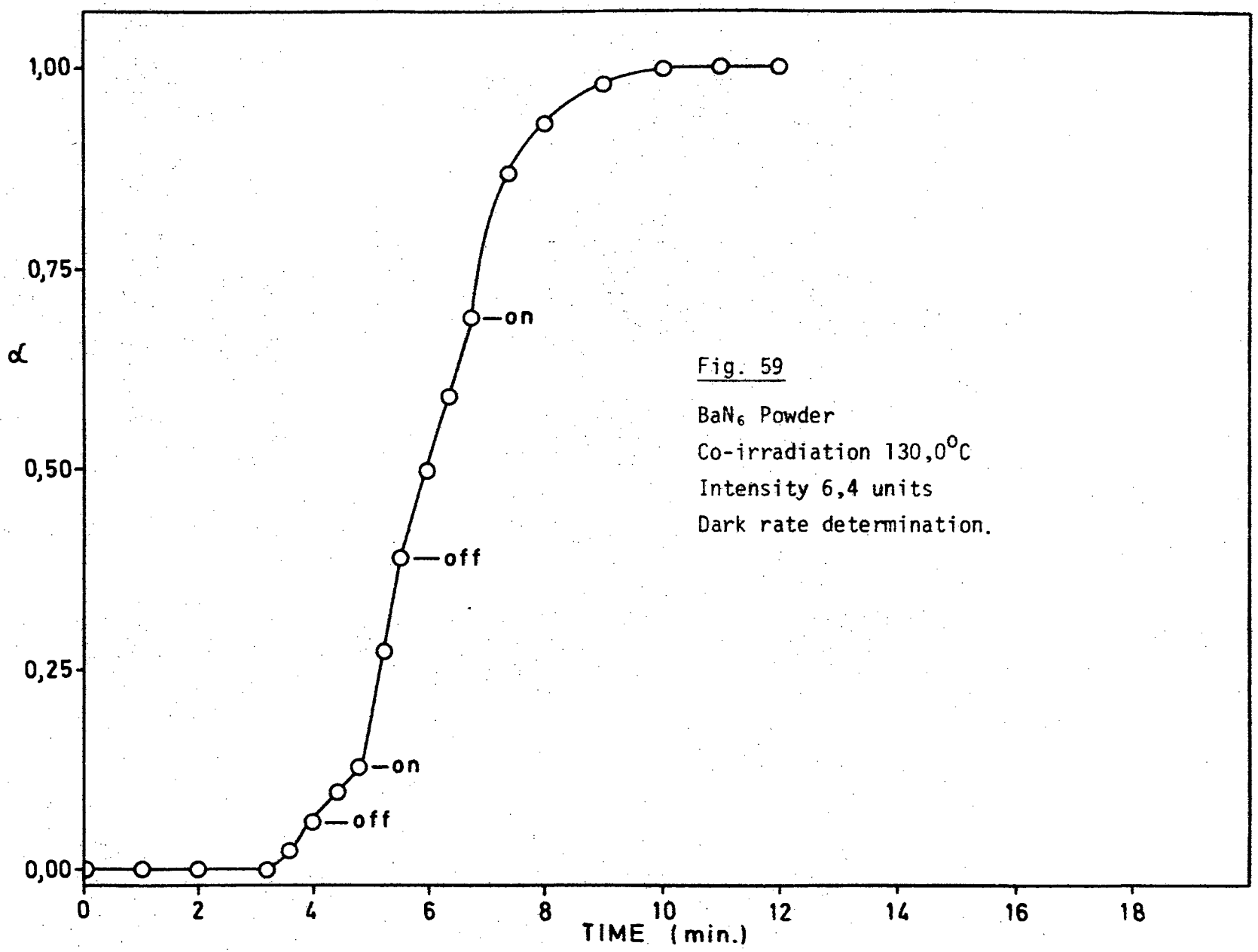

Fig. 59

BaN_6 Powder
Co-irradiation 130,0°C
Intensity 6,4 units
Dark rate determination.

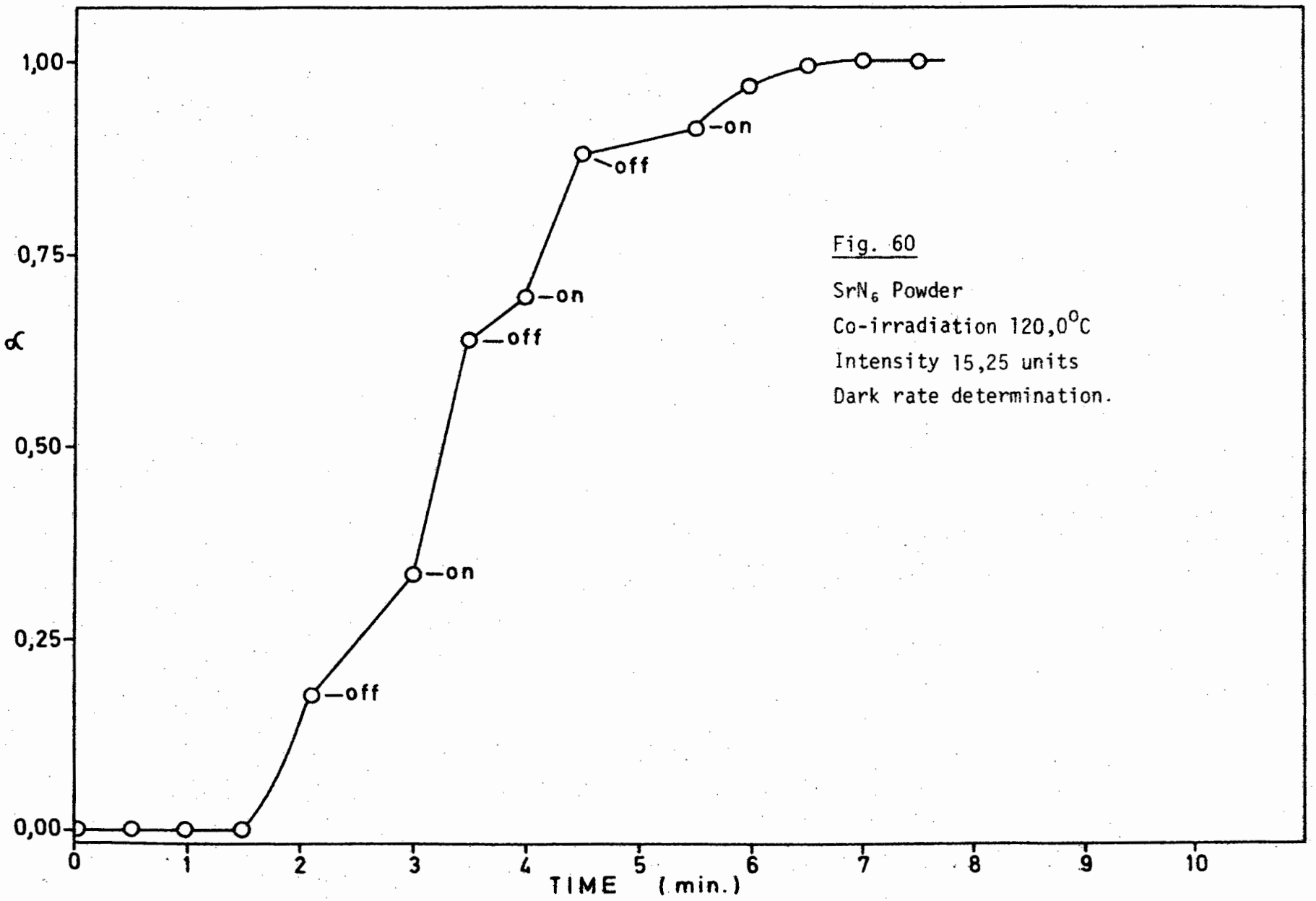

Fig. 60

SrN_6 Powder
Co-irradiation 120,0°C
Intensity 15,25 units
Dark rate determination.

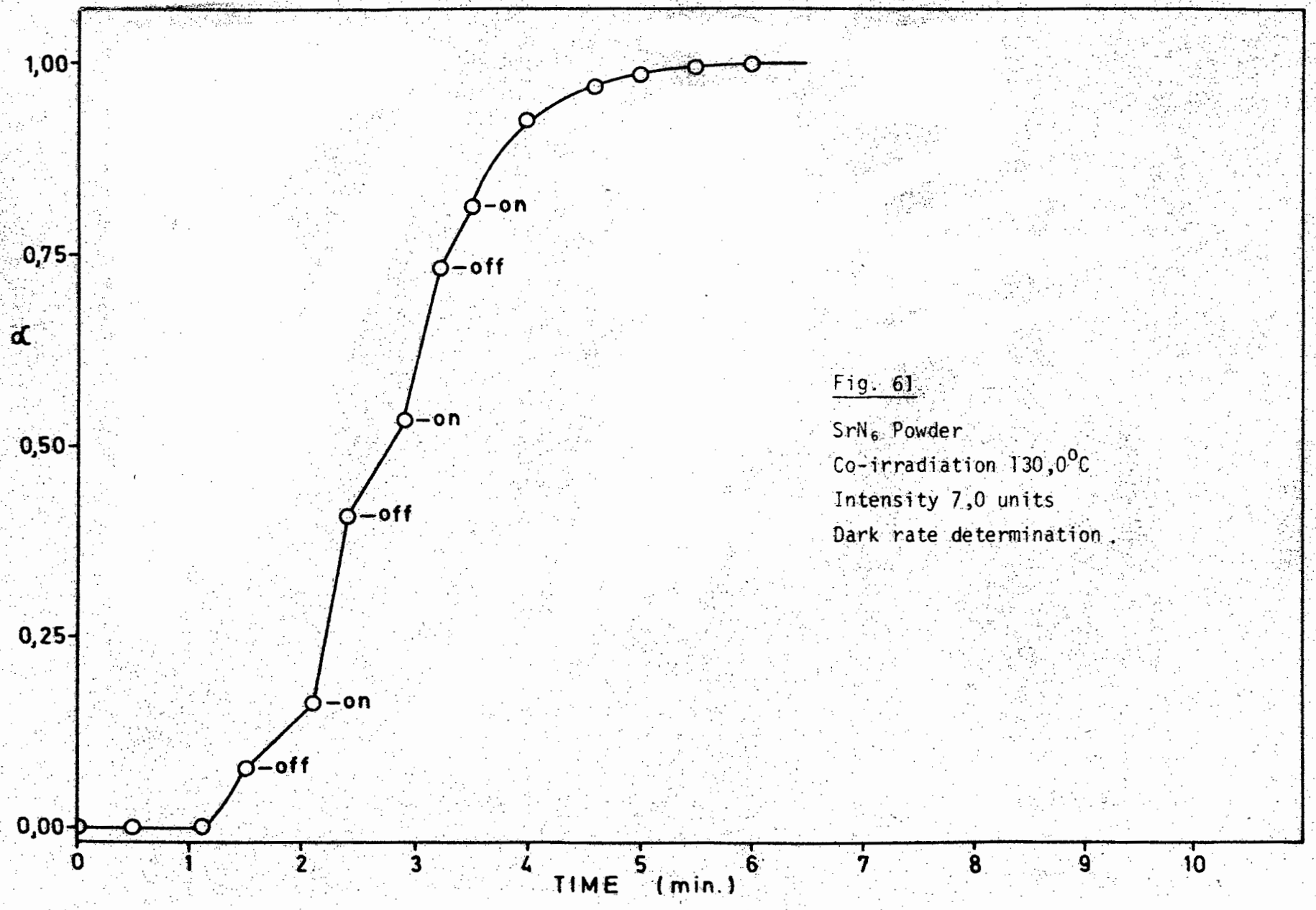

Fig. 61

SrN_6 Powder
Co-irradiation 130,0°C
Intensity 7,0 units
Dark rate determination .

was introduced at t = o; midway along the induction period and at α values of 0,01; 0,10; 0,22; 0,38; 0,47; 0,53. Water vapour was allowed to react with strontium azide at t = o; midway along the induction period and at α values of 0,01; 0,18; 0,31; 0,50.

The results of the interaction of water vapour at various stages of decomposition were the same for both compounds and similar to those found for the corresponding reactions in the photolytic temperature range. Water vapour introduced at t = o and midway along the induction period had no effect on the subsequent co-irradiated reaction i.e. the run continued as though no interruption had occurred. Water vapour introduced at the end of the induction period and at positions further along the decomposition curve caused the subsequent reaction to proceed after an induction period. The length of the new induction period following an interruption at α = 0,01 was shorter than that of the uninterrupted run. These new induction periods increased in duration as the point of interruption along the decomposition curve increased. The acceleratory and decay reactions following the new induction periods were slower than that of an uninterrupted decomposition. Water vapour introduced at the inflection point and in the decay period destroyed the subsequent reaction. The final pressure of the reactions following a "water interruption" was much lower than that of an uninterrupted decomposition. The results for barium azide are illustrated in Fig. 62 and those for strontium azide are illustrated in Fig. 63. The curves have been plotted as pressure against time and not the usual α vs t, to show the effect of water vapour on the final pressure.

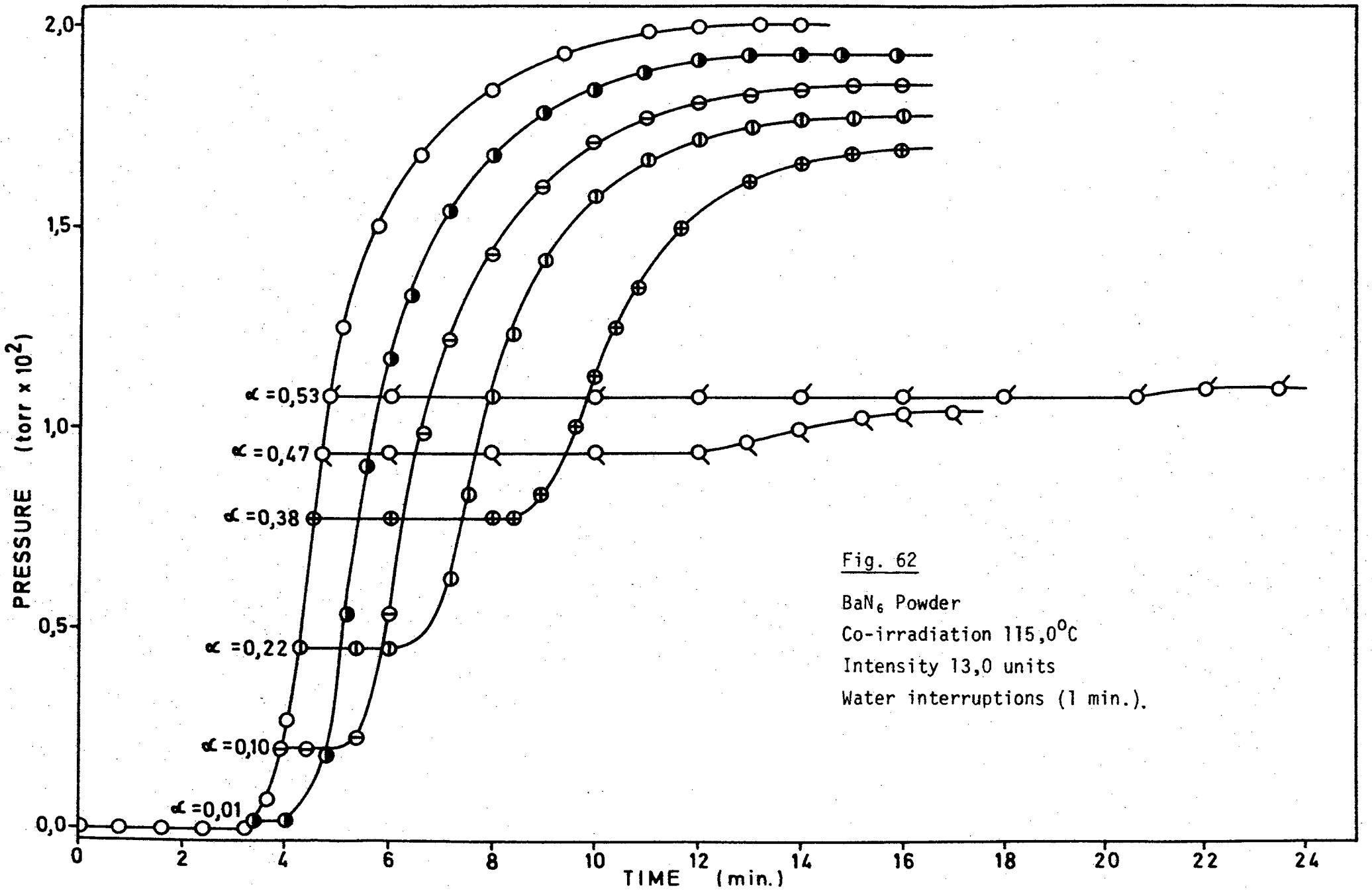

Fig. 62

BaN_6 Powder
Co-irradiation 115,0°C
Intensity 13,0 units
Water interruptions (1 min.).

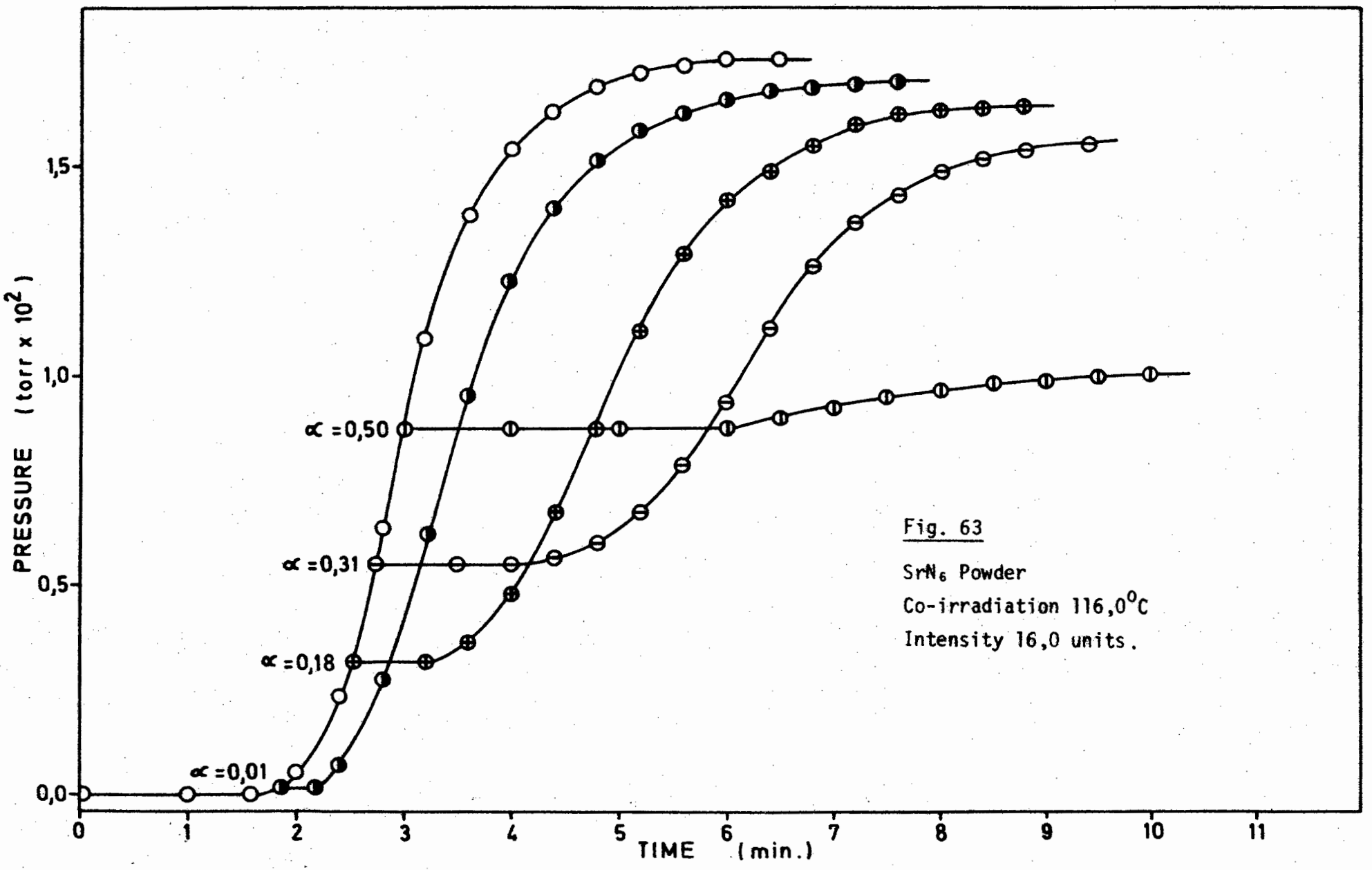

Fig. 63

SrN_6 Powder
Co-irradiation 116,0°C
Intensity 16,0 units.

(ih) The effect of filtering the high intensity arc with blue and ultraviolet transmission filters

The high intensity ultraviolet arc was filtered with various Schott filters in order to determine the wavelengths most effective for the co-irradiation of barium and strontium azides. For barium azide a decomposition temperature of 115,8°C was chosen and for strontium azide a temperature of 116,0°C was chosen. An incident light intensity of 27,5 units was chosen for both compounds. Table 10 in the corresponding section on photolysis, lists the blue and ultraviolet transmissions used, giving the Chance equivalents for reference purposes. The intensity of the transmitted wavelengths is also listed.

The results for barium and strontium azides were analogous. The rate of the reaction decreased in the order of 3mm UG5 > 1mm UG1 > 5mm BG12. The results are plotted out in Fig. 64 and Fig. 65 for barium and strontium azides respectively.

(ii) Pellets

It was found that irradiation of barium and strontium azide pellets (8mg; 0,25mm thick and 0,5mm in diameter) with ultraviolet light during thermal decomposition (110,0° - 135,0°C) had the same effect as found with co-irradiated powder viz a shortening of the induction period and an increase in the rate of the acceleratory and decay reactions. A significant dark rate was measurable with both azides throughout this temperature range due to the thermal decomposition of the pellet. The percentage decomposition of a pellet

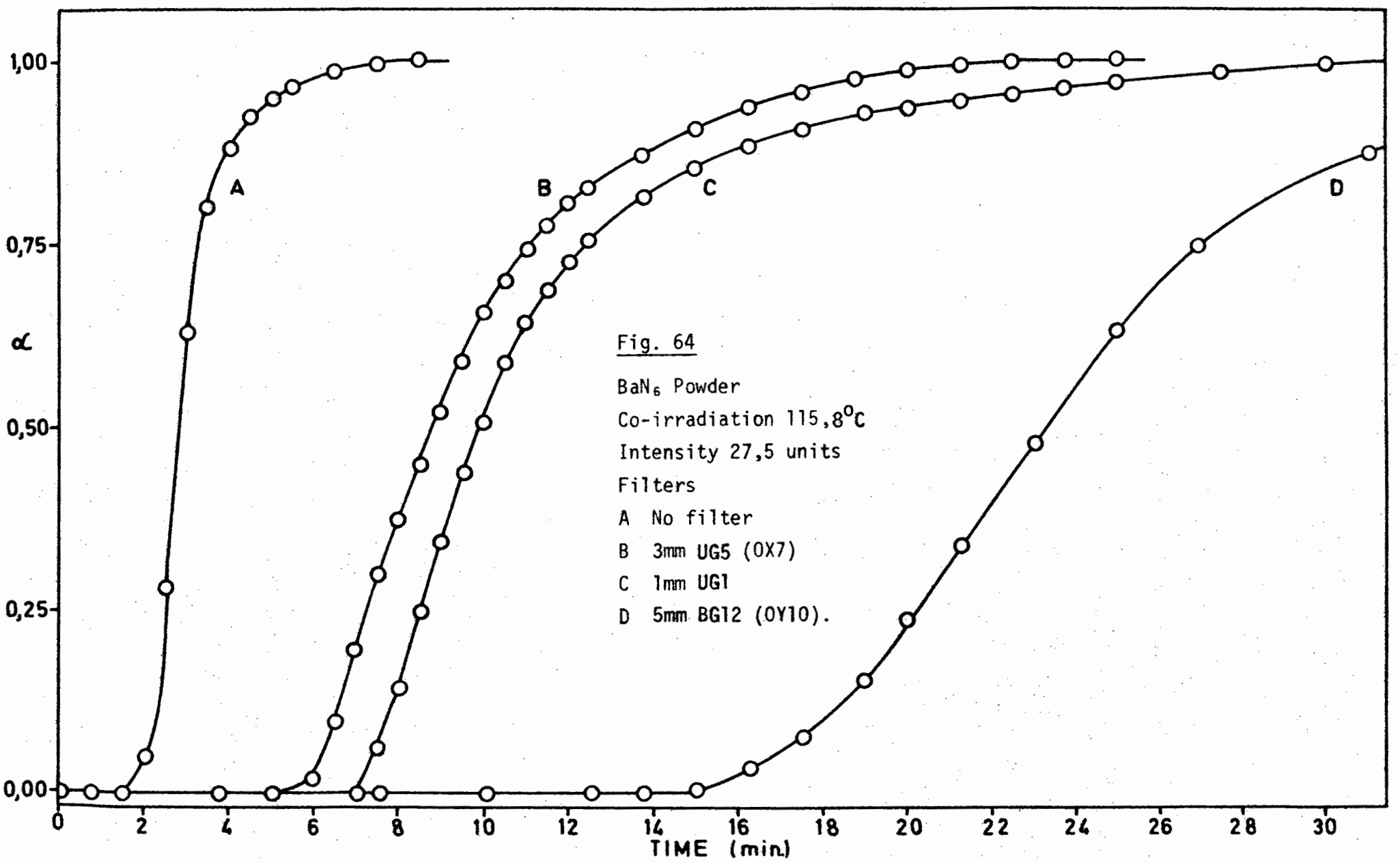

Fig. 64

BaN_6 Powder
Co-irradiation 115,8°C
Intensity 27,5 units
Filters
A No filter
B 3mm UG5 (0X7)
C 1mm UG1
D 5mm BG12 (0Y10).

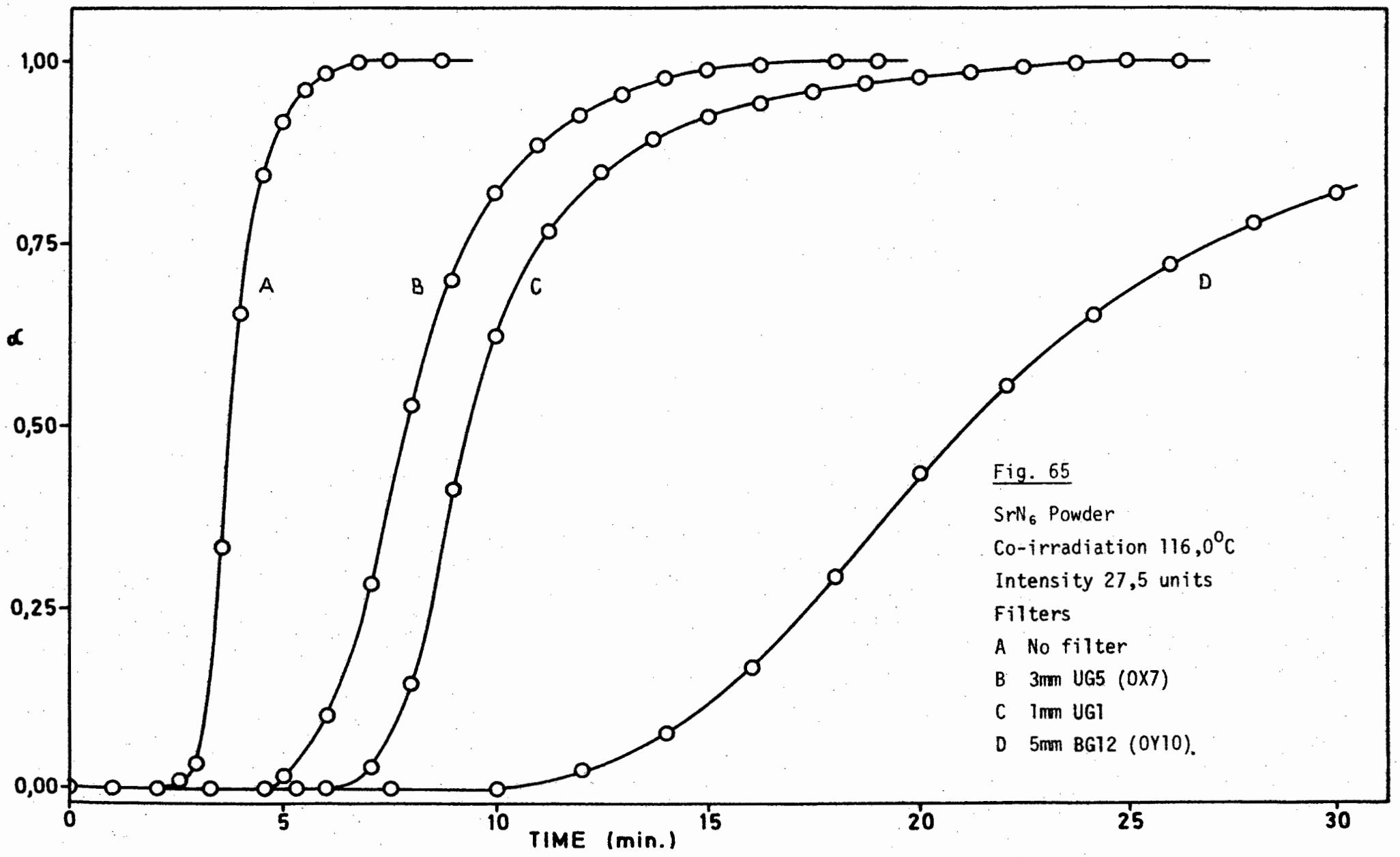

Fig. 65

SrN_6 Powder
Co-irradiation 116,0°C
Intensity 27,5 units
Filters
A No filter
B 3mm UG5 (0X7)
C 1mm UG1
D 5mm BG12 (0Y10).

irradiated during thermal decomposition was found to be the same as that of an unirradiated pellet in this temperature range viz 95,0% for barium azide and 71,2% for strontium azide. A comparison between a thermal and a co-irradiated decomposition of barium azide pellets is shown in Fig. 66 (decomposition temperature 115,8°C, intensity 14,0 units) and Fig. 67 for strontium azide (decomposition temperature 115,0°C, intensity 15,0 units). A pelleting pressure of 2000 lb/sq.in. was used for all pellets.

(iia) Shape of decomposition curve, mathematical analyses and reproducibility

The shape of the co-irradiated decomposition curves, of both barium and strontium azides with pelleting pressure either 2000 lb/sq.in. or 600 lb/sq.in., did not resemble that obtained from photolysed pellets but rather the shape of the co-irradiated powder decomposition curves. These curves of co-irradiated pellets showed an induction period, during which there was no evolution of gas, followed by an acceleratory and decay reaction.

The mathematical analyses for these curves were identical to those found for co-irradiated powder i.e. the Avrami-Erofeyev equation with n = 2 fitted the acceleratory period and the unimolecular law fitted the decay period. The fit of these analyses for the curves obtained from co-irradiated barium and strontium azide pellets, was identical. The inflection point on the curves obtained from either azide occurred at $\alpha = 0,54$. The Avrami-Erofeyev equation fitted the curves from $0,01 < \alpha < 0,54$ while the unimolecular decay law fitted the curves from $0,54 < \alpha < 0,98$.

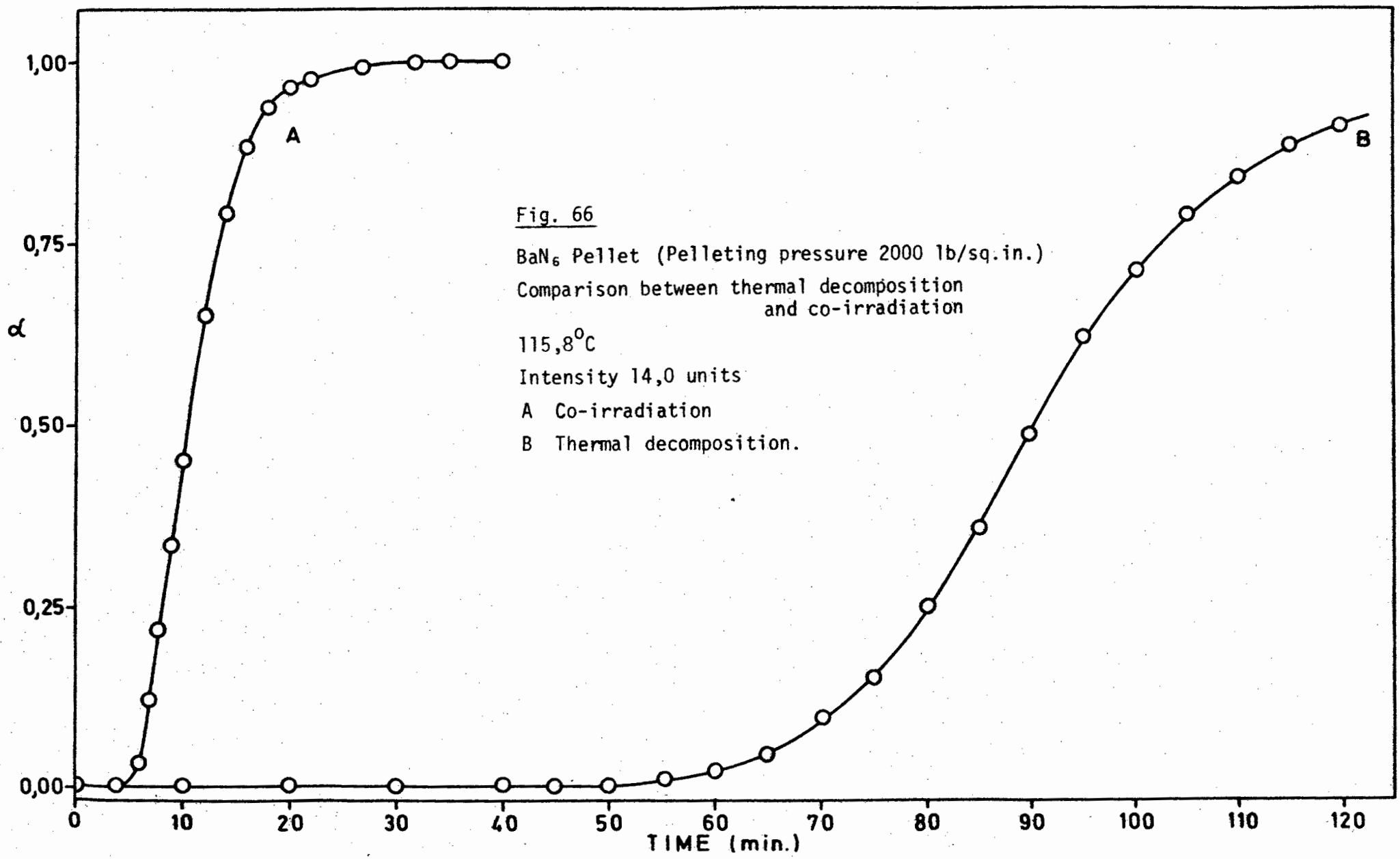

Fig. 66

BaN_6 Pellet (Pelleting pressure 2000 lb/sq.in.)

Comparison between thermal decomposition and co-irradiation

115,8°C

Intensity 14,0 units

A Co-irradiation

B Thermal decomposition.

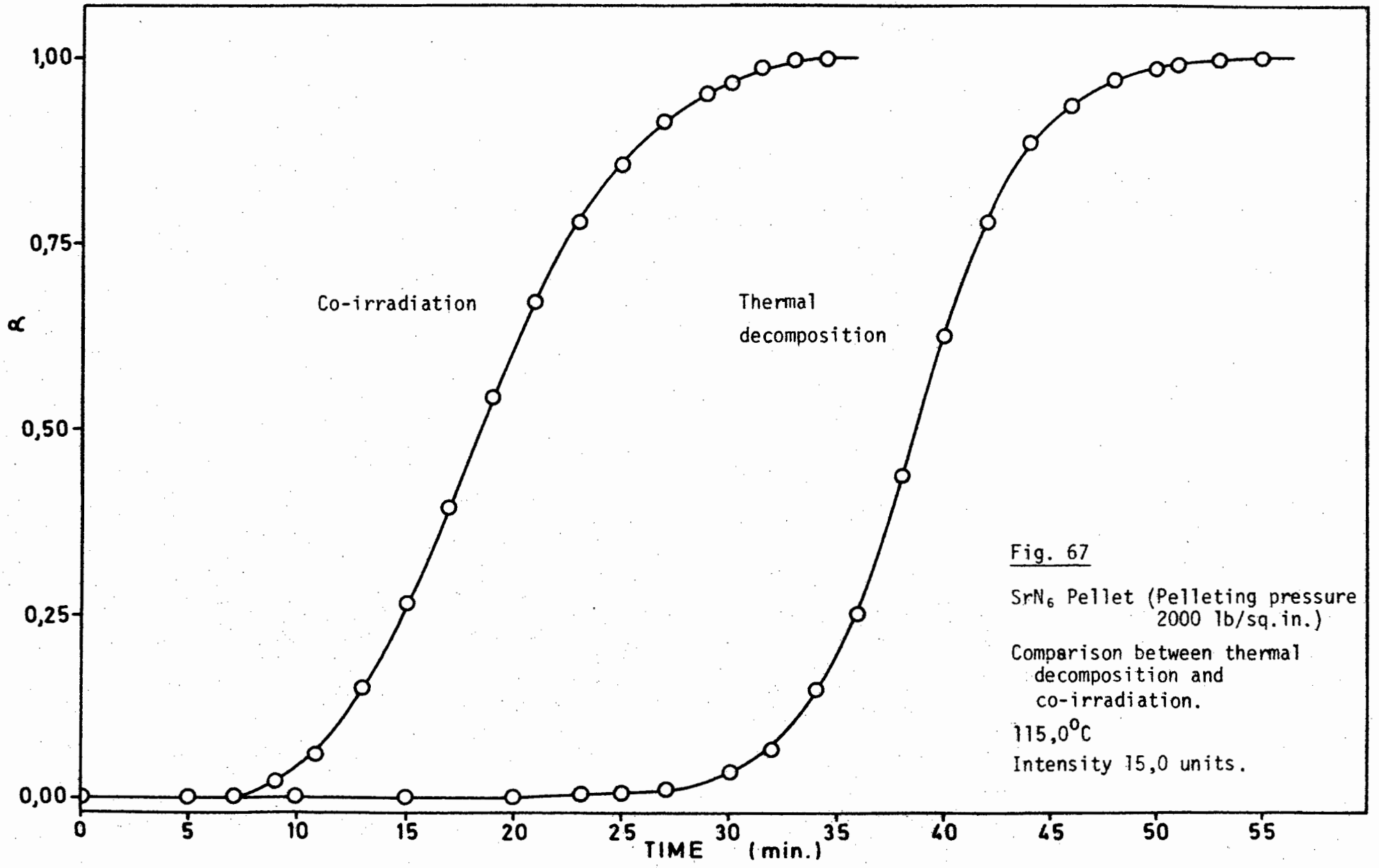

Fig. 67

SrN_6 Pellet (Pelleting pressure 2000 lb/sq.in.)

Comparison between thermal decomposition and co-irradiation.

115,0°C

Intensity 15,0 units.

A typical α vs t curve with analyses for a barium azide pellet (decomposition temperature 115,8^{o}C, intensity 14,0 units) is illustrated in Fig. 68 and for a strontium azide pellet (decomposition temperature 115,0^{o}C, intensity 15,0 units) in Fig. 69.

Reproducibility for co-irradiated barium and strontium azide pellets was unobtainable. The nature of the irreproducibility is shown in Fig. 70 for barium azide (decomposition temperature 112,0^{o}C and intensity 15,5 units) and Fig. 71 for strontium azide (decomposition temperature 115,0^{o}C and intensity 15,0 units).

(iib) Evaluation of activation energies

Since the reproducibility of co-irradiated decompositions was not at all good for either barium or strontium azide pellets, activation energies could not be determined using individual runs. An attempt was made to find rate constants for the acceleratory and decay periods of pellets of the two azides using the split run technique. The procedure was identical to that used for the determination of rate constants for the decay reaction of photolysed pellets. The method was not successful since on returning the furnace into position around the cell, for the determination of the second rate constant, a large volume of gas was given off during the warm-up stage due to thermal decomposition of the pre-irradiated pellet. This resulted in the pellet being in the decay stage when the cell had reached the temperature required for the determination of the second rate constant for the acceleratory period. Thus the attempt to determine rate constants for the pellets failed and consequently no activation energies could be found.

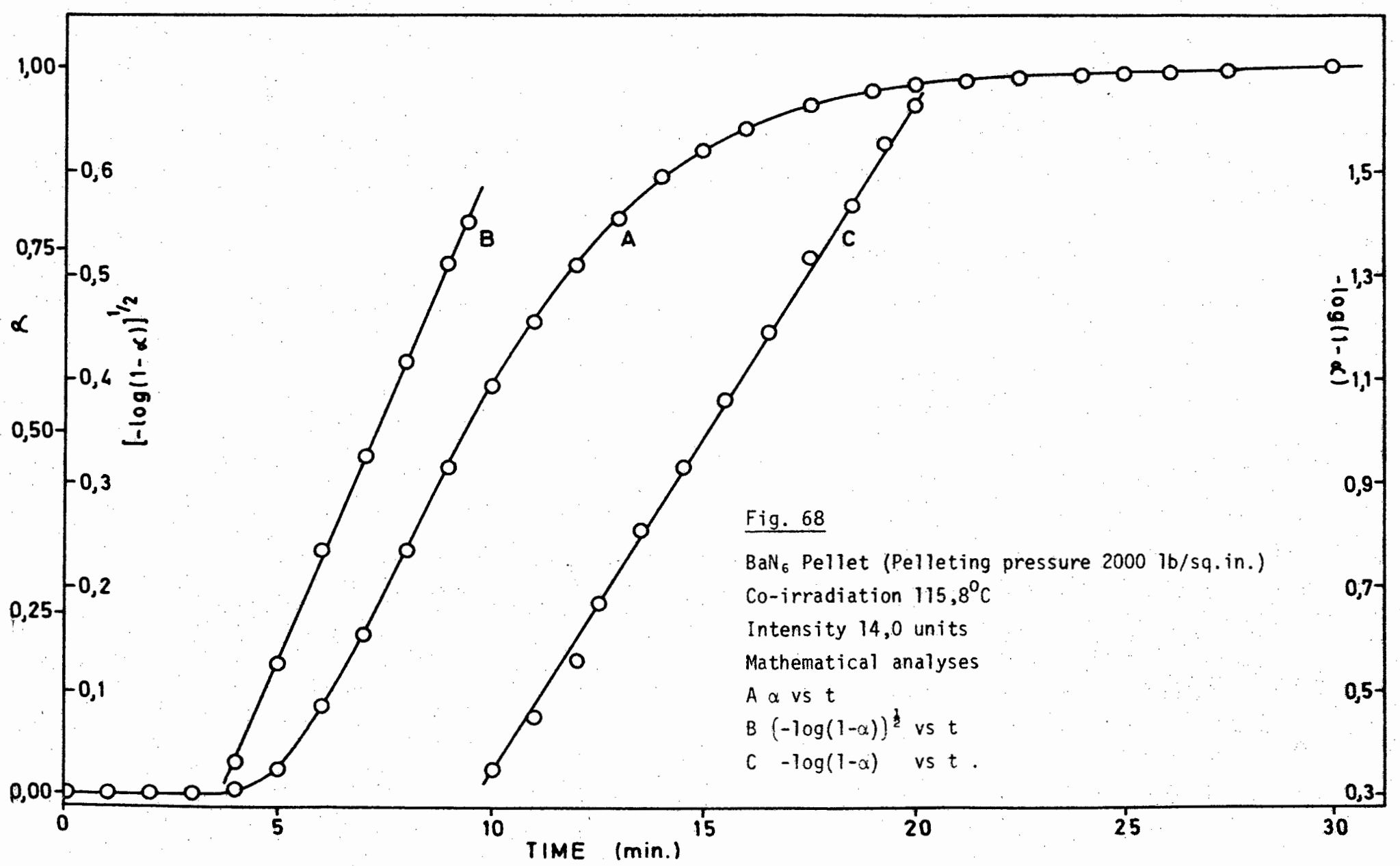

Fig. 68

BaN_6 Pellet (Pelleting pressure 2000 lb/sq.in.)
Co-irradiation 115,8°C
Intensity 14,0 units
Mathematical analyses
A α vs t
B $(-\log(1-\alpha))^{\frac{1}{2}}$ vs t
C $-\log(1-\alpha)$ vs t .

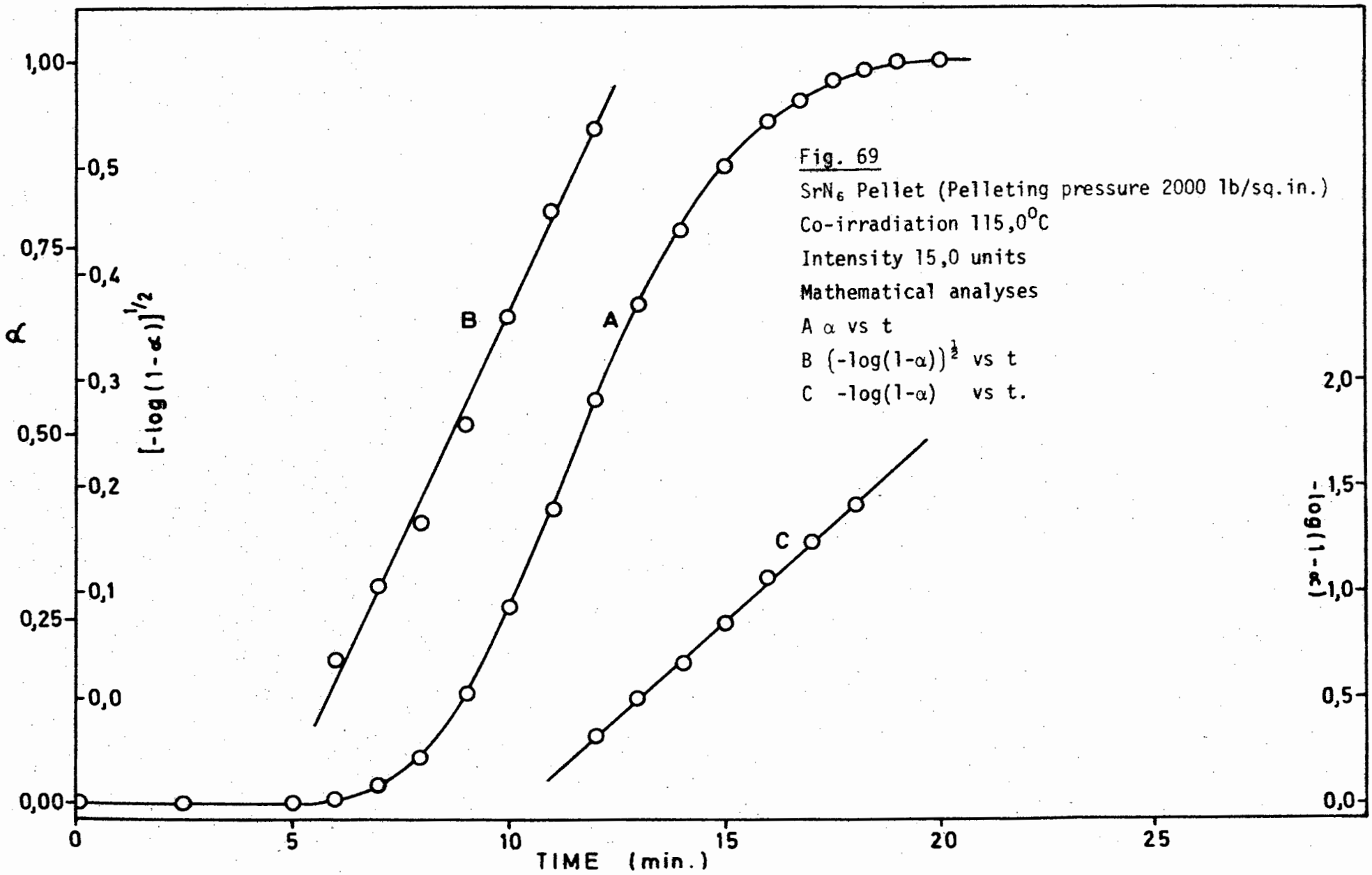

Fig. 69

SrN_6 Pellet (Pelleting pressure 2000 lb/sq.in.)

Co-irradiation 115,0°C

Intensity 15,0 units

Mathematical analyses

A α vs t

B $(-\log(1-\alpha))^{\frac{1}{2}}$ vs t

C $-\log(1-\alpha)$ vs t.

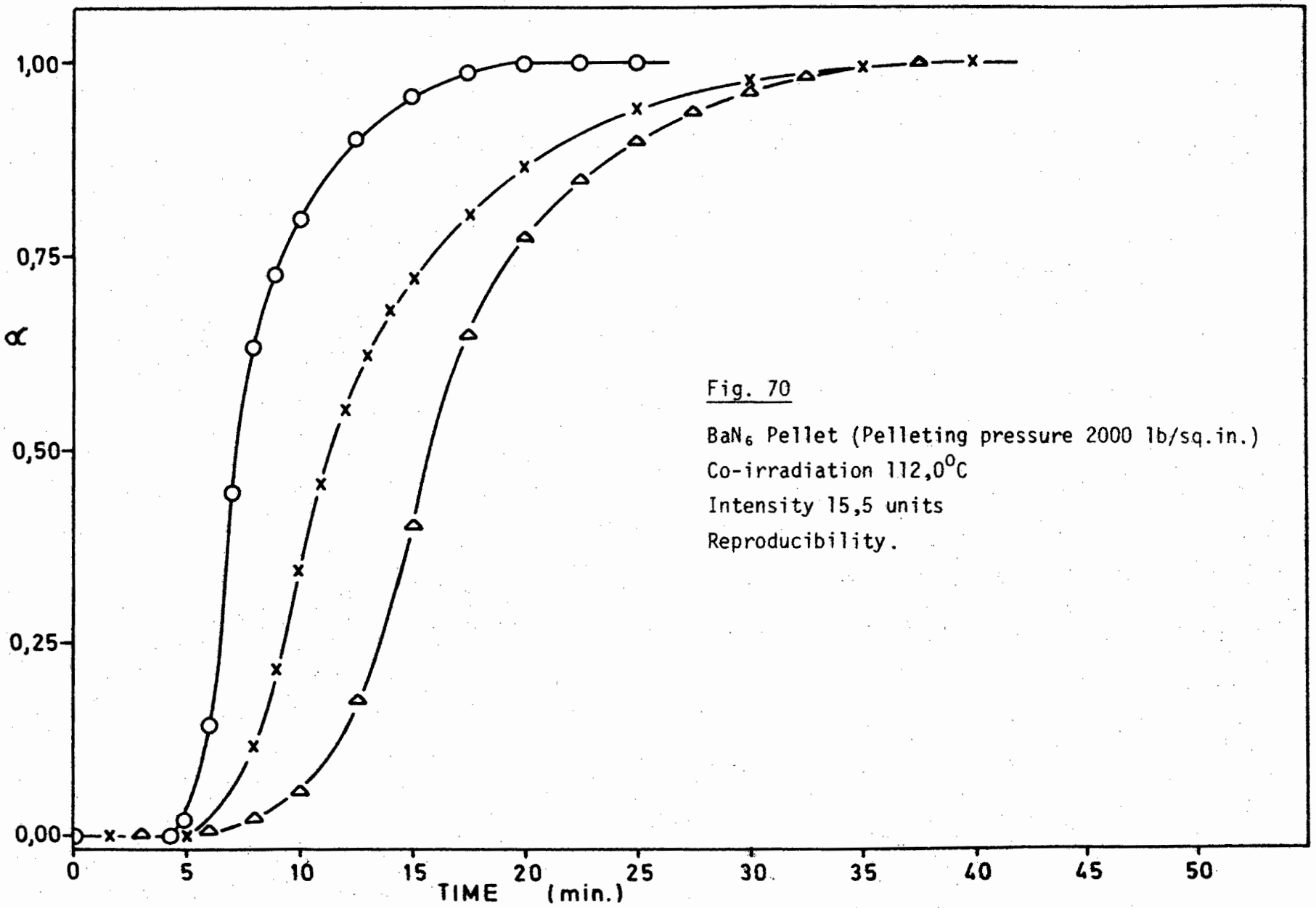

Fig. 70

BaN_6 Pellet (Pelleting pressure 2000 lb/sq.in.)
Co-irradiation 112,0°C
Intensity 15,5 units
Reproducibility.

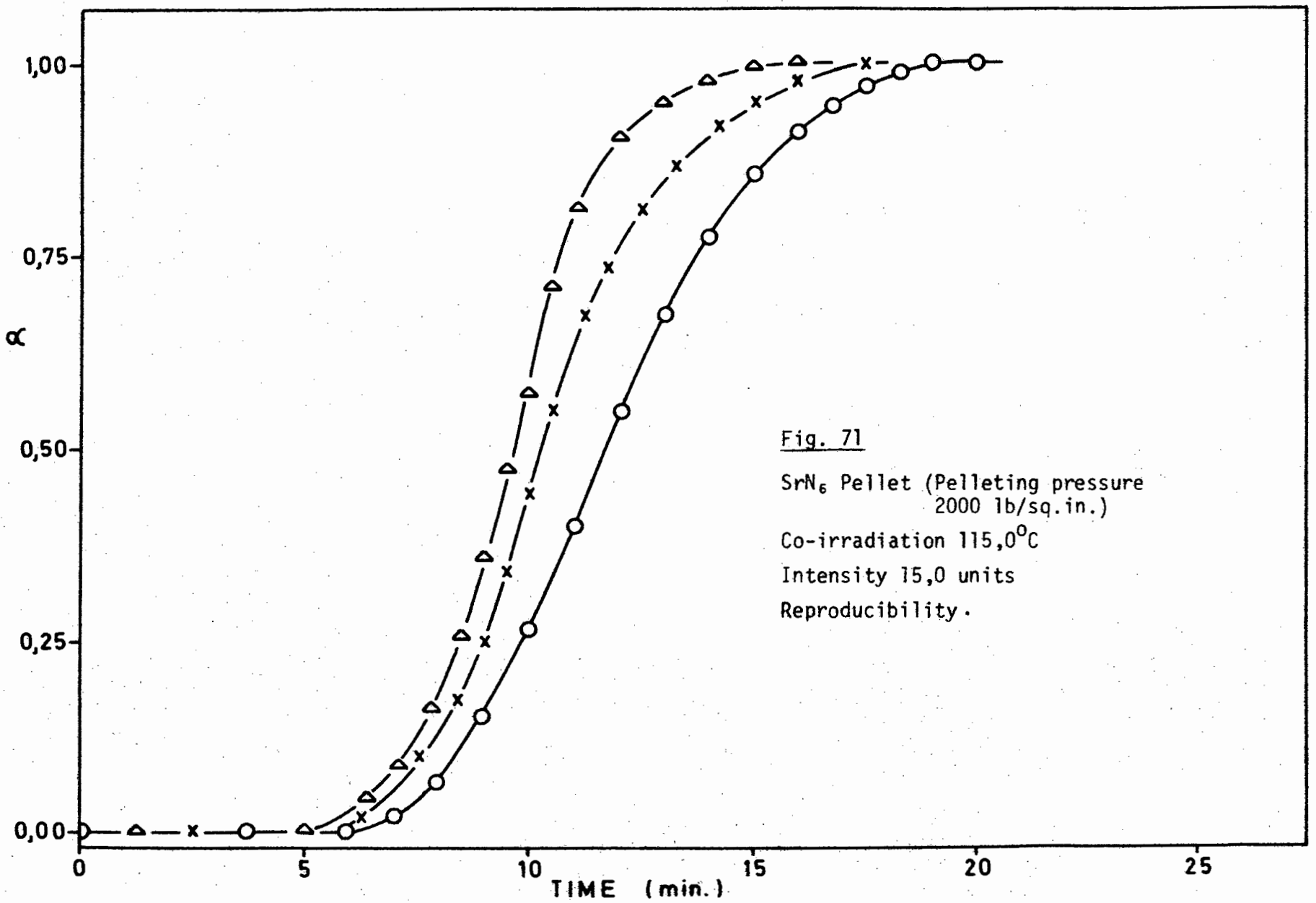

Fig. 71

SrN_6 Pellet (Pelleting pressure 2000 lb/sq.in.)

Co-irradiation 115,0°C

Intensity 15,0 units

Reproducibility.

(iic) Visual observations

The colour of barium and strontium azide pellets pressed at both 600 lb/sq.in. and 2000 lb/sq.in. was observed at various stages of the co-irradiated decomposition. A temperature of 115,0°C and light intensity of 10,0 units were employed for both azides. The results were similar to those found for co-irradiated powders of barium and strontium azides.

Irrespective of pelleting pressure and compound pressed, the upper surface of the pellet changed to a light grey colour when the reaction reached the end of the induction period, the lower surface showed no change in colour at this stage of reaction. At α = 0,25 the lower surface had changed to a light grey while the upper surface had changed to a dark grey colour. The surfaces continued to darken as the reaction progressed and at α = 0,54 the pellet was dark black on both surfaces.

(iid) Admittance of water vapour following an interruption

Water vapour (17 torr pressure) was allowed to react with barium azide pellets (pressed at 2000 lb/sq.in.) for 1 min. at various stages of a co-irradiated decomposition. This was done in order to determine the importance of barium metal at various stages of the decomposition. The method employed and results obtained were identical to those obtained for co-irradiated powder. A decomposition temperature of 115,0°C and light intensity of 10,0 units were chosen.

The subsequent reaction following an interruption at α = 0,54, the inflection point, was completely destroyed. Reactions after interruptions between 0,01 < α < 0,54, proceeded after a new induction

period. Water vapour was found to have no effect on the subsequent reaction when the interruption occurred during the induction period.

Identical results were obtained when strontium azide pellets (pressed 2000 lb/sq.in.) were reacted with water vapour for 1 min. A decomposition temperature of 115,0^{o}C and light intensity of 10,0 units were chosen for these tests on strontium azide pellets.

5 DISCUSSION

Both barium and strontium azides were subjected to ultraviolet radiation from a high intensity 100 watt "point source" high pressure mercury arc lamp, over a wide range of temperatures : 27,0° - 135,0°C for barium azide and 30,0° - 135,0°C for strontium azide. Decompositions of barium azide in the temperature range 27,0° - 100,0°C and strontium azide in the temperature range 30,0° - 90,0°C with ultraviolet light are referred to as photolytic decompositions, while decompositions of both azides in the temperature range 110,0° - 135,0°C with ultraviolet light are referred to as co-irradiated decompositions (122). The results obtained on the effects of ultraviolet light on powdered and pelleted barium azide will be considered initially and will be followed by a similar discussion for strontium azide.

5A PHOTOLYSIS OF BARIUM AZIDE

(i) Powder

The pressure-time plots obtained from barium azide powder when photolysed in the temperature range 27,0° - 100,0°C were sigmoid in shape, as was found for the low temperature photolysis using a low intensity lamp (61).

Reproducibility of the acceleratory and decay reactions in the photolytic temperature range was satisfactory. Due to variation in the defect surfaces of the powders the induction period did not prove to be highly reproducible.

The pressure-time curves of photolysed barium azide powder exhibited true induction periods during which there was no evolution

of gas. This period was followed by an acceleratory period, described by the Avrami-Erofeyev equation with n = 2, and finally a decay period which conformed to the unimolecular decay law.

The volume of gas obtained during photolysis was found to be the same as that expected if the test sample had been thermally decomposed at 130,0°C. Another feature of the photolysis was that the decay reaction commenced the moment the particles of the powder had turned black on all external surfaces.

Investigation of the dark rate at all temperatures in the photolytic temperature range showed that it was non-existent.

Photolysis of a sample after thermal pre-treatment, for a period of time equal to that of the thermal induction period, resulted in the usual photolytic reaction but without an induction period. Reversal of this procedure by photolysing the sample to the end of the induction period and then decomposing it thermally, resulted in a normal pre-irradiated decomposition with the absence of an induction period. This leads to the conclusion that thermal centres and photolytic centres are similar in nature.

In the temperature range 27,0° - 100,0°C two distinct activation energies were found for the photolysis of the barium salt, the transition temperature occurring at 60,0°C. At this temperature the activation energy increased from 6,2 Kcal.mol.$^{-1}$ to 11,4 Kcal.mol.$^{-1}$ over the induction period and from 7,6 Kcal.mol.$^{-1}$ to 11,3 Kcal.mol.$^{-1}$ over the acceleratory period and from 6,6 Kcal.mol.$^{-1}$ to 12,9 Kcal.mol.$^{-1}$ over the decay period. The dependence of the reciprocals of the duration of the induction periods on intensity (I) were found to be $I^{0,7}$ below 60,0°C and $I^{0,6}$ above 60,0°C. In view of the bad reproducibility of the induction period the relationship may be approximated to $I^{1,0}$. The rate constants for the acceleratory and decay reactions depended

approximately on the square of the light intensity at temperatures below 60,0°C and on the first power of the light intensity at temperatures above 60,0°C. The results in these two temperature ranges will be discussed separately.

(ia) Photolysis in the temperature range 27,0° - 60,0°C

A brown colouration, marked by the first evolution of gas at the end of the induction period of photolysed samples of barium azide powder, was observed. This colouration can be attributed to barium metal which is formed at the end of the induction period. It is assumed that the sites at which decomposition can take place are those where severe strain exists such as at localities on the surface of the particles e.g. surface cracks or lines where disorganization or mechanical damage has taken place and where there is a higher thermodynamic instability and unsaturation of cohesive forces. At the core of an emergent edge dislocation, either isolated or in emergent grain boundaries terminating at the surface, large stresses exist. The chemical potential and stereochemical environment of ionic species in the immediate vicinity of a dislocation differ from those of similar species at ideal lattice sites.

In the samples of barium azide used, large stresses exist through dehydration and grinding, leading to the formation of dislocations which will have grouped to form high angle grain boundaries.

Since the crystal structure of barium azide is known to be layered (125) it is likely that a large number of incomplete planes of the edge dislocations in an emergent grain boundary will contain only azide ions or Ba^{2+} ions. Thus decomposition will commence when azide ions at positions of stress on the surface and along the planes of the

particles become optically excited.

The optical absorption spectrum, obtained by Deb (41), of thin films and pellets of barium azide showed three bands with multiple structure in the wavelength region 1400 - 2500 Å. The spacings in the band structure were shown to correspond with the fundamental vibration frequencies of the azide ion, which led to the conclusion that each of the absorption peaks is associated with the azide ion itself. From the appearance of the well-resolved vibrational structure of the bands at 2000 Å and 1800 Å and the low magnitude of the absorption coefficient of these two bands, it was concluded that the electronic transitions would be forbidden. Thus after comparison with the electronic spectrum of the isoelectronic molecule N_2O (126) it was decided that absorption bands in the range 1400 - 2500 Å could be interpreted as transitions involving excited states of the azide ion itself. Moreover the absence of any photocurrent at wavelengths longer than 1700 Å indicated that electronic transitions in this region involved bound excited or exciton states. But due to the fact that the exciton transitions are associated with vibrational structure, it was concluded that the excitons are trapped on the molecule on which they are formed (127).

The absorption peak at 1550 Å showed a large absorption coefficient indicating allowed optical transitions of electrons from the valence band to the conduction band i.e. the production of free electrons and positive holes.

From the results of filtering the high intensity ultraviolet arc it can be seen that the rate of decomposition with the 3mm UG5 filter was reduced from that of the unfiltered arc. This lowered rate is not due entirely to the change in wavelength of irradiation, but also due to the reduction in the arc intensity by simple reflection from the

polished filter surface. If this is considered to be constant for all filters used then the reduction in rate with the UG1 and the BG12 filters is very marked. This leads to the assumption that the most effective wavelengths from the ultraviolet spectrum for the photolysis of barium azide would be in the region 2200 - 2800 Å. From the above discussion it can be concluded that the most effective wavelengths used were of less energy than that required for the formation of positive holes and electrons, and it can be assumed that absorption leads to excited azide ions rather than excitons. The absorbed energy is localized at the favoured sites in the form of vibrational or internal electronic excitation. A similar assumption has been made for nitronium perchlorate (34), silver oxalate (93) and sodium bromate (36). It was concluded for these compounds that the primary excitations, which eventually lead to decomposition, result in the localization of energy in a trapped anion.

The reduction in rate observed with the use of the UG1 and the BG12 filters (i.e. reduced rates with the use of long wavelengths) is most probably due to the very low absorption coefficient of long wavelengths as compared with the shorter wavelengths and consequently a low rate of excitation of the internal transition.

The reaction scheme proposed here for the formation of nuclei during the induction period, is similar to that proposed by Jacobs et.al. (40) for the photolysis of barium azide:

$$N_3^- \rightleftharpoons^{h\nu} N_3^{-*} \quad \ldots\ldots\ldots\ldots\ldots\ldots\ldots\ldots \quad (1)$$

The excited azide ion N_3^{-*} will only decay to the ground state N_3^- when the azide ion is situated at an ideal lattice site. An excited azide ion adjacent to a ground state azide ion at a surface defect S

(most probably an anion vacancy) reacts with a barium ion, Ba^{++}

$$N_3^-SN_3^{-*} + Ba^{++} \xrightarrow{\Delta} Ba + 3N_2 + S \text{ ..... } (2)$$

The measured activation energy of 6,2 Kcal.mol.$^{-1}$ is associated with this second step.

It is considered that the nuclei formed during the induction period of a photolytic decomposition are similar to those formed during the corresponding period in a thermal decomposition. From the studies of pre-irradiation of barium azide with ultraviolet light (111), it was proved that formation of barium metal nuclei during thermal decomposition occurs on the surface of the azide particles and along the core of a dislocation as it climbs along the surface. However with the high intensity ultraviolet arc used it is expected that barium atoms, formed in step (2), will be located on the surface and on the planes of the crystal, each plane starting at the surface at an emergent grain boundary. These atoms will initially be at the interatomic spacing of barium azide. With time diffusion will take place and at a critical concentration the barium metal atoms will aggregate to form barium metal specks i.e. nuclei. The duration of the induction period is proportional to the time required for the aggregation of metal atoms, which in turn is dependent upon the temperature of decomposition and intensity of light source used. From the mechanism proposed, the duration of the induction period will be inversely proportional to the light intensity which is in accordance with the observed experimental result.

With the aggregation of barium metal atoms to form metal specks growth proper will begin, causing the reaction to accelerate from the rapidly expanding metal/salt interface.

The existence of metal at the end of the induction period has been indicated by "water interruption" photolytic decompositions.

Water vapour introduced at the end of the induction period caused the barium metal on the surface to be destroyed. The subsequent reaction proceeded after a new induction period, shorter than that of the uninterrupted decomposition. This indicates that water vapour only reacted with the nuclei on the surface, leaving those in the bulk of the material i.e. along the planes of the particles, intact. These are possibly newly formed and small. It is assumed that after reaction with water vapour, reaction then proceeds from growth nuclei still present in the bulk of the material. The length of the new induction period is the time required for these growing nuclei to reach a significant critical size. Reaction of water vapour with the salt before the end of the induction period had no effect on the subsequent photolytic reaction, supporting the postulate that barium metal nuclei are formed at the end of the induction period only.

From the work done on the structure and properties of thin films of metal (128), it can be concluded that the barium metal formed at the end of the induction period will have electronic properties associated with the metal. Thin films of metal have been shown to have the same characteristics as those of the bulk metal. These films are formed by lateral growth of nuclei and may become continuous at thicknesses as low as 50 Å. The character of the conductivity of such metal films corresponds very closely to that of the massive metal. Thus it seems likely that very thin 2-dimensional plates of metal nuclei with electronic properties of the bulk metal will form on the surface of the particles and along the planes of the crystal at discrete centres by the end of the induction period.

At the end of the induction period growth of the nuclei commences and the reaction accelerates. The acceleratory period was described mathematically by the Avrami-Erofeyev equation with the exponent taking

the value of n = 2. The general equation takes into account centres of decomposition which are increasing in number according to a fixed power of time and growing 1-, 2- or 3- dimensionally, and includes the effects of ingestion of potential nucleus forming sites by growing nuclei or the overlapping of such nuclei. The value of n = 2 in the equation can be ascribed to one of the following:

(i) one-dimensional growth of nuclei increasing in number linearly with time, or

(ii) two-dimensional growth of nuclei increasing from a fixed number of centres.

The former mechanism for nucleus growth is thought to be highly unlikely since the decay reaction commences at α = 0,43, and such a mechanism would not account for this high fractional decomposition.

Due to the high intensity light source used it is thought that the effect of the radiation would be very pronounced. Therefore if there was any linear increase in the number of nuclei with time during the acceleratory period it would be swamped by the very large number of nuclei formed at the end of the induction period. Thus mechanism (ii) is thought to operate. The growth centres of metal are considered to be plate-like in nature advancing along the grain boundaries in which they were initiated.

These metal nuclei are discrete at the onset of the acceleratory period, but as the acceleratory reaction progresses independent growth of the individual reaction centres is no longer ensured and overlapping occurs, as is indicated by the excellent conforming of the acceleratory reaction to Avrami-Erofeyev type kinetics.

The dependence of the acceleratory period on the square of the light intensity below 60,0^{o}C, indicates that the overall mechanism must

involve the decomposition of two excited azide ions.

The most likely process by which the metal nuclei, formed at the end of the induction period, can grow is postulated to be one which involves the decomposition of two singly excited azide ions. The barium metal nuclei formed during the induction period undergo reaction via the photo-electric effect to produce barium ions and electrons. A singly excited azide ion results through the absorption of a photon. As before it can be assumed that the absorbed electromagnetic energy is localized at the favoured sites in the form of vibrational or internal electronic excitation. This excited azide ion may then either revert to the ground state (if situated at an ideal lattice position) by the tunnel effect or react with a barium ion formed through the photo-electric effect to give barium metal and an azide radical (positive hole). The radical then reacts with an adjacent singly excited azide ion to give three molecules of nitrogen and an electron and two anion vacancies. The reaction is therefore an acceleratory one in which the barium metal is regenerated. The reaction scheme (i) is thus:

$$Ba_n \overset{h\nu}{\rightleftharpoons} Ba_n^{+} + e \quad \ldots\ldots\ldots\ldots\ldots\ldots \quad (1)$$

$$N_3^{-} \overset{h\nu}{\rightleftharpoons} N_3^{-*} \quad \ldots\ldots\ldots\ldots\ldots\ldots \quad (2)$$

$$Ba_n^{+} + N_3^{-*} \xrightarrow{\Delta} Ba_n + N_3 \quad \ldots\ldots\ldots\ldots\ldots\ldots \quad (3)$$

$$N_3 + N_3^{-*} \longrightarrow 3N_2 + e + 2A \longrightarrow 3N_2 + F + A \quad \ldots\ldots \quad (4)$$

where A = anion vacancy

and F = F-centre.

Growth of barium metal nuclei to the interface occurs via the collapse of these F-centres as follows:

$$2F \longrightarrow 2A + 2e \qquad \ldots\ldots\ldots\ldots\ldots\ldots (5)$$

$$Ba_n + 2e + Ba^{++} \longrightarrow Ba_{n+1} \qquad \ldots\ldots\ldots (6)$$

A similar process, for the growth of sodium metal nuclei, has been proposed by Jacobs and Tariq Kureishy (51) to occur during the photolysis of sodium azide.

Step (3) is considered to be the rate determining step and has an activation energy of 7,6 Kcal.mol.$^{-1}$ associated with it during the acceleratory phase.

It is also possible that the growth of barium metal nuclei below 60,0^{o}C can take place via an overall mechanism which involves the decomposition of an excited intermediate which has absorbed directly or indirectly, the energy from two photons of the incident light. Two basic schemes, (ii) and (iii) can be postulated for this type of mechanism.

(ii) This mechanism involves the successive absorption of two photons by an azide ion. The barium metal nuclei formed during the induction period undergo reaction via the photo-electric effect to produce barium ions and electrons. A singly excited azide ion results through the absorption of a photon. This excited azide ion may then revert to the ground state by the tunnel effect or become doubly excited by the absorption of another quantum of light energy. A second excitation will occur of only singly excited ions situated at a defect site since at such positions the imbalance of forces will allow the absorbed energy to be localized on a particular ion long enough for a secondary excitation to occur. Azide ions located at ideal lattice points, on absorption of energy will revert after a time to the ground state by communication of their energy to the vibrational modes of adjacent ions. This doubly excited azide ion may either become thermally ionized to produce an electron and a positive hole or be de-excited to the singly excited

state. If thermal ionization occurs the electron reacts with an adjacent Ba^+ ion, formed via the photo-electric effect, to give barium metal, and the positive hole reacts with an adjacent ground state azide ion to give three molecules of nitrogen, an electron and two additional anion vacancies. The reaction is therefore an acceleratory one in which the barium metal is regenerated. This mechanism can be written schematically as

$$Ba_n \overset{h\nu}{\rightleftharpoons} Ba_n^+ + e \qquad \text{photo-electric effect .....(1)}$$

$$N_3^- \xrightarrow[h\nu]{k_1} N_3^{-*} \qquad \text{primary excitation .....(2)}$$

$$N_3^{-*} \xrightarrow{k_2} N_3^- \qquad \text{de-excitation .....(3)}$$

$$N_3^{-*} \xrightarrow[h\nu]{k_3} N_3^{-**} \qquad \text{secondary excitation .....(4)}$$

$$N_3^{-**} \xrightarrow{k_4} N_3^{-*} \qquad \text{de-excitation .....(5)}$$

$$N_3^{-**} \xrightarrow[\Delta]{k_5} N_3 + e \qquad \text{decomposition .....(6)}$$

The following fast reactions follow.

An electron, produced through thermal ionization in step (6), combines with an adjacent barium metal ion formed in step (1)

$$Ba_n^+ + e \longrightarrow Ba_n \qquad \text{.....(7)}$$

The positive hole formed in step (6) reacts with an adjacent ground state azide ion in the strained region at the interface in a fast reaction

$$N_3^- + N_3 \longrightarrow 3N_2 + e + 2A \longrightarrow 3N_2 + F + A \qquad \text{.....(8)}$$

where F and A have the same meaning as in process (i), and growth of barium metal nuclei to the interface occurs as before by the collapse

of the F-centre complex which is bound to the nucleus, on attaining a critical size i.e.

$$2F \longrightarrow 2A + 2e \quad \ldots\ldots\ldots (9)$$

$$Ba_n + 2e + Ba^{++} \longrightarrow Ba_{n+1} \quad \ldots (10)$$

Step (6) is considered to be the rate determining step.

The overall rate can be expressed as

$$R = k_5(N_3^{-**}).$$

On application of the steady state conditions

$$\frac{d(N_3^{-*})}{dt} = \frac{d(N_3^{-**})}{dt} = 0$$

it can be shown that the rate equation can be written as

$$R = k_1 k_3 k_5 (N_3^-) I^2 / (k_2 + k_3 I)(k_4 + k_5).$$

Since $R \alpha I^2$ it can be assumed that $k_2 >> k_3 I$ and since there is a single experimental activation energy $k_4 >> k_5$. Thus the rate equation reduces to

$$R = k_1 k_3 k_5 (N_3^-) I^2 / k_2 k_4 .$$

Thus the proposed mechanism is in accordance with the observed dependence, of rate of reaction on the square of the light intensity.

(iii) This scheme involves the transfer of energy from an excited ion to an adjacent ion:

$Ba_n \overset{h\nu}{\rightleftharpoons} Ba_n^+ + e$ photo-electric effect ... (1)

$N_3^- \xrightarrow[h\nu]{k_1} N_3^{-*}$ primary excitatation..... (2)

$N_3^{-*} \xrightarrow{k_2} N_3^-$ de-excitation ..... (3)

$$N_3^{-*} + N_3^{-*} \xrightarrow{k_3} N_3^{-**} + N_3^- \quad \text{energy transfer .... (4)}$$

$$N_3^{-**} \xrightarrow{k_4} N_3^{-*} \quad \text{de-excitation ..... (5)}$$

$$N_3^{-**} \xrightarrow[\Delta]{k_5} N_3 + e \quad \text{decomposition ..... (6)}$$

As for process **(ii)** the electrons generated in step (6) react with Ba^+ ions formed via the photo-electric effect in step (1)

$$Ba_n^+ + e \longrightarrow Ba_n \quad \text{..... (7)}$$

and the positive hole formed in step (6) reacts with an adjacent azide ion to give three molecules of nitrogen and an electron

$$N_3^- + N_3 \longrightarrow 3N_2 + e + 2A \longrightarrow 3N_2 + F + A \quad \text{..... (8)}$$

$$2F \longrightarrow 2A + 2e \quad \text{..... (9)}$$

$$Ba_n + 2e + Ba^{++} \longrightarrow Ba_{n+1} \quad \text{..... (10)}$$

This reaction is an acceleratory process in which the barium metal is regenerated. The rate determining step is considered to be step (6).

When the steady state conditions, as defined above, are applied again, it can be shown that

$$k_1(N_3^-)I = C_1(N_3^{-**})^{\frac{1}{2}} + C_2(N_3^{-**})$$

where C_1 and C_2 are constants expressed in terms of the rate constants. If it is assumed that $C_2(N_3^{-**}) \ll 1$, then by substituting in the overall rate equation

$$R = k_5(N_3^{-**})$$

a rate equation of the form

$$R \simeq k_1 k_5 C_k (N_3^-) I^2$$

is obtained, where C_k is a combination of the rate constants. As before the proposed mechanism has been proved to be proportional to the square of the light intensity as found experimentally.

Thus for both processes the incident energy is absorbed by the electrons of the N_3^- ions. Absorbing ions situated at normal lattice sites will be de-excited by communication of their energy to the vibrational modes of the ion, while for those at positions of stress the energy will be localized long enough for secondary excitation to occur. Both processes are in accordance with the observed dependence of rate of reaction on the square of the light intensity.

These two processes ((ii) and (iii)), in which an excited intermediate has absorbed directly or indirectly the energy from two photons of incident light, can be modified to fit the experimental results obtained for the photolytic reactions in the temperature range $60{,}0^{o}$ - $100{,}0^{o}C$ i.e. an increase in the activation energy and a linear dependence of reaction rate on light intensity. In each scheme the reaction steps (1), (2), (3) are unaltered while the step governed by k_3 is now the rate determining step and becomes

$$N_3^{-*} \xrightarrow[\Delta]{k_3} N_3 + e \qquad \text{decomposition} \qquad \ldots\ldots\ldots (4)$$

As for reactions below $60{,}0^{o}C$, the electron generated in step (4) reacts with an adjacent Ba^+ ion formed via the photo-electric effect to give barium metal

$$Ba_n^+ + e \longrightarrow Ba_n \qquad \ldots\ldots\ldots\ldots\ldots\ldots\ldots (5)$$

and the positive hole reacts with an adjacent azide ion to give three molecules of nitrogen

$$N_3^- + N_3 \longrightarrow 3N_2 + e + 2A \longrightarrow 3N_2 + F + A \qquad \ldots\ldots (6)$$

$$2F \longrightarrow 2A + 2e \quad \ldots\ldots\ldots\ldots \quad (7)$$

$$Ba_n + 2e + Ba^{++} \longrightarrow Ba_{n+1} \quad \ldots \quad (8)$$

As for the lower temperature range, it can be shown after application of the steady state condition

$$\frac{d(N_3^{-*})}{dt} = 0$$

that $R \alpha I$. Thus the overall rate equation

$$R = k_3(N_3^{-*})$$

becomes

$$R = k_3k_1(N_3^{-})I \; / \; (k_2 + k_3).$$

Since there is a single experimental activation energy it can be assumed that $k_2 >> k_3$ and therefore the rate equation reduces to

$$R = k_3k_1(N_3^{-})I \; / \; k_2 \; .$$

Thus the rate of reaction is proportional to I and the measured activation energy of 11,3 Kcal.mol.$^{-1}$ is associated with step (4).

These latter two mechanisms satisfactorily fit the experimental results (increase in activation energy but decrease in the molecularity of the reactions as the temperature of decomposition is increased) obtained from the photolysis of barium azide powder in the temperature range 27,0^{o} - 100,0^{o}C. However, on comparison of the results obtained from the photolysis of barium and strontium azide powders it was found that although both compounds showed that the energy required for the rate determining step increased with increase in decomposition temperature, barium azide showed a change from a bimolecular dependence on light intensity to a linear dependence on intensity above 60,0^{o}C

while strontium azide powder showed a constant bimolecular dependence on light intensity throughout the photolytic temperature range. This dependence of reaction rate, of photolysed strontium azide powder, on the square of the light intensity throughout the photolytic temperature range forces one to conclude that a decomposition process involving the decomposition of an excited intermediate which has absorbed, directly or indirectly, the energy from two photons of incident light, is more than likely not possible for the photolysis of barium azide since such a process was not found adaptable to the results obtained from the photolysis of strontium azide powder. It is assumed that the most probable mechanism occuring during the photolysis of barium azide in the temperature range 27,0^{o} - 60,0^{o}C involves the decomposition of two singly excited azide ions i.e. scheme (i).

However the processes (ii) and (iii), involving the decomposition of an excited intermediate which has absorbed directly or indirectly the energy from two photons of incident light, has been widely used by many workers in the theoretical postulation of the processes occuring during photolysis.

A similar scheme to process (ii) has been invoked by Finch, Jacobs and Tompkins (93) for the photolytic decomposition of silver oxalate, taking place more than likely by an interface reaction. They envisaged that a single oxalate radical may decompose to carbon dioxide. Excitation of the silver oxalate by the ultraviolet light results in a mobile exciton which is then trapped at an anion vacancy involving the capture of the excited electron by the vacancy which may accommodate two electrons. The complex formed may have two fates: either it can become further excited by light absorption so that a second electron is captured by the anion vacancy giving an oxalate radical associated with an anion vacancy containing two electrons; or it may be destroyed by the tunnelling effect from the anion vacancy

back to the singly charged ion. The oxalate radical formed in the first possibility can decompose to give two molecules of carbon dioxide or revert to a singly charged oxalate ion by regaining an electron from the anion vacancy. The proposed mechanism can be summarized as follows:

$$(Ox^{2-}) \rightleftharpoons (Ox^{2-})^{*} \quad h\nu$$

$$(Ox^{2-})^{*} \rightleftharpoons (Ox^{2-})^{**} \quad h\nu$$

$$(Ox^{2-})^{**} \longrightarrow 2CO_2 + 2e \quad \text{(anion vacancy + 2 electrons).}$$

Process (ii) has also been applied to the photolysis of potassium permanganate in the temperature range $30,0^{o}$ - $180,0^{o}C$ by Prout and Lownds (96). Account was taken of the fact that the rate of reaction below $110,0^{o}C$ was dependent on the cube of the light intensity and above $110,0^{o}C$ dependent on the square of the light intensity i.e. a mechanism was postulated in which either three photons (below $110,0^{o}C$) or two photons (above $110,0^{o}C$) are required to raise the energy of the permanganate ion to a level at which the excited ion dissociates thermally.

Thus below $110,0^{o}C$:

$$M \rightleftharpoons M^{*} \quad h\nu$$

$$M^{*} \rightleftharpoons M^{**} \quad h\nu$$

$$M^{**} \rightleftharpoons M^{***} \quad h\nu$$

$$M^{***} \xrightarrow{\Delta} \text{Products}$$

and above $110,0^{o}C$:

$$M \rightleftharpoons M^{*} \quad h\nu$$

$$M^{*} \rightleftharpoons M^{**} \quad h\nu$$

$$M^{**} \xrightarrow{\Delta} \text{Products}$$

where M = MnO_4^- ion .

Thus the overall photolytic reaction below 110,0^oC was thought to be

$$MnO_4^- \xrightleftharpoons{3h\nu} (MnO_4^-)^{***} \xrightarrow{\Delta} MnO_2^- + O_2$$

and at temperatures above 110,0^oC

$$MnO_4^- \xrightleftharpoons{2h\nu} (MnO_4^-)^{**} \xrightarrow{\Delta} MnO_4^o + e$$

$$MnO_4^o \longrightarrow MnO_2 + O_2$$

$$MnO_4^- + e \longrightarrow MnO_4^= .$$

The reaction product ions MnO_2^- and $MnO_4^=$ have been detected spectrophotometrically by Lee (38) during flash photolysis of potassium permanganate at low intensity (and thus low temperatures) and high intensity light sources (and thus high temperatures), thus justifying the mechanism for product formation.

Herley and Levy (36) have considered that sodium bromate will photolyse by either process (ii) or by process (iii). Using process (ii) they propose

$$BrO_3^- \xrightleftharpoons{h\nu} (BrO_3^-)^*$$

$$(BrO_3^-)^* \xrightleftharpoons{h\nu} (BrO_3^-)^{**}$$

or process (iii)

$$BrO_3^- \xrightleftharpoons{h\nu} (BrO_3^-)^*$$

$$2(BrO_3^-)^* \rightleftharpoons (BrO_3^-)^{**} + BrO_3^- .$$

This doubly excited site can now either

(i) generate an additional singly excited site

$$(BrO_3^-)^{**} + BrO_3^- \longrightarrow (BrO_3^-)^* + (BrO_3^-)^*$$

or (ii) cause decomposition

$$(BrO_3^-)^{**} \longrightarrow BrO^- + O_2 \ .$$

These mechanisms, postulated by other workers for the photolysis of some ionic solids, illustrate the feasibility of a reaction scheme which involves either successive excitations of a single ion by direct absorption of photons, or transfer of energy from one excited site to another to account for rate equations of the form $R \alpha I^n$ where $n>1$.

The importance of the metal nuclei during the acceleratory period has been illustrated by the effect of interrupting a decomposition during the acceleratory period and then continuing it after allowing a reaction with water vapour to occur. Water vapour was found to destroy the reaction and a new induction period of length shorter than that of the uninterrupted decomposition, but increasing in length as the position of interruption along the curve increased, was observed. The acceleratory rate of the subsequent reaction was found to have decreased. The new reaction is presumed to begin from growth nuclei not destroyed by the water vapour. The growth nuclei are assumed to be situated on the planes of the particles and the new induction period observed is the time required for the growth of these nuclei to a critical size. Thus the water vapour is assumed to attack only those metal nuclei on the surface of the particles. The fall in the acceleratory rate after admission of water vapour is due to the commencement of reaction from fewer centres. The value of the acceleratory rate constant is dependent on the number of nuclei at the start of the reaction and a decrease in the number will decrease the rate of reaction.

Interruption of the reaction at the inflection point and at positions further along the decomposition curve was found to destroy

all subsequent reactions. At the inflection point the particles are completely covered by a layer of barium metal, observed as a black coating on the external surfaces of the particles. A formation of a layer of barium hydroxide results from the destruction of the barium metal by water vapour. This layer of hydroxide is opaque to ultra-violet light, thus even if growth nuclei are present below the surface they cannot be activated by the light and reaction ceases. The observed final pressures were lower than expected on exposing barium azide to water vapour and this is attributed to partial hydrolysis of the azide. Thus it can be concluded that barium metal nuclei have a "catalytic" effect on the photolytic reaction. The observance of a continual darkening of the salt from the end of the induction period till the inflection point indicates the increase in the metal nuclei concentration as the reaction proceeds.

The decay reaction commences when the 2-dimensional nuclei overlap and the surface of the small particles are covered by reaction product. During this period penetration of the product interface into the particles takes place according to the unimolecular decay law. Because of the difference in molecular volume between product and reactant phases, the interface collapses leaving isolated blocks of material in which no nuclei are present. This arises from the extensive growth of plate-like nuclei. In these isolated blocks each molecule has an equal probability of decomposition and the rate of reaction becomes proportional to the amount of unreacted substance. Thus the decay reaction conforms to the unimolecular decay law.

The mechanism operating during the decay reaction is thought to be similar to that during the acceleratory period since the energy required for the rate determining step and the dependence of the experimental rate constant on intensity of light source is within experimental error analogous to that found for the acceleratory period.

(ib) Photolysis in the temperature range 60,0° - 100,0°C

The generalized reaction schemes postulated for the decomposition below 60,0°C have to be modified to describe the situation above 60,0°C where the rate of reaction varies linearly with light intensity and the activation energy increases from 6,2 Kcal.mol.$^{-1}$ to 11,4 Kcal.mol.$^{-1}$ for the induction period, 7,6 Kcal.mol.$^{-1}$ to 11,3 Kcal.mol.$^{-1}$ for the acceleratory period and 6,6 Kcal.mol.$^{-1}$ to 12,9 Kcal.mol.$^{-1}$ for the decay period.

The mathematical analyses, visual observations, and the effect of water vapour at various stages of reaction were found to be analogous to the results obtained in the temperature range 27,0° - 60,0°C. Thus it is thought that the topochemical decomposition in the higher temperature range is similar to that in the lower temperature range.

Formation of barium metal nuclei during the induction period is postulated to occur according to the following mechanism:

$$N_3^- \xrightleftharpoons{h\nu} N_3^{-*} \quad \ldots\ldots\ldots\ldots (1)$$

$$Ba^{++} + N_3^- \xrightarrow{\Delta} Ba^+ + N_3 \quad \ldots\ldots\ldots\ldots (2)$$

$$N_3 + N_3^{-*} \longrightarrow 3N_2 + e \quad \ldots\ldots\ldots\ldots (3)$$

$$Ba^+ + e \longrightarrow Ba \quad \ldots\ldots\ldots\ldots (4)$$

This mechanism is in accordance with the observed linear dependence of the inverse of the duration of the induction period on light intensity. Step (2) is considered to be the rate determining step, the energy of activation being 11,4 Kcal.mol.$^{-1}$.

The mechanism for nucleus growth below 60,0°C can be modified for nucleus growth above 60,0°C where the rate of reaction varies linearly

with intensity and the activation energy increases from 7,6 Kcal.mol.$^{-1}$ to 11,3 Kcal.mol.$^{-1}$. The proposed mechanism is as follows:

$$Ba_n \overset{h\nu}{\rightleftharpoons} Ba_n^+ + e \qquad \ldots\ldots\ldots\ldots (1)$$

$$N_3^- \overset{h\nu}{\rightleftharpoons} N_3^{-*} \qquad \ldots\ldots\ldots\ldots (2)$$

$$Ba_n^+ + N_3^- \overset{\Delta}{\longrightarrow} Ba_n + N_3 \qquad \ldots\ldots\ldots\ldots (3)$$

The positive hole formed in step (3) reacts with an adjacent singly excited azide ion

$$N_3 + N_3^{-*} \longrightarrow 3N_2 + e + 2A \longrightarrow 3N_2 + F + A \ldots\ldots (4)$$

Through the collapse of aggregates of F-centres barium atoms are formed, which add to the interface

$$F + F \longrightarrow 2A + 2e \qquad \ldots\ldots\ldots\ldots\ldots (5)$$

$$Ba_n + 2e + Ba^{++} \longrightarrow Ba_{n+1} \qquad \ldots\ldots\ldots\ldots (6)$$

Step (3) is considered to be the rate determining step with an activation energy of 11,3 Kcal.mol.$^{-1}$. At temperatures above 60,0^{o}C there is sufficient thermal energy for the thermal transfer of an electron from a ground state azide ion to a Ba^+ ion formed via the photoelectric effect.

This mechanism proposed for the photolytic decomposition of barium azide above 60,0^{o}C, is in accordance with the linear dependence of photolytic rate on light intensity and is similar to the mechanism proposed by Jacobs et.al. for the photolysis of barium azide (40).

It is assumed that the mechanism occurring during the decay reaction is analogous to that occurring during the acceleratory region since the activation energy for the acceleratory period and the decay

period are similar and both reaction rates vary linearly with light intensity when the experimental error is taken into account.

(ii) Pellets

The pressure-time plots obtained from photolysed pellets showed an induction period in which there was no evolution of gas, followed by a linear rate of evolution of gas till $\alpha = 0,20$, and a decay reaction fitted by the unimolecular decay law from $0,20 < \alpha < 0,96$.

The reproducibility was found to be highly unsatisfactory at all temperatures of decomposition and pelleting pressures used. Very often the pellets were observed to explode at the end of the induction period.

Pelleting the ground material results in the production of large numbers of crystal defects throughout the pellet. This process will also cause the accumulation of dislocations to form new high angle grain boundaries. Steps will be formed at the surfaces of the pellets and in general a highly damaged pellet will be produced with a high concentration of point and line defects. These defects will vary in concentration from pellet to pellet, thus the decomposition of each pellet will vary. Pellets containing large concentrations of defects will be most likely to explode at the end of the induction period.

During the induction period barium metal nuclei are formed on the surface of the pellet at emergent grain boundaries and along internal grain boundaries and dislocations in the pellet. As with the photolysis of powder, decomposition will commence when azide ions at positions of stress become optically excited. Barium metal nuclei are assumed to form, during the induction period, via the same mechanisms as proposed for the photolysis of powder in the temperature range

27,0° - 100,0°C. The duration of the induction period will be proportional to the time required for the barium metal atoms, formed initially at the interatomic spacing of barium azide, to aggregate to barium metal specks. The presence of barium metal on the surface of the pellet is confirmed by the appearance of a brown colouration at the end of the induction period. Furthermore interaction for 1 min. with water vapour at the end of the induction period caused the subsequent reaction to proceed after a new induction period of duration equal to that of the uninterrupted pellet, indicating the presence of barium metal at the end of the induction period. Interaction with water vapour before the end of the induction period had no effect on the subsequent decomposition, indicating that no metal nuclei exist before the end of this period.

The reaction proceeds into the acceleratory phase on the aggregation of the barium atoms. The acceleratory period of photolysed pellets was observed to consume only a small fraction of the total reaction i.e. $0,01 < \alpha < 0,22$ as compared with the acceleratory period of photolysed powder i.e. $0,01 < \alpha < 0,43$. The difference can be accounted for when the areas of the two specimens are taken into account. The surface to volume ratio of pellets is small compared with the same value for powder. Thus the time required to cover the complete surface with product would be expected to be a small fraction of the time required for complete decomposition. The linear acceleratory period is assumed to result from rapid surface reactions which cover the faces of the pellet with product. The acceleration is assumed to proceed in the form of linear chains, solely from the nuclei formed during the induction period and each nucleus is assumed to grow in one-dimension. The rate of reaction will then be a constant. The growth of the nuclei will be small before overlap occurs and at over-

lap the product interface moves into the pellet following the unimolecular decay law.

At the onset of the decay reaction the pellet was observed to be black on all external surfaces, the interior being white. The thickness of the black layer on each face was estimated to be 50 000 unit cell layers thick. Interaction with water vapour at this stage killed any further reaction, indicating the importance of metal for the continuation of the reaction, the hydroxide formed being opaque to ultraviolet light. Interaction with water vapour between $0,01 < \alpha < 0,22$ resulted in the reaction being returned to zero time.

Due to the irreproducible nature of the photolysis of pellets activation energies for the decay reaction only were obtained using the split run technique, over the temperature ranges $30,0^{o}$ - $60,0^{o}C$ and $60,0^{o}$ - $100,0^{o}C$. The linear acceleratory period was too short to determine activation energies by this method. The effect of pelleting pressure on activation energy in these two temperature ranges was also investigated. Activation energies were found to increase with pelleting the powdered material and increased as the pelleting pressure increased. The increase can be accounted for if it is assumed that diffusion of nitrogen will be hindered by high compression. The values of activation energies for the decay reactions were found to be 9,4 Kcal.mol.$^{-1}$ and 14,8 Kcal.mol.$^{-1}$ for pellets pressed at 600 lb/sq.in. in the temperature ranges $30,0^{o}$ - $60,0^{o}C$ and $60,0^{o}$ - $100,0^{o}C$ respectively. At a pelleting pressure of 2000 lb/sq.in. activation energies of 12,4 Kcal.mol.$^{-1}$ and 17,0 Kcal.mol.$^{-1}$ were measured in the temperature ranges $30,0^{o}$ - $60,0^{o}C$ and $60,0^{o}$ - $100,0^{o}C$ respectively. The mean activation energies for the powders in these temperature ranges were 6,8 Kcal.mol.$^{-1}$ and 11,9 Kcal.mol.$^{-1}$ respectively. The difference between the mean activation energies for the powder in the two temperature ranges is 5,1 Kcal.mol.$^{-1}$; for the 600 lb/sq.in. pressing, 5,4 Kcal.mol.$^{-1}$,

and for the 2000 lb/sq.in. pressing 4,6 Kcal.mol.$^{-1}$. This supports the assumption that the increase in activation energy with pelleting pressure is due to the hindrance of the diffusion of nitrogen gas from the pellet.

The two stage photodecomposition observed when two pellets resting on each other were decomposed, indicates a possibility of transparency of the product of barium metal to ultraviolet light. Only on completion of the decomposition of the upper pellet does the lower one commence to react. The rate of decomposition of the latter is slower because of the attenuation of the light beam in passing through the top pellet. A further point indicating the possible transparency of barium metal product to ultraviolet light is the result found when barium azide powder is pressed between two barium metal pellets. The powder between the barium metal pellets was found to decompose but more slowly than expected for a usual pellet. This decrease in reaction rate is attributed to the diffusion of nitrogen being hindered by compression, and the attenuation of the light beam in passing through the top pellet.

The mechanism of decomposition occurring during the acceleratory and decay reactions is assumed to be the same as that occurring during the corresponding reactions of photolysed powder.

5B CO-IRRADIATION OF BARIUM AZIDE

Garner and Moon (123) were the first to study the effect of radiation during the thermal decomposition of barium azide. Irradiation with a radium needle during thermal decomposition was found to have a four-fold increase on the reaction rate. The nuclei on the faces of the crystal nearest the needle were larger than those on other faces. The main effect of the emission was on the nucleus growth and not on the formation of nuclei.

Maggs (124) studied the effect of emission from a radium needle on the thermal decomposition of strontium azide. A large reduction in the duration of the induction period and an increase in k in the equation $\log p = kt + c$ was observed. It was postulated that the effect of the radiation was either to increase the rate of growth of the nuclei or to increase their rate of formation.

The effect of X-rays at the instant of thermal decomposition of barium azide has been investigated to some extent (122, 129, 130). Boldyrev and Skorik (129) found that the pre-irradiation effect was greater at decomposition temperatures than at ambient temperatures. They suggested that nuclei, which were only stable above a critical size, were formed and grew by trapping of electrons followed by neutralization of the charge by migrating vacancies. The nuclei were originally aggregates of atoms or F-centres. At room temperature it was thought that the mobility of vacancies was low and hence only a few stable nuclei were formed, while at the threshold temperature their mobility had increased. Thus a large number of stable nuclei could form and hence a higher rate of decomposition took place.

These authors (130) later extended their study to include silver azide. No influence on the rate of thermal decomposition was

observed when a silver azide pellet was irradiated with X-rays or ultraviolet light at the moment of decomposition.

In a further study of the decomposition of barium azide, irradiated with X-rays at the moment of decomposition (130) an increase in maximum rate and decrease in duration of the induction period was observed. This led to the belief that the process of excitation of electrons, from the valence band into the conduction band is the limiting step, operating at the stage of the decomposition when the reaction is catalysed by the decomposition products.

The effect of X-rays during the thermal decomposition (co-irradiation) (122) of barium, strontium and calcium azides has been investigated. Pre-irradiation with X-rays had a greater effect than co-irradiation on the thermal decomposition of calcium and strontium azides, whereas co-irradiation of barium azide had a more marked effect on the thermal decomposition than pre-irradiation. They stated that the proportional effect of pre-irradiation and co-irradiation on the thermal decomposition is dependent on the sensitivity of the salt to irradiation and the temperature dependence of the pre-irradiation effect. Pre-irradiation of barium azide was found to have a larger temperature dependence than strontium or calcium azide, which would account for the greater sensitivity of barium azide to co-irradiation.

The permanganates of potassium and silver have also been subjected to X-radiation during thermal decomposition (122). No effect on the thermal decomposition was produced by either pre-irradiation or co-irradiation of the potassium salt with an X-ray dose of 400 rad/min. The rate of thermal decomposition of silver permanganate increased five times when pre-irradiated or co-irradiated with this dose.

Pre-irradiation with ultraviolet light at ambient temperature on barium, strontium (111), calcium (73), potassium (74) and lithium azides (110) was found to shorten the duration of the induction period and

increase the rate of reaction, when the salts were decomposed isothermally. The ultraviolet radiation was assumed to produce large numbers of anion vacancies which enhanced reaction rates of the subsequent thermal decomposition of strontium (111) and calcium azides (73). The effects of pre-irradiation on barium (111 , 112), potassium (74) and lithium azides (110) however have been attributed to F-centre formation.

The results found when barium azide is irradiated with ultraviolet light during thermal decomposition will now be discussed. The extension of photolysis into the region 110,0° - 135,0°C in which the thermal decomposition of barium azide has been investigated is called co-irradiation after Skorik et. al. (122).

The essential feature of this decomposition is the existence of a dark rate at all temperatures in the decomposition temperature range due to the thermal decomposition of the pre-irradiated azide. The effects of co-irradiation on barium azide powder will be discussed initially followed by a discussion of the results obtained from the co-irradiation of barium azide pellets.

(i) Powder

The pressure-time plots obtained from co-irradiated decompositions were sigmoid in shape as found for the unirradiated decomposition (114). The reproducibility of the powdered material of uniform particle size, was found to be satisfactory when the pressure-time plots of three runs at the same temperature and light intensity were superimposed. The curves exhibited a true induction period in which there was no evolution of gas, followed by an acceleratory period fitted by the Avrami-Erofeyev equation with n = 2 and finally a decay period conforming to the unimolecular decay law.

The percentage decomposition of a thermal run was found to be unaltered by co-irradiation i.e. irradiation with ultraviolet light during thermal decomposition had no effect on the percentage decomposition of a

thermal run.

Irradiation of the sample with ultraviolet light during thermal decomposition had the effect of shortening the induction period and causing an increase in the rate of the acceleratory and decay reactions.

The overall mechanism of thermal decomposition in terms of topographical considerations was found to be altered by co-irradiation. Also the activation energies of the process(es) occurring during co-irradiation were found to be lower than that of an unirradiated decomposition. At low light intensities the activation energies were found to approximate to those of the thermal decomposition of the azide. The activation energies of the inverse of the duration of the induction period and the acceleratory and decay reactions were found to be 18,5 Kcal.mol.$^{-1}$, 21,7 Kcal.mol.$^{-1}$ and 24,1 Kcal.mol.$^{-1}$ respectively when a light intensity of 6,4 units was used, while the activation energies changed to values of 16,5 Kcal.mol.$^{-1}$, 19,2 Kcal.mol.$^{-1}$ and 15,6 Kcal.mol.$^{-1}$ for the induction period and acceleratory and decay reactions respectively when a light intensity of 15,5 units was used. The thermal activation energies (114) for these three reactions were found to be 26,5 Kcal.mol.$^{-1}$, 26,8 Kcal.mol.$^{-1}$ and 26,1 Kcal.mol.$^{-1}$ respectively.

The dependence of the inverse of the duration of the induction period and the rates of acceleration and decay on the intensity of the ultraviolet light source were found to be 0,7 by a method of least squares. This value was approximated to unity.

Due to the approximations of the co-irradiated activation energies to the thermal activation energies at low light intensities and to the photolytic activation energies in the temperature range 60,0^{o} - 100,0^{o}C at high light intensities, it is proposed that parallel reactions, namely the photolytic reaction proposed for the temperature range

60,0° - 100,0°C and the thermal reaction occurring in the temperature range 110,0° - 140,0°C for barium azide (114) occur simultaneously during co-irradiation.

Three-dimensional nucleus formation is assumed to occur during the induction period of a purely thermal decomposition (114). These nuclei are formed at positions of stress such as along the core of an emergent edge dislocation. From the layered structure of barium azide (125) it can be expected that incomplete planes of edge dislocations in an emergent grain boundary will contain only Ba^{++} ions or only N_3^- ions. Two such adjacent surface azide ions at the core of the dislocation will be favourably situated for decomposition producing a barium atom and three molecules of nitrogen i.e.

$$N_3^- + N_3^- \longrightarrow 3N_2 + 2e .$$

The freed electrons will combine with a barium ion on the surface in the rate determining step to form barium atoms

$$Ba^{++} + 2e \longrightarrow Ba.$$

More barium atoms will be formed, initially at the interatomic spacing in barium azide, as the dislocation climbs along the surface and down the core. At a critical concentration the barium atoms will aggregate to give barium metal specks i.e. nuclei.

During the induction period of a photolytic decomposition of barium azide in the temperature range 60,0° - 100,0°C a thermal transfer of an electron from a ground state azide ion to a barium metal ion, Ba^{++}, occurs resulting in the formation of a Ba^+ ion and a positive hole. This positive hole then reacts with an adjacent single optically excited azide ion to give three molecules of nitrogen and an electron. Barium metal atoms are formed initially at the interatomic spacing in barium azide, by the combination of the freed electron with

the Ba^+ ion.

The barium metal atoms are assumed to form in thin plates starting on the surface and moving down the core of the dislocation. Aggregation of barium atoms, as during thermal decomposition, to give barium metal nuclei, occurs at the end of the induction period. This mechanism is consistent with the observed linear dependence of the reciprocal of the duration of induction period on light intensity i.e. the rate of formation of barium metal nuclei will be linearly dependent on light intensity.

Thus the end of the induction period of a thermal or photolytic decomposition of barium azide is marked by the aggregation of barium atoms to give barium metal nuclei. It can be assumed that the photolytic and thermal processes for barium metal nucleus formation proceeds concurrently during a co-irradiated decomposition.

It can be seen from the comparison (see Fig. 44) of a thermal decomposition and a decomposition irradiated during thermal decomposition that the decomposition curve obtained from the unirradiated material indicates a gradual transition from the induction period to the acceleratory period and the rate of change during the initial part of the region is small. With co-irradiation the transition from the induction period to the acceleratory period is very abrupt. The slow reaction in the thermal decomposition represents the time required for the nuclei to grow to a critical size before the reaction accelerates. Irradiation with ultraviolet light during the thermal induction period accelerates the growth of the nuclei to the critical size, thus reducing the growth time and the transition from the induction period to the acceleratory period. Alternatively the increase in rate with co-irradiation could be due to an increase in the number of nuclei originally formed. Thus the reduction in time for the transition from the induction period to the acceleratory period with co-irradiation can be attributed to either a reduction in growth time of the nuclei or to an increase in the

number of nuclei originally formed.

Once the nuclei have reached a critical size or extent the induction period processes become unimportant and are superseded by the acceleratory process. On the reaction entering the acceleratory period the salt has "forgotten" whether the induction period nucleus formation was induced by heat or radiation, although the thermal and radiation induced formation may not be described by the same equation. It must be assumed that the irradiation effects do not modify the heating effects and vice versa i.e. it must be assumed that the combined effects are additive. This accounts for the observed decrease in duration of the induction period with co-irradiation since the time required to create barium metal nuclei during thermal decomposition will be decreased by the added action of light.

The energy for the rate determining step for the creation of metal nuclei will therefore be expected to be somewhere between the energy for pure thermal decomposition and photolysis above 60,0^{o}C. This was found experimentally by the decrease in activation energy from the thermal value of 26,5 Kcal.mol.$^{-1}$ to 12,1 Kcal.mol.$^{-1}$ when a light intensity of 26,5 units was used, and a decrease to 16,5 Kcal. mol.$^{-1}$ using a light intensity of 15,5 units and a decrease to 18,5 Kcal.mol.$^{-1}$ when a light intensity of 6,4 units was used. The activation energy for the induction period of samples photolysed above 60,0^{o}C was found to be 11,4 Kcal.mol.$^{-1}$.

Irradiation of barium azide with ultraviolet light during thermal decomposition was found to change the topography of the acceleratory and decay reactions of the pure thermal decomposition. The acceleratory period of the pure thermal decomposition was found to obey the Avrami-Erofeyev equation with the exponent taking the value of 4. The value of n = 4 was interpreted as the growth of three-dimensional nuclei, the nuclei increasing in number linearly with time. The fit of the equation

was from $0,01 < \alpha < 0,66$; the inflection point occurring at $\alpha = 0,62$. However pre-irradiation of barium azide with ultraviolet light was found to increase the exponent in the Avrami-Erofeyev equation from 4 to 6 (111). This increase was accounted for by assuming that after irradiation the number of nuclei increased as the cube of the time. Pre-irradiation has the effect of changing the number of potential nuclei and the linear rate of growth of these nuclei. The growth of the additional nuclei over the acceleratory period will accelerate the decomposition and the growth rate increases from a linear relationship with time to a cubic relationship with time with pre-irradiation. This change in growth rate can be expected since the growth process involves a charge transfer mechanism. Pre-irradiation is thought to form F-centres which aggregate and collapse on heating with the formation of barium atoms, thus accelerating thermal decomposition by increasing the number of barium nuclei at the end of the induction period. The activation energies for the induction period and the acceleratory and decay reactions of ultraviolet pre-irradiated decompositions were found to be approximately equal to that of the thermal decomposition, indicating that although the rate of reaction was increased by pre-irradiation, the rate determining step is identical in the two modes of decomposition i.e. the mode of reaction was found to be unaltered by pre-irradiation with ultraviolet light.

The acceleratory period of a co-irradiated decomposition was fitted by Avrami-Erofeyev type kinetics with the exponent taking the value of 2. The extent of the fit was from $0,01 < \alpha < 0,47$, the inflection point occurring at $\alpha = 0,47$.

Thus the exponent n, in the Avrami-Erofeyev equation, changes from 4 for a purely thermal decomposition to 6 for a thermal decomposition pre-irradiated with ultraviolet light and to 2 for a co-irradiated

decomposition.

The value of n = 2 for a co-irradiated decomposition indicates that growth of two-dimensional nuclei will occur from a fixed number of nuclei. The irradiation effect is very pronounced since a high intensity light source was employed. Thus it would be expected that growth of these nuclei produced rapidly and in large numbers at the end of the induction period on the surface and down the planes of the particles would swamp any further formation of new nuclei during the acceleratory period. This discounts the possibility that n = 2 represents one-dimensional growth of nuclei increasing linearly with time. The growth of these additional nuclei, produced through co-irradiation, over the acceleratory period will cause an acceleration of the decomposition and decrease the time required to reach the decay stage of reaction i.e. decrease the value of the inflection point. The growth centres of metal are considered, as in the case of photolysis, to be plate-like in nature advancing along the grain boundaries in which they were initiated. The activation energy of thermal decomposition was found to be lowered by co-irradiation, indicating that a different mode of reaction occurs during co-irradiation.

The mechanism for the growth of metal nuclei during the acceleratory period of a thermal decomposition (114) involves the transfer of an electron from an azide ion (N_3^-) into the lowest level (conduction band) of the metal nucleus. This results in a positive hole (azide radical) which is stable to decomposition. This hole may then react with an adjacent azide ion when the latter has received sufficient thermal energy to raise one of the electrons to an excited state with the production of three molecules of nitrogen, according to the equation

$$(N_3^-)^* + N_3 \longrightarrow 3N_2 + A + F$$

where A = anion vacancy,

F = F-centre

and $(N_3^-)^*$ = thermally excited azide ion (internal excitation).

After liberation of the nitrogen the freed electrons are trapped at the newly formed anion sites forming an F-centre complex which is bound to the nucleus. On attaining a critical size the aggregate collapses to yield barium atoms which add to the nucleus.

The rate determining step in the reaction is considered to be the elevation of the electron from a ground state azide ion to the conduction band of the metal nucleus and has an activation energy of 26,8 Kcal.mol.$^{-1}$.

For photodecomposition below 100,0^{o}C, the rate determining step is considered to be the thermal transfer of an electron from a ground state azide ion to a positively charged Ba^+ ion, formed via the photo-electric effect when barium metal formed at the end of the induction period, is irradiated with ultraviolet light. This produces barium metal and an azide radical. This positive hole then reacts with an adjacent azide ion which has absorbed the energy from a photon (resulting in a singly excited azide ion) producing three molecules of nitrogen, an F-centre and an anion vacancy. As for thermal decomposition, barium metal atoms add to the nucleus on collapse of these F-centres. This reaction is unimolecular with respect to azide ions. For photodecomposition exciton formation or photo-ionization was not postulated since the wavelengths of light used were of insufficient energy to create these energy carriers.

Thus it appears that during co-irradiation, where the reaction rate shows a linear dependence on light intensity, the mechanism proposed for the photolysis of barium azide in the temperature range 60,0^{o} - 100,0^{o}C and the mechanism proposed for the thermal decomposition in the temperature range 110,0^{o} - 135,0^{o}C (114) could occur

concurrently.

In the thermal decomposition temperature range considerable thermal ionization of the azide ion will occur in the absence of ultraviolet light and electrons will be promoted thermally into the conduction band of the metal nucleus with an activation energy of 26,8 Kcal.mol.$^{-1}$. However irradiation with ultraviolet light will cause the barium metal formed at the end of the induction period to become positively charged through the photo-electric effect. Electrons from adjacent ground state azide ions can now be thermally transferred to the positively charged metal ions, with an activation energy of 11,3 Kcal.mol.$^{-1}$. Thus during co-irradiation growth of barium metal nuclei occurs either from the thermal ionization of electrons from a ground state azide ion into the conduction band of the barium metal nucleus or the thermal transfer of electrons from a ground state azide ion to a positively charge barium metal ion Ba^{+}. The measured rate of a co-irradiated decomposition will be proportional to the concentration of azide radicals formed. Since two parallel reactions are responsible for the creation of these positive holes, the measured rate of reaction of a co-irradiated decomposition at a particular temperature in the decomposition temperature range can be expressed as

$$R = R_T + R_{co}$$

where R_T = rate of decomposition if thermal ionization of an electron from a ground state azide ion into the conduction band of the barium metal nucleus takes place exclusively

and R_{co} = rate of decomposition if thermal transfer of an electron from a ground state azide ion to a positively charged barium metal ion formed via the photo-electric effect, takes place exclusively.

The experimental rate constant of the acceleratory period of a co-irradiated decomposition was found to be proportional to the light intensity. It can be shown that the measured rate of a co-irradiated decomposition at a particular value of α, is proportional to the light intensity.

The activation energies associated with the acceleratory and decay reactions of a co-irradiated decomposition, at a particular constant light intensity are found to be approximately the same value. A similar statement can be said about a purely thermal decomposition. Thus it can be assumed that the kinetic processes outlined above for a co-irradiated decomposition occur during both the acceleratory and decay periods.

The rate of decomposition at $\alpha = 0{,}55$ is described by the unimolecular decay law

$$-\log(1-\alpha) = kt$$

or $$\frac{d\alpha}{dt} = R = k(1-\alpha)$$

i.e. the rate is proportional to the amount of undecomposed material. Thus for a particular value of α in the decay stage, the measured rate is proportional to the experimental rate constant. A linear dependence of the rate constant on light intensity was found for the decay period of the co-irradiated decomposition. Thus the dependence of rate constant on intensity can be written as

$$k = a_1 I + b_1$$

or $$R = a_2 I + b_2$$

where a and b are constants.

From the above discussion the overall rate can be expressed as the sum of the rates of two parallel reactions. Therefore

$$R_T + R_{co} = a_2 I + b_2 \ .$$

The dark rate measured at any stage of the co-irradiated decomposition is the rate of thermal decomposition of the pre-irradiated salt. It can be taken that this will be constant at constant temperature and all values of light intensity. The powerful light source used will saturate the sample with decomposition centres, and the dark rate will be a constant at all the intensities used.

Thus at constant decomposition temperature but varying light intensity R_T will have a constant value at a particular value of α. The rate vs intensity relation can now be rewritten as

$$R_{co} = a_2 I + b_3$$

which implies that the reaction

$$N_3^- \underset{}{\overset{h\nu}{\rightleftharpoons}} N_3^{-*} \xrightarrow[\text{radical}]{N_3} 3N_2 + e + 2A \longrightarrow 3N_2 + F + A$$

is directly proportional to the light intensity. Thus only one optical excitation occurs before reaction with an N_3 radical which is in accordance with the observed linear dependence of reaction rate on light intensity.

Since the reaction mechanism in the acceleratory period is identical to that in the decay stage, it would be expected similarly that the co-irradiated rate, R_{co}, at a particular value of α in the acceleratory period, would be directly proportional to the light intensity.

The above mechanism for the co-irradiated decomposition is consistent with the observed behaviour of the Arrhenius activation energy for the acceleratory and decay reactions. From the study of photo-

decomposition below 100,0^{o}C it was found that an energy of 11,3 Kcal.mol.$^{-1}$ was required for the thermal transfer of an electron from a ground state azide ion to a positively charged barium metal ion (Ba^{+}); while an energy of 26,8 Kcal.mol.$^{-1}$ was required for the thermal ionization of an electron from a ground state azide ion into the conduction band of a barium metal nucleus during thermal decomposition. Thus the energy required for co-irradiation, in which these two reactions are occurring, should be a value somewhere between 11,3 Kcal.mol.$^{-1}$ and 26,8 Kcal.mol.$^{-1}$. The Arrhenius equation applying to parallel reactions can be written as

$$k_T + k_{co} = A_T \exp(-E_T/RT) + A_{co} \exp(-E_{co}/RT)$$

where the subscripts T and co have the same meanings as before. As k_{co} increases with respect to k_T as the light intensity increases, the measured activation energy of the parallel reactions should approach E_{co}. The occurrence of parallel reactions during co-irradiation is then verified by the decrease in the activation energy from 21,7 Kcal.mol.$^{-1}$ to 19,2 Kcal.mol.$^{-1}$ for increases in light intensity from 6,4 units to 15,5 units respectively.

The mechanism for photodecomposition in the temperature range 60,0^{o} - 100,0^{o}C could perhaps (as outlined in the discussion on photolysis) be taken to be the single excitation of an azide ion, through the absorption of one photon, followed by the rate determining step in which the excited azide ion undergoes thermal ionization with an activation energy of 11,3 Kcal.mol.$^{-1}$. The generated electron combines with a Ba^{+} ion formed through the photo-electric effect and the positive hole reacts with an adjacent ground state azide ion in a strained position to yield nitrogen. The reaction mechanism can be

summarised as

$$N_3^- \underset{}{\overset{h\nu}{\rightleftharpoons}} N_3^{-*} \xrightarrow[\text{slow reaction}]{\Delta=11,3\text{Kcal.mol.}^{-1}} (N_3 + e) \xrightarrow[\text{fast reactions}]{Ba_n^+ + N_3^-} Ba_n + 3N_2 + F + A .$$

Addition of barium metal to the nucleus occurs, as during thermal decomposition via the collapse of aggregates of F-centres.

This mechanism proposed for the photolysis of barium azide in the temperature range $60,0^o$ - $100,0^oC$ and the mechanism for thermal decomposition in the temperature range $110,0^o$ - $135,0^oC$ (outlined earlier) (114), could occur concurrently during co-irradiation. During thermal decomposition, considerable ionization of azide ions (producing electrons and positive holes) will occur in the absence of ultraviolet light. Irradiation with ultraviolet light will cause electrons of suitably situated azide ions to be optically excited into the vibrational and electronic energy levels of the ions. These excited azide ions can then be thermally ionized resulting in electrons, which combine with Ba^+ ions formed via the photo-electric effect, and positive holes. Hence barium metal nuclei will be able to grow during a co-irradiated decomposition by two processes: (i) thermal transfer of electrons from a ground state azide ion into the conduction band of a barium metal nucleus and (ii) by the thermal transfer of electrons from a single optically excited azide ion to a Ba^+ ion. Thus during co-irradiation the two thermal ionization processes of the azide ion can be represented by the following equations:

$N_3^- \xrightarrow{\Delta} N_3 + e$ for a pure thermal ionization of the N_3^- ion

and $N_3^{-*} \xrightarrow{\Delta} N_3 + e$ for an optically assisted thermal ionization of a singly excited azide ion.

These two parallel reactions are responsible for the creation of positive holes and hence as before the measured rate of reaction of a co-irradiated decomposition at a particular temperature in the decomposition temperature range can be expressed as

$$R = R_T + R_{co'}$$

where R_T = the rate of decomposition if thermal ionization of the N_3^- ion occurs exclusively, and

$R_{co'}$ = the rate of decomposition if optically assisted ionization of the N_3^- ion occurs exclusively.

By following the argument put forward earlier it can be shown again that $R_{co'}$, at a particular value of α in either the acceleratory or decay reactions, is directly proportional to the light intensity. This implies that the reaction

$$N_3^- \rightleftharpoons N_3^{-*} \xrightarrow{\Delta} N_3 + e$$

is directly proportional to the light intensity and only one optical excitation occurs before thermal ionization of the excited azide ion gives an azide radical.

Again this mechanism for the co-irradiated decomposition is consistent with the observed behaviour of the Arrhenius activation energy for the acceleratory and decay reactions. From the study of the photodecomposition below 100,0°C it was postulated that the energy required for the reaction

$$N_3^{-*} \xrightarrow{\Delta} N_3 + e$$

is 11,3 Kcal.mol.$^{-1}$. For the reaction

$$N_3^- \xrightarrow{\Delta} N_3 + e$$

occurring during thermal decomposition (114), the energy has been found to be 26,8 Kcal.mol.$^{-1}$. Therefore the energy required for co-irradiation in which the reactions

$$N_3^- \xrightarrow{\Delta} N_3 + e$$

and $$N_3^{-*} \xrightarrow{\Delta} N_3 + e$$

are postulated to occur simultaneously, should be a value somewhere between 26,8 Kcal.mol.$^{-1}$ and 11,3 Kcal.mol.$^{-1}$. Since the Arrhenius equation applying to parallel reactions can be written as

$$k_T + k_{co'} = A_T \exp(-E_T/RT) + A_{co'} \exp(-E_{co'}/RT)$$

(subscripts T and co' have the same meanings as before), the occurrence of parallel reactions during co-irradiation is verified by the decrease in the activation energy from 21,7 Kcal.mol.$^{-1}$ to 19,2 Kcal. mol.$^{-1}$ for increases in light intensity from 6,4 units to 15,5 units respectively.

However the mechanism for photolysis below 100,0^{o}C, in which there is a thermal transfer of an electron from a singly excited azide ion to an adjacent Ba^+ ion, has been pointed out in the discussion on the photolysis of barium azide powder, to be highly unlikely. If this mechanism is discounted for photolysis in the temperature range 60,0^{o} - 100,0^{o}C, then it is not probable that it will constitute part of the mechanism occurring during co-irradiation and the first theory forwarded for the processes occurring during co-irradiation is postulated to be the most likely mechanism.

A similar approach has been made by Prout and Lownds (131) to explain the co-irradiated decomposition of potassium permanganate. The thermal decomposition has been proposed by Boldyrev (132) to proceed

via the rate determining step

$$MnO_4^- \xrightarrow{\Delta} MnO_4^{o} + e \qquad \ldots\ldots\ldots\ldots\ldots (1)$$

The activation energy of this step was found to be 39 Kcal.mol.$^{-1}$. The rate determining step for photolysis of potassium permanganate above 110,0^{o}C was postulated to be

$$(MnO_4^-)^{**} \xrightarrow{\Delta} MnO_4^{o} + e \qquad \ldots\ldots\ldots\ldots (2)$$

in the temperature range 110,0^{o} - 180,0^{o}C. The activation energy of this step was found to be 14 Kcal.mol.$^{-1}$. Thus during photolysis, thermal ionization occurs following the successive absorption of two photons by a permanganate ion. The mechanism for photolysis below 180,0^{o}C was modified to apply to the co-irradiated decomposition. A linear dependence of rate on the light intensity at constant temperature was found for co-irradiation, indicating that one excitation of the MnO_4^- ion occurs before thermal ionization of the electron into the conduction band occurs i.e.

$$MnO_4^- \rightleftharpoons^{h\nu} (MnO_4^-)^{*} \xrightarrow{\Delta} MnO_4^{o} + e \qquad \ldots\ldots\ldots (3)$$

Thus the two parallel reactions, (1) and (3) were thought to be responsible for the creation of the MnO_4^{o} radical during the co-irradiated decomposition. The measured rate of decomposition at a particular temperature and fractional decomposition was expressed as

$$R = R_T + R_o$$

where R_T and R_o are the rates of formation of MnO_4^{o} radicals by thermal ionization and optically assisted thermal ionization respectively. Therefore it was postulated that the average energy of reactions (1)

and (3) which both occur during co-irradiation should be something between 14 Kcal.mol.$^{-1}$ and 39 Kcal.mol.$^{-1}$. The values of the activation energies for the decomposition of $KMnO_4$ above 195,0^{o}C were 39 Kcal.mol.$^{-1}$, 33 Kcal.mol.$^{-1}$ and 29 Kcal.mol.$^{-1}$ for light intensities of 0, 10 and 44 units respectively.

Since the activation energies and dependence of reaction rates on light intensity associated with the decay reaction of co-irradiated barium azide powder are approximately equal to those of the acceleratory period, it is assumed that mechanisms analogous to those occurring during the acceleratory period occur during the decay period. The decay reaction commences when the surface nuclei touch and reaction takes place according to the unimolecular decay law, indicating that the rate of reaction in the product coated grains,is proportional to the amount of undecomposed material. As postulated for the decay reaction of photolysed powder, due to extensive growth of plate-like nuclei with the use of a high intensity light source, the interface collapses through differences in volume between product and reactant phases leaving isolated blocks of material in which no nuclei are present. In these isolated blocks each molecule has an equal probability of decomposition and the rate of reaction becomes proportional to the amount of substance undecomposed. Thus decay follows the unimolecular decay law.

For a purely thermal decomposition (114) or a thermal decomposition pre-irradiated with ultraviolet light (111) of low intensity, the decay reaction conformed to the contracting sphere equation. This is due to rapid efficient surface nucleation of the particles, causing them to become coated with a layer of product on the surface only. The decay reaction corresponds to the penetration of the continuous

interface into the particles according to the contracting sphere formula. With the high intensity light source used for co-irradiation, nuclei are formed on the surface and on the planes of the particles resulting in different topographical kinetics.

The presence of barium metal nuclei at the end of the induction period of a co-irradiated decomposition is supported by the observation of a grey colouration on the surface of the particles. It can be assumed that no nuclei are present until the end of the induction period since water vapour, when interacted with the salt before the end of the induction period, had no effect on the subsequent reaction, also no changes in the colour of the salt were observable until the end of the induction period. For a pure thermal decomposition of barium azide (114) it has been reported that barium metal nuclei have been detected at positions midway along the thermal induction period in which there was no detectable evolution of gas. However a slow evolution of nitrogen was detected, after a period in which there was no evolution of gas and before the reaction entered the acceleratory stage, when a sensitive pressure gauge was used to monitor the course of the reaction instead of a McLeod gauge (see Fig. 44). It can be assumed that the metal nuclei destroyed midway along the apparent induction period, of a thermal decomposition, are those in the process of growth to the critical size before acceleration proper can commence. This slow growth period is insignificant when the sample is subjected to co-irradiation.

The importance of the presence of metal nuclei during co-irradiation was again illustrated by the interaction of the sample with water vapour at various stages of decomposition. Interaction with water vapour at the end of the induction period and at positions in the acceleratory stage was found to destroy the metal nuclei on the surface

only since the reaction following a water interruption proceeded after an induction period shorter than that of an uninterrupted decomposition. This supports the proposal that growth nuclei are formed on the surface and on planes below the surface of the particles. Water vapour is assumed to cause the destruction of the surface nuclei only and leave the nuclei in the bulk of the sample intact, the new reaction proceeding from these centres. The duration of the induction period represents the time for those nuclei remaining in the bulk of the sample to grow to a critical size. The decrease in the acceleratory and decay reaction rates following a new induction period can be attributed, as before, to the commencement of the acceleratory reaction from fewer centres.

The increase in metal nuclei concentration as the reaction proceeded was observed by the gradual darkening of the salt through the acceleratory stage of the reaction. Reaction with water vapour at the inflection point was found to destroy any further reaction. Although after the inflection point growth nuclei may exist below the surface, they cannot be activated by the light due to the opaque layer of barium hydroxide (produced through the reaction of barium metal with water vapour) formed on the surface of the particles. The decrease in the acceleratory rate constant after a water interruption, is due to the removal of potential nucleus sites by the water vapour, when already growing nuclei are destroyed. The decrease in the expected final pressure after a water interruption is due to the partial hydrolysis of the azide by the water vapour.

(ii) Pellets

The pressure-time curves obtained from co-irradiated pellets

were found to resemble those of co-irradiated powder. The characteristics of the curves were an induction period during which there was no evolution of gas, followed by an acceleratory reaction obeying the Avrami-Erofeyev equation with n = 2 and finally a decay reaction conforming to the unimolecular decay law. Co-irradiation was found to accelerate the thermal decomposition of the pellet.

Since the results of mathematical analyses, visual observations and the effect of water vapour at various stages of decomposition were found to be analogous with the results obtained from co-irradiated powder it can be assumed that the topochemistry of the reaction occurring during co-irradiation of pellets will be similar.

No activation energies could be obtained for the co-irradiated decomposition of the pellets due to the irreproducible nature of the pressure-time curves. The split run technique was found to be unsuccessful since the pellet was highly susceptible to pre-irradiation with ultraviolet light. This caused the pellet, after the determination of the first velocity constant, to begin decomposing during the warm-up period required for the pellet to reach the second decomposition temperature, thus preventing the determination of a second velocity constant. The irreproducibility of the co-irradiated decomposition can be accounted for in the same way as was done for the photolytic decomposition of pellets.

5C PHOTOLYSIS OF STRONTIUM AZIDE

The discussion that has applied to the photolysis and co-irradiation of barium azide powder and pellets can, in general, be applied to the decomposition of strontium azide powder and pellets.

The photolysis of the strontium salt will be discussed followed by a discussion of the co-irradiated decomposition pointing out the essential differences between the behaviour of the barium and strontium salts when exposed to ultraviolet light over the temperature range $30,0^{o}$ - $135,0^{o}C$.

(i) Powder

Two distinct activation energies were obtained in the photolytic temperature range ($30,0^{o}$ - $90,0^{o}C$), the transition temperature occurring at $50,0^{o}C$. The change in activation energy at this temperature was found to be from 2,6 Kcal.mol.$^{-1}$ to 6,5 Kcal.mol.$^{-1}$ for the induction period; 3,2 Kcal.mol.$^{-1}$ to 12,9 Kcal.mol.$^{-1}$ for the acceleratory period and from 5,7 Kcal.mol.$^{-1}$ to 12,9 Kcal.mol.$^{-1}$ for the decay period.

Unlike barium azide, the dependence of the photolytic rate of strontium azide on the intensity of the ultraviolet light source was not found to change at the transition temperature. The reciprocals of the duration of the induction periods and the rates of acceleration and decay were found to vary approximately as the square of the light intensity over the whole of the photolytic temperature range ($30,0^{o}$ - $90,0^{o}C$).

The topography of the photolytic reaction of strontium azide can be assumed to be analogous to that described for barium azide

since the kinetic equations, used to describe the photolysis of strontium azide, visual observations and the effect of the interaction of water vapour at various stages of photolytic decomposition of strontium azide were identical to those found for barium azide. A variation in the photolytic mechanism is needed to explain the bimolecular dependence of photolytic reaction on the intensity of the ultraviolet light source.

The formation of strontium metal nuclei at the end of the induction period of photolytic decomposition in the temperature range $30{,}0^{o}$ - $50{,}0^{o}C$ is assumed to proceed via the following mechanism

$$N_3^- \overset{h\nu}{\rightleftharpoons} N_3^{-*} \quad \ldots\ldots\ldots\ldots\ldots\ldots \quad (1)$$

As proposed for barium azide this primary excitation corresponds to an internal transition on the azide ion. Reaction now takes place with an Sr^{++} ion when there are two singly excited azide ions at a surface defect S (possibly an anion vacancy)

$$N_3^{-*}\ SN_3^{-*} + Sr^{++} \xrightarrow{\Delta} 3N_2 + Sr + S \quad \ldots \quad (2)$$

Step (2) is considered to be the rate determining step with an activation energy of 2,6 $Kcal.mol.^{-1}$ associated with it. The strontium atoms formed in this step are located on the surface and on the planes of the crystal initially at the interatomic spacings in strontium azide. With time diffusion of these strontium atoms will occur resulting in aggregation to give strontium metal nuclei. The aggregation of metal atoms to metal nuclei marks the end of the induction period.

This mechanism, proposed for the production of strontium metal nuclei, is in accordance with the observed dependence of the inverse of the duration of the induction period on the square of the light intensity; the duration being dependent on the time required for the

strontium atoms to aggregate, through diffusion, to form strontium metal nuclei, this in turn being dependent on the intensity of the light source.

A variation of this mechanism for the production of strontium metal nuclei, is needed for photolysis in the temperature range $50{,}0^{o}$ - $90{,}0^{o}C$, to account for the observed increase in activation energy but the same square dependence of the duration of the inverse of the induction period on light intensity. The following mechanism is proposed:

$$N_3^- \rightleftharpoons^{h\nu} N_3^{-*} \quad \ldots\ldots\ldots\ldots\ldots\ldots (1)$$

From the increase in thermal energy due to the increase in decomposition temperature, there is sufficient thermal energy now for the transfer of an electron from an excited azide ion thermally to an adjacent Sr^{++} ion

$$Sr^{++} + N_3^{-*} \xrightarrow{\Delta} Sr^{+} + N_3 \quad \ldots\ldots\ldots\ldots (2)$$

The positive hole formed in this step can react with an adjacent excited azide ion

$$N_3 + N_3^{-*} \longrightarrow 3N_2 + e \quad \ldots\ldots\ldots\ldots (3)$$

and the generated electron can now combine with the Sr^{+} ion formed in step (2)

$$e + Sr^{+} \longrightarrow Sr \quad \ldots\ldots\ldots\ldots\ldots (4)$$

Step (2) is considered to be the rate determining step with an activation energy of 6,5 $Kcal.mol.^{-1}$ associated with it. The strontium metal atoms formed in step (4) are again assumed to be formed on the surface and on the planes of the crystal, the metal nuclei being

formed after diffusion of these atoms. The duration of the induction period is still inversely proportional to the square of the light intensity and dependent on the time required for the concentration of strontium atoms to aggregate to strontium metal nuclei.

The growth of the strontium metal nuclei during the accelera-tory period of photolysis in the temperature range $30{,}0^{o}$ - $50{,}0^{o}C$ is postulated to take place via an overall mechanism which involves the decomposition of an excited intermediate which has absorbed, directly or indirectly, the energy from two photons of incident light since the mechanism must be in accordance with the observed dependence of reaction rate on the square of the light intensity. The two basic schemes by which this can occur have been outlined under the section on photolysis of barium azide, but for completeness will be repeated briefly here again.

(i) This first scheme involves the successive absorption of two photons by an azide ion. The strontium metal nuclei formed at the end of the induction period undergo reaction via the photo-electric effect to produce positive strontium ions. A single excitation of an azide ion results on the absorption of a photon. This singly excited azide ion if situated at a defect site will absorb a second photon of light energy to give a doubly excited azide ion. The absorbed energy is assumed to be localized in the form of vibrational or internal electronic excitation. This doubly excited azide ion can now undergo thermal ionization to give an electron and an excited positive hole or revert to the singly excited state.

Thus $Sr_n \overset{h\nu}{\rightleftharpoons} Sr_n^{+} + e$ photo-electric effect ..... (1)

$N_3^{-} \xrightarrow[h\nu]{k_1} N_3^{-*}$ primary excitation ..... (2)

$$N_3^{-*} \xrightarrow{k_2} N_3^- \qquad \text{de-excitation} \quad \ldots\ldots\ldots (3)$$

$$N_3^{-*} \xrightarrow[h\nu]{k_3} N_3^{-**} \qquad \text{secondary excitation} \quad \ldots\ldots (4)$$

$$N_3^{-**} \xrightarrow{k_4} N_3^{-*} \qquad \text{de-excitation} \quad \ldots\ldots\ldots (5)$$

$$N_3^{-**} \xrightarrow[\Delta]{k_5} N_3^* + e \qquad \text{decomposition} \quad \ldots\ldots\ldots (6)$$

As proposed for barium azide the electron, produced through thermal ionization in this step now combines with an adjacent Sr^+ ion formed in step (1)

$$Sr_n^+ + e \longrightarrow Sr_n \qquad \ldots\ldots\ldots\ldots\ldots (7)$$

The positive hole created in step (6) is highly energetic i.e. it retains energy received from the light, and can react with an adjacent azide ion in a strained position to give nitrogen

$$N_3^- + N_3^* \longrightarrow 3N_2 + e + 2A \longrightarrow 3N_2 + F + A \quad \ldots\ldots (8)$$

where A = anion vacancy

and F = F-centre.

Strontium metal nuclei, which add to the interface, are formed via the collapse of the F-centres (which are attached to the nucleus) on attaining a critical size

$$2F \longrightarrow 2A + 2e \qquad \ldots\ldots\ldots\ldots\ldots\ldots (9)$$

$$Sr_n + 2e + Sr^{++} \longrightarrow Sr_{n+1} \qquad \ldots\ldots\ldots\ldots\ldots (10)$$

Steps (7), (8), (9) and (10) are fast reactions following the rate determining step (6).

The overall rate can be expressed as

$$R = k_5(N_3^{-}**) \ .$$

When the steady state conditions

$$\frac{d(N_3^{-}*)}{dt} = \frac{d(N_3^{-}**)}{dt} = 0$$

are applied it can be shown that the rate equation reduces to

$$R = k_1k_3k_5(N_3^{-})I^2 \ / \ k_2k_4$$

when it is assumed that $k_2 >> k_3I$ and $k_4 >> k_5$ and when it is remembered that $R \propto I^2$. Thus the proposed mechanism is in accordance with the observed dependence of reaction rate on the square of the light intensity.

(ii) The second scheme involves the transfer of energy from an excited ion to an adjacent azide ion :

Sr_n	$\overset{h\nu}{\rightleftharpoons}$	$Sr_n^{+} + e$	photo-electric effect ..... (1)
N_3^{-}	$\xrightarrow[h\nu]{k_1}$	$N_3^{-}*$	primary excitation ..... (2)
$N_3^{-}*$	$\xrightarrow{k_2}$	N_3^{-}	de-excitation ..... (3)
$N_3^{-}* + N_3^{-}*$	$\xrightarrow{k_3}$	$N_3^{-}** + N_3^{-}$	energy transfer ..... (4)
$N_3^{-}**$	$\xrightarrow{k_4}$	$N_3^{-}*$	de-excitation ..... (5)
$N_3^{-}**$	$\xrightarrow[\Delta]{k_5}$	$N_3* + e$	decomposition ..... (6)

As before the electron, generated through thermal ionization in step (6), combines with an adjacent Sr^{+} ion formed in step (1) and the excited positive hole, N_3*, reacts with an adjacent N_3^{-} ion in a strained

position to give nitrogen. Thus the fast decomposition reactions are

$$Sr_n^+ + e \longrightarrow Sr_n \quad \ldots\ldots\ldots\ldots\ldots\ldots\ldots\ldots (7)$$

$$N_3^* + N_3^- \longrightarrow 3N_2 + e + 2A \longrightarrow 3N_2 + F + A \quad \ldots\ldots (8)$$

where F and A have the same meanings as before.

On aggregation of these F-centres to a critical size collapse occurs, yielding strontium metal atoms which add to the nucleus. Thus

$$2F \longrightarrow 2A + 2e \quad \ldots\ldots\ldots\ldots\ldots\ldots (9)$$

$$Sr_n + 2e + Sr^{++} \longrightarrow Sr_{n+1} \quad \ldots\ldots\ldots\ldots\ldots\ldots (10)$$

The rate determining step is considered to be step (6). When the steady state conditions defined above are applied and the overall rate equation is assumed to be

$$R = k_5(N_3^{-**})$$

a rate equation of the form

$$R \simeq k_1 k_5 C_k (N_3^-) I^2$$

can be obtained, where C_k is a combination of the rate constants. The mechanism is therefore in accordance with the observed dependence of reaction rate on the square of the light intensity.

Thus for both processes the incident energy is absorbed by the electrons of the N_3^- ions. Absorbing ions situated at normal lattice sites will be de-excited by communication of their energy to the vibrational modes of the ion, while for those at positions of stress the energy will be localized long enough for secondary excitation to occur.

The measured activation energy of 3,2 Kcal.mol.$^{-1}$ for

photolysed strontium azide powder below 50,0°C is associated with the rate determining step (6) in processes (i) and (ii). The mechanisms proposed are in accordance with the observed dependence of rate of reaction with the square of the light intensity.

As shown under the section on photolysis of barium azide, these reaction schemes have been used by other workers to explain photolysis of ionic salts and it is thought that these are the most likely mechanisms whereby strontium azide photolysis, in the temperature range 30,0° - 50,0°C occurs.

For photolysis of strontium azide in the temperature range 50,0° - 90,0°C, modifications to the mechanisms postulated for photolysis in the lower temperature range are needed to account for the increase in activation energy although the reaction remains dependent upon the square of the light intensity. The following mechanism is proposed: the strontium metal formed at the end of the induction period undergoes reaction via the photo-electric effect to give strontium metal, Sr^+, ions. A singly excited azide ion results through the absorption of one photon of electromagnetic energy. Again it can be assumed that the energy is localized at the favoured sites in the form of vibrational and internal electronic excitation. An azide ion, located at a normal lattice point, which has absorbed a photon will revert to the ground state by communication of its energy to the vibrational modes of an adjacent ion. However azide ions situated at defect sites,on absorbing a photon, due to the imbalance of forces will allow the absorbed energy to be localized at a particular ion long enough for reaction to occur with a Sr^+ ion to produce an azide radical and strontium metal. The azide radical will then react with an adjacent single optically excited azide ion to give nitrogen, an electron and two newly formed anion vacancies.

Thus $Sr_n \rightleftharpoons Sr_n^+$ ..... (1)

$N_3^- \rightleftharpoons N_3^{-*}$ ..... (2)

$Sr_n^+ + N_3^{-*} \xrightarrow{\Delta} Sr_n + N_3$ ..... (3)

$N_3 + N_3^{-*} \longrightarrow 3N_2 + e + 2A \longrightarrow 3N_2 + F + A$ ... (4)

where A = anion vacancy

and F = F-centre.

Strontium metal atoms add to the nucleus on the collapse of the F-centre complex (which is bound to the nucleus) on it attaining a critical size

$2F \longrightarrow 2A + 2e$ ..... (5)

$Sr_n + 2e + Sr^{++} \longrightarrow Sr_{n+1}$ ..... (6)

Step (3) is considered to be the rate determining step with an activation energy of 12,9 Kcal.mol.$^{-1}$ associated with it. This reaction is bimolecular with respect to azide ions and is an acceleratory one in which the strontium metal is regenerated.

It is thought that the reaction, occurring during the decay stage of photolysed samples of strontium azide powder, follows the same mechanism as proposed for the photolytic acceleratory period in the corresponding decomposition temperature range. The slight increase in activation energy from 3,2 Kcal.mol.$^{-1}$ for the acceleratory period to 5,7 Kcal.mol.$^{-1}$ i.e. an increase of 2,5 Kcal.mol.$^{-1}$ for the decay reaction in the lower decomposition temperature range, is thought to be due to a change in crystal structure of the product causing possible hindrance to the diffusion of nitrogen from the particles of partly decomposed powder. Thus the increase in activation energy is due to the activation energy of diffusion of nitrogen. At the higher decomposition

temperature range it is thought that the increase in activation energy of the decay reaction due to the diffusion of nitrogen from the partly decomposed powder is not observed owing to experimental error. The protracted nature of the decay reaction is thought to be caused by the hindrance to the diffusion of nitrogen from the partly decomposed powder.

(ii) Pellets

The discussion applying to photolysed pellets of barium azide can be applied to photolysed strontium azide pellets since the shape of the photolytic decomposition curve obtained from strontium azide pellets, the change in activation energies with change in pelleting pressure of the strontium azide pellets, and the results obtained when two strontium azide pellets are decomposed simultaneously, is analogous to that found for the corresponding tests on barium azide pellets.

5D CO-IRRADIATION OF STRONTIUM AZIDE

(i) Powder

The results obtained from the irradiation of strontium azide powder with ultraviolet light during thermal decomposition were similar to those obtained from the barium salt when co-irradiated. Co-irradiation of strontium azide was found to decrease the duration of the induction period and increase the rate of the acceleratory and decay reactions of a purely thermal decomposition. At all stages of the acceleratory and decay reactions a dark rate was detected due to the thermal decomposition of the pre-irradiated azide.

A change in the topography of the thermal reaction was found to occur with co-irradiation. As with the co-irradiation of barium azide the activation energies of the process(es) occurring during co-irradiation were found to be on the whole lower than that of an un-irradiated decomposition. At low values of light intensity the activation energies were found to approximate to those of thermal decomposition while at high values of light intensity the activation energies were found to approximate to those occurring in the photolytic decomposition temperature range 50,0^{o} - 90,0^{o}C. The activation energies of the induction period and the acceleratory and decay reactions were found to be 22,6 Kcal.mol.$^{-1}$, 25,9 Kcal.mol.$^{-1}$ and 28,3 Kcal.mol.$^{-1}$ respectively when a light intensity of 7,0 units was employed, while a decrease to 15,4 Kcal.mol.$^{-1}$, 18,8 Kcal.mol.$^{-1}$ and 20,9 Kcal.mol.$^{-1}$ was observed for the stages of reaction when a light intensity of 15,25 units was used. The activation energies for the induction period, and the acceleratory and decay reactions of a purely thermal decomposition (89) were found to be 23,3 Kcal.mol.$^{-1}$, 25,0 Kcal.mol.$^{-1}$ and

21,7 Kcal.mol.$^{-1}$ respectively. The activation energies, found for the acceleratory and decay reactions of a co-irradiated decomposition when a light intensity of 7,0 units was employed, are in fact slightly higher than that of the corresponding values of the pure thermal decomposition. This is due most probably to the slightly irreproducible nature of the co-irradiated powder and thus the increase can be attributed to experimental error.

The dependence, of the inverse of the duration of the induction period and rates of acceleration and decay on the intensity of the ultraviolet light source was found to be $I^{0,8}$, $I^{0,6}$ and $I^{0,8}$ respectively. These values were approximated to $I^{1,0}$ for all stages of reaction.

As for the co-irradiation of barium azide, it can be proposed for the co-irradiation of strontium azide that the parallel reactions: (i) a modification of the photolytic reaction occurring in the temperature range 50,0^{o} - 90,0^{o}C and (ii) the thermal reaction occurring in the temperature range 110,0^{o} - 135,0^{o}C for strontium azide both occur during co-irradiation.

Two-dimensional reaction centres are assumed to form during the induction period of a purely thermal decomposition (89) of strontium azide. These nuclei are produced most probably at localities on the surface of the particles where disorganization or mechanical damage has taken place such as at an emergent edge dislocation, either isolated or in a grain boundary terminating at the surface. From the layered structure of strontium azide (133) it is probable that a large number of incomplete planes of the edge dislocations in an emergent grain boundary will contain only azide ions or Sr^{2+} ions. The decomposition of two adjacent azide ions at the core of a dislocation will be favoured, particularly if they both lie on the surface. Decomposition will

produce a strontium atom and three molecules of nitrogen i.e.

$$N_3^- + N_3^- \longrightarrow 3N_2 + 2e \quad \ldots\ldots\ldots\ldots\ldots (1)$$

The freed electrons will combine with a strontium ion on the surface to form strontium atoms in the rate determining step

$$Sr^{++} + 2e \longrightarrow Sr \quad \ldots\ldots\ldots\ldots\ldots\ldots (2)$$

These strontium atoms will be at the interatomic spacing in strontium azide. More strontium atoms will form as the dislocation climbs along the surface. When a critical concentration of strontium atoms is reached, a strontium metal speck will crystallize to form a nucleus.

During the induction period of a photolytic decomposition of strontium azide above 50,0^{o}C there is a thermal transfer of an electron from an azide ion which has absorbed one photon from the incident light, to an adjacent Sr^{++} ion resulting in a Sr^{+} ion and an azide radical. Strontium atoms result when the electron generated in the reaction between the azide radical and a singly excited azide ion, combines with an adjacent Sr^{+} ion. The reaction scheme can be written as

$$N_3^- \overset{h\nu}{\rightleftharpoons} N_3^{-*} \quad \ldots\ldots\ldots\ldots\ldots (1)$$

$$Sr^{++} + N_3^{-*} \xrightarrow{\Delta} Sr^{+} + N_3 \quad \ldots\ldots\ldots\ldots\ldots (2)$$

$$N_3 + N_3^{-*} \longrightarrow 3N_2 + e \quad \ldots\ldots\ldots\ldots\ldots (3)$$

$$Sr^{+} + e \longrightarrow Sr \quad \ldots\ldots\ldots\ldots\ldots (4)$$

These strontium metal nuclei are at the interatomic spacing in strontium azide and are assumed to form as in the case of the photolysis of barium azide, in thin plates starting on the surface and moving

down the core of the dislocation. Aggregation of the metal atoms to form strontium metal nuclei as described for thermal decomposition, takes place when the concentration of atoms reaches a critical value. The rate of formation of metal nuclei will be dependent on the square of the light intensity.

It appears that the mechanism proposed for strontium metal nucleus formation above 50,0^{o}C can be modified to apply to the co-irradiated decomposition where the duration of the induction period i.e. the time required for the strontium metal atoms to reach a critical concentration for aggregation to metal nuclei, is dependent on the first power of intensity.

With an increase in thermal energy through an increase in decomposition temperature, sufficient thermal energy is now available for the thermal transfer of an electron from a ground state azide ion to a Sr^{++} ion, resulting in the formation of a Sr^{+} ion and a positive hole. As for photolysis above 50,0^{o}C, nitrogen and an electron are produced when the positive hole reacts with an adjacent singly excited azide ion. Strontium atoms are formed by the combination of the generated electron and the Sr^{+} ion. Thus the reaction scheme for the production of strontium metal nuclei during a co-irradiated decomposition can be written as

$$N_3^- \rightleftharpoons^{h\nu} N_3^{-*} \quad \ldots\ldots\ldots\ldots (1)$$

$$Sr^{++} + N_3^- \xrightarrow{\Delta} Sr^{+} + N_3 \quad \ldots\ldots\ldots (2)$$

$$N_3 + N_3^{-*} \longrightarrow 3N_2 + e \quad \ldots\ldots\ldots\ldots (3)$$

$$Sr^{+} + e \longrightarrow Sr \quad \ldots\ldots\ldots\ldots (4)$$

The rate of formation of strontium metal will be proportional to the first power of light intensity.

Thus the end of the induction period of a co-irradiated decomposition is marked by the formation of strontium metal nuclei, the nuclei being formed by the thermal process and a modification to the photolytic process occurring below 90,0°C. As was stated in the discussion on the co-irradiation of barium azide, once the nuclei have reached a critical size or extent the reaction will enter the acceleratory period, the induction period processes becoming unimportant i.e. the salt has "forgotten" whether the induction period nucleus formation was induced by heat or radiation at the onset of the acceleratory reaction. The combined effects of the radiation must be taken as additive with either process not modifying the other. A slow transition from the induction period to the acceleratory period was noticed when a purely thermal decomposition was carried out on strontium azide. A marked reduction in this transition from the induction period to the acceleratory period was noticed with co-irradiation of the salt. This could be attributed, as was done for barium azide, to either a reduction in the time required for the metal nuclei to grow to a critical size or to an increase in the number of nuclei originally formed.

The energy of the rate determining step of nucleus formation was found to be between that expected if the reaction was a purely thermal one and that expected if the reaction was a purely photolytic decomposition in the temperature range 50,0° - 90,0°C. This is feasible if it is assumed that nucleus formation occurs by the purely thermal process and by a modification to the photolytic process occurring during photolysis in the temperature range 50,0° - 90,0°C.

A change in the topography of the acceleratory and decay reactions occurring during thermal decomposition was found with co-irradiation of strontium azide powder. During thermal decomposition (89) the acceleratory period was found to obey the power law with the

exponent taking the value of 3. The expression was found to fit the whole of the acceleratory period, which led to the conclusion that no significant overlap or ingestion of nuclei occurred before the decay reaction commenced. It was assumed that reaction proceeded from a steadily expanding 2-dimensional reaction centre, the nuclei increasing in number linearly with time. The decay reaction commenced when the surface nuclei touched, reaction then proceeding by the inward progression of the interface. Thus the kinetics of the reaction was described by the contracting sphere formula. The activation energies during the course of reaction were found to be 23,3 Kcal. $mol.^{-1}$, 25,0 $Kcal.mol.^{-1}$ and 21,7 $Kcal.mol.^{-1}$ for the induction period and acceleratory and decay reactions respectively. When the salt was pre-irradiated (111) with a low intensity ultraviolet light source, the exponent in the power law expression was found to change from 3 to 2. The exponent taking the value of 2 was assumed to represent the growth of two-dimensional nuclei occurring from a fixed number produced at the end of the induction period. The power law with n = 2 fitted the complete acceleratory period, indicating again that even with pre-irradiation no significant overlap or ingestion of nuclei occurred before the decay reaction commenced. It was concluded that this change in the exponent from 3 to 2 was due to a large number of surface nuclei, produced at the end of the induction period through pre-irradiation, causing any further increase with time to be virtually swamped. The decay reaction followed the contracting sphere formula, as was found for the purely thermal process. The activation energies for the thermal decomposition of ultraviolet light pre-irradiated strontium azide (111) were found to be 19,5 $Kcal.mol.^{-1}$, 23,0 $Kcal.mol.^{-1}$ and 25,7 $Kcal.mol.^{-1}$ for the induction period, and the acceleratory and decay reactions

respectively and can be said to be, within experimental error, comparable with the activation energies obtained for the corresponding reactions of a purely thermal decomposition. This indicates that the mechanism of thermal decomposition is unaltered by pre-irradiation of the material.

The acceleratory period of the co-irradiated decomposition was found to obey Avrami-Erofeyev type kinetics, the exponent taking the value of 2 in the equation. The applicability of this equation indicates that significant overlap or ingestion of nuclei occurs before the decay reaction commences. With the powerful light source employed for co-irradiation studies it is expected that the number of nuclei created at the end of the induction period of a co-irradiated decomposition is significantly larger than with pre-irradiation, consequently overlap and ingestion of nuclei occurs. It can be concluded as was done for barium azide that n = 2 represents the growth of two-dimensional nuclei from a fixed number of nuclei, and the growth centres can again be considered to be plate-like in nature advancing along the grain boundaries in which they were initiated. As for barium azide a general decrease in the thermal activation energies were observed with co-irradiation indicating that a different mode of reaction mechanism from that occurring during thermal decomposition occurs during co-irradiation.

The growth of strontium metal nuclei during the acceleratory period of a thermal decomposition (89) is assumed to follow the same mechanism as proposed for barium azide i.e. an electron is transferred from the full band of the azide ion to the lowest vacant level (conduction band) of the strontium metal nucleus which has crystallized at the end of the induction period. The activation energy for growth is identified with the energy difference of the electron in the full band and in the lowest level of the metal. The generated positive hole

reacts with an adjacent azide ion whenever sufficient thermal energy is available to raise one of its electrons to an excited state. After liberation of the nitrogen, the freed electrons are trapped in newly formed anion vacancies, forming an F-centre complex which is bound to the nucleus. Collapse of the aggregate occurs on it reaching a critical size to yield strontium atoms which add to the nucleus.

For photodecomposition below 90,0^{o}C the rate determining step during the acceleratory reaction is considered to be the thermal transfer of an electron from a singly excited azide ion to a Sr^{+} ion formed via the photo-electric effect when ultraviolet light acts on strontium metal. The positive hole produced then reacts with an adjacent single optically excited azide ion to produce three molecules of nitrogen, an electron and two anion vacancies. The electron combines with one of the newly formed anion vacancies to produce an F-centre which is bound to the nucleus. As during thermal decomposition, strontium atoms add to the nucleus on collapse of the F-centre aggregate on it attaining a critical size. This reaction is bimolecular with respect to azide ions.

It appears that the mechanism proposed for the decomposition below 90,0^{o}C can be modified for the co-irradiated decomposition where the reaction is unimolecular with respect to azide ions. With the increase in temperature to that of the thermal decomposition temperature range, there is now sufficient thermal energy for the thermal transfer of an electron from a ground state azide ion to a Sr^{+} ion formed via the photo-electric effect. The positive hole formed reacts with an adjacent single optically excited azide ion to give three molecules of nitrogen. Thus the reaction scheme can be written as

$$Sr_n \overset{h\nu}{\rightleftharpoons} Sr_n^{+} + e \qquad \ldots\ldots\ldots\ldots (1)$$

$$N_3^- \rightleftharpoons^{h\nu} N_3^{-*} \quad \ldots\ldots\ldots\ldots\ldots\ldots\ldots\ldots \quad (2)$$

$$Sr_n^+ + N_3^- \xrightarrow{\Delta} Sr_n + N_3 \quad \ldots\ldots\ldots\ldots\ldots\ldots\ldots \quad (3)$$

$$N_3 + N_3^{-*} \longrightarrow 3N_2 + e + 2A \longrightarrow 3N_2 + F + A \quad \ldots \quad (4)$$

where F = F-centre

and A = anion vacancy.

Strontium metal nuclei add to the interface when the F-centres (which are bound to the nucleus) collapse after reaching a critical size.

Thus $$2F \longrightarrow 2A + 2e \quad \ldots\ldots\ldots\ldots\ldots \quad (5)$$

$$Sr_n + 2e + Sr^{++} \longrightarrow Sr_{n+1} \quad \ldots\ldots\ldots\ldots\ldots \quad (6)$$

The reaction is thus unimolecular with respect to azide ions.

Thus it can be expected that the thermal ionization of an electron from a ground state azide ion into the conduction band of the strontium metal nucleus and the thermal transfer of such an electron to a positively charged strontium metal ion occurs concurrently during co-irradiation, both reactions producing azide radicals. As for the co-irradiation of barium azide, since two parallel reactions are responsible for the production of azide radicals, the measured rate of reaction of a co-irradiated decomposition at a particular temperature in the decomposition temperature range can be expressed as

$$R = R_T + R_{co}$$

where R_T = rate of decomposition if thermal ionization of an electron from a ground state azide ion into the conduction band of the strontium metal nucleus takes place exclusively, and

R_{co} = rate of decomposition if thermal transfer of an electron from

a ground state azide ion to a positively charged strontium metal ion formed via the photo-electric effect takes place exclusively.

As for barium azide it can be shown that the measured rate of a co-irradiated decomposition of strontium azide at a particular value of α, is proportional to the light intensity, from which it can be concluded that the reaction

$$N_3^- \underset{}{\overset{h\nu}{\rightleftharpoons}} N_3^{-*} \xrightarrow[\text{radical}]{N_3} 3N_2 + e + 2A \longrightarrow 3N_2 + A + F$$

is directly proportional to the light intensity. Thus only one optical excitation occurs before reaction with an N_3 radical which is in accordance with the observed linear dependence of reaction rate on light intensity.

The activation energy for the thermal decomposition has been found to be 25,0 Kcal.mol.$^{-1}$ i.e. it is associated with the thermal ionization of an electron, from a ground state azide ion, into the conduction band of the metal nucleus :

$$N_3^- + \text{strontium metal} \xrightarrow[25,0\ \text{Kcal.mol.}^{-1}]{\Delta} N_3 + (\text{electron in conduction band of strontium metal}).$$

The reaction

$$N_3^{-*} + Sr^+ \xrightarrow[12,9\ \text{Kcal.mol.}^{-1}]{\Delta} N_3 + Sr$$

which occurs during photolysis in the temperature range 50,0^o - 90,0^{o}C has an activation energy of 12,9 Kcal.mol.$^{-1}$ associated with it. Therefore the average energy of the reactions

$$N_3^- + \text{strontium metal} \xrightarrow{\Delta} N_3 + (\text{electron in conduction band of strontium metal})$$

and $N_3^- + Sr^+ \xrightarrow{\Delta} N_3 + Sr$

which both occur during co-irradiation, should be some value between 12,9 Kcal.mol.$^{-1}$ and 25,0 Kcal.mol.$^{-1}$. As shown for barium azide, it can be expected that as k_{co} increases with respect to k_T (i.e. as the light intensity increases) the measured activation energy of the parallel reactions should approach E_{co}. The activation energy of the accelerator stage decreased from 25,9 Kcal.mol.$^{-1}$ to 18,8 Kcal.mol.$^{-1}$ for light intensities of 7,0 units and 15,25 units respectively, which verifies this situation of parallel reactions, and indicates that E_{co} is less than 18,8 Kcal.mol.$^{-1}$, but by the previous argument, is greater than 12,9 Kcal.mol.$^{-1}$. Therefore the observed activation energies and the dependence of reaction rate on intensity show that the following situations apply:

(i) 50,0^{o} - 90,0^{o}C, E_a = 12,9 Kcal.mol.$^{-1}$,

thermal ionization of an electron from a single optically excited azide ion which has absorbed one photon, to a positively charged Sr^{+} ion to give a strontium metal atom and an azide radical;

(ii) 110,0^{o} - 135,0^{o}C, 12,9 Kcal.mol.$^{-1} \leqslant E_a \leqslant$ 18,8 Kcal.mol.$^{-1}$,

thermal ionization of an electron from a ground state azide ion to a positively charged Sr^{+} ion to give strontium metal and an azide radical;

(iii) 110,0^{o} - 135,0^{o}C, E_a = 25,0 Kcal.mol.$^{-1}$,

thermal ionization of an electron from the full band of the azide ion to the lowest vacant level of the strontium metal nucleus which has crystallized at the end of the induction period.

It can be assumed that the mechanism of decomposition occurring during the decay stage of co-irradiated strontium azide powder is analogous to that occurring during the acceleratory period, as was assumed for the co-irradiation of barium azide. The activation energies of the decay reactions, when light intensities of 7,0 units or 15,25 units were

employed, are greater than the activation energies of the corresponding acceleratory periods by 2,4 Kcal.mol.$^{-1}$ and 2,1 Kcal.mol.$^{-1}$ respectively. This increase in activation energy during the decay stage is thought to be due to hindrance to the diffusion of nitrogen from the partly decomposed particles of powder caused by a change in the crystal structure of the product. A similar increase in activation energy (by 2,5 Kcal.mol.$^{-1}$) was observed for photolysis in the temperature range 30,0^{o} - 50,0^{o}C.

The decay reaction of a co-irradiated decomposition followed the unimolecular law while the decay reaction of a purely thermal decomposition (89), or a thermal decomposition following pre-treatment with a low intensity ultraviolet light source, was found to obey the contracting sphere equation. The use of a high intensity light source with co-irradiation leads to the growth of plate-like nuclei causing a collapse of the interface due to differences in volume between product and reactant phases. This leaves isolated blocks of material in which no nuclei are present, each molecule now having equal probability of decomposing and the rate of reaction becomes proportional to the amount of substance undecomposed. Thus decay follows the unimolecular law.

During the thermal decomposition of either a pure sample or one pre-treated with ultraviolet light, rapid efficient surface nucleation of the particles occurs, causing a coating of product to form on the surface only. The decay reaction corresponds to the penetration of the continuous interface into the particles according to the contracting sphere formula. With the high intensity light source used for co-irradiation, nuclei are formed on the surface and on the planes of the particles, resulting in different topographical kinetics.

(ii) Pellets

The discussion applying to co-irradiated pellets of strontium azide follows similarly to that of co-irradiated pellets of barium azide since the results obtained were analogous for pellets of the two salts.

6 COMPARISON TABLE OF THE EFFECTS OF ULTRAVIOLET LIGHT ON BARIUM AND STRONTIUM AZIDES (POWDER AND PELLETS)

Note: Throughout the table $\alpha = p/p_f$ (p_f = observed final pressure); and $\alpha' = p/p'_f$ (p'_f = estimated final pressure)

A PHOTOLYSIS		
(i) Powder		
	Barium azide	Strontium azide
Kinetic equations used for analyses	Acceleratory period Avrami-Erofeyev equation: $(-\log(1-\alpha))^{\frac{1}{2}} = k_{acc}t + c$ Decay period Unimolecular law: $-\log(1-\alpha) = k_{decay}t + c$	Acceleratory period Avrami-Erofeyev equation: $(-\log(1-\alpha'))^{\frac{1}{2}} = k_{acc}t + c$ Decay period Unimolecular law: $-\log(1-\alpha') = k_{decay}t + c$
Inflection point α_i	0,43	0,36
Fit of analyses	Acceleratory period $0,01 < \alpha < 0,43$ Decay period $0,43 < \alpha < 0,92$	Acceleratory period $0,01 < \alpha < 0,36$ Decay period $0,36 < \alpha < 0,95$

	Barium azide		Strontium azide	
Activation energies Kcal.mol.$^{-1}$	Temperature range 27,0° - 60,0°C		Temperature range 30,0° - 50,0°C	
	Induction period	6,2	Induction period	2,6
	Acceleratory period	7,6	Acceleratory period	3,2
	Decay period	6,6	Decay period	5,7
	Temperature range 60,0° - 100,0°C		Temperature range 50,0° - 90,0°C	
	Induction period	11,4	Induction period	6,5
	Acceleratory period	11,3	Acceleratory period	12,9
	Decay period	12,9	Decay period	12,9
	Light intensity used for both ranges		Light intensity used for both ranges	
	25,0 units		40,5 units	
Dependence on intensity (m in the equation $k = I^m + c$)	Temperature 50,0°C		Temperature 40,0°C	
	Induction period	0,7	Induction period	2,0
	Acceleratory period	2,0	Acceleratory period	2,3
	Decay period	2,1	Decay period	1,9
	Temperature 80,0°C		Temperature 70,0°C	
	Induction period	0,6	Induction period	1,6
	Acceleratory period	1,0	Acceleratory period	1,8
	Decay period	1,2	Decay period	1,9
Type of nuclei	Two-dimensional growth of plate-like nuclei, increasing from a fixed number of centres. Marked overlap and ingestion of nuclei.		As for barium azide.	

	Barium azide	Strontium azide
Mechanism (i) Nucleus formation	Ba atoms formed on the surface and on the planes of the crystal, each plane starting at the surface at an emergent grain boundary. Nuclei form by aggregation at the end of the induction period.	As for barium azide.
	Temperature range $27,0^{o}$ - $60,0^{o}C$	Temperature range $30,0^{o}$ - $50,0^{o}C$
	$N_3^- \overset{h\nu}{\rightleftharpoons} N_3^{-*}$	$N_3^- \overset{h\nu}{\rightleftharpoons} N_3^{-*}$
	$N_3^-SN_3^{-*} + Ba^{++} \xrightarrow{\Delta}$ $Ba + 3N_2 + S$	$N_3^{-*}SN_3^{-*} + Sr^{++} \xrightarrow{\Delta}$ $Sr + 3N_2 + S$
	Temperature range $60,0^{o}$ - $100,0^{o}C$	Temperature range $50,0^{o}$ - $90,0^{o}C$
	$N_3^- \overset{h\nu}{\rightleftharpoons} N_3^{-*}$	$N_3^- \overset{h\nu}{\rightleftharpoons} N_3^{-*}$
	$Ba^{++} + N_3^- \xrightarrow{\Delta} Ba^+ + N_3$	$Sr^{++} + N_3^{-*} \xrightarrow{\Delta} Sr^+ + N_3$
	$N_3 + N_3^{-*} \longrightarrow 3N_2 + e$	$N_3 + N_3^{-*} \longrightarrow 3N_2 + e$
	$Ba^+ + e \longrightarrow Ba$	$Sr^+ + e \longrightarrow Sr$
(ii) Nuclear growth over the **accelerat**-ory period	Temperature range $27,0^{o}$ - $60,0^{o}C$	Temperature range $30,0^{o}$ - $50,0^{o}C$
	$Ba_n \overset{h\nu}{\rightleftharpoons} Ba_n^+ + e$	(i)
	$N_3^- \overset{h\nu}{\rightleftharpoons} N_3^{-*}$	$Sr_n \overset{h\nu}{\rightleftharpoons} Sr_n^+ + e$
	$Ba_n^+ + N_3^{-*} \xrightarrow{\Delta} Ba_n + N_3$	$N_3^- \overset{h\nu}{\rightleftharpoons} N_3^{-*}$
	$N_3 + N_3^{-*} \longrightarrow 3N_2 + e + 2A$ $\longrightarrow 3N_2 + A + F$	

	Barium azide	Strontium azide
	$2F \longrightarrow 2A + 2e$	$N_3^{-*} \overset{h\nu}{\rightleftharpoons} N_3^{-**}$
	$Ba_n + 2e + Ba^{++} \longrightarrow Ba_{n+1}$	$N_3^{-**} + Sr^{+} \xrightarrow{\Delta} Sr + N_3^{*}$
		$N_3^{*} + N_3^{-} \longrightarrow 3N_2 + e + 2A$
		$\longrightarrow 3N_2 + F + A$
		$2F \longrightarrow 2A + 2e$
		$Sr_n + 2e + Sr^{++} \longrightarrow Sr_{n+1}$
		or (ii)
		$Sr_n \overset{h\nu}{\rightleftharpoons} Sr_n^{+} + e$
		$N_3^{-} \overset{h\nu}{\rightleftharpoons} N_3^{-*}$
		$N_3^{-*} + N_3^{-*} \rightleftharpoons N_3^{-**} + N_3^{-}$
		$N_3^{-**} + Sr^{+} \xrightarrow{\Delta} Sr + N_3^{*}$
		$N_3^{*} + N_3^{-} \longrightarrow 3N_2 + e + 2A$
		$\longrightarrow 3N_2 + F + A$
		$2F \longrightarrow 2A + 2e$
		$Sr_n + 2e + Sr^{++} \longrightarrow Sr_{n+1}$
	Temperature range $60,0^{o} - 100,0^{o}C$	Temperature range $50,0^{o} - 90,0^{o}C$
	$Ba_n \overset{h\nu}{\rightleftharpoons} Ba_n^{+} + e$	$Sr_n \overset{h\nu}{\rightleftharpoons} Sr_n^{+} + e$
	$N_3^{-} \overset{h\nu}{\rightleftharpoons} N_3^{-*}$	$N_3^{-} \overset{h\nu}{\rightleftharpoons} N_3^{-*}$
NB	$Ba_n^{+} + N_3^{-} \xrightarrow{\Delta} Ba_n + N_3$	$Sr_n^{+} + N_3^{-*} \xrightarrow{\Delta} Sr_n + N_3$
	$N_3 + N_3^{-*} \longrightarrow 3N_2 + e + 2A$	$N_3 + N_3^{-*} \longrightarrow 3N_2 + e + 2A$
	$\longrightarrow 3N_2 + F + A$	$\longrightarrow 3N_2 + F + A$

	Barium azide	Strontium azide
(iii) Reaction in decay	$2F \rightarrow 2A + 2e$ $Ba_n + 2e + Ba^{++} \rightarrow Ba_{n+1}$ Temperature range 27,0° - 60,0°C A continuation of the reaction occurring during the acceleratory period. Temperature range 60,0° - 100,0°C A continuation of the reaction occurring during the acceleratory period.	$2F \rightarrow 2A + 2e$ $Sr_n + 2e + Sr^{++} \rightarrow Sr_{n+1}$ Temperature range 30,0° - 50,0°C A continuation of the reaction occurring during the acceleratory period. Temperature range 50,0° - 90,0°C A continuation of the reaction occurring during the acceleratory period.
Percentage decomposition	95,0%	71,2%
	(ii) Pellets	
Kinetic equations used for analyses	Acceleratory period Constant rate of evolution of gas. Decay period Unimolecular law: $-\log(1-\alpha) = k_{decay}t + c$	Acceleratory period Constant rate of evolution of gas. Decay period Unimolecular law: $-\log(1-\alpha) = k_{decay}t + c$
Fit of analyses	Acceleratory period $0,01 < \alpha < 0,22$ Decay period $0,22 < \alpha < 0,96$	Acceleratory period $0,01 < \alpha < 0,20$ Decay period $0,20 < \alpha < 0,93$

	Barium azide	Strontium azide
Activation energies (decay reaction) Kcal.mol.$^{-1}$	Temperature range $30,0^{o}$ - $60,0^{o}$C Pelleting pressure 600 lb/sq.in. 9,4 Pelleting pressure 2000 lb/sq.in. 12,4 Temperature range $60,0^{o}$ - $100,0^{o}$C Pelleting pressure 600 lb/sq.in. 14,8 Pelleting pressure 2000 lb/sq.in. 17,0 Light intensity used for both ranges 25,0 units	Temperature range $30,0^{o}$ - $50,0^{o}$C Pelleting pressure 600 lb/sq.in. 8,8 Pelleting pressure 2000 lb/sq.in. 11,7 Temperature range $50,0^{o}$ - $90,0^{o}$C Pelleting pressure 600 lb/sq.in. 16,1 Pelleting pressure 2000 lb/sq.in. 18,9 Light intensity used for both ranges 30,0 units
Type of nuclei	One-dimensional growth of nuclei (from the nuclei formed during the induction period) in the form of linear chains.	As for barium azide.
Mechanism	Assumed to be the same as that occurring during the corresponding reactions of photolysed powder.	As for barium azide.
Percentage decomposition	0,25mm thick pellet 95,0% 1mm thick pellet 90,0%	0,25mm thick pellet 71,2% 1mm thick pellet 65,0%

B CO-IRRADIATION		
(i) Powder		
	Barium azide	Strontium azide
Kinetic equations used for analyses	Acceleratory period Avrami-Erofeyev equation: $(-\log(1-\alpha))^{\frac{1}{2}} = k_{acc}t + c$ Decay period Unimolecular law: $-\log(1-\alpha) = k_{decay}t + c$	Acceleratory period Avrami-Erofeyev equation: $(-\log(1-\alpha))^{\frac{1}{2}} = k_{acc}t + c$ Decay period Unimolecular law: $-\log(1-\alpha) = k_{decay}t + c$
Inflection point α_i	0,47	0,48
Fit of analyses	Acceleratory period $0,01 < \alpha < 0,47$ Decay period $0,47 < \alpha < 0,97$	Acceleratory period $0,03 < \alpha < 0,48$ Decay period $0,48 < \alpha < 0,98$
Activation energies Kcal.mol.$^{-1}$	Temperature range 110,0° - 135,0°C Intensity 0,0 units (114) Induction period 26,5 Acceleratory period 26,8 Decay period 26,1 Intensity 6,4 units Induction period 18,5 Acceleratory period 21,7 Decay period 24,1	Temperature range 110,0° - 135,0°C Intensity 0,0 units (89) Induction period 23,0 Acceleratory period 25,0 Decay period 21,7 Intensity 7,0 units Induction period 22,6 Acceleratory period 25,9 Decay period 28,3

	Barium azide	Strontium azide
	Intensity 15,5 units Induction period 16,5 Acceleratory period 19.2 Decay period 15,6 Intensity 26,5 units Induction period 12,1 Acceleratory period - Decay period -	Intensity 15,25 units Induction period 15,4 Acceleratory period 18,8 Decay period 20,9
Dependence on intensity (m in the equation $k = I^m + c$)	Temperature 115,0°C Induction period 0,7 Acceleratory period 0,7 Decay period 0,7	Temperature 116,5°C Induction period 0,8 Acceleratory period 0,6 Decay period 0,8
Type of nuclei	Two-dimensional growth of plate-like nuclei, increasing from a fixed number of centres. Marked overlap and ingestion of nuclei.	As for barium azide.
Mechanism (i) Nucleus formation	Atoms formed on the surface and on the planes of the crystal, each plane starting at the surface at an emergent grain boundary. Nuclei form by aggregation at the end of the induction period.	As for barium azide.

	Barium azide	Strontium azide
	Temperature range 110,0° - 135,0°C The following two processes occur concurrently: (i) $N_3^- + N_3^- \xrightarrow{\Delta} 3N_2 + 2e$ $Ba^{++} + 2e \longrightarrow Ba$ and (ii) $N_3^- \overset{h\nu}{\rightleftharpoons} N_3^{-*}$ $Ba^{++} + N_3^- \xrightarrow{\Delta} Ba^+ + N_3$ $N_3 + N_3^{-*} \longrightarrow 3N_2 + e$ $Ba^+ + e \longrightarrow Ba$ Both processes produce Ba atoms which aggregate at the end of the induction period.	Temperature range 110,0° - 135,0°C The following two processes occur concurrently: (i) $N_3^- + N_3^- \xrightarrow{\Delta} 3N_2 + 2e$ $Sr^{++} + 2e \longrightarrow Sr$ and (ii) $N_3^- \overset{h\nu}{\rightleftharpoons} N_3^{-*}$ $Sr^{++} + N_3^- \xrightarrow{\Delta} Sr^+ + N_3$ $N_3 + N_3^{-*} \longrightarrow 3N_2 + e$ $Sr^+ + e \longrightarrow Sr$ Both processes produce Sr atoms which aggregate at the end of the induction period.
(ii) Nuclear growth over the accelerat-ory period	Temperature range 110,0° - 135,0°C The following two processes occur concurrently: (i) $N_3^- + Ba(metal) \xrightarrow{\Delta}$ (electron in conduction band of barium metal) + N_3 $N_3 + N_3^- \longrightarrow 3N_2 + e + 2A$ $\longrightarrow 3N_2 + F + A$	Temperature range 110,0° - 135,0°C The following two processes occur concurrently: (i) $N_3^- + Sr(metal) \xrightarrow{\Delta}$ (electron in conduction band of strontium metal) + N_3 $N_3 + N_3^- \longrightarrow 3N_2 + e + 2A$ $\longrightarrow 3N_2 + F + A$

	Barium azide	Strontium azide
(iii) Reaction in decay	$2F \longrightarrow 2A + 2e$ $Ba_n + 2e + Ba^{++} \longrightarrow Ba_{n+1}$ and (ii) $Ba_n \overset{h\nu}{\rightleftharpoons} Ba_n^+ + e$ $N_3^- \overset{h\nu}{\rightleftharpoons} N_3^{-*}$ $Ba_n^+ + N_3^- \xrightarrow{\Delta} Ba_n + N_3$ $N_3 + N_3^{-*} \longrightarrow 3N_2 + e + 2A$ $\longrightarrow 3N_2 + F + A$ $2F \longrightarrow 2A + 2e$ $Ba_n + 2e + Ba^{++} \longrightarrow Ba_{n+1}$ A continuation of the reaction occurring during the acceleratory period.	$2F \longrightarrow 2A + 2e$ $Sr_n + 2e + Sr^{++} \longrightarrow Sr_{n+1}$ and (ii) $Sr_n \overset{h\nu}{\rightleftharpoons} Sr_n^+ + e$ $N_3^- \overset{h\nu}{\rightleftharpoons} N_3^{-*}$ $Sr_n^+ + N_3^- \xrightarrow{\Delta} Sr_n + N_3$ $N_3 + N_3^{-*} \longrightarrow 3N_2 + e + 2A$ $\longrightarrow 3N_2 + F + A$ $2F \longrightarrow 2A + 2e$ $Sr_n + 2e + Sr^{++} \longrightarrow Sr_{n+1}$ A continuation of the reaction occurring during the acceleratory period.
Percentage decomposition	95,0%	71,2%

(ii) Pellets		
	Barium azide	Strontium azide
Kinetic equations used for analyses	<u>Acceleratory period</u> Avrami-Erofeyev equation: $(-\log(1-\alpha))^{\frac{1}{2}} = k_{acc}t + c$ <u>Decay period</u> Unimolecular law: $-\log(1-\alpha) = k_{decay}t + c$	<u>Acceleratory period</u> Avrami-Erofeyev equation $(-\log(1-\alpha))^{\frac{1}{2}} = k_{acc}t + c$ <u>Decay period</u> Unimolecular law: $-\log(1-\alpha) = k_{decay}t + c$
Inflection point α_i	0,54	0,54
Fit of analyses	<u>Acceleratory period</u> $0,01 < \alpha < 0,54$ <u>Decay period</u> $0,54 < \alpha < 0,98$	<u>Acceleratory period</u> $0,01 < \alpha < 0,54$ <u>Decay period</u> $0,54 < \alpha < 0,98$
Type of nuclei and mechanism	Most probably the same as for co-irradiated powder.	As for barium azide.
Percentage decomposition	<u>0,25mm thick pellet</u> 95,0%	<u>0,25mm thick pellet</u> 71,2%

7 REFERENCES

1 Levy, Herley : Material Science Research 4, 156 Chap.8 (1969).

2 Dodd : J. Chem. Phys. 35, 1815 (1961).

3 Jacobs, Tompkins : Proc. Roy. Soc. (Lond.) A215, 254 (1952).

4 Garner (Ed.) : "Chemistry of the Solid State", Butterworths (1955).

5 Hannay : "Solid State Chemistry", Prentice-Hall (1967).

6 Deb : J. Chem. Phys. 35, 2122 (1961).

7 Deb, Yoffe : Proc. Roy. Soc. (Lond.) A256, 514 (1960).

8 McLaren, Rogers : Proc. Roy. Soc. (Lond.) A240, 484 (1957).

9 Seitz : Rev. Mod. Phys. 26, 7 (1954).

10 Tamm : Phys. Z. U.S.S.R. 1, 733 (1932).

11 Swank, Brown : Phys. Rev. 130, 34 (1963).

12 Pohl : Proc. Phys. Soc. Lond. 49 (extra number), 3 (1937).

13 De Boer : "Electron and Emission Phenomena", Cambridge (1935).

14 Carlson, King, Miller : J. Chem. Phys. 33, 1266 (1960).

15 Cunningham, Tompkins : Proc. Roy. Soc. (Lond.) A251, 27 (1959).

16 King, Miller, Carlson, McMillan : J. Chem. Phys. 35, 1442 (1961).

17 Mollwo : Ann. Phys. Lpz. 29, 394 (1937).

18 Pick : Ann. Phys. Lpz. 31, 365 (1938).

19 Martienssen, Pohl : Z. Phys. 131, 488 (1952).

20 Burnstein, Oberly : Phys. Rev. 76, 1254 (1949).

21 Duerig, Markham : Phys. Rev. 79, 341 (1950).

22 Mott : Proc. Roy. Soc. A172, 325 (1939).

23 Garner, Maggs : Proc. Roy. Soc. A172, 299 (1939).

24 Wischin : Proc. Roy. Soc. A172, 314 (1939).

25 Mitchell : J. Phot. Sci. 5, 49 (1957).

26 Luckey : J. Phys. Chem. 57, 791 (1953).

27 Verwey : J. Phys. Chem. Solids 31, 163 (1970).

28 Schoonman : Physica 39, 244 (1968).

29 Kaldor, Somojai : J. Phys. Chem. 70, 3538 (1966).

30 Levine, Mark : Phys. Rev. 144, 751 (1966).

31 Kröger : "The Chemistry of Imperfect Crystals", Amsterdam (1964).

32 Arends, Verwey : Phys. Status Solidi 23, 137 (1967).

33 Dawood, Forty, Tubbs : Proc. Roy. Soc. 284, 272 (1965).

34 Maycock, Pai Verneker, Witten : J. Phys. Chem. 71, 2107 (1967).

35 Pai Verneker, Maycock : J. Phys. Chem. 72, 2798 (1968).

36 Herley, Levy : J. Chem. Phys. 46, 627 (1967).

37 Prout, Lownds : Inorg. Nucl. Chem. Let. 9, 377 (1973).

38 Shu-ti Lee : Univ. Microfilms, Ann. Arbor, Mich., 6711878.

39 Jacobs, Sheppard, Tompkins : International Symposium on the Reactivity of Solids R5 - 45, 509 (1964).

40 Jacobs, Tompkins, Pai Verneker : J. Phys. Chem. 66, 1113 (1962).

41 Deb : Trans. Fara Soc. 59, 1423 (1963).

42 Deb : Trans. Fara. Soc. 59, 1414 (1963).

43 Tompkins, Young : Proc. Roy. Soc. A236, 10 (1956).

44 Heal, Pringle : J. Phys. Chem. Solids 15, 261 (1960).

45 Papazian : J. Phys. Chem. Solids 21, 81 (1961).

46 Miller : J. Chem. Phys. 33, 889 (1960).

47 King, Carlson, Miller, McMillan : J. Chem. Phys. 34, 1499 (1961).

48 Shuskus, Young, Gilliam, Levy : J. Chem. Phys. 33, 622 (1960).

49 Horst, Anderson, Milligan : J. Phys. Chem. Solids 23, 157 (1962).

50 Wylie, Shuskus, Young, Gilliam, Levy : Phys. Rev. 125, 451 (1962).

51 Jacobs, Tariq Kureishy : Can. Jou. Chem. 44, 703 (1966).

52 Pai Verneker : J. Phys. Chem. 72, 1733 (1968).

53 Jacobs, Tariq Kureishy : J. Chem. Soc., 4723 (1964).

54 Prout, Sears : Inorg. Nucl. Chem. Let. 9, 31 (1973).

55 Thomas, Tompkins : Proc. Roy. Soc. A209, 550 (1951).

56 Baidins : Disc. Fara. Soc. 28, 248 (1959).

57 Jacobs, Tompkins, Young : Disc. Fara. Soc. 28, 234 (1959).

58 Tompkins : Welch Found. Conf. XIV, 203 (1970).

59 Marinkas, Bartram : J. Chem. Phys. 48, 927 (1968).

60 Owen : J. Phys. Chem. Solids 88, 2646 (1971).

61 Prout, Sears : J. Inorg. Nucl. Chem. 35, 2163 (1973).

62 Boldyrev : Kinet. i Katal. 1, 203 (1960).

63 Bartlett, Tompkins, Young : J. Chem. Soc., 3323 (1956).

64 Singh : Trans. Fara. Soc. 52, 1623 (1956).

65 Bowden, MacAuslan : Nature 178, 408 (1956).

66 Thomas, Renshaw : J. Chem. Soc., 2058 (1967).

67 Bartlett, Tompkins, Young : Proc. Roy. Soc. A246, 206 (1958).

68 Prout, Moore : ASTM Spec. Tech. Pub. No. 400, 45 (1966).

69 Bright and Garner : J. Chem. Soc., 1872 (1934).

70 Boldyrev, London, Zhuravlev : Phys. Status Solidi 30, K13 (1968).

71 Garner, Hailes : Proc. Roy. Soc. A139, 576 (1933).

72 Secco ; J. Phys. Chem. Solids 24, 469 (1963).

73 Tompkins, Young : Trans. Fara. Soc. 61, 1470 (1965).

74 Jacobs, Tompkins : Proc. Roy. Soc. A215, 265 (1952).

75 Garner, Tanner : J. Chem. Soc., 47 (1930).

76 Freeman, Anderson, Campisi : J. Phys. Chem. 64, 1727 (1960).

77 Komarov, Boldyrev, Zhuravlev, Ivanov : Kinet. i Katal. 7, 788 (1966).

78 Herley, Prout : Nature 184, 445 (1959).

79 Erofeyev, Protashchik : Dokl. Akad. Nauk SSSR 172, 1129 (1967).

80 Groocock, Tompkins : Proc. Roy. Soc. A172, 299 (1939).

81 Flanagan : J. Phys. Chem. 66, 416 (1962).

82 Jach, Griffel : J. Phys. Chem. 68, 737 (1964).

83 Herley, Jacobs, Levy : Proc. Roy. Soc. A318, 197 (1970).

84 Herley, Jacobs, Levy : J. Chem. Soc. A, 434 (1971).

85 Herley, Levy : 7th Int. Symp. on React. Solids (1972).

86 Herley, Levy : CFSTI, BNL 15654 (1970).

87 Prout, Liddiard : J. Phys. Chem. 72, 2281 (1968).

88 Prout, Brown : Nature 205, 1314 (1965).

89 Prout, Moore : J. Inorg. Nucl. Chem. 31, 1595 (1969).

90 Yankwich, Zavitsansos : J. Phys. Chem. 68, 457 (1964).

91 Hailes : Trans. Fara. Soc. 29, 544 (1933).

92 McDonald : J. Chem. Soc., 839 (1936).

93 Finch, Jacobs, Tompkins : J. Chem. Soc., 2053 (1954).

94 Prout, Tompkins : Trans. Fara. Soc. 40, 488 (1944).

95 Herley, Prout : J. Phys. Chem. 66, 961 (1962).

96 Prout, Lownds : Inorg. Nucl. Chem. Let. 9, 617 (1973).

97 Maycock, Pai Verneker : J. Phys. Chem. 71, 4077 (1967).

98 Herley, Levy : Nature 211, 1287 (1966).

99 Phillips, Taylor : J. Chem. Soc. A, 5583 (1963).

100 Markowitz, Boryta : Chem. Abs. 55, 26618 (1961).

101 Prout, Tompkins : Trans. Fara. Soc. 42, 482 (1946).

102 Avrami : J. Chem. Phys. 7, 1103 (1939);
8, 121 (1940);
9, 177 (1941).

103 Erofeyev : Acad. Sci. U.R.S.S. 52, 511 (1946).

104 Bond, Jacobs : J. Chem. Soc. A9, 1265 (1966).

105 Herley, Levy : J. Chem. Phys. 49, 1500 (1968).

106 Bel'kevich, Osinovik : Chem. Abs. 50, 11790 (1956).

107 Prout, Brown : ASTM Spec. Tech. Pub. No. 359, 38 (1964).

108 Jacobs, Kureishy : J. Chem. Soc. 4718 (1964).

109 Boldyrev, Oblivantsev : Kinet. i Katal. 3, 887 (1962).

110 Prout, Liddiard : J. Inorg. Nucl. Chem. 35, 2183 (1973).

111 Prout, Moore : Unpublished results, Moore Ph.D. thesis Rhodes University (1966).

112 Garner, Reeves : Trans. Fara. Soc. 51, 694 (1955).

113 Prout, Tompkins : Trans. Fara. Soc. 43, 148 (1947).

114 Prout, Moore : ASTM Spec.Tech. Pub. No. 400, 45 (1966).

115 Tompkins : Trans. Fara. Soc. 44, 206 (1948).

116 Benton, Cunningham : J. Am. Chem. Soc. 57, 2227 (1935).

117 McDonald : J. Chem. Soc., 832 (1936).

118 Bartlett : Thesis, (London 1956).

119 Haynes, Young : Disc. Fara. Soc. 31, 229 (1961).

120 Boldyrev, Eroshkin, Zakharov : Nauk, Dokl., Vysshikh, Shkolei, 3 (1959); Chem. Abs. 54, 16146e (1960).

121 Boldyrev, Zakharov, Eroshkin, Sokolova : Dokl. Akad. Nauk SSSR 129, 365 (1959).

122 Skorik, Boldyrev, Komarov : Kinet. i Katal. 8, 1258 (1967).

123 Garner, Moon : J. Chem. Soc. 1398 (1933).

124 Maggs : Trans. Fara. Soc. 35, 433 (1939).

125 Choi : Acta Cryst. B25, 2638 (1969).

126 Walsh : J. Chem. Soc., 2266 (1953).

127 Seitz : "Imperfections in nearly Perfect Crystals", John Wiley and Sons Inc. New York (1952).

128 Nuegebauer : "The Structure and Properties of Thin Films", Wiley (1959).

129 Boldyrev, Skorik : Fiz. Shchel. Kristallov, Latv. Gos. Univ., Tr. 2-go Vses. Soveshch., Riga, 527 (1961).

130 Boldyrev, Skorik : Dokl. Akad. Nauk S.S.S.R. 156, 1143 (1964).

131 Prout, Lownds : Inorg. Nucl. Chem. Let. 9, 617 (1973).

132 Boldyrev : J. Phys. Chem. Solids 30, 1215 (1969).

133 Llewellyn, Whitmore : J. Chem. Soc., 881 (1947).

134 Menter : Proc. Roy. Soc. A236, 119 (1956).

135 Prout, Moore : ASTM Spec. Tech. Pub. No. 400, 1 (1966).